Thèse présentée pour obtenir le grade de
Docteur de l'université de bordeaux

École doctorale : Sciences de la vie et de la santé
Spécialité : Sciences agronomiques
Par **Vincent LAILHEUGUE**

Influence du génotype de porte-greffe de vigne sur la composition des microbiotes rhizosphérique et racinaire : mécanismes moléculaires impliqués et impact sur le développement du plant

Sous la direction du Maître de Conférences : **Virginie LAUVERGEAT**

Soutenue le 28/11/2023

Membres du jury :

Mme LAUVERGEAT, Virginie, Maître de conférences, Université de Bordeaux, Directrice de thèse
Mme. DELLAGI, Alia, Professeur, AgroParisTech, Rapporteur
M. WIPF, Daniel, Professeur, Université de Bourgogne, Rapporteur
Mme. VACHER, Corinne, Directrice de recherche, Université de Bordeaux, Examinateur
M. LA CAMERA, Sylvain, Professeur, Université de Poitiers, Examinateur
Mme. CLUZET, Stéphanie, Professeur, Université de Bordeaux, Examinateur

Influence des génotypes de porte-greffe et de greffon de vigne sur la composition des microbiotes rhizosphérique et racinaire : mécanismes moléculaires impliqués et impact sur le développement du plant

Résumé de la thèse :

La viticulture est un secteur d'activité économique et culturelle majeur, nécessitant de s'adapter rapidement aux contraintes actuelles de changement climatique et de réduction des intrants, afin d'assurer sa pérennité. Le sol viticole contient une multitude de microorganismes en interaction étroite avec le système racinaire de la vigne. Au sein de la rhizosphère (i.e., zone de terre collée aux racines) et de l'endosphère racinaire, ils influencent de manière bénéfique, neutre ou défavorable, la croissance et le développement de l'hôte, et par conséquent le rendement et la qualité des baies et du vin. Grâce à la rhizodéposition, mécanisme regroupant l'exsudation de composés de faible poids moléculaire (e.g. sucres, acides aminés et organiques) et le mucilage (sucres polymérisés) par les racines, ainsi que le relargage de cellules spécialisées, les plantes influencent la composition du microbiote du système racinaire.

Comprendre les interactions entre la vigne greffée et le microbiote du sol est donc indispensable pour proposer des techniques innovantes et efficaces dans l'adaptation du secteur aux enjeux actuels. L'influence des génotypes du plant greffé, et plus particulièrement du porte-greffe (PG), en contact direct avec le sol, revêt donc une importance fondamentale. En effet, il est nécessaire de comprendre comment le PG interagit avec ce microbiote, afin de définir des stratégies d'amélioration variétale en identifiant quel génotype interagira le mieux avec le microbiote indigène d'une parcelle, ou un consortium de micro-organismes stimulateurs de croissance ou des défenses de la plante, tels que les champignons mycorhiziens arbusculaires (CMA). Plusieurs travaux semblent montrer une influence des deux génotypes du plant greffé sur la composition des bactéries et des champignons du microbiote du système racinaire de la vigne. Cependant, l'influence réciproque des deux partenaires n'est pas toujours clairement démontrée. Par ailleurs il est difficile de comparer ces études à cause de différences dans les méthodes d'analyses employées, les micro-organismes, les compartiments racinaires et les génotypes étudiés, ainsi que le contexte pédoclimatique des parcelles analysées. De plus, la plupart de ces études se sont concentrées sur l'identification des microorganismes mais très peu sur leurs rôles environnementaux et sur la plante. Enfin, l'influence du génotype de PG sur la communauté de CMA est très peu étudiée.

Dans ce contexte, les objectifs de la thèse étaient : (i) d'étudier l'influence des deux génotypes du plant greffé de vigne sur la composition des bactéries et des champignons associés au système racinaire, (ii) de comparer la capacité d'association de différente combinaisons PG × greffon avec les CMA, (iii) caractériser le rôle fonctionnel du microbiote du système racinaire et (iv) de comparer chez différents génotypes de PG les profils métaboliques de la rhizosphère et des racines, afin de les relier à leur composition taxonomique. Les résultats acquis sur le dispositif GreffAdapt au cours des trois dernières années confirment l'influence du génotype de PG sur la composition et la fonction des bactéries et des champignons du microbiote racinaire, ainsi qu'une contribution moindre du génotype du cépage. Même si la capacité de mycorhization ne semble pas dépendante des deux génotypes du plant greffé, la diversité des CMA dans l'endosphère racinaire est fortement influencée par le PG. L'observation de corrélations entre la composition du microbiote du système racinaire avec le phénotype et la nutrition minérale de la plante met en évidence le rôle fondamental de ces communautés microbiennes sur le développement de la vigne. Enfin, l'acquisition récente d'un jeu de données caractérisant la composition métabolique des compartiments racinaires de différents génotypes de PG, semble prometteuse pour caractériser une partie des mécanismes impliqués dans la sélection des microorganismes du sol par les racines.

Mots clés : Microbiote de la rhizosphère, Microbiote de l'endosphère racinaire, Bactéries, Champignons, Champignon mycorhizien arbusculaire.

Influence of grapevine rootstock and scion genotypes on the composition of rhizospheric and root endophyte microbiota: molecular mechanisms involved and impact on plant development

Abstract:

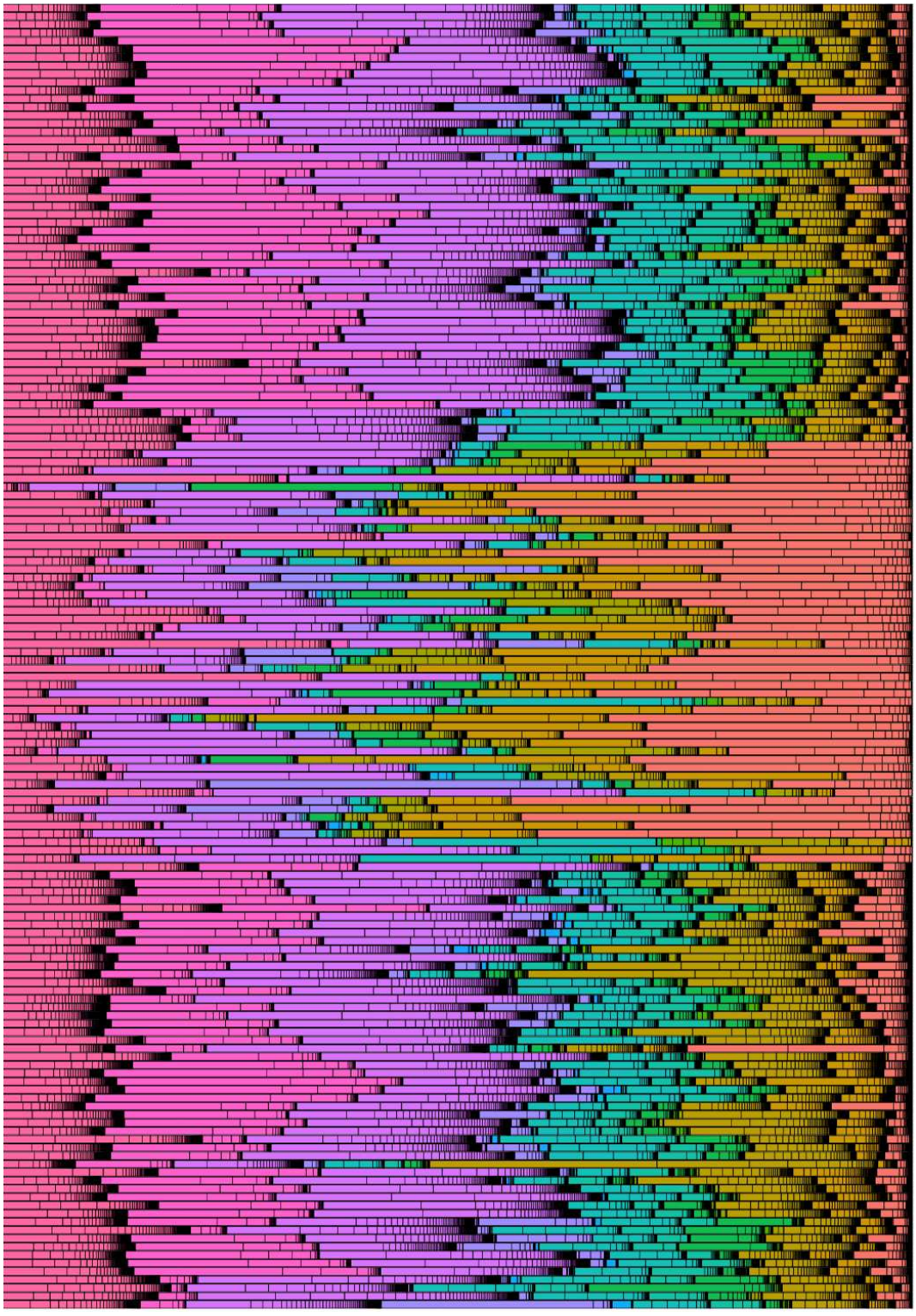
Viticulture is a major sector of economic and cultural activity, requiring rapid adaptation to the current constraints of climate change and reduced inputs to ensure its long-term perennity. Vineyard soil contains a multitude of microorganisms that interact closely with the grapevine root system. Within the rhizosphere (i.e., the zone of soil attached to the roots) and the root endosphere, microorganisms have a beneficial, neutral, or adverse effect on the growth and development of the host, and consequently on the yield and quality of the berries and wine. Through rhizodeposition, a mechanism involving the exudation of low molecular weight compounds (e.g., sugars, amino acids and organics) and mucilage (polymerized sugars) by the roots, as well as the release of specialized cells, plants influence the composition of the microbiota in the root system.

Understanding the interactions between the grafted vine and the soil microbiota is therefore essential to propose innovative and effective techniques for adapting the sector to current challenges. The influence of the genotypes of the grafted plant, and more particularly of the rootstock, in direct contact with the soil, is therefore of fundamental importance. We need to understand how the rootstock interacts with this microbiota, to define varietal improvement strategies by identifying which genotype will interact best with the plot indigenous microbiota, or with a consortium of microorganisms that stimulate plant growth or defenses, such as arbuscular mycorrhizal fungi (AMF). Several studies showed that both genotypes of the grafted plant influence the composition of bacteria and fungi in the microbiota of the grapevine root system. However, the reciprocal influence of the two partners is not always clearly demonstrated. It is also difficult to compare these studies because of differences in the analysis methods used, the micro-organisms, the root compartments and the genotypes studied, as well as the soil and climate conditions of the vineyards analyzed. In addition, most of these studies focused on the identification of microorganisms, but few about their environmental roles and impact on plant health. Finally, the influence of the rootstock genotype on the AMF community still poorly characterized.

In this context, the objectives of the thesis were: (i) to study the influence of both genotypes of the grafted plant on the composition of bacteria and fungi associated with the root system, (ii) to compare the association capacity of the different rootstock × scion combinations with AMF, (iii) to characterize the functional role of the root system microbiota and (iv) to compare the metabolic profiles of the rhizosphere and roots of different rootstock genotypes, in order to link them to their taxonomic composition. The results obtained from the GreffAdapt plot over the last three years confirm the influence of the rootstock genotype on the composition and function of the bacteria and fungi in the root microbiota, as well as a lesser contribution from the scion genotype. Although mycorrhization capacity does not seem to depend on the two genotypes of the grafted plant, the AMF diversity in the root endosphere is strongly influenced by the rootstock. The observation of correlations between the composition of the root system microbiota and plant phenotype and mineral nutrition highlights the fundamental role of these microbial communities in grapevine development. Finally, the recent acquisition of a dataset characterizing the metabolic composition of the root compartments of different rootstock genotypes seems promising for characterizing some of the mechanisms involved in the root selection of microorganisms.

Keywords: Rhizosphere microbiota, Root endosphere microbiota, Bacteria, Fungi, Arbuscular mycorrhizal fungi.





Au sein de son système racinaire, la vigne abrite des communautés microbiennes complexes, riches et diversifiées ...

Remerciements

Tout d'abord, je souhaite remercier les membres du jury pour le temps consacré à l'évaluation de mes travaux de thèse. Merci infiniment à vous Madame Alia Dellagi et Monsieur Daniel Wipf d'évaluer mon travail en tant que rapporteurs, ainsi qu'à vous Madame Corinne Vacher, Madame Stéphanie Cluzet et Monsieur Sylvain La Camera de l'évaluer en tant qu'examinateurs.

Mes remerciements vont ensuite naturellement s'adresser à ma directrice de thèse Virginie Lauvergeat, ainsi qu'à Romain Darriaut, Joseph Tran et Elisa Marguerit, sans qui, l'aboutissement de ce travail au cours des trois dernières années n'aurait jamais réussi. Merci à toi Virginie pour ton encadrement dans lequel tu m'as donné toute ton expertise scientifique en me laissant une certaine liberté, je n'ai manqué de rien. Merci pour ta bienveillance, ta confiance et les nombreuses discussions, scientifiques ou non, que nous avons eu au cours de la thèse. Merci à toi Docteur Dolgov pour ton appui indispensable lors de la première moitié de ma thèse, ainsi que les nombreux conseils de microbiologiste russe pasteurien que tu m'as transmis. C'est un honneur d'avoir servi à tes cotés ! Merci à toi Joseph, pour les nombreux après-midis passés ensemble à résoudre mes problèmes sur R ou sur FROGS, je n'aurais jamais réussi à me former au monde de la bio-informatique sans toi. Enfin, merci à toi Élisa de m'avoir laissé réaliser mes expérimentations sur ton dispositif unique, ainsi que pour tes précieux conseils d'agronome aguerrie.

Vous vous doutez bien que la science n'aboutit jamais loin lorsqu'elle est exercée par un petit groupe de personne. C'est pourquoi je remercie l'ensemble de la grande famille de l'UMR 1287 EGFV (directrice, chercheurs, ingénieurs, techniciens et stagiaires), pour leur accueil, les supers moments passés avec eux et leur aide au cours des nombreuses expérimentations. Je tiens aussi à remercier l'ensemble des stagiaires que j'ai eu la chance d'encadrer au cours de ma thèse, Tania Marzari et Ulysse Tuquoi en première année, Charlotte Barthel en seconde, et enfin Rachid Benr'Kia lors de la dernière. Merci à vous, sans qui, les grosses campagnes de prélèvement et le traitement des échantillons frais ne se seraient pas déroulés dans d'aussi bonnes conditions. Beaucoup d'entre vous ont un gros potentiel, je vous souhaite le meilleur pour la suite.

De plus, je tiens particulièrement à adresser mes remerciements à toutes les personnes qui ont travaillé dans les deux bureaux des non-permanents, même à nos rivaux de celui des coquillages au caryotype douteux. Je tiens infiniment à vous remercier Louis Blois, Marine Morel, Mathieu Larrey,

Margot Berger, Grégoire Loupit, Etienne Patin, Xi Zhan, Cécile Prévot, Marc Plantevin, Anne Janoueix, et enfin toi Marilou Camboué, pour tous les moments passés ensemble, au travail, au Stag, au Edwood, en club, à Condom, à la plage, en congrès, au ski, ainsi que dans le No Man's Land de GreffAdapt armés d'une cuillère à soupe. Je remercie aussi les MIBettes Anthony Pébarthé et David Taillis, ainsi que mes amis d'autres UMR Sabri Najai et Kilian Dehlouz, pour avoir partagé beaucoup de ces moments avec nous, ainsi que l'ensemble de mes amis d'enfance bordelais.

Pour clôturer ces remercîments, je les adresse à l'ensemble de ma famille, les Lailheugue, les Jammes, les Fragne, les Verdon, et les Kocimski, grâce à qui le soutien infaillible m'a permis d'arriver jusqu'ici. Je les adresse en hommage particulièrement à toi mon oncle Jean. Enfin, merci surtout à vous Papa, Maman et Gautier. Je ne vous l'ai jamais dit mais, je vous suis infiniment reconnaissant d'avoir grandi à vos côtés, encore plus depuis l'arrivée du bouledogue des ténèbres Sauron.

Table des matières

Introduction *14*

I) Contexte socio - économique de la vigne **14**
1) La vigne, une histoire qui se confond avec celle de l'humanité **14**
2) La viticulture, un secteur d'intérêt économique majeur **17**
3) La vigne est cultivée greffée **18**
a) Le choix du greffon **18**
b) Le choix du porte-greffe **19**
4) Les enjeux de la filière viti-vinicole **22**
a) L'adaptation aux contraintes biotiques dans un contexte d'agriculture durable **22**
b) La viticulture face au changement climatique **24**
c) Les attentes des consommateurs **26**

II) Le microbiote du système racinaire et son rôle dans la croissance de la vigne et l'adaptation à l'environnement **28**
1) Le sol viticole : un réservoir de micro-organismes aux fonctions multiples **28**
2) Des micro-organismes prometteurs pour l'adaptation de la viticulture **30**
a) Les Plant Growth Promoting Rhizobacteria (PGPR) améliorent la croissance du plant par divers mécanismes **30**
b) Le cas des champignons mycorhiziens arbusculaires (CMA) **33**
3) Des méthodologies pour étudier le microbiote de la vigne **36**
a) Les approches de culture in vitro sur milieux nutritifs **36**
b) Les méthodes basées sur la biologie moléculaire **37**
c) Les autres méthodologies utilisées dans la thèse **41**

III) Le porte-greffe de vigne et le microbiote du système racinaire **45**
1) La composition du microbiote du système racinaire est soumise à de nombreux facteurs **45**
2) Influence des génotypes de porte-greffe et de greffon sur la composition des microbiomes rhizosphériques et racinaires chez la vigne **47**
3) Les exsudats racinaires influencent la communauté microbienne rhizosphérique **52**
a) Le rôle des exsudats racinaires dans la rhizosphère **52**
b) La caractérisation des exsudats racinaires chez la vigne **55**

IV) Les objectifs de la thèse **57**

Chapitre 1 : Influence des génotypes de porte-greffe et de greffon de la vigne sur la composition des microbiotes de la rhizosphère et de l'endosphère racinaire *61*

Préface **61**

The genotypes of the two components of grafted grapevines influence the rhizosphere and root endophyte microbiomes, with rootstocks having a greater impact **62**
Abstract: **62**
Background **64**
Materials and methods **67**
Results **72**
Discussion **88**
Conclusion **92**
Supplementary tables **93**
Supplementary figures **98**

Chapitre 2 : Influence des génotypes du plant greffé de vigne sur la communauté des champignons mycorhiziens arbusculaires des racines *107*

Préface **107**

Influence of grapevine rootstock and scion genotypes on the structure and composition of arbuscular mycorrhizal fungi associated with the root system **108**
Abstract: **108**
Background **110**
Material and methods **112**

Results 115
Discussion 125
Conclusion 128
Supplementary tables 129
Supplementary figures 131

Chapitre 3 : Mécanismes moléculaires induits par le porte-greffe dans la sélection des microorganismes du système racinaire ***132***

Préface 132

Molecular mechanisms of rootstocks involved in the selection of rhizosphere and root endosphere microbiomes 134
Abstract 134
Background 134
Conclusion 135
Background 136
Material and methods 139
Results 145
Discussion 167
Conclusion 171
Supplementary tables 172
Supplementary figures 180

Discussion de la thèse ***184***

I- Synthèse des résultats acquis dans la thèse 184

II- Continuer et améliorer le décryptage des interactions de la vigne avec son microbiome racinaire 187
a) Le couplage des approches de métabarcoding et de métabolomique pour comprendre l'influence du porte-greffe sur le microbiome du sol 187
b) Relier la composition du microbiome du système racinaire au développement de la plante 188
c) Proposition d'une approche intégrative pour l'étude du microbiome de la vigne 190

III- Conclusion et perspectives 194

Bibliographie ***196***

Publications ***211***

Liste des figures

Introduction

Figure 0-1 : Comparaison entre V. vinifera ssp sylvestris et sativa. 15
Figure 0-2 : La domestication de V. vinifera. 16
Figure 0-3 : La viticulture, un secteur d'intérêt économique majeur. 18
Figure 0-4 Croisement des espèces de Vitis pour l'obtention des hybrides de porte-greffe tolérants au phylloxera. 20
Figure 0-5 : Impact du changement climatique sur la phénologie de la vigne (A) et la composition de la baie (B) (Adapté de : Venios et al., 2020) 25
Figure 0-6 : Interactions entre le plant de vigne et le microbiote du sol. 29
Figure 0-7 : Les bénéfices des PGPR face aux problématiques de la viticulture. 32
Figure 0-8 : Proposition de classification taxonomique des CMA basée sur l'homologie de séquences codantes la petite sous-unité du ribosome (SSU). 34
Figure 0-9 : Les bénéfices des CMA pour la vigne face aux problématiques de la viticulture. 35
Figure 0-10 : Champignons et bactéries rhizosphériques 36
Figure 0-11 : Schéma de l'opéron de l'ADN ribosomique sur les chromosomes eucaryotes (A) et procaryote (B) 38
Figure 0-12 : Pipeline utilisé pour traiter les données de métabarcoding (A) et indices de diversité (B) 40
Figure 0-13 : Liste des différents substrats présents dans les plaques Biolog Ecoplate™ 42
Figure 0-14 : Gamme étalon utilisée pour le dosage de l'arylamidase 43
Figure 0-15 : Évaluation de la capacité de mycorhization des racines au microscope (A) à l'aide d'une échelle semi-quantitative (B). 43
Figure 0-16 : Schéma du fonctionnement de la spectrométrie de masse en tandem (MS/MS) 44
Figure 0-17 : Les facteurs qui influencent la composition des microbiomes du sol et de la rhizosphère chez la vigne. 45
Figure 0-18 : Schéma des interactions complexes entre les racines de la plante et les microbiotes rhizosphériques et racinaires. 52
Figure 0-19 : Influence de la rhizodéposition les communautés microbiennes du sol et du système racinaire 53
Figure 0-20 : Schéma récapitulatif des expérimentations menées dans les trois chapitres de la thèse. 60

Chapitre 1

Figure 1-1: Comparison of microbial communities between the root endosphere (RE, light brown) and the rhizosphere (RH, dark brown). 72
Figure 1-2: Comparison of bacterial communities in the rhizosphere (dark brown, top panel) and the root endosphere (light brown, bottom panel) between the 6 rootstock genotypes grafted onto CS (n=6). 77
Figure 1-3: Histogram of the linear discriminant analysis (LDA) scores reveals the most differentially abundant taxa of bacteria (A, B), fungi (C, D) and AMF (D, E) in the rhizosphere (RH) and the root endosphere (RE) between rootstock genotypes. 79
Figure 1-4: Comparison of fungal communities in the rhizosphere (top panel, dark brown) and the root endosphere (bottom panel, light brown) between the 6 rootstock genotypes grafted with CS (n=6). 81
Figure 1-5: Comparison of AMF communities in the rhizosphere (top panel) and the root endosphere (bottom panel) between the 6 rootstock genotypes grafted with CS (n=6). 83

Figure 1-6: PICRUSt inference of bacterial metabolic pathways and functions. 85
Figure 1-7: Comparisons of the predicted trophic modes and guilds between the root system compartments (A, C) or the rootstock genotypes in the rhizosphere (B, D) and the root endosphere (C, E) 86
Figure 1-8: Matrices of significant correlations established between the variables measured to characterize the root system microbiomes and the plant phenotype (A), the mineral status of petioles (B) and the mineral status of roots (C) 87

Chapitre 2

Figure 2-1: Comparison of the mycorrhization frequency (F%), the overall mycorrhization intensity (M%) and the mycorrhization intensity of mycorrhized fragments (m%) between genotypes of rootstock (A, B) or scion (C, D). 116
Figure 2-2: Comparison of AMF community assessed with the 28S rRNA gene between rootstocks. 118
Figure 2-3 : Comparison of AMF community assessed with the 18S rRNA gene between the rootstock genotypes. 120
Figure 2-4: Comparison of AMF community assessed with the 18S rRNA gene between the scion genotypes. 121
Figure 2-5: Matrix showing Pearson correlations of the variables to assess AMF community with plant phenotypic traits measured in the 10 rootstock combinations. 122
Figure 2-6: Pearson correlations of α-diversity metrics measured by sequencing 18S and 28S rRNA genes. 124

Chapitre 3

Figure 3-1: Comparison of the number of copies of bacterial 16S rRNA, fungal 18S rRNA and archaeal 16S rRNA genes between soil compartments (A, D, G) or rootstock genotypes in BS (B, E, H, dark grey) and RH (C, F, I, dark brown). 146
Figure 3-2: Comparison of microbial communities between the bulk soil (grey), the rhizosphere (dark brown) and the root endosphere (RE, light brown) (n=54). 148
Figure 3-3: Comparison of bacterial communities between the rootstock genotypes in the bulk soil (grey), the rhizosphere (dark brown) and the root endosphere (RE, light brown) (n=9). 152
Figure 3-4: Histogram of the linear discriminant analysis (LDA) scores reveals the most differentially abundant taxa of bacteria (A, B and C), fungi (D, E and F) and AMF (G, H and I) within the bulk soil, the rhizosphere and the root endosphere. 153
Figure 3-5: Comparison of fungal communities between the rootstock genotypes in the bulk soil (grey), the rhizosphere (dark brown) and the root endosphere (RE, light brown) (n=9). 156
Figure 3-6: Comparison of AMF communities between the rootstock genotypes in the bulk soil (grey), the rhizosphere (dark brown) and the root endosphere (RE, light brown) (n=9). 159
Figure 3-7: Comparison of the trophic modes and the guilds of fungi between compartments (A and E) (n=54), and rootstock genotypes within the bulk soil (B and F), the rhizosphere (C and G) and the root endosphere (D and H) (n=9). 161
Figure 3-8: Heatmap showing the abundance of bacterial metabolic pathways which were significantly influenced by the compartments (A) (n = 18), or the rootstock genotype in the bulk soil (B), the rhizosphere (C) and the root endosphere (D) (n = 9). 162
Figure 3-9: Comparison of the activities of the arylamidase (A), the β-glucosidase (B) and the phosphatase (C) in the rhizosphere between rootstock genotypes (n = 9). 163
Figure 3-10: Comparison of the parameters measured by community-level physiological profiling (CLPP) using Biolog EcoplateTM between rootstock genotypes (n = 9). 164

Figure 3-11: Matrices of significant correlations established between the variables measured to characterize the root system microbiomes (qPCR, metabarcoding, Biolog, microscopy) and the plant phenotype or the activity of enzymes involved in biogeochemical cycles (n = 54). 166

Liste des tables

Introduction

Tableau 0-1 : Superficies des vignes mères de cépages en France 19
Tableau 0-2 : Origines génétiques et principales caractéristiques agronomiques des six porte-greffes étudiés dans la thèse. 20
Tableau 0-3 : Superficies des vignes mères de porte-greffes en France 21
Tableau 0-4 : Liste non exhaustive des principaux agents pathogènes de la vigne 22
Tableau 0-5 : Principales caractéristiques des études des effets du porte-greffe et du greffon sur le microbiome du système racinaire de la vigne 48

Chapitre 1

Table 1-1: Influence of the rootstock and the scion genotypes on the α-diversity (richness = Chao1, diversity= Simpson) and the β-diversity metrics (Bray-Curtis dissimilarity) amongst bacteria, fungi and AMF, in the rhizosphere (RH) and the root endosphere (RE). 75

Chapitre 2

Table 2-1: Effects of the genotype of rootstock or scion on the root colonization by AMF, assessed by measuring the mycorrhization frequency (F%), the overall mycorrhization intensity (M%) and the mycorrhization intensity of mycorrhized fragments (m%). 115
Table 2-2: Effects of the genotype of rootstock or scion on α-diversity (Chao1, Simpson) and β-diversity metrics. 116

Chapitre 3

Table 3-1: Influence of the rootstock genotype and the block on the quantity of bacteria, fungi, and archaea in the bulk soil (BS) and the rhizosphere (RH). 145
Table 3-2: Influence of the studied compartment (BS, RH and RE) on the α-diversity (richness = Chao1, diversity= Simpson) and the β-diversity metrics (Bray-Curtis dissimilarity) amongst bacteria, fungi and AMF. 147
Table 3-3: Influence of the rootstock genotype and the block on the α-diversity (richness = Chao1, diversity= Simpson) and the β-diversity metrics (Bray-Curtis dissimilarity) measured for bacteria. 150
Table 3-4: Influence of the rootstock genotype and the block on the α-diversity (richness = Chao1, diversity= Simpson) and the β-diversity metrics (Bray-Curtis dissimilarity) measured for fungi. ... 154
Table 3-5: Influence of the rootstock genotype and the block on the α-diversity (richness = Chao1, diversity= Simpson) and the β-diversity metrics (Bray-Curtis dissimilarity) measured for AMF. ... 157

Introduction

I) Contexte socio - économique de la vigne

Dans cette première partie introductive du manuscrit, nous verrons que l'histoire de la vigne est intimement liée à celle de l'homme, et que les produits issus de sa culture présentent un intérêt économique majeur en France et dans le monde. Nous verrons que cette plante est principalement cultivée greffée et nous établirons une liste non exhaustive des caractéristiques importantes pour le choix des génotypes de porte-greffe et de greffon. Enfin, nous discuterons des principales problématiques auxquelles la viticulture doit s'adapter : l'agriculture durable, le changement climatique et les attentes des consommateurs.

1) La vigne, une histoire qui se confond avec celle de l'humanité

Le genre *Vitis* appartient à la famille des Vitacées et comprend 80 espèces qui se répartissent en deux sous-genres : *Muscadinia* (2n = 40 chromosomes) et *Euvitis* (2n = 38 chromosomes) (*Distribution variétale du vignoble dans le monde, OIV 2017*). Les *Muscadinia* comprennent 3 espèces appelées *Vitis popenœi*, *Vitis munsoniana* et *Vitis rotundifolia*. Même si *V. Rotundifolia* est cultivée dans le Sud-Est de l'Amérique du Nord, la majeure partie des vignes cultivées dans le monde appartient au sous-genre *Euvitis*, lui-même découpé en trois groupes. On retrouve le groupe américain constitué d'une vingtaine d'espèces telles que *V. berlandieri*, *V. riparia* ou *V. rupestris*. Ces espèces ont fortement participé à la création de porte-greffes permettant de faire face à la crise phylloxérique en Europe lors de la seconde moitié du XIX^{ème} siècle. Il existe aussi le groupe d'Asie orientale, constitué d'environ 55 espèces, présentant une importance jugée réduite pour la viticulture à ce jour. Enfin, le groupe eurasiatique est constitué d'une espèce unique appelée *V. vinifera L*. Cette espèce réunit la plupart des variétés de *Vitis* cultivées dans le monde et a acquis un intérêt économique et culturel important au fil du temps. Elle comprend des espèces sauvages (*V. vinifera* subsp. *sylvestris*) et cultivées (*V. vinifera* subsp. *sativa*) dans le monde entier. A l'état sauvage, c'est une liane héliophile qui pousse généralement le long des berges des rivières, ainsi que dans les forêts alluviales et colluviales décidues et semi-décidues (*Arnold, 2002*). Elle est distribuée dans une vaste zone géographique s'étalant de l'Europe occidentale à la zone transcaucasienne et autour du bassin méditerranéen, à l'exception des zones infra-méditerranéennes et non méditerranéennes les plus méridionales (Grassi and De Lorenzis, 2021). Elle se distingue de la forme cultivée grâce à certains traits morphologiques tels que la forme des feuilles et la taille réduite de celles-ci, la réduction du bec des pépins leur donnant une forme plus

arrondie, ainsi que des grappes moins fournies, portant des fruits plus acides et amers. Enfin, les fleurs des individus de la sous-espèce *sylvestris* sont dioïques (fleurs mâles et femelles), alors que celles de la forme cultivée *vinifera* sont monoïques (fleurs hermaphrodites) (Figure 1).

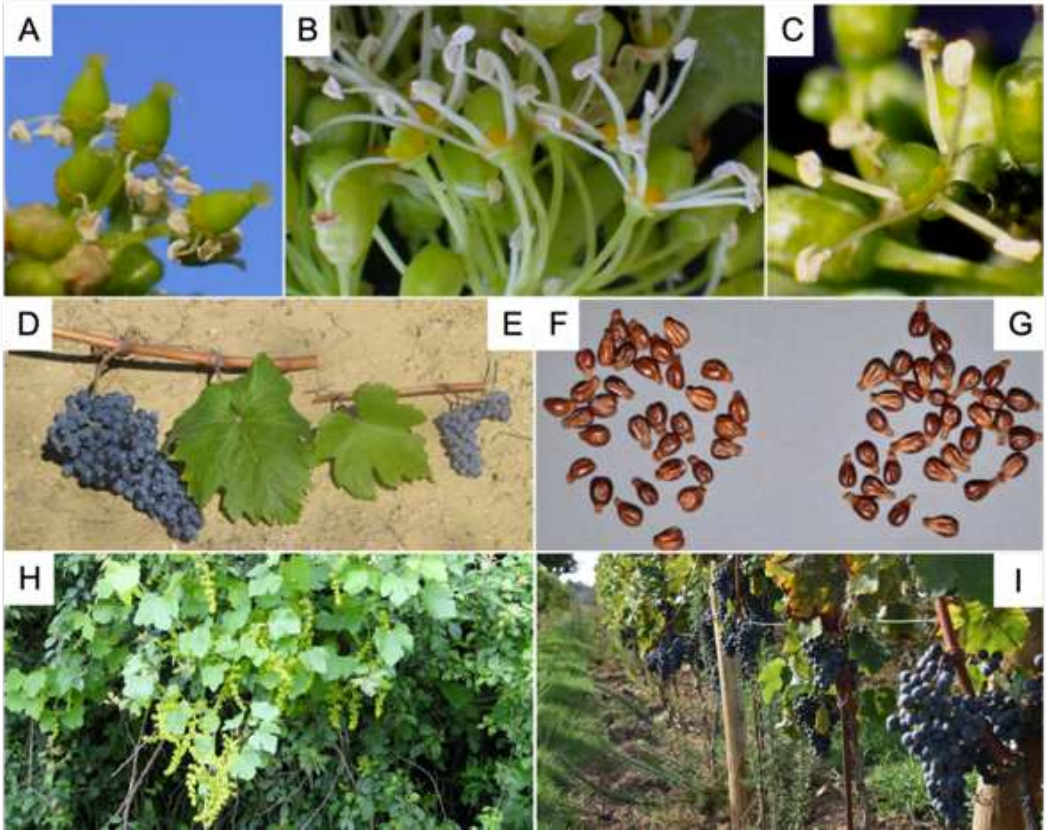


Figure 0-1 : Comparaison entre *V. vinifera* ssp *sylvestris* et *sativa*.
Fleurs femelles (A) et mâles (B) chez *sylvestris*. Fleur hermaphrodite chez *sativa* (C). Feuille et grappe chez *sativa* (D) et *sylvestris* (E). Pépins chez *sylvestris* (F) et *sativa* (G). Plante entière de *sylvestris* (H) et de *sativa* (I) (Adapté de : Grassi et De Lorenzis, 2021).

Aujourd'hui, le débat portant sur la date de la domestication de la vigne reste ouvert. Certaines recherches proposent un modèle d'origine unique avec une domestication de la vigne dans une zone restreinte bien définie (McGovern et al., 1996). En revanche, d'autres travaux proposent un modèle aux origines multiples, avec la création de différentes lignées sur l'ensemble de l'aire de répartition des vignes sauvages (Dong et al., 2023). Dans la revue de Grassi and De Lorenzis (2021), les auteurs proposent une première domestication de la vigne autour du mont Ararat dans le Caucase qui aurait été diffusée autour du bassin méditerranéen par trois voies principales (Figure 2). À l'âge de bronze, elle aurait traversé la Mésopotamie, puis l'Égypte, pour atteindre la Grèce, présentée comme un centre de domestication secondaire (Flèche 1a). D'autres études indiquent une arrivée de la vigne en Grèce par l'Anatolie (Flèche 1b). Sous l'influence des Grecs, des Étrusques et des Phéniciens, la seconde

route se serait ensuite dirigée vers l'Italie du Sud, la France et l'Espagne (Flèches 2, 3a et 3b). Sous l'influence de l'Empire Romain, la vigne aurait empruntée une troisième route de la France vers le Nord de l'Europe (Flèche 4). Enfin, l'Italie du Nord aurait aussi été un centre de mélange des populations du Sud de l'Italie et d'Europe centrale (Flèche 5 et 6). Une étude récente de génétique propose que la domestication de la vigne aurait eu lieu il y a 11 000 ans simultanément dans deux régions. Une domestication dans le Caucase aurait donné naissance aux vignes destinées à la production de vin et une autre en Asie de l'Ouest aux vignes destinées à la production de raisin de table (Dong et al., 2023). Cependant, de nombreux travaux sont encore nécessaires pour élucider l'histoire de la domestication de la vigne.

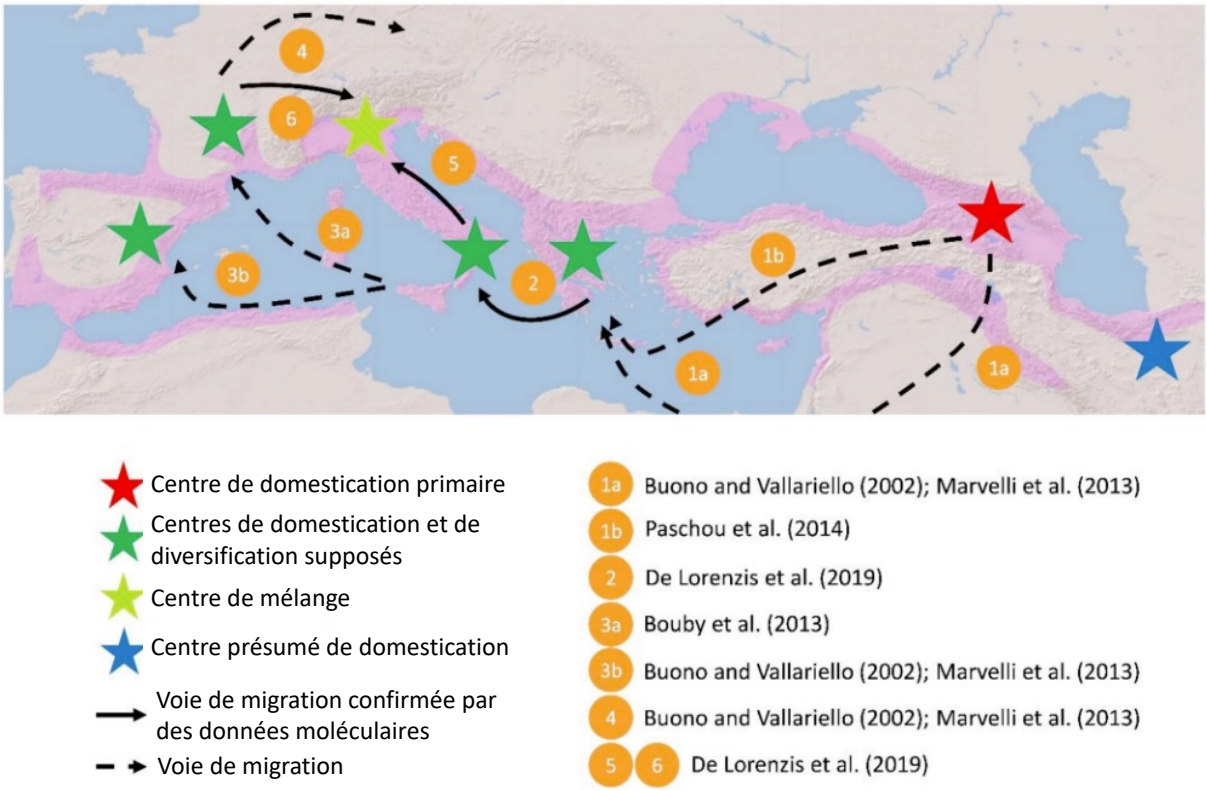


Figure 0-2 : La domestication de *V. vinifera.*
Carte représentant les centres probables de domestication et de diversification (étoiles), ainsi que les principales voies de migration de la vigne (flèches). (Adapté de : Grassi and De Lorenzis, 2021)

La découverte d'une jarre datant de plus de 5000 ans avant J-C contenant des résidus d'acide tartrique et d'un additif (résine térébinthe) permettant d'inhiber la croissance de bactéries transformant le vin en vinaigre, laisse penser que le procédé de vinification serait apparu au cours du Néolithique (McGovern et al., 1996). En tant que source de nourriture et d'ingrédient de base pour la fabrication du vin, *V. vinifera* est devenu un emblème d'identité culturelle chez la plupart des civilisations euro-

méditerranéennes (Dong et al., 2023). En effet, cette espèce a souvent été associée à des divinités ou des rituels. On la retrouve fréquemment sur des artefacts provenant de plusieurs anciennes civilisations telles que les Égyptiens, les Grecs ou les Romains. De plus, de nombreuses caractéristiques de la vigne et du vin furent associées à des significations symboliques. Par exemple, les fruits ronds, charnus et colorés, devinrent des symboles d'abondance, de fertilité et de richesse. Le dimorphisme saisonnier de la plante fût utilisé pour imager la renaissance, la régénération et les cycles de la vie. La vinification du jus des baies permit d'illustrer la métamorphose ou la transformation (Savo et al., 2016).

2) La viticulture, un secteur d'intérêt économique majeur

L'Organisation Internationale de la Vigne et du Vin (OIV) estime la surface mondiale des vignobles à 7,3 millions d'hectares (mha) en 2022. Avec 13.1% de la surface viticole mondiale, l'Espagne détient la plus grande superficie, suivie de la France (11,2%), la Chine (10,8%), l'Italie (9,9%), la Turquie (5,6%) et les Etats-Unis (5,4%). La majorité du rendement en raisin est destinée à la vinification (57%), contre 36 et 7% à la production de raisins de table et de raisins secs. La production mondiale de vin (hors jus et moûts) est estimée à 258 millions d'hectolitres (mhl) en 2022. Les principaux pays producteurs sont l'Italie (19,3%), la France (17,7%), l'Espagne (13,8%), les Etats-Unis (8,7%) et l'Australie (4,9%). Avec une consommation mondiale de 232 mhl au cours de la même année, le vin est principalement consommé par les Etats-Unis (15%), la France (11%), l'Italie (10%), l'Allemagne (8%) et le Royaume-Uni (6%). Il est estimé que 46% de la production mondiale (107 mhl) est destinée à l'export vers l'international, représentant un chiffre d'affaires de 37,6 milliards d'euro (Md€). En termes de volume, les principaux pays exportateurs sont l'Italie (21,9 mhl), l'Espagne (21,2 mhl), la France (14 mhl), le Chili (8,3 mhl) et l'Australie (6,4 mhl). En revanche, si l'on s'intéresse au chiffre d'affaires, la France se hisse en première place avec une valeur à l'export de sa production de vin à 12,279 Md€. Elle est suivie par l'Italie (7,834 Md€), l'Espagne (2,984 Md€), le Chili (1,818 Md€) et les Etats-Unis (1,392 Md€). Avec une légère réduction des surfaces viticoles (7,7 à 7,3 mha), de légères fluctuations dans la production (250 à 295 mhl) et la consommation du vin (225 à 250 mhl), mais une augmentation du prix au litre (2,30 à 3,30€), ainsi que du volume (60 à 110 mhl) et de sa valeur à l'export (14 à presque 40 Md€ d'euros) au cours des 20 dernières années, la viticulture représente un secteur d'intérêt économique majeur à l'échelle de la France et du globe (Figure 3).

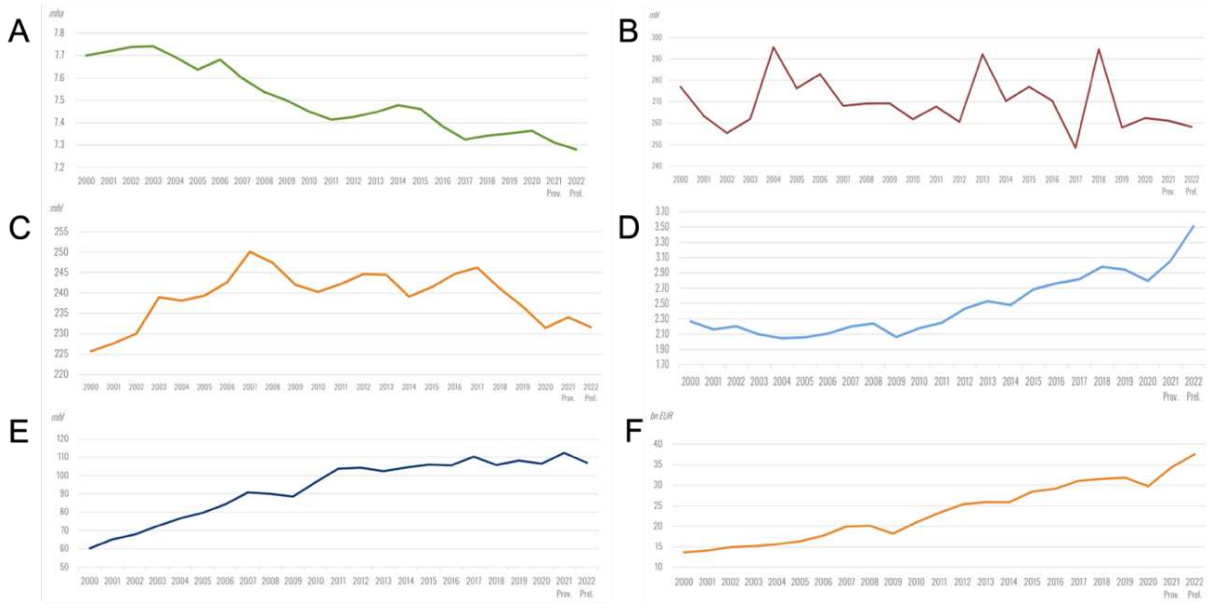


Figure 0-3 : La viticulture, un secteur d'intérêt économique majeur.
Évolution mondiale au cours des 20 dernières années de la superficie des vignobles (mha, A), de la production (mhl, B) et la consommation (mhl, C) de vin, du prix (bn €, D), du volume (mhl, E) et de la valeur (bn €, F) à l'export. (Adapté de : State of the world vine and wine sector in 2022, OIV)

3) La vigne est cultivée greffée

a) Le choix du greffon

Aujourd'hui, on estime qu'il existe plus de 6000 cépages de *V. vinifera* à travers le monde. Le choix d'un cépage va d'abord être défini par la destination des baies. Un cépage producteur de raisins de table sera sélectionné pour l'apparence (taille, forme et couleur), le goût, les arômes, la texture et la capacité de conservation des baies. Au sein des raisins de cuve, le choix du cépage sera principalement orienté par la nature de vin que l'on veut produire (rouge, blanc, rosé), mais aussi pour les propriétés organoleptiques souhaitées au sein de chacun des types. Par exemple, les attributs de qualité du raisin pour un cépage blanc vont être liés à un bon rapport sucre/acidité, associé à un pH modéré du moût et un caractère variétal propre. Pour un cépage rouge, on va rechercher des réserves non limitantes en sucres et en anthocyanes qui doivent fusionner avec une texture idéale des tanins dans la peau et les pépins (Poni et al., 2018). Le choix du cépage sera aussi dicté par la qualité de vin escomptée (vin de table versus noble), si l'on souhaite le faire vieillir ou non (vin de garde versus jeune), ainsi que par le cahier des charges des appellations.

Tableau 0-1 : Superficies des vignes mères de cépages en France

Variétés	Production Antérieure	2014	2015	2016	2017	Total
Total	1295.04.79	53.25.35	53.39.13	36.02.71	10.11.93	1447.83.91
MERLOT N	154.91.61	3.10.55	1.30.60	1.14.93	1.00.11	161.47.80
SYRAH N	95.45.38	5.90.54	2.27.55	3.05.98	0.72.01	107.41.46
UGNI BLANC B	89.51.90	8.29.50	7.56.27	1.92.54	0.06.93	107.37.14
CABER.SAUVIGNON N	103.13.07	0.06.68	1.17.44	1.60.86	nd	105.98.05
CHARDONNAY B	93.60.26	4.64.30	2.12.88	4.17.02	0.22.19	104.76.65
GRENACHE N	89.64.09	3.38.80	1.76.06	2.06.56	1.26.69	98.12.20
SAUVIGNON B	72.19.99	0.74.89	6.56.03	4.12.50	1.13.42	84.76.83
PINOT NOIR N	78.41.21	1.65.61	1.76.95	0.73.60	nd	82.57.37
CABERNET FRANC N	38.66.05	0.05.01	1.64.42	1.13.26	nd	41.48.74
CINSAUT N	26.53.58	2.02.65	2.26.59	0.65.03	0.16.25	31.64.10

Surfaces mesurées en hectares (ha.a.ca).
(Adapté de : Les chiffres de la pépinière viticole 2017, France Agrimer)

Les propriétés de tolérance à des stress abiotiques tels que la chaleur, la sécheresse ou la lumière sont aussi des critères importants dans la sélection du cépage (Carvalho et al., 2016), tout comme la sensibilité aux maladies. Par exemple, il a été démontré que les génotypes de cépage présentent des sensibilités différentes au mildiou (Boso et al., 2010) et à l'eutypiose (Munkvold and Marois, 1995). Enfin, la phénologie est aussi prise en compte en fonction de l'environnement du cep (Parker et al., 2020). En France, comme en témoigne la superficie des vignes mères de cépages entre 2014 et 2017, les plus utilisés correspondent aux Merlot N, Syrah N, Ugni blanc B, Cabernet Sauvignon N, Chardonnay B, Grenache N, Sauvignon B, Pinot noir N, Cabernet franc N et Cinsaut N, représentant 54% de la superficie totale (Tableau 1).

b) Le choix du porte-greffe

Depuis la crise phylloxérique, *V. vinifera* est cultivée greffée sur des cultivars ou des hybrides de porte-greffes américains dans la grande majorité des vignobles mondiaux (Ollat et al., 2017). Cette maladie est causée par le ravageur américain *Daktulosphaira vitifoliae*, accidentellement introduit en Europe aux alentours de 1860, qui a induit en quelques décennies une crise sur l'ensemble des vignobles français. Ce puceron occasionne de sévères dégâts sur le système racinaire de *V. vinifera*, entrainant une baisse de rendement et de la qualité des baies, et pouvant conduire à la mort du cep. En piquant les racines, il perturbe l'absorption en eau et en nutriments des racines et accroit indirectement l'entrée de pathogènes fongiques (Powell, 2008). Le greffage de la vigne européenne sur des porte-greffes tolérants aux piqûres du puceron a permis de lutter efficacement contre ce ravageur. Les porte-greffes hybrides sont principalement issus de croisements entre *V. cordifolia*, *V. riparia*, *V. rupestris*,

V. berlandieri et même *V. vinifera* (Corso and Bonghi, 2014) (Figure 4). Certains d'entre eux sont obtenus par croisement de deux espèces de *Vitis* uniquement, tels que 1103P ou 3309C, quand d'autres ont eu recours à quatre fonds génétiques pour leur création, tels que le Nemadex (Table 2).

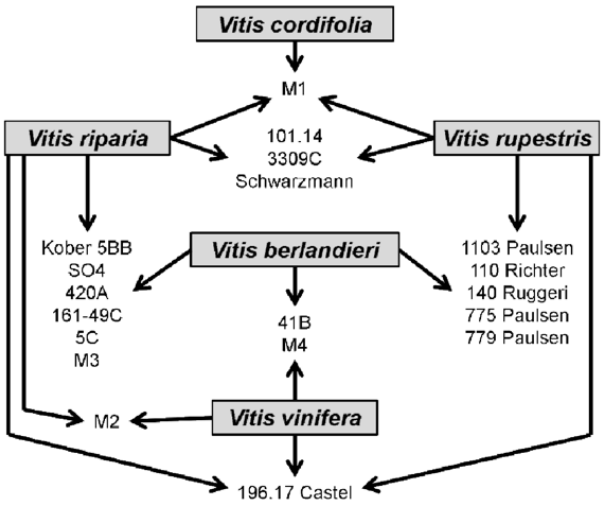


Figure 0-4 Croisement des espèces de Vitis pour l'obtention des hybrides de porte-greffe tolérants au phylloxera.
(Adapté de : Corso and Bonghi, 2014)

Tableau 0-2 : Origines génétiques et principales caractéristiques agronomiques des six porte-greffes étudiés dans la thèse.

Génotype	Croisement	Vigueur conférée	Tolérance au phylloxera radicicole	Tolérance aux nématodes	Tolérance à la sécheresse	Tolérance à la chlorose ferrique	Tolérance à l'acidité du sol
1103P	*V. berlandieri - V. rupestris*	Forte	Très forte	Faible à moyenne	Très forte	Moyenne	Moyenne
3309C	*V riparia - V rupestris*	Faible à moyenne	Très forte	Faible	Faible	Faible à moyenne	Moyenne
41B MGt	*V. vinifera - V. berlandieri*	Moyenne à forte	Moyenne à forte	Faible	Moyenne	Forte	/
Nemadex	hybride F1 *V. vinifera - M. rotundifolia* - 140 Ruggeri (*V. berlandieri - V. rupestris*)	Faible	Très forte	Très forte	Faible	Faible à moyenne	/
RGM	*V. riparia*	Très faible	Très forte	Moyenne à forte	Très faible	Très faible	Forte
SO4	*V. berlandieri - V. riparia*	Forte	Très forte	Moyenne à forte	Moyene à forte	Moyenne	Moyenne

Source : Pl@ntGrap

En jouant le rôle d'interface entre la composante édaphique du milieu et le greffon, le porte-greffe est un levier d'adaptation aux contraintes environnementales. En effet, ce dernier absorbe l'eau et les nutriments du sol, puis transfère ces ressources au greffon en échange des sucres issus de la photosynthèse. En plus de leur tolérance au phylloxera, les porte-greffes sont sélectionnés pour leurs performances agronomiques qui dépendent de la topologie du vignoble et des attentes des viticulteurs (Ollat et al., 2017). Il est aujourd'hui bien connu que le porte-greffe impacte profondément la nutrition minérale du greffon (Gautier et al., 2020), ainsi que sa physiologie (e.g., conductance stomatique,

photosynthèse, statut hydrique) et sa productivité (e.g., croissance, rendement et composition des fruits) (Zhang et al., 2016). Le choix du porte-greffe est souvent orienté en fonction de la vigueur qu'il confère au greffon (Tableau 2). Par exemple, 1103P est connu pour conférer une forte vigueur au greffon, contrairement à RGM dont la vigueur conférée est réduite (Rossdeutsch et al., 2021). De plus, les porte-greffes sont sélectionnés en fonction de la texture du sol (argile, sable, limon), ainsi que pour leur tolérance à divers stress d'origine biotique (e.g. Black-rot, maladie de Petri, galle du collet et les nématodes) ou abiotique (e.g. salinité, sécheresse, chlorose ferrique et l'acidité du sol) (Khan et al., 2020). Par exemple, RGM présente une forte résistance à certains nématodes mais une très faible tolérance à la chlorose ferrique, alors que l'inverse est observé pour ces deux caractéristiques chez 41B MGt (Tableau 2). Enfin, le dernier critère sera la compatibilité du génotype de porte-greffe avec le cépage souhaité lors du greffage. En effet, même si les raisons restent encore peu claires, certaines combinaisons présentent un faible taux de réussite au greffage (Loupit et al., 2023). En France, 89% de la superficie de vignes mères de porte-greffes est représentée par 110 Richter, SO4, 3309C, Fercal, 140 Ruggeri, 41B MGt, Gravesac, 101-14 M Gt, 1103P et Kober 5BB (Tableau 3).

Tableau 0-3 : Superficies des vignes mères de porte-greffes en France

Variétés	Production Antérieure	2014	2015	2016	Total
Total	1915.45.57	123.85.51	106.88.45	74.30.65	2220.50.18
110 RICHTER	324.17.71	27.11.72	25.44.91	11.40.76	388.15.10
S.O.4	336.71.97	18.07.77	15.04.13	15.15.89	384.99.76
3309 COUDERC	239.25.11	19.93.53	14.73.50	14.64.46	288.56.60
FERCAL	208.98.11	15.43.54	15.29.75	6.80.85	246.52.25
140 RUGGERI	135.02.23	9.43.60	8.04.21	6.39.54	158.89.58
41 B MGT.	121.98.59	7.05.05	9.97.47	0.78.75	139.79.86
GRAVESAC	102.03.61	5.25.98	3.00.35	3.18.33	113.48.27
101-14 MGT.	99.23.64	3.16.62	2.54.61	2.82.37	107.77.24
1103 PAULSEN	77.37.35	4.37.91	0.68.06	3.95.01	86.38.33
5 B B.	60.34.14	3.84.18	5.14.78	2.05.49	71.38.59

Surfaces mesurées en hectares (ha.a.ca).
(Adapté de : Les chiffres de la pépinière viticole 2017, France Agrimer)

4) Les enjeux de la filière viti-vinicole

a) L'adaptation aux contraintes biotiques dans un contexte d'agriculture durable

Tableau 0-4 : Liste non exhaustive des principaux agents pathogènes de la vigne

Agent pathogène	Impact sur la plante	Symptômes	Moyens de lutte
Botrytis cinerea	Champignon parasite des tissus verts et saprophytes des tissus morts ou sénescents, il s'établit sur l'intégralité des grappes et provoque la maladie de la « pourriture grise », affectant la conservation des baies et le résultat aromatique de leur vinification.		Mesures prophylactiques et application de fongicides
Erysphe necator	Champignon responsable de l'oïdium qui se traduit par l'apparition d'une poudre blanchâtre sur les organes infectés (principalement les feuilles et les tiges). La maladie entraine une diminution des rendements et de la qualité des baies.		Lutte chimique préventive avec application de fongicides (Cu^{2+})
Plasmopara viticola	Oomycète responsable du mildiou de la vigne, maladie aux épidémies fulgurantes occasionnant de grosses pertes de rendement. Elle se caractérise par des tâches grisâtres sur la surface adaxial de la feuille, ainsi que des tâches blanchâtres sur la face abaxial.		Application de fongicides cuivre (Cu^{2+})
Agrobacterium vitis	Agent causal de la galle du collet. Il forme des tumeurs au site d'infection pour augmenter le prélèvement des nutriments de son hôte et induit des nécroses sur les racines et les tissus non infectés.		Pas de traitement curatif mais le Cu^{2+} réduit la sévérité de la maladie
phytoplasme de la Flavescence dorée	Maladie causée par une bactérie sans paroi de la classe des Mollicutes, transmise par une cicadelle vectrice (*Scaphoideus titanus*) ou lors du greffage, entrainant un flétrissement des inflorescences, une décoloration des feuilles, une diminution du rendement et des qualités organoleptiques des baies et un empêchement de l'aoûtement des bois.		Destruction des plants infectés et utilisation d'insecticides contre les insectes vecteurs
GLRaV	Virus appartenant aux *Clostéroviridae*, responsables de la maladie de l'enroulement de la vigne. La transmission du virus est assurée par des insectes vecteurs tels que des cochenilles. Entraine des symptômes de rougissement et d'enroulement du limbe.		Utilisation d'insecticides contre les insectes vecteurs
Maladie du bois Esca *Phomopsis Eutypa*	Maladies causées par un complexe de champignons pathogènes. Se caractérisent par une décoloration et des lésions sur les feuilles lors de sa forme lente, avant d'induire la présence d'amadou, de nécroses brunes et de ponctuations noires exprimés dans le bois, pouvant conduire à la mort du cep.		Mesure prophylactiques

(Sources : Armijo et al., 2016 ; Fontaine et al., 2016 ; Euphytia.inrae)

Introduction

Le concept d'agriculture durable est apparu à la fin des années 1980. Il peut se définir comme « un système de production (animal ou végétal) qui satisfera les besoins humains en nourriture et en fibres ; améliorera la qualité de l'environnement ; utilisera efficacement les ressources non renouvelables, ainsi que celles de l'exploitation en intégrant les cycles et les contrôles biologiques naturels appropriés ; soutiendra la viabilité économique des exploitations agricoles ; et améliorera la qualité de vie des agriculteurs et de la société dans son ensemble » (Farm Bill, 1990). La viticulture est une filière qui a longtemps omis de respecter certains de ces principes. En effet, la vigne est soumise à de nombreux stress d'origine biotique, qui impactent les rendements, la qualité de la baie et peuvent conduire à la mort du cep. On retrouve parmi les principaux agents pathogènes de la vigne des champignons tels que *Botrytis cinerea* ou *Erysphe necator* ; des Oomycètes tels que *Plasmopara viticola* ; des bactéries tels que *Agrobacterium vitis* ou *Xyllela fastidiosa* ; ainsi que des virus tels que le *Grapevine Leaf Roll associated Viruses* (GLRaV) ou les *Grapevine Virus A and B* (GVA et GVB, respectivement) (Armijo et al., 2016) (Tableau 4). Il est aussi important de citer les champignons associés aux maladies du bois tels que *Phomopsis*, *Eutypa* et le complexe Esca dans les vignobles établis, ainsi que ceux provoquant la maladie de Petri ou le Black-rot chez les jeunes plants (Fontaine et al., 2016).

En agriculture conventionnelle, il existe des moyens de lutte chimique contre certains de ces agents pathogènes ou leurs insectes vecteurs (Tableau 4). Cependant, ces substances chimiques peuvent exercer une influence négative sur la santé de l'environnement, ainsi que sur celle du consommateur. Par exemple, les applications à long terme de fongicide à base de cuivre (hydroxyde ou sulfate de cuivre) pour lutter notamment contre le mildiou, ont conduit à une accumulation de cet élément dans les sols jusqu'à des niveaux toxiques dans plusieurs régions du monde. Par conséquent, la contamination des sols au cuivre, ainsi que le transfert subséquent de cet élément du sol vers la vigne, puis vers l'homme, suscite des préoccupations à l'échelle mondiale (Marastoni et al., 2019; Shirani Bidabadi and Sabbatini, 2020). Pour contrôler certaines maladies, notamment virales, les exploitations peuvent adopter une tolérance zéro à l'égard des insectes vecteurs. Par exemple, il existe des insecticides efficaces contre les cochenilles vectrices du GLRaV, tels que des néonicotinoïdes (Almeida et al., 2013). Cette dernière classe de molécules est la plus utilisée dans le monde en tant qu'insecticide. Or, les néonicotinoïdes peuvent entrainer la pollution de l'environnement en persistant et en s'accumulant dans les sols. Par sa haute toxicité pour la plupart des arthropodes, son action non sélective va à l'encontre des principes établis de la lutte intégrée contre les ravageurs. De plus, l'exposition des oiseaux et des mammifères à ces insecticides, au travers de résidus présents sur leur nourriture, peut représenter une cause de leur mortalité. En impactant un large éventail d'organismes

non ciblés, l'utilisation des néonicotinoïdes est présumée menaçante sur une série de services écosystémiques (Goulson, 2013). Dans la liste des produits phytosanitaires largement utilisés, on retrouve aussi des herbicides tels que le glyphosate, le flazasulfuron ou le glufosinate. Or, il a été démontré qu'en plus de modifier la physiologie de la vigne, ces derniers impactent la composition des micro-organismes du sol et réduisent la capacité de mycorhization des racines, pouvant donc présenter un risque sur l'environnement (Zaller et al., 2018). Même si la dangerosité du glyphosate pour l'homme reste encore débattue, des études réalisées *in vitro* et *in vivo* suggèrent un potentiel effet cancérigène. Il pourrait donc présenter un risque pour le consommateur par sa présence sous forme de traces dans les aliments, ainsi que pour le viticulteur lors de son épandage (Lacroix and Kurrasch, 2023).

Pour diminuer l'utilisation des produits phytosanitaires contre les agents pathogènes, l'adaptation de la viticulture repose sur la sélection ou la création de variétés de porte-greffe ou de greffon tolérantes ou résistantes aux ravageurs (Dewasme et al., 2023; Dry et al., 2019). De plus, des pratiques culturales sont étudiées pour limiter le développement des maladies, comme par exemple l'orientation des vignes ou l'espacement des rangs qui permettent de réduire la sévérité de l'oïdium (De Bem et al., 2016). L'utilisation de biostimulants ou d'agents de biocontrôle pour remplacer à termes les produits phytosanitaires est aussi prometteuse (Halleen et al., 2016; Monteiro et al., 2022). Enfin, il a récemment été proposé que la vigne pourrait tirer parti des bénéfices des micro-organismes de la rhizosphère pour parvenir à une viticulture plus durable (Cobos et al., 2022; Dries et al., 2021; Darriaut et al., 2022).

b) La viticulture face au changement climatique

Selon les rapports de l'IPCC (Intergovernmental Panel of Climate Change), le changement climatique est l'un des plus grands défis environnementaux auxquels l'humanité sera confrontée au cours des prochaines décennies. Il désigne l'altération du climat terrestre qui s'est développée à partir de la fin du XIXème siècle jusqu'à nos jours, résultant de l'augmentation des gaz à effet de serre émis dans l'atmosphère par les activités anthropiques, tels que le CO_2. Il se traduit par une augmentation de la température moyenne globale (+ 0,5 à 1°C au cours du XX^{ème} siècle et prévision de + 0,2 à 0,3°C par décennie), ainsi que par les phénomènes atmosphériques associés, tels que des épisodes de vagues de chaleur et de fortes sécheresses, des modifications du cycle de l'eau (inondation, fonte des glaces, montée des océans) et des schémas de circulation atmosphérique (provoquant des orages et des tempêtes) (Cataldo et al., 2023).

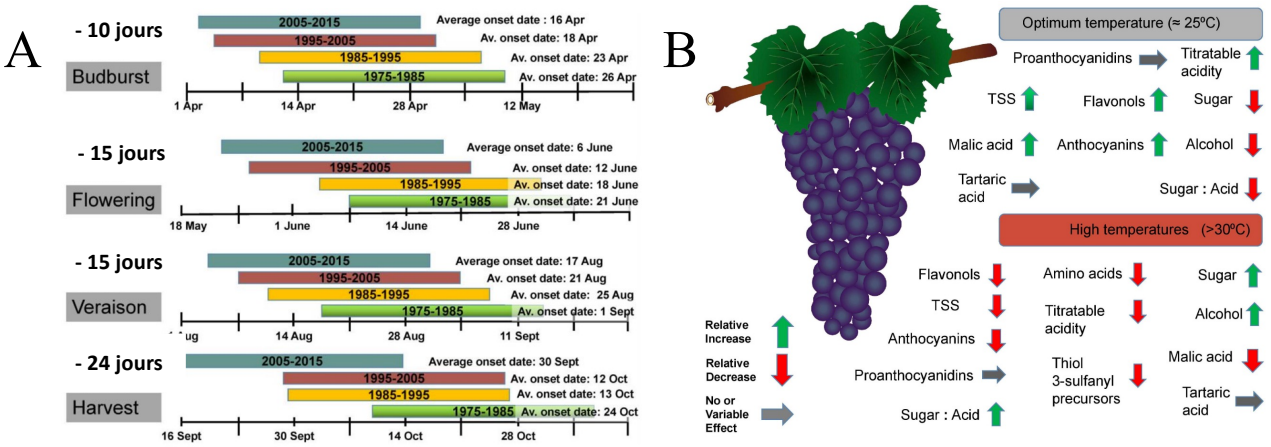


Figure 0-5 : Impact du changement climatique sur la phénologie de la vigne (A) et la composition de la baie (B).
(Adapté de : Venios et al., 2020)

Comme le climat est un élément fondamental du concept de « terroir », la viticulture n'échappe pas aux effets négatifs du changement climatique (Biasi et al., 2019). Ce dernier va principalement impacter le développement de la vigne en avançant la plupart des stades phénologiques. En effet, une étude réalisée en Allemagne sur quatre cépages a révélé un décalage moyen de 10 à 24 jours des principaux stades phénologiques du raisin entre 1975 er 2015 (Koch and Oehl, 2018) (Figure 5 A). Cela peut avoir un effet délétère sur le métabolisme des baies et la qualité du jus, paramètres influencés à la fois par le début et la durée des stades phénologiques (Fraga et al., 2012). De plus, un débourrement avancé peut exposer les vignes plus fréquemment au gel printanier dans certaines régions (Van Leeuwen et al., 2019). Les températures extrêmes de plus de 35°C peuvent impacter négativement la conductance stomatique et empêcher la transpiration de la plante, ainsi que la photosynthèse en perturbant les processus biochimiques actifs dans le chloroplaste (Venios et al., 2020). Les températures élevées perturbent aussi plusieurs voies métaboliques au sein de la baie, entraînant des altérations dans la biosynthèse de composés qui sont essentiels pour la qualité du moût de raisin (Venios et al., 2020, Cataldo et al., 2023). Par exemple, cela va réduire l'acidité et augmenter la teneur en sucre des baies, donnant des vins déséquilibrés compte tenu d'une teneur en alcool plus élevée et dépourvus de fraîcheur et de complexité aromatique (Figure 5 B). Les effets de la sécheresse sont connus pour inhiber la transpiration de la plante et altérer la composition moléculaire de la baie, et peuvent s'additionner à ceux causés par les fortes températures (Gambetta et al., 2020). Diverses solutions sont envisagées à court et moyen terme pour s'adapter aux contraintes exercées par le changement climatique. Il est par exemple possible de modifier les pratiques culturales sur la canopée de la vigne (éclaircissement avant floraison, coupe sévère des apex ou effeuillage parcimonieux),

pratiquer l'irrigation ou travailler le sol pour augmenter sa capacité de rétention en l'eau, augmenter la hauteur des troncs ou retarder la taille pour ralentir la maturation des raisins. À long terme, il est envisagé de délocaliser les vignobles dans des régions plus propices ou de sélectionner des cultivars ou des porte-greffes adaptés (Bucur and Dejeu, 2022). Récemment, il a été proposé que le microbiome du sol de la vigne pourrait offrir de nouvelles solutions d'ingénierie pour lutter contre les problèmes liés au changement climatique (Darriaut et al., 2022b). Dans ce contexte, les champignons mycorhiziens arbusculaires (CMA) ou les Plant Growth Promoting Rhizobacteria (PGPR) représentent des ressources prometteuses d'adaptation (Shah et al., 2021; Trouvelot et al., 2015).

c) Les attentes des consommateurs

Le premier argument de choix pour un consommateur de vin porte sur les qualités organoleptiques du produit. Or, la fabrication du vin implique de multiples facteurs regroupés dans le terme de « terroir ». Il englobe dans sa définition l'emplacement et l'environnement du vignoble, la qualité des sols qui le composent, le choix des cépages, ainsi que les pratiques viticoles et vinicoles associées. Chacun de ces facteurs influence la composition chimique et les caractéristiques du vin, laissant apparaitre le concept de « typicité ». La typicité d'un vin est la résultante d'une juxtaposition de traits uniques qui définissent une classe de vin ayant des aspects communs liés au terroir, impliquant des dimensions biophysiques et humaines rendant les vins reconnaissables et, en théorie, incapables d'être reproduits sur un autre territoire (Souza Gonzaga et al., 2021). La France a été pionnière dans l'adoption d'un système destiné à protéger légalement l'authenticité de ces produits grâce à la création en 1935 de l'Appellation d'Origine Contrôlée (AOC). En plus des caractéristiques organoleptiques typiques d'un vin, les informations sur l'origine du produit sont perçues comme un gage de qualité par le consommateur, ayant un impact positif sur le prix des bouteilles. Il est donc important pour l'industrie de comprendre les facteurs impliqués dans la typicité du vin afin d'être en mesure de gérer et conserver ses caractéristiques. Il est aujourd'hui admis que les microbiomes du sol et de la plante sont des facteurs déterminants dans la définition d'un terroir ou de la typicité des vins (Belda et al., 2017; Gobbi et al., 2022; Mezzasalma et al., 2017). En effet, le microbiome de la vigne influence son développement et donc le métabolome de ses produits (e.g. raisin et vin). De plus, les levures naturellement présentes sur les raisins dans le vignoble, dans l'environnement de la cave ou inoculées avant le processus de fermentation ont un impact significatif sur les caractéristiques finales des vins (Bettenfeld et al., 2022). Il est donc crucial de comprendre le rôle des micro-organismes dans l'ensemble du processus de vinification, en étudiant leurs niches écologiques, la dynamique de leurs

populations, leur rôle sur la santé de la vigne, ainsi que leur impact sur le métabolome du vin (Belda et al., 2017).

La sensibilisation croissante de l'opinion publique sur le lien entre l'alimentation et la santé, ainsi que sur les effets négatifs de la viticulture conventionnelle sur l'environnent, incite les consommateurs à être plus attentifs dans le choix des produits alimentaires qu'ils consomment au quotidien (Bazoche et al., 2008). Les consommateurs vont alors chercher des produits présentant de meilleurs qualités organoleptiques (e.g. goût, taux de sucre et acidité) et nutritionnelles (e.g. minéraux et vitamines) (Noceto et al., 2021). Ce phénomène va aussi se traduire par un gain d'intérêt envers des vins présentant des certifications durables et écologiques, tels que des vins naturels, organiques, et biodynamiques ou sans sulfites (González and Parga-Dans, 2020). Il est donc nécessaire de mener une viticulture plus durable, sans pour autant impacter les rendements ou la qualité des vins, notamment dans un contexte de changement climatique. Le développement de méthodes visant à encourager la prolifération de populations microbiennes bénéfiques du sol, pour améliorer le développement de la vigne (e.g. nutrition minérale et lutte contre les maladies), ainsi que les qualités nutritionnelles et organoleptiques de ces produits, offre une perspective intéressante pour répondre aux exigences des consommateurs (Darriaut et al., 2022; Dries et al., 2021; Noceto et al., 2021).

II) Le microbiote du système racinaire et son rôle dans la croissance de la vigne et l'adaptation à l'environnement

Dans cette partie, nous verrons que le sol viticole comporte une multitude de microorganismes qui interagissent avec le système racinaire des plantes et influencent leur développement. Nous discuterons ensuite des microorganismes bénéfiques du sol qui semblent prometteurs dans l'adaptation de la viticulture aux problématiques actuelles, c'est-à-dire des Plant-Growth Promoting Rhizobacteria (PGPR) et des champignons mycorhiziens arbusculaires (CMA). Enfin, nous ferons l'état de l'art des méthodologies employées pour caractériser la composition taxonomique et le rôle des communautés microbiennes du système racinaire de la vigne.

1) Le sol viticole : un réservoir de micro-organismes aux fonctions multiples

Au sein des sols viticoles, il existe une multitude de micro-organismes tels que les bactéries, les archées, les champignons, les protistes ou encore les virus (Darriaut et al., 2022b). Une étude récente menée sur 200 parcelles viticoles, réparties dans 13 pays sur les 5 continents, a montré que les taxons procaryotes les plus largement représentés dans le sol correspondaient aux phyla bactériens des *Proteobacteria*, des *Actinobacteria* et des *Acidobacteria*, ainsi qu'à la classe des *Nitrososphaera* pour les archées (Gobbi et al., 2022). Le phyla des *Proteobacteria* est impliqué dans un grand nombre de fonctions relatives aux cycles du carbone (C), du souffre (S) et de l'azote (N). Il regroupe par exemple pour ce dernier élément des bactéries bénéfiques du sol aux propriétés fixatrices d'azote atmosphérique, d'oxydation de l'ammoniac ou de dégradation de la cellulose (Zhang et al., 2022). Les *Actinobacteria* sont des bactéries filamenteuses productrices d'une grande source de métabolites secondaires, de protéines, d'inhibiteurs enzymatiques et d'antibiotiques dans les sols. Elles jouent un rôle dans la décomposition des substances organiques et sont également bénéfiques pour les plantes en stimulant leur croissance et en jouant le rôle d'agent de biocontrôle (Hazarika and Thakur, 2020). Le phyla des *Acidobacteria* est moins connu à cause de la difficulté de culture de ses bactéries. Cependant, les techniques modernes d'édition génomique laissent entrevoir un intérêt bénéfique de certaines souches d'*Acidobacteria*, grâce à la présence de gènes impliqués dans le métabolisme du carbone (C), de l'azote (N) et du souffre (Su), ainsi que dans des processus environnementaux (Kalam et al., 2020). Enfin, les *Nitrososphaera* rassemblent des archées bénéfiques du sol, interagissant dans le cycle de l'azote, notamment grâce à leur capacité d'oxydation de l'ammoniac (Tourna et al., 2011).

La communauté fongique des sols viticoles est dominée par les champignons des genres *Solicoccozyma*, *Mortierella* et *Alternaria* (Gobbi et al., 2022). Le genre *Solicoccozyma* appartient au phylum des *Basidiomycota* et rassemble des levures du sol. Certaines souches présentent des caractéristiques bénéfiques sur le développement des plantes et ont été classées en tant que Plant Growth-Promoting Fungi (PGPF) (Stosiek et al., 2019). Les *Mortierella* sont des champignons appartenant au phylum des *Mucoromycota* et sont capables de coloniser le système racinaire. Certaines souches présentent aussi des caractéristiques de PGPF (Ozimek and Hanaka, 2020). Enfin, le genre *Alternaria* appartient au phylum des *Ascomycota* et contient des espèces néfastes pour les plantes en incluant des organismes saprotrophes, endophytes des tissus végétaux et pathogènes (Lou et al., 2013).

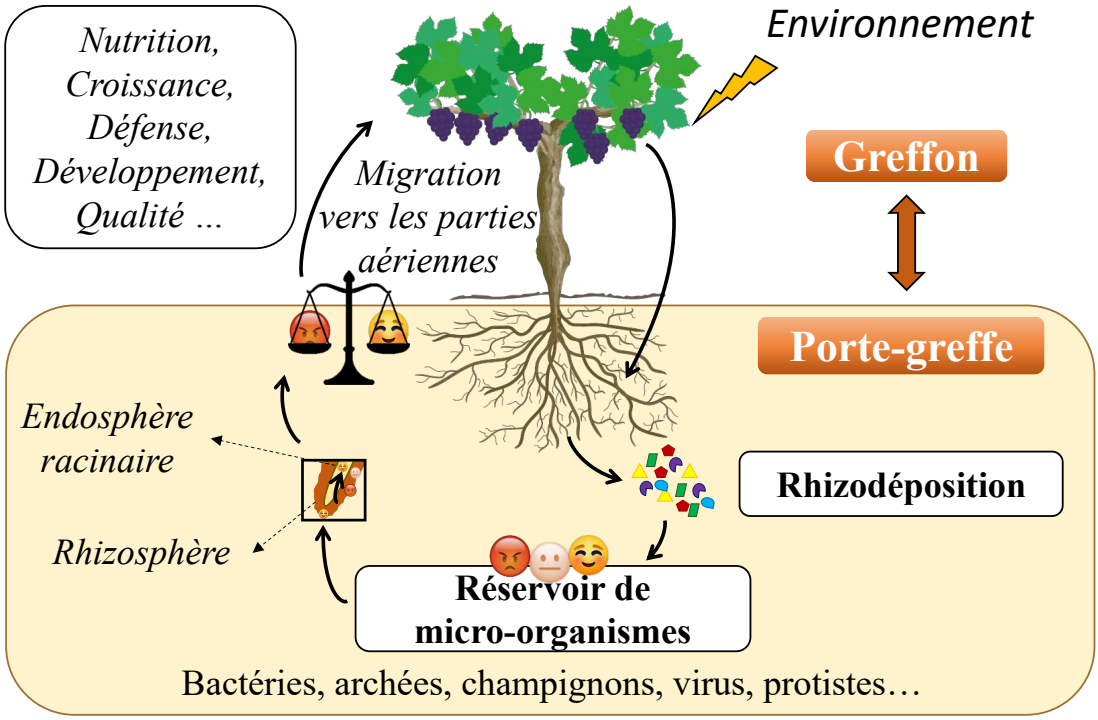


Figure 0-6 : Interactions entre le plant de vigne et le microbiote du sol.

Au vignoble, le sol joue le rôle de réservoir des micro-organismes qui composeront le microbiote de la plante (Figure 6). Le microbiote est défini par l'ensemble des micro-organismes vivant en communautés complexes dans un environnement spécifique, appelé microbiome, chez un hôte ou une matrice d'origine biologique. Ces micro-organismes peuvent être présents sans impact sur leur hôte (i.e. commensalisme) ou mener des interactions étroites avec lui (i.e. mutualisme, parasitisme). Le microbiome a récemment été redéfini comme le microbiote et son théâtre d'activité qui combine des éléments structurels (e.g. protéines, peptides, lipides, polysaccaride) et des métabolites (e.g. molécules de signalisation, toxines, molécules organiques) microbiens, ainsi que les

conditions environnementales (Berg et al., 2020). Il a été démontré chez la vigne que la vaste majorité des taxons microbiens associés aux différents compartiments (rhizosphère, endosphère racinaire, grappes, feuilles et fleurs) sont originaires du sol (Zarraonaindia et al., 2015). Certains micro-organismes sont attirés par les racines et se retrouvent enrichis dans la zone rhizosphérique, c'est-à-dire la zone de sol collée aux racines. Parmi eux, des micro-organismes bénéfiques, mais aussi pathogènes, peuvent pénétrer dans les racines et devenir endophytes racinaires ou être transportés *via* le système vasculaire vers les parties aériennes de l'hôte, représentant respectivement 28 et 4% des micro-organismes du sol chez la vigne (Bettenfeld et al., 2022). Le système racinaire constitue ainsi un point d'entrée pour les micro-organismes du sol par les jonctions intercellulaires du rhizoderme où émergent les poils absorbants ou les racines latérales, ainsi que les zones de blessures. Par la variété de rôles évoqués précédemment, les micro-organismes du sol impactent, directement ou indirectement, la physiologie (e.g. croissance, nutrition, défense) de la plante de différentes manières (bénéfique, neutre ou néfaste), depuis la rhizosphère jusqu'à la phyllosphère. En fonction de l'environnement et de la génétique de la plante (i.e. porte-greffe et greffon), les racines influencent la composition taxonomique du microbiome de la rhizosphère au travers d'un mécanisme appelé la rhizodéposition, processus que nous détaillerons plus tard dans l'introduction (Ma et al., 2022).

2) Des micro-organismes prometteurs pour l'adaptation de la viticulture

a) Les Plant Growth Promoting Rhizobacteria (PGPR) améliorent la croissance du plant par divers mécanismes

De plus en plus d'études rapportent les effets bénéfiques de certaines bactéries du sol, qui en colonisant la rhizosphère ou l'endosphere des racines, améliorent la croissance des plantes, ainsi que leur défense vis-à-vis des agents pathogènes. Ces bactéries pourraient donc jouer le rôle de levier dans la mise en place d'une agriculture plus durable, ainsi que dans l'adaptation au changement climatique, y compris chez la vigne (Darriaut et al., 2022b; Duan et al., 2021). Ces bactéries bénéfiques sont regroupées sous le terme générique de Plant Growth Promoting Rhizobacteria (PGPR) et présentent divers mécanismes pour améliorer le développement de la plante (Figure 7).

Certains PGPR influencent positivement la disponibilité et l'absorption des minéraux par la plante (Shah et al., 2021), qui sont essentiels pour le maintien de son métabolisme (Shrivastaz et al., 2020). L'azote (N) est un macro-élément très important par son implication dans la plupart des processus physiologiques, tels que la photosynthèse, ou la constitution des acides nucléiques et des protéines. Certains taxons bactériens permettent d'enrichir les sols en N, directement grâce à la fixation

de l'azote atmosphérique, ou indirectement en aidant les bactéries fixatrices d'azote grâce à leurs sécrétions. Parmi les bactéries fixatrices d'azote, certaines vont établir une symbiose avec la plante telles que celles du genre *Rhizobium*, tandis que d'autres vont rester autonomes. Le phosphore (P) est aussi très important pour la plante car il est impliqué dans la respiration et la photosynthèse, ainsi que la constitution des acides nucléiques, des sucres et des lipides. D'autres bactéries vont améliorer l'absorption de cet élément par la plante en transformant des formes non assimilables par le système racinaire en formes assimilables ($H_2PO_4^-$ et HPO_4^{2-}). Ce phénomène peut être réalisé grâce à la solubilisation du P inorganique, ainsi que la minéralisation du P organique. Le potassium (K) est impliqué dans la régulation du potentiel osmotique des cellules végétales, ainsi que l'activation d'enzymes impliquées dans la photosynthèse et la respiration. Certains PGPR sont aussi capables de solubiliser le K dans les sols grâce à la sécrétion d'acides organiques qui vont dégrader et chélater les minéraux silicatés. Le fer (Fe) est un élément vital pour la plante car il intervient entre autres dans le transfert d'électrons lors des réactions d'oxydoréductions de divers processus métaboliques. Certains PGPR permettent de séquestrer cet élément dans le sol en libérant des composés de faible poids moléculaire, appelés sidérophores, capables de lier les ions ferriques, et par conséquent de les rendre facilement assimilables par les cellules végétales. Enfin, le zinc (Zn) est un microélément important impliqué dans l'activation de certaines enzymes du métabolisme de l'auxine, des sucres, ainsi que la synthèse des protéines, des lipides et des acides aminés. Il a été reporté que certains PGPR peuvent solubiliser des formes non assimilables de Zn dans le sol grâce à la sécrétion d'acides organiques comme pour le K. Chez la vigne, l'inoculation de plants avec des bactéries présentant des activités PGPR (fixation de l'azote atmosphérique, solubilisation du phosphore ou productrice de sidérophore), seules ou combinées, a montré une augmentation significative de la teneur en nutriment des feuilles, associée à une stimulation de la croissance générale des plantes (Erdogan et al., 2018; Sabir et al., 2012).

Les phytohormones sont de petites molécules qui jouent un rôle essentiel dans la régulation de la croissance et du développement des plantes, ainsi que dans la tolérance au stress pour favoriser la survie et l'acclimatation aux contraintes environnementales (Fahad et al., 2015). Des études réalisées chez d'autres modèles végétaux ont démontré que certaines souches de bactéries (e.g. *Kocuria turfanensis* 2M4, *Pseudomonas fluorescens* G20-18, *Leifsonia soli* SE134) du sol étaient capables de sécréter des phytohormones telles que la classe d'auxine correspondant à l'acide indole-3-acétique (IAA) (Goswami et al., 2014), les cytokinines (Mekureyaw et al., 2022) ou les gibbérellines (Kang et al., 2014). En s'additionnant avec les hormones de la plante, les analogues produits par ces bactéries symbiotiques du système racinaire (i.e. rhizosphérique, endophyte) promeuvent différentes réactions

bénéfiques pour la plante tels que la germination des graines, le développement du système racinaire, le développement et l'élaboration des tissus vasculaires, l'élongation des pousses, la floraison et la croissance globale de la plante (Shah et al., 2021). Certaines souches productrices de phytohormones, tels que l'IAA, ont déjà été isolées à partir du système racinaire de la vigne (Zhao et al., 2016). Enfin, l'inoculation de plants de vigne avec des PGPR présentant ces caractéristiques a montré une amélioration du développement général du plant de vigne après inoculation (Sabir et al., 2012).

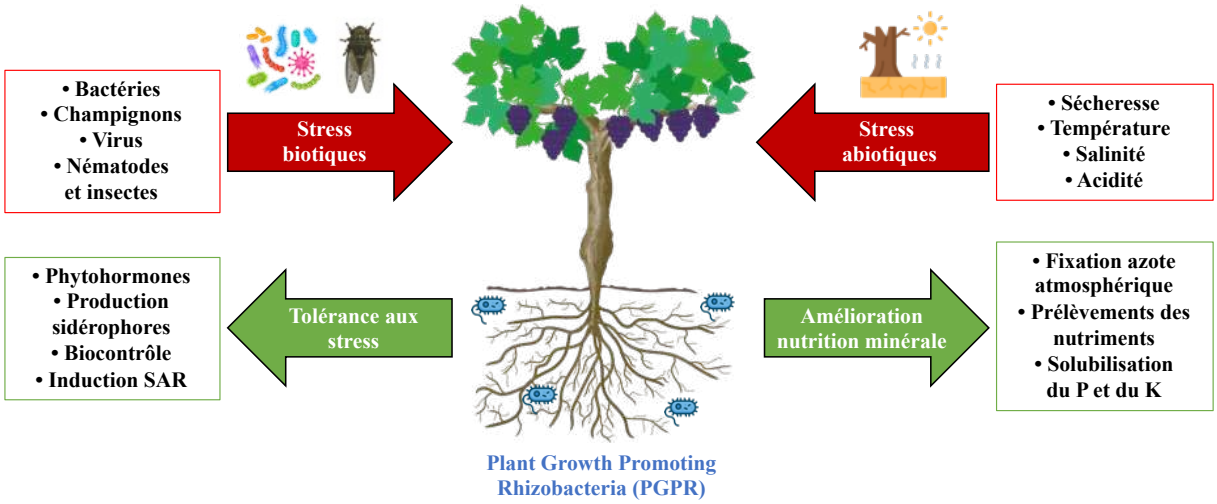


Figure 0-7 : Les bénéfices des PGPR face aux problématiques de la viticulture.
(Adapté de : Shah et al., 2021)

Parmi les PGPR, se trouvent aussi des agents de biocontrôle, permettant la protection des plantes contre divers agents pathogènes (e.g. bactéries, champignons, virus ou insectes). Outre l'induction des mécanismes de défense de la plante, certains PGPR permettent de lutter contre les agents pathogènes *via* l'antibiose, l'hyper-parasitisme, la sécrétion de composés antimicrobiens (e.g. cyanure d'hydrogène), ou d'enzymes de défense tels que l'1-aminocyclopropane-1-carboxylate (ACC) désaminase. Cette enzyme réduit la production d'éthylène par la plante en hydrolysant son substrat, l'ACC, pour former de l'α-cétobutyrate et de l'ammoniaque. Or, l'éthylène est une hormone produite en réponse aux stress qui peut avoir un impact négatif sur le développement et la croissance de la plante, pouvant conduire à sa mort, lorsqu'elle est accumulée en excès (Orozco-Mosqueda et al., 2020). D'autres PGPR réduisent la présence d'agents pathogènes indirectement, en créant une compétition pour l'accès aux nutriments et aux niches écologiques, en interférant avec la signalisation qu'ils utilisent (i.e. quorum sensing), ainsi que par l'induction de la résistance systémique de la plante (Compant et al., 2013; Shah et al., 2021). Chez la vigne, il a déjà été démontré que certaines bactéries rhizosphériques pourraient être utilisées dans la lutte contre certains agents pathogènes, notamment contre les champignons associés aux maladies du bois (Cobos et al., 2022). Par exemple, l'utilisation

d'isolats d'*Actinobacteria* présentant des activités antifongiques a permis de réduire significativement les niveaux d'infection de la vigne aux espèces du genre *Dactylonectria* et *Ilyonectria*, ainsi qu'à *Phaeomoniella chlamydospora,* et *Phaeoacremonium minimum*, et par conséquent le taux de mortalité de plants greffés en pépinière (Álvarez-Pérez et al., 2017).

Grâce à la production d'hormones, l'amélioration de la nutrition minérale et leurs rôles d'agent de biocontrôle, les PGPR procurent des bénéfices chez la plante, permettant une meilleure tolérance aux contraintes abiotiques, ainsi qu'une amélioration de sa défense vis-à-vis des agents pathogènes. Il est intéressant de noter ici que beaucoup de caractéristiques des PGPR sont retrouvées chez certains champignons du sol. Ces derniers sont alors qualifiés de Plant Growth-Promoting Fungi (PGPF) (Hossain et al., 2017). Parmi eux, on retrouve par exemple certaines souches des genres *Solicoccozyma* (Stosiek et al., 2019) et *Mortirellomycota* (Ozimek and Hanaka, 2020), ainsi que le groupe des champignons mycorhiziens à arbuscules (CMAs) (Trouvelot et al., 2015), particulièrement ciblés dans le cadre de ce travail.

b) Le cas des champignons mycorhiziens arbusculaires (CMA)

L'effet des champignons mycorhiziens arbusculaires (CMA) sur la réduction possible de la quantité de produits phytosanitaires et sur l'adaptation au changement climatique en viticulture a été discuté par de nombreux auteurs (Aguilera et al., 2022; Darriaut et al., 2022; Torres et al., 2018; Trouvelot et al., 2015). La symbiose mycorhizienne à arbuscules est probablement l'interaction la plus répandue entre les plantes et les micro-organismes. En effet, plus de 80% des espèces de plantes terrestres, vivants dans un large spectre d'environnements, sont capables d'établir cette association, incluant la vigne (Wang et al., 2021). La découverte d'hyphes et de spores fossilisés semblables à ceux des CMA actuels laisse entrevoir que cette symbiose serait apparue il y a 460 millions d'années, jouant un rôle clé dans l'évolution des plantes terrestres (Redecker et al., 2000). Depuis la première description des CMA en 1845 par Tulasne et Tulasne, plus de 260 espèces de CMA ont été découvertes et ce chiffre est continuellement en augmentation (Likar and Regvar, 2017). Toutes ces espèces sont regroupées dans la sous-division fongique des Glomeromycètes. Même si la phylogénie des CMA reste aujourd'hui débattue à cause de la publication d'un grand nombre de taxons qui a donné lieu à des schémas systémiques contradictoires, Redecker et al. (2013) propose une classification consensus des espèces en quatre ordres : *Paraglomerales*, *Archaeosporales*, *Glomerales* et *Diversisporales*, subdivisé en onze familles (Figure 8).

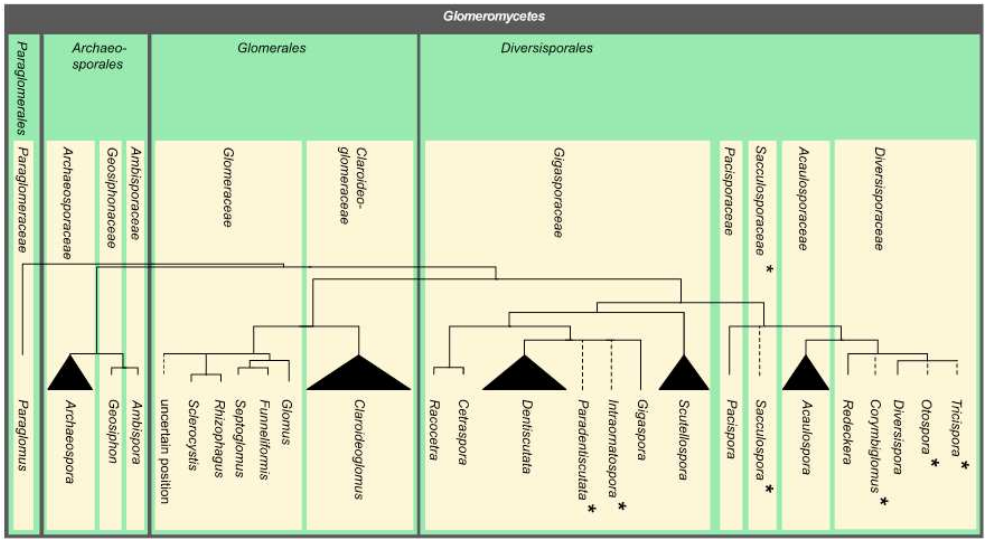


Figure 0-8 : Proposition de classification taxonomique des CMA basée sur l'homologie de séquences codantes la petite sous-unité du ribosome (SSU).
Les lignes pointillées indiquent les genres dont la position est incertaine, les astérisques représentent les taxons dont les preuves ne sont pas suffisantes pour pouvoir les exclure, les triangles inversés indiquent les taxons déjà rejetés dans des publications antérieures. (Adapté de : Redecker et al., 2013)

Les CMA sont des biotrophes qui colonisent l'endosphere racinaire et améliorent les nutritions hydrique et minérales des plantes, principalement en phosphore (P) et en azote (N), en échange de 4 à 23% des sucres issus de la photosynthèse (Salmeron-Santiago et al., 2021). Lors de la colonisation, les CMA vont former des structures appelées arbuscules dans les cellules corticales des racines, délimitées par une membrane péri-arbusculaire. Les arbuscules vont jouer le rôle de sites d'échanges entre les deux symbiotes. L'amélioration des prélèvements minéraux de la plante est attribuée à une augmentation de la surface d'exploration du sol grâce à la prolifération des hyphes extra-radiculaires. Les minéraux sont absorbés par deux voies indépendantes, celle de l'absorption racinaire classique, ainsi que celle formée par le champignon, qui transfèrera ensuite les nutriments aux cellules hôtes colonisées dans l'espace péri-arbusculaire (Schreiner, 2005). La principale forme absorbée par les plantes est le phosphate inorganique Pi (HPO_4^{2-}). La lente transformation des formes organiques en Pi par les micro-organismes du sol, ainsi que sa faible diffusion dans les sols, peut créer une zone de déplétion en Pi autour des racines, pouvant impacter la physiologie de la plante. Chez les racines mycorhizées, le réseau d'hyphes extra-radiculaires permet d'augmenter l'accès au Pi dans les sols (Trouvelot et al., 2015). Les CMA peuvent aussi jouer un rôle important dans l'absorption de N dans le sol. En effet, ces derniers sont capables d'assimiler différentes formes de N, inorganiques (NO_3^- ou le NH_4^+) et organiques, ainsi que de les convertir en arginine pour les transporter sous cette forme jusqu'à la plante (Wipf et al., 2019). Même si les études sur l'absorption des autres micro/macro-

éléments par les CMA sont rares chez la vigne, il est suggéré que la symbiose mycorhizienne peut augmenter l'absorption de certains d'entre eux (e.g. K, Ca, Mg, Fe et B) (Schreiner, 2005; Trouvelot et al., 2015).

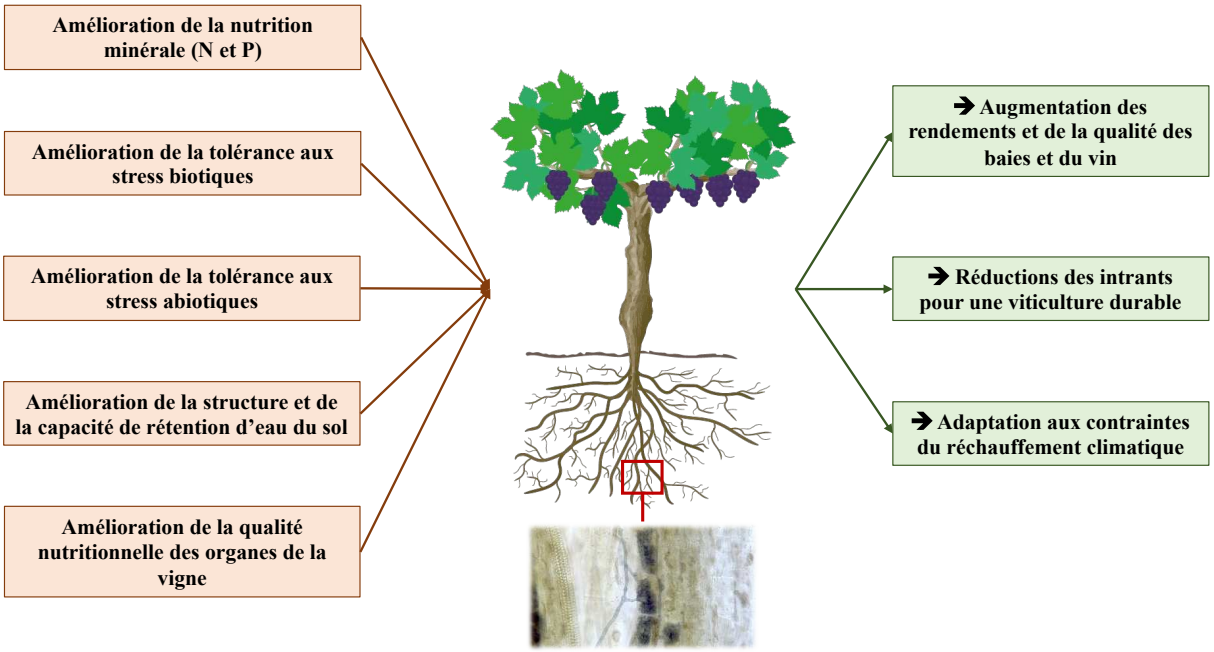


Figure 0-9 : Les bénéfices des CMA pour la vigne face aux problématiques de la viticulture. (Adapté de : Trouvelot et al., 2015)

En améliorant la nutrition hydrique et minérale, l'interaction symbiotique avec les CMA améliore la santé et la tolérance aux contraintes environnementales de la vigne (Figure 9). Des effets positifs des CMA ont été rapportés sur la tolérance de la vigne à divers stress d'ordre abiotique tels que le stress hydrique, la chlorose ferrique induite dans les sols calcaires, la salinité ou l'accumulation de métaux lourds dans le sol (Likar and Regvar, 2017; Trouvelot et al., 2015). Des effets positifs de l'addition de CMA vis-à-vis de la tolérance aux stress d'origine biotique ont aussi été démontrés chez la vigne, comme par exemple aux maladies virales (Gaši et al., 2023) ou à la maladie du pied noir (Moukarzel et al., 2022). Cela s'explique par l'amélioration de la santé générale du plant mycorhizé, la compétition exercée par les CMA envers les agents pathogènes dans la rhizosphère (Aguilera et al., 2022), la mise en place de la résistance induite par les CMA appelée MIR (Mycorrhiza-Induced Resistance) (Cameron et al., 2013), ainsi que par l'induction de la résistance systémique acquise de la plante (Trouvelot et al., 2015). Grâce leur réseau extra-mycélien pouvant mesurer jusqu'à 30 mètres de long par gramme de sol, ainsi que la sécrétion abondante de glomaline (glycoprotéine aux propriétés collantes), les CMA améliorent la structure et la rétention d'eau des sols (Wilson et al., 2009; Rillig et al., 2015). Enfin, il est suggéré que les CMA parviennent à améliorer les qualités nutritionnelles des

produits issus de la vigne, notamment des baies, et par conséquent du vin (Noceto et al., 2021; Torres et al., 2018).

3) Des méthodologies pour étudier le microbiote de la vigne

a) Les approches de culture *in vitro* sur milieux nutritifs

Traditionnellement, l'étude des micro-organismes est basée sur l'utilisation de la culture *in vitro*. Cette technique, encore appelée « cultivable », permet de quantifier et d'identifier les micro-organismes présents dans un environnement donné, capables de pousser sur le milieu de culture utilisé. Elle repose sur l'étalement d'un échantillon provenant d'un environnement quelconque (e.g. sol brut, rhizosphère ou racines), dilué ou non dans de l'eau stérile, sur un milieu de culture solide, afin de multiplier *in vitro* les micro-organismes associés. Après une étape d'incubation dans des conditions adaptées aux micro-organismes ciblés (e.g. température, lumière, oxygénation), leur quantification est alors opérée en comptant le nombre de colonies macroscopiquement détectables, appelées unités formant colonies (UFC) (Figure 10). Comme ces dernières sont obtenues à partir d'échantillons frais, le nombre d'UFC est ensuite exprimé après normalisation avec le poids sec de l'échantillon, afin de réduire la variabilité dû à sa teneur en eau.

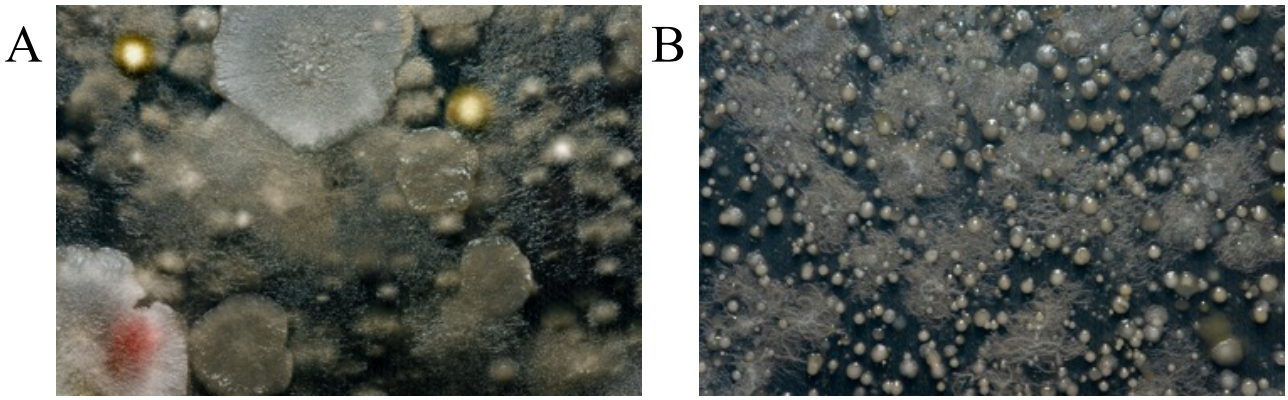


Figure 0-10 : Champignons et bactéries rhizosphériques
Photographies (échelle 1 : 1) sur fond noir de champignons (A) et de bactéries (B) après une semaine de culture sur les milieux PDA (Potato Dextrose Agar) et R2A (Reasoner's 2A Agar), ©Vincent Lailheugue.

Pour assurer leur développement, les micro-organismes utilisent des macroéléments (C, O, H, N, S, P, K, Ca, Mg and Fe) qui entrent dans la synthèse de biomolécules essentielles (e.g. sucres, lipides, protéines et les acides nucléiques) ou jouent le rôle de cations dans diverses fonctions au sein des cellules. Ils ont aussi besoin de microéléments (Mn, Zn, Co, Mo, Ni et Cu) pour constituer les

enzymes ou des cofacteurs, ainsi que des facteurs de croissance, généralement sous la forme d'acides organiques (Basu et al., 2015). En fonction de sa composition, le milieu va donc drastiquement impacter la culture des différentes communautés microbiennes. Pour celle des bactéries, il est possible d'utiliser des milieux simples dont la composition chimique exacte est connue (e.g. gélose nutritive), des milieux synthétiques contenant les ingrédients minimums pour assurer la croissance (e.g. Davis and Mingioli), ou encore des milieux complexes dont la composition exacte n'est pas connue (e.g. bouillon de soja). Pour la culture des champignons, il est possible d'utiliser des milieux naturels composés de substrats biologiques tels que des composés issus des plantes (e.g. gélose de farine de maïs ou milieu PDA), ainsi que des milieux synthétiques contenant des ingrédients connus (e.g. gélose de Czapek-Do) (Basu et al., 2015). Chez la vigne, il a été reporté que les milieux R2A (Reasoner's 2A Agar) et PDA (Potato Dextrose Agar) sont adaptés à la culture respective des bactéries et des champignons du sol (Darriaut et al., 2021). En plus de pouvoir évaluer la quantité de micro-organismes présents dans un environnement, les approches de cultivable permettent d'isoler des colonies. Il est alors possible de les identifier par une analyse au MALDI-TOF-MS ou en les séquençant, ainsi que de cribler de potentielles fonctions bénéfiques pour la plante *in vitro* ou *in silico* (Darriaut et al., 2022a; Marasco et al., 2018; Duan et al., 2021). Le principal problème de ces approches est que près de 99% de tous les micro-organismes restent encore incultivables. Cela s'explique par l'absence d'une variabilité suffisante de composition des milieux, ainsi que par la complexité de reproduction des conditions environnementales exactes en laboratoire (Basu et al., 2015).

b) Les méthodes basées sur la biologie moléculaire

Le développement des techniques de biologie moléculaire au cours des dernières décennies ont permis de révolutionner l'identification et la quantification des micro-organismes. Le recours à la PCR (Polymerase Chain Reaction) ou la PCR quantitative (qPCR) a par exemple permis de diagnostiquer et de quantifier certains agents pathogènes présents dans les différents compartiments de la vigne. Ainsi, des amorces ont été conçues pour détecter *Plasmapora viticola* dans les feuilles (Si Ammour et al., 2020), *Phaeomoniella chlamydospora* and *Phaeoacremonium aleophilum* dans le bois (Pouzoulet et al., 2013), ainsi que les nématodes (Blanco-Pérez et al., 2020) ou *Daktulosphaira vitifoliae* (Giblot-Ducray et al., 2016) dans les sols. Récemment, Darriaut et al. (2021) ont utilisé des amorces ciblant les gènes codant l'ARN ribosomique (ARNr) 16S des bactéries ou des archées, ainsi que le gène codant l'ARNr 18S des champignons, pour quantifier leurs populations dans les sols. Il est aussi possible d'utiliser la RT-qPCR (Reverse transcription-qPCR) pour faire du diagnostic chez la vigne, notamment pour quantifier les maladies virales tels que le GLRaV-3 (Diaz-Lara et al., 2018) ou le GFLV (Krebelj

et al., 2015). Enfin ces techniques peuvent aussi être utilisées pour quantifier des organismes symbiotiques tels que les CMA dans les racines (Bodenhausen, 2021; Duret et al., 2022).

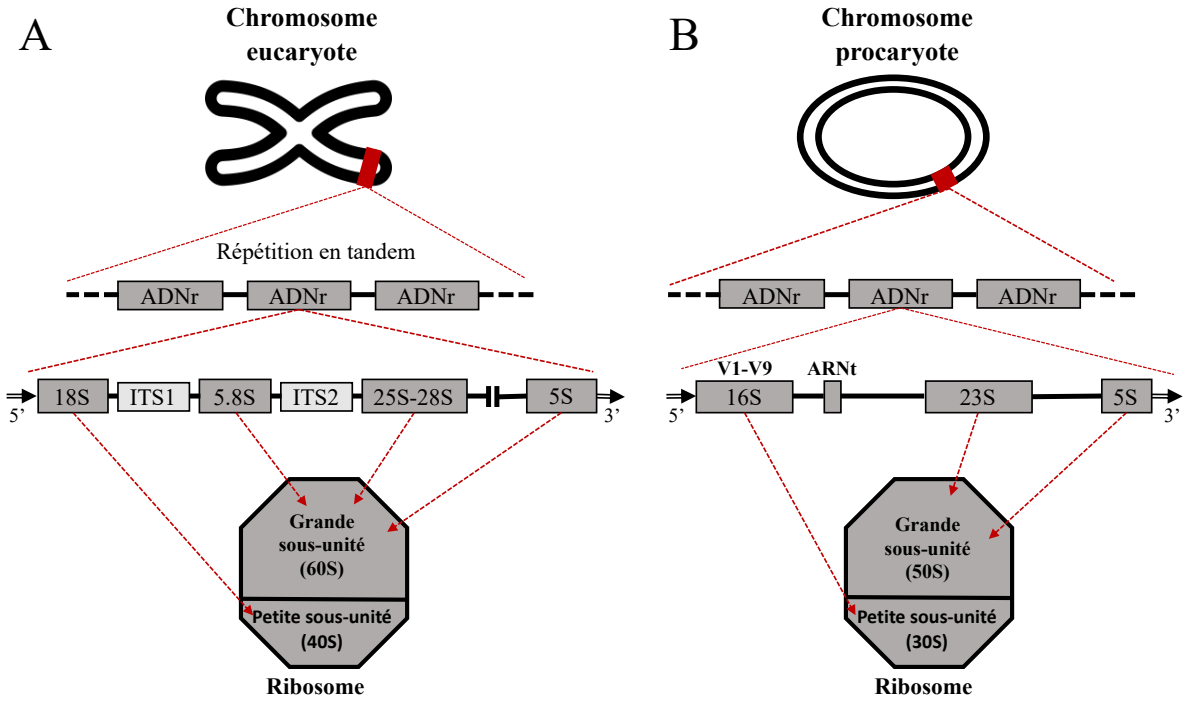


Figure 0-11 : Schéma de l'opéron de l'ADN ribosomique sur les chromosomes eucaryotes (A) et procaryote (B).
(Adapté de : Lavrinienko et al., 2021)

L'utilisation de la PCR couplée aux nouvelles technologies de séquençage (e.g. Illumina), regroupées sous le terme de métabarcoding, est une approche très utilisée en écologie microbienne. Elle permet notamment d'intégrer les espèces non-cultivables dans l'étude des micro-organismes d'un environnement. L'ADNr codant les ARN ribosomique est rapidement devenu une cible de choix pour les études de métabarcoding. Les ribosomes sont des complexes ribonucléoprotéiques responsables de la synthèse des protéines dans toutes les formes de vie. Ils polymérisent des chaînes polypeptidiques programmées par des séquences de nucléotides dans l'ARN messager (ARNm) grâce à un mécanisme médié par l'ARN de transfert (ARNt) (Noller et al., 2017). Les gènes de l'ADNr ont l'avantage d'être constitués à la fois de fragments hautement conservés au sein des populations microbiennes (e.g. bactéries, champignons et archées) pouvant être utilisés comme site d'annexion des amorces, ainsi que des domaines variables permettant de distinguer les différents taxons microbiens. Les gènes de l'ADNr sont regroupés en opéron sur les chromosomes et sont présents en plusieurs copies, également connues sous le nom de répétitions en tandem (Figure 11) (Lavrinienko et al., 2021). Les études modernes de métabarcoding des bactéries et des archées reposent généralement sur l'analyse des séquences de

l'ARNr 16S. Ce fragment de 1600 paires de bases est subdivisé en neuf régions hypervariables (V1-V9) (Bukin et al., 2019). Chez la vigne, l'étude du microbiote procaryote du système racinaire est principalement basée sur l'analyse des régions hypervariables V3-V4 (Berlanas et al., 2019; Marasco et al., 2022; D'Amico et al., 2018). Il est également possible d'étudier d'autres régions tels que la V5-V7 (Darriaut et al., 2022b) ou la V6-V8 (Wright et al., 2022). Pour étudier les champignons, les gènes codants l'ARNr 18S ou l'ARNr 28S et les séquences ITS (Internal Transcribed Spacer) offrent une bonne résolution taxonomique (Tedersoo et al., 2022). Chez la vigne, ces approches ciblent généralement les séquences ITS2 (Berlanas et al., 2019; Darriaut et al., 2023; Marasco et al., 2022). Comme les CMA présentent des hyphes multinucléés avec des copies de séquences ITS très variables, il est préférable de cibler les gènes codant l'ARNr 18S ou 28S pour leur étude (Suzuki et al., 2020)

En sortie de plateforme de séquençage, les données de métabarcoding sont traitées grâce à des pipelines tels que celui de FROGS proposé par le serveur Galaxy (Escudié et al., 2018) (Figure 12 A). Brièvement, le processus est initié par une étape de démultiplexage si nécessaire. Lors de l'étape de préprocessing, le pipeline va joindre les séquences R1 (Read1) et R2 avec un taux de non-concordance personnalisable (fixé à 10 % par défaut) dans la région recoupée. Il va aussi supprimer les séquences pour lesquelles les deux amorces ne sont pas présentes avec l'outil cutadapt (Martin, 2011), nettoyer les données sur des critères de taille de séquence, supprimer celles contenant une base ambiguë, ainsi que les dé-répliquer. Ensuite, les unités taxonomiques opérationnelles (OTUs) vont être clustérisées grâce à la méthode Swarm (Mahé et al., 2014). La détection et l'élimination des chimères seront réalisées grâce à l'outil VSEARCH (Rognes et al., 2016) avec la méthode *de novo* UNCHIME (Edgar et al., 2011). FROGS va utiliser ici une étape innovante de validation inter-échantillons pour confirmer le statut chimérique des séquences. Les OTUs vont ensuite être filtrées selon leur abondance et leur distribution parmi les échantillons. Ici, certaines séquences seront éliminées si elles sont retrouvées dans des banques de contaminant (e.g. phiX). La dernière étape du pipeline consiste à réaliser l'affiliation des OTUs. Pour cela différentes bases de données peuvent être utilisées tels que Silva138.1 pour les bactéries (Quast et al., 2012), Unite8.2 pour les champignons (Nilsson et al., 2019) ou MaarjAM pour les CMA (Öpik et al., 2010). Après obtention des données, il est alors possible de les traiter sur des logiciels statistiques tels que RStudio à l'aide de package conçus pour les études de métabarcoding tels que *phyloseq* (McMurdie and Holmes, 2013). La composition des micro-organismes est alors quantifiée grâce à des indices de diversité-α, mesurés au sein d'une communauté, tels que la richesse et les indices Chao1, de Simpson et de Shannon. Pour comparer la diversité entre différentes communautés microbiennes, on utilise des indicateurs de β-diversité basés sur la mesure de distances, tels que celles de Bray-Curtis, de Jaccard ou de l'Unifrac (pondérée ou non) (Figure 12

B). Enfin, il est possible de prédire *in silico* le rôle des communautés microbiennes grâce à des outils tels que PICRUSt2 pour les bactéries (Douglas et al., 2020) ou FUNGuild pour les champignons (Nguyen et al., 2016).

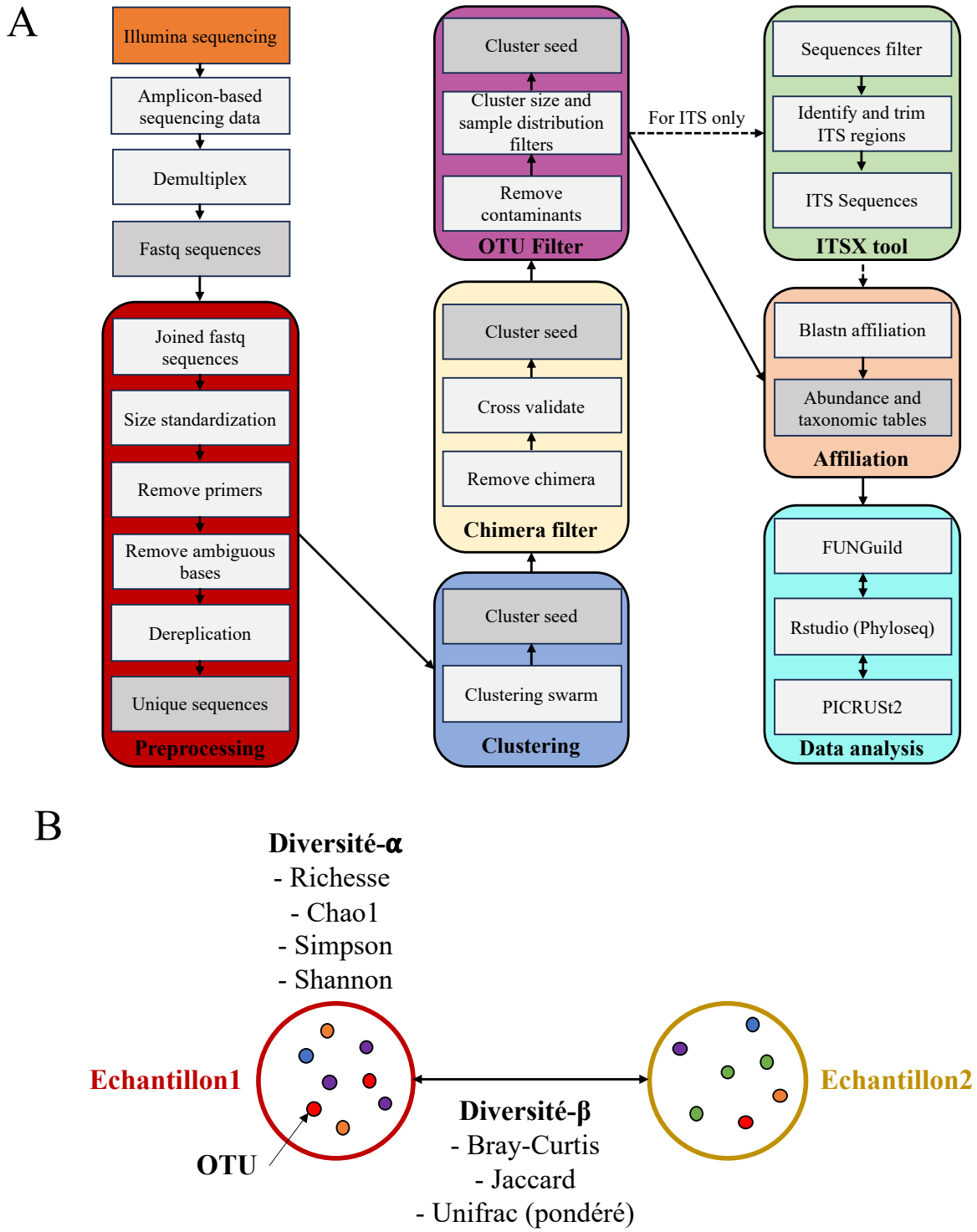


Figure 0-12 : Pipeline utilisé pour traiter les données de métabarcoding (A) et indices de diversité (B). (Adapté de : Escudié et al., 2018)

La métatranscriptomique est aussi utilisée en écologie microbienne. Il est en effet possible de faire le même type d'analyse de métabarcoding sur des ADNc (ADN complémentaire) après une étape de RT (reverse-transcription). Cela a par exemple été réalisé chez la vigne pour étudier les communautés bactériennes de la rhizosphère en séquençant la région V4-V5 de l'ARNr 16S (Dries et al., 2023). Il est aussi possible de réaliser des analyses de métatranscriptomique en séquençant l'ensemble de l'ARN extrait après l'étape de RT, afin d'identifier les gènes ou les voies actives dans une communauté microbienne (Enespa and Chandra, 2022). On observe aussi l'émergence de la métagénomique « Shotgun » dans les études d'écologie microbienne. Contrairement aux approches de métabarcoding qui repose sur l'utilisation de gènes marqueurs, la métagénomique « Shotgun » consiste en le séquençage de tous les ADN présents dans un échantillon biologique (microbien ou non). Cette technique est utilisée pour établir la composition taxonomique des micro-organismes, étudier leurs fonctions au travers des nombreux gènes séquencés (e.g. processus physiologiques, voie de biosynthèse), ainsi que reconstruire des génomes d'espèces entiers (Quince et al., 2017). Récemment, cette technologie prometteuse a été testée avec succès chez la vigne sur des échantillons de feuille, de rhizosphère et de sol (Azevedo-Silva et al., 2021). Enfin, il existe d'autres méthodologies de biologie moléculaire pouvant être utilisées en écologie microbienne tels que l'hybridation d'acides nucléiques (e.g. FISH), l'électrophorèse sur gel en gradient dénaturant (DGGE), les puces à ADN ou l'étude de l'empreinte génétique (DNA fingerprinting) (Enespa and Chandra, 2022).

c) Les autres méthodologies utilisées dans la thèse

Le profilage physiologique des communautés microbiennes avec le système Biolg Ecoplate™

L'analyse de la diversité métabolique d'une communauté microbienne peut être réalisée en examinant son comportement catabolique à l'égard de plusieurs substrats. En effet, les données de dégradation de ces substrats peuvent être rassemblées pour former un profil métabolique, caractéristique d'un échantillon environnemental. Cette technique est appelée profilage physiologique de communautés (Community-Level Physiological Profiling en anglais) et s'effectue à l'aide de plaques Biolog EcoPlate™. Ce système est composé de microplaques de 96 puits contenant trois répétitions de 31 sources de carbone réparties dans six grandes familles (i.e. amines, acides aminés, carbohydrates, acides carboxyliques, composés phénoliques et polymères) (Figure 13). La consommation des substrats par les micro-organismes est alors révélée grâce à la libération d'un indicateur coloré violet (i.e. sel de tétrazolium) proportionnellement à leurs dégradations. Les plaques sont inoculées avec un échantillon de sol dilué, puis incubées à l'obscurité pendant 7 jours en effectuant

une lecture par spectrophotométrie toutes les 24h. Plusieurs indicateurs de diversité sont alors mesurés tels que l'AWCD (Average Well Color Development), la richesse fonctionnelle ou l'indice de Simpson (Németh et al., 2021; Gryta and Fr, 2014). Ce type de plaque présente l'avantage de mener une analyse rapide à moindre coût de la diversité microbienne d'un échantillon. Certaines études reportent déjà l'utilisation de plaques Biolog Ecoplate™ pour analyser les microbiotes d'organes de la vigne tels que le bois (Bruez et al., 2015) ou les feuilles (Nerva et al., 2019), ainsi que le sol de parcelles viticoles (Darriaut et al., 2021).

	1	2	3	4	5	6	7	8	9	10	11	12
A	Water	B-methyl-D-glucoside	D-galactonic Acid γ-lactone	L-arginine								
B	Pyruvic acid methyl ester	D-Xylose	D-galacturonic acid	L-asparagine								
C	Tween 40	i-Erythritol	2-hydroxy benzoic acid	L-phenylalanine								
D	Tween 80	D-Mannitol	4-hydroxy benzoic acid	L-serine								
E	α-cyclodextrin	N-acethyl-D-glucosamine	γ-hydroxybutyric acid	L-threoinine								
F	Glycogen	D-glucosaminic acid	Itaconic acid	Glycyl-L-glutamic acid								
G	D-cellobiose	Glucose-1-phosphate	α-ketobutyric acid	Phenylethyl-amine								
H	α-D-lactose	D,L-α-glycerol-phosphate	D-malic acid	Putrescine								

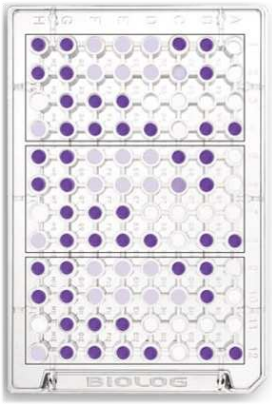


Figure 0-13 : Liste des différents substrats présents dans les plaques Biolog Ecoplate™.

Le dosage des enzymes microbiennes impliquées dans les cycles biogéochimiques

Les micro-organismes du sol jouent des rôles dans plusieurs processus biogéochimiques. Par conséquent, il est intéressant de doser l'activité enzymatique de certaines protéines impliquées dans ces cycles, afin de caractériser fonctionnellement les communautés microbiennes dans leur environnement. Ces méthodes sont basées sur le dosage par spectrophotométrie d'un produit coloré (i.e. β-naphtylamine ou p-nitrophénol), issu de la réaction de l'enzyme avec ses substrats, observé après révélation (Figure 14) (Darriaut et al., 2021). Certaines protéines du sol ont des rôles clefs tels que :

- l'arylamidase qui est impliquée dans le cycle de l'azote en catalysant l'hydrolyse des acides aminés en N-terminal à partir de peptides, d'amides ou d'arylamines (Acosta-Martinez and Tabatabai, 2000).
- la β-glucosidase qui est impliquée dans le cycle du carbone en catalysant l'hydrolyse de différents glycosides (Eivazi and Tabatabai, 1988).
- la phosphatase qui est impliquée dans le cycle du phosphore en catalysant l'hydrolyse d'une large variété de phosphomonoesters (Tabatabai and Bremner, 1969).

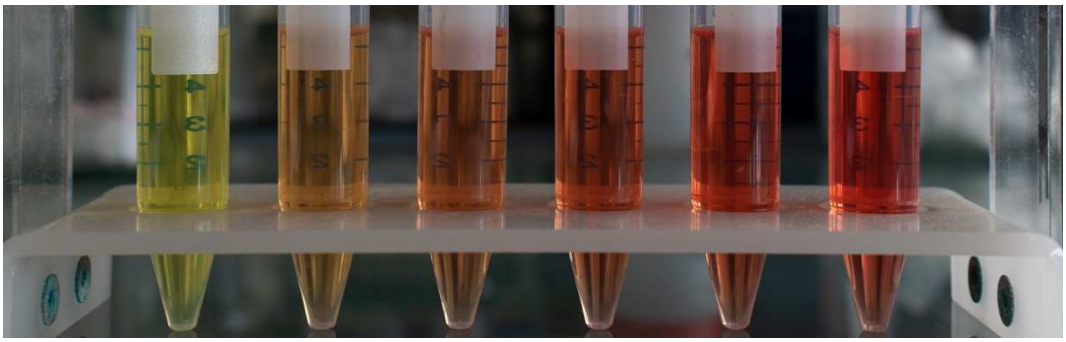


Figure 0-14 : Gamme étalon utilisée pour le dosage de l'arylamidase.
©Vincent Lailheugue.

La quantification de la mycorhization par microscopie

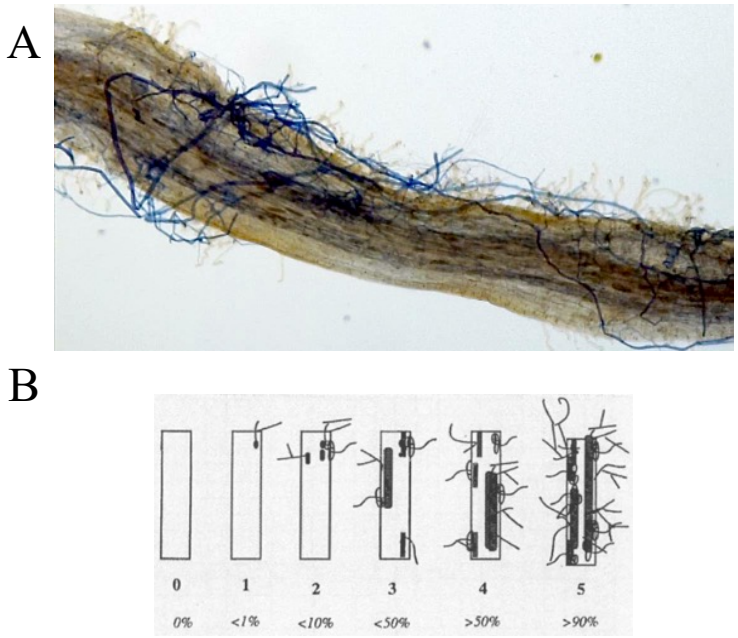


Figure 0-15 : Évaluation de la capacité de mycorhization des racines au microscope (A) à l'aide d'une échelle semi-quantitative (B).

Parmi les nombreuses méthodes permettant d'étudier les CMA (i.e. métabarcoding, analyse de biomarqueurs lipidiques, (RT-)qPCR et PCR-DGGE), une approche intéressante et peu coûteuse repose sur la microscopie. Après coloration des racines à l'encre bleue grâce à une méthode adaptée de Phillips and Haymann (1970), il est possible d'observer les structures des CMA (i.e. hyphes, arbuscules et vésicules) et de les quantifier au microscope, grâce à des paramètres (e.g. fréquence de mycorhization ou l'intensité de mycorhization des fragments mycorhizés) mesurés après notation des racines à l'aide d'une échelle semi-quantitative allant de 0 à 5 (Figure 15). Cela permet alors de comparer statistiquement la capacité de mycorhization des racines entre différents plants *via* ces

indices (Trouvelot et al., 1986). Ce type de méthodologie reste encore largement utilisé pour étudier les CMA chez la vigne (Binet et al., 2017; Moukarzel et al., 2021)

La métabolomique non ciblée

La métabolomique est une approche consistant à identifier et à quantifier l'ensemble ou une partie de petites molécules (<1500 Da), appelées métabolites, dans des échantillons biologiques, afin de pouvoir les comparer entre eux. Il existe des approches de métabolomique ciblée qui se concentrent sur un groupe spécifique de métabolites liés à une voie métabolique ou une classe de composés, ainsi que des approches non ciblées permettant une analyse globale des changements métaboliques entre conditions. Les communautés du sol et du système racinaire sont extrêmement diverses et une multitude d'interactions biochimiques sont réalisées entre elles, ainsi qu'avec la plante (Van Dam and Bouwmeester, 2016). La chromatographie en phase liquide avec spectrométrie de masse en tandem (LC/MS-MS), en mode non ciblée, est utilisée pour faciliter la compréhension des mécanismes des processus biologiques et biochimiques impliqués. Tout d'abord, la chromatographie en phase liquide va permettre de séparer les différents métabolites en fonction de leur hydrophobicité. Ils vont ensuite arriver séquentiellement dans la source du spectrophotomètre de masse dans laquelle ils seront ionisés (en mode négatif ou positif). Le rapport masse sur charge (m/z) d'un ion moléculaire d'intérêt est obtenu et recherché dans une base de données. Les métabolites sont alors identifiés de manière putative s'ils se situent dans une plage de tolérance spécifiée. Cependant, ces identifications putatives sont rarement uniques en raison de l'existence d'isomères et de la précision limitée des spectromètres de masse. Ces composés peuvent alors être soumis à l'étape de spectrométrie de masse en tandem (MS/MS), qui va fragmenter l'ion en phase gazeuse et permettre d'obtenir des éléments de structure primaire (Figure 16). En comparant les spectres MS/MS avec les temps de rétention obtenus pour les différents composés identifiés dans l'échantillon, il est alors possible de confirmer leurs identités (Xiao et al., 2012).

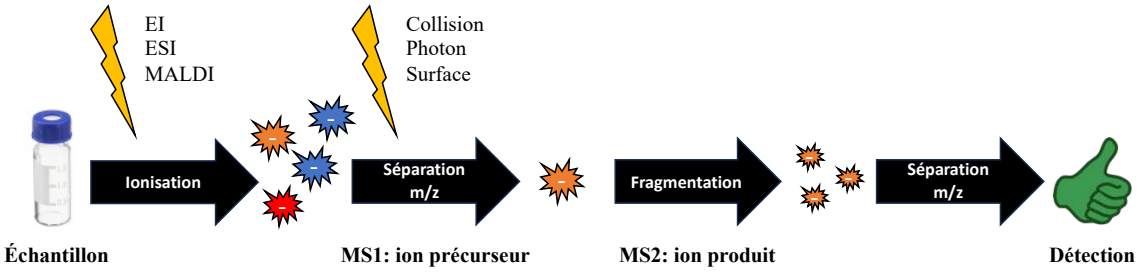


Figure 0-16 : Schéma du fonctionnement de la spectrométrie de masse en tandem (MS/MS) (Adapté de : Kang et al., 2012).

III) Le porte-greffe de vigne et le microbiote du système racinaire

Précédemment, nous avons vu que les microorganismes présents autour et dans le système racinaire, influencent le développement des plantes, et que certains microorganismes bénéfiques sont prometteurs pour adapter la viticulture aux enjeux actuels. Dans cette dernière partie introductive, nous verrons quels sont les facteurs qui influencent la composition du microbiote du système racinaire, en s'attardant sur le rôle des génotypes de porte-greffe et de greffon chez la vigne. Nous discuterons ensuite du rôle des exsudats racinaires impliqués dans les interactions de la plante avec les micro-organismes du sol et finirons par un état de l'art de la caractérisation des exsudats chez la vigne.

1) La composition du microbiote du système racinaire est soumise à de nombreux facteurs

Il existe dans le système racinaire de la vigne un core microbiome, défini par des taxons bactériens ou fongiques retrouvés en proportion semblables dans la rhizosphère ou l'endosphère racinaire de plants de différentes parcelles viticoles (Gobbi et al., 2022 ; Marasco et al., 2022). Cependant, la composition de ces niches écologiques reste variable et dépendante de l'intégration des divers facteurs environnementaux, ainsi que de la plante (Figure 17) (Bettenfeld et al., 2022).

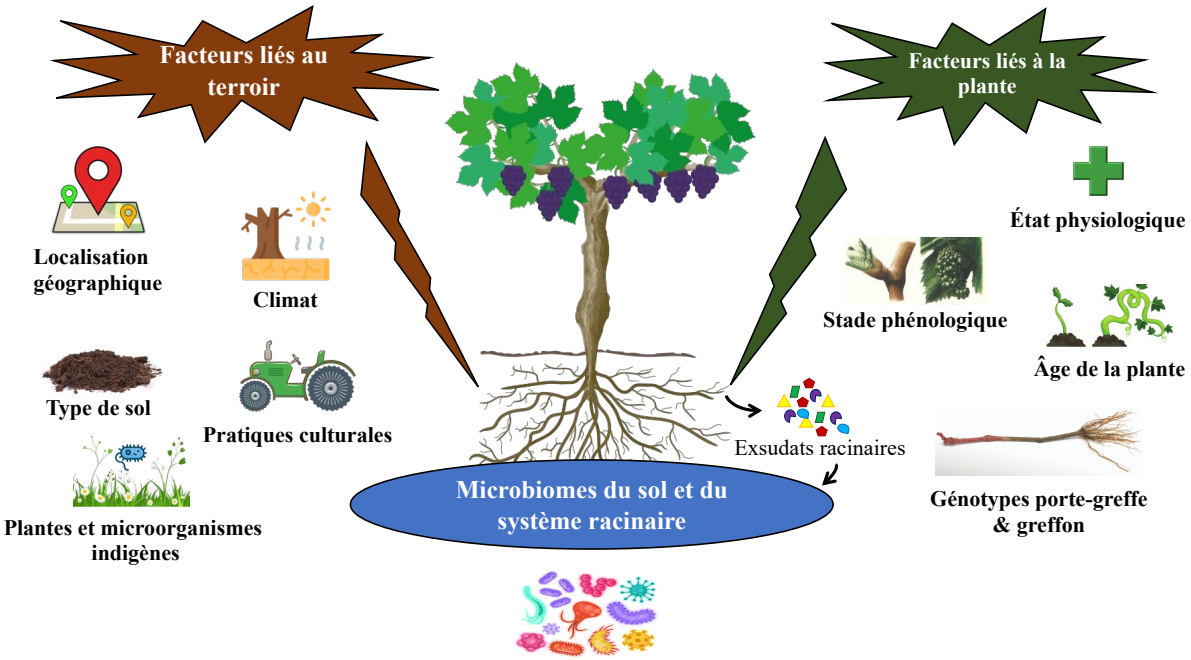


Figure 0-17 : Les facteurs qui influencent la composition des microbiomes du sol et de la rhizosphère chez la vigne.

Premièrement, la composition du microbiote du système racinaire est dépendante des populations indigènes du sol (Zarraonaindia et al., 2015). En comparant l'effet de la zone de la parcelle (saine ou dépérissante), de la saison (été et automne) et du terroir (Graves et Haut-Médoc) sur la composition en bactéries, champignons et CMA du sol, Darriaut et al. (2023) montrent que le terroir est le principal facteur influençant les communautés bactériennes et fongiques du sol. Ces résultats sont cohérents avec ceux obtenus par Marasco et al. (2022), qui ont comparé les effets de la région (au nombre de deux en Italie), de la parcelle viticole (au nombre de dix), des génotypes de porte-greffe et de greffon, ainsi que leur interaction (sept combinaisons porte-greffe × greffon), sur la diversité des bactéries et des champignons du sol, de la rhizosphère et du sol brut. Les auteurs montrent que la parcelle est le facteur exerçant la plus forte influence sur la diversité des deux groupes de microorganismes au sein des trois compartiments étudiés. Comme le terroir regroupe une multitude de facteurs d'ordre biotique et abiotique, il est très difficile d'étudier ces facteurs séparément. Il est aujourd'hui établi que la composition des micro-organismes du sol est dépendante de ses caractéristiques physico-chimiques (e.g. texture, disponibilité des nutriments, structure, humidité, température, radiation et pH) et biologiques (e.g. interactions avec les insectes, les nématodes, les autres micro-organismes et les espèces végétales présentes sur le site) (Islam et al., 2020). Par exemple, Oyuela Aguilar et al. (2020) ont montré que certains taxons bactériens (e.g. β- γ- ε-*Proteobacteria*, *Acidobacteria* Gp7) et fongiques (e.g. *Saccharomycetes*, *Glomeromycetes*, *Rozellomycotina*) étaient influencés par des paramètres du sol tels que les teneurs en matière organique et en nutriments, le pH ou la structure. Des corrélations positives ont récemment été établies entre la richesse fongique du sol et la température, ainsi qu'avec les précipitations, suggérant un effet du climat sur la composition du microbiote du sol (Gobbi et al., 2022). Il a été démontré que le type de conduites viticulturales impacte significativement la composition bactérienne et fongique du sol, avec des différences plus marquées chez les bactéries, pouvant s'expliquer par l'utilisation du cuivre en agriculture biologique ou par le labourage du sol en agriculture conventionnelle (Likar et al., 2017). Enfin, des études ont également montré que la richesse et la diversité des bactéries et des champignons peuvent varier au cours d'années successives, suggérant une influence du millésime sur les microbiomes du sol et du système racinaire de la vigne (Oyuela Aguilar et al., 2020; Berlanas et al., 2019; Darriaut et al., 2022a). La saison de l'année est aussi un facteur déterminant sur la composition et la diversité microbienne des sols, comme cela a été démontré pour la diversité des champignons par Hernandez and Menéndez (2019), ou pour la diversité des bactéries et des champignons, ainsi que la richesse des CMA par Darriaut et al. (2023).

Au travers la rhizodéposition, les plantes sont capables de modifier la composition des micro-organismes de la rhizosphère par différents procédés que nous détaillerons plus tard. Chez la vigne, la

comparaison des bactéries et des champignons de la rhizosphère chez des individus prélevés dans une parcelle jeune de 7 ans avec ceux d'une parcelle établie depuis 25 ans montre des différences significatives en terme de composition, les auteurs concluent un effet de l'âge de la vigne sur la composition du microbiome rhizosphérique (Berlanas et al., 2019). Une étude récente réalisée sur trois parcelles viticoles d'âges différents (i.e. 11, 36 et 110 ans), géographiquement proches et présentant des paramètres pédologiques similaires, montre des différences significatives dans la composition des communautés de CMA associées aux racines de la vigne (Noceto et al., 2023). Il est aussi présumé que le stade phénologique de la plante puisse avoir un impact sur la composition des microbiomes du système racinaire. Par exemple, il a été démontré que la richesse des CMA dans les racines était significativement plus élevée au stade de la véraison qu'au stade de la floraison (Schreiner, 2020). Enfin, tout comme le choix de l'espèce végétale, il a récemment été démontré que les génotypes des deux composants du plant greffé influencent la composition des microbiomes de la rhizosphère et de l'endosphère racinaire (Marasco et al., 2022; Vink et al., 2021). Même si la rhizodéposition est peu caractérisée chez la vigne, il est établi dans le règne végétal que la physiologie, le stade phénologique, l'âge et la génétique de la plante influencent la composition métabolique des racines et de leurs rhizodépots et leurs exsudats. Indirectement, ces paramètres vont influencer la composition du microbiome du système racinaire (Ma et al., 2022).

2) Influence des génotypes de porte-greffe et de greffon sur la composition des microbiomes rhizosphériques et racinaires chez la vigne

Chez la vigne, plusieurs équipes ont récemment démontré un effet du génotype de porte-greffe, sur la composition des microbiomes du système racinaire. Encore plus récemment, d'autres travaux montrent un effet du greffon ou de la combinaison des deux génotypes du plant greffé sur la composition de ces communautés microbiennes. Ces expérimentations diffèrent par les composants du plant (greffé ou non greffé) et les compartiments du système racinaire étudiés, les communautés microbiennes ciblées, les méthodologies d'analyse et les génotypes employés, ainsi que la localisation géographique et les caractéristiques des parcelles viticoles. Ces expérimentations sont résumées dans le Tableau 5.

Tableau 0-5 : Principales caractéristiques des études des effets du porte-greffe et du greffon sur le microbiome du système racinaire de la vigne

Références	Composants étudiés	Micro-organismes ciblés	Compartiments étudiés	Méthodologies	Porte-greffe	Greffon	Plants greffés	Date de prélèvement	Culture des plants
D'Amico et al., 2018	Porte-greffe	Bactéries	Sol brut, Rhizosphère, Racine	Métabarcoding: - 16S rRNA gene (région V3-V4)	1103P, Kober 5BB	Lambrusco	Oui	Novembre 2016	Une parcelle en Italie
Marasco et al., 2018	Porte-greffe	Bactéries	Sol brut, Rhizosphère, Racine	Métabarcoding: -16S rRNA gene (région V3-V4)	402A, 157.11, SO4, 16.49, Barbera	Barbera	Oui et non	-	Une parcelle en Italie
Berlanas et al., 2019	Porte-greffe	Bactéries Champignons	Rhizosphere	Métabarcoding: - 16S rRNA gene (région V3-V4) - ITS2	110 R, 140 Ru, 1103 P, 41 B, 161-49 C	Tempranillo	Oui	Juin et Novembre 2016 et 2917	Une parcelle jeune (7ans) et une établie en Espagne (25 ans)
Darriaut et al., 2022	Porte-greffe	Bactéries, Champignons	Sol brut, Rhizosphère, Root endosphère	Métabarcoding: - 16S rRNA gene (région V5-V7) - ITS2	RGM, 1103P	Cabernet Sauvignon	Oui	-	Une parcelle en France (10 ans) et une expérimentation en serre
Dries et al., 2021	Porte-greffe	Bactéries	Rhizosphère	Métabarcoding: -16S rRNA gene (région V4-V5)	1103P, 140 Ru, 161- 49 Couderc, Kober 5BB	-	Non	Juillet 2020	Plantation dans des tubes dans une parcelle en Allemagne (5ans)
Wright et al., 2022	Porte-greffe	Bactéries Champignons	Sol brut, Racines	Métabarcoding: - 16S rRNA gene (région V6 -V8) - ITS2	RGM, 3309C, New York Muscat	New York Muscat	Oui et non	-	Une parcelle au Canada (5 ans)
Swift et al., 2021	Porte-greffe	Bactéries Champignons	Sol brut, Racines, Feuilles, Baies	Métabarcoding: - 16S rRNA gene (région V4) - ITS2	Chambourcin, 1103P, 3309C, SO4	Chambourcin	Oui et non	Septembre 2018	Une parcelle aux Etats-Unis (9ans)
Moukarzel et al., 2021	Porte-greffe	CMA	Racines	Denaturing gradient gel electrophoresis (DGGE) et trap cultures	101-14, Schwarzmann, SO4, 5C, 3309C, 420A, 5C, 99R, Fercal, RGM,	Pinot noit	Oui et non	-	Trois parcelle en nouvelle zelande
Marasco et al., 2023	Porte-greffe, Greffon, Combinaison	Bactéries, Champignons	Sol brut, Rhizosphère, Racine	Métabarcoding: - 16S rRNA gene (région V3-V4) - ITS2	420A, SO4, 110R, 3309C	Chardonnay, Merlot, Sangiovese	Oui	Octobre 2016	Dix paarcelles en Italie
Vink et al., 2021	Porte-greffe, Greffon, Combinaison	Bactéries	Rhizosphère	Métabarcoding: - 16S rRNA gene (région V4)	125 AA, 5 BB, Binova, SO4	Calandro, Reberger, Felicia, Villaris	Oui	Octobre 2016	Une parcelle en Allemagne (11ans)
Dries et al., 2023	Porte-greffe, Greffon	Bactéries	Rhizosphere	Métatranscriptomique -16S rRNA gene (région V4-V5)	Mueller-Thurgau, Riesling, SO4, Boemer, 125AA, Teleki 8 B	Riesling, Mueller-Thurgau	Oui et non	Mai 2019, Octobre 2019 et 2020	Plantation dans des pots dans une serre ouverte

Introduction

Parmi les études de métabarcoding qui s'intéressent à l'effet du porte-greffe sur le microbiome du système racinaire, D'Amico et al. (2018) ont montré que 1103P présentait une diversité bactérienne dans la rhizosphère et les racines significativement inférieure à celle de 5BB, notamment pour les bactéries impliquées dans la solubilisation du K, pouvant expliquer l'absorption insuffisante de cet élément par 1103P. En étudiant quatre porte-greffes et un cépage (greffé ou non sur les porte-greffes), Marasco et al. (2018) ont montré que la richesse et la diversité bactérienne, ainsi que les réseaux microbiens, étaient significativement influencés par le génotype de porte-greffe au sein de la rhizosphère et de l'endosphère racinaire. Cependant, la culture et l'isolement de bactéries du système racinaire, suivis de la prédiction d'activités PGPR *in silico*, retrouvées similaires entre les différents porte-greffes, suggèrent que les fonctions bactériennes ne diffèrent pas. Berlanas et al. (2019) ont comparé le microbiome de la rhizosphère de cinq génotypes de porte-greffe, sur une jeune parcelle (7 ans), ainsi qu'une autre bien établie (25 ans). Chez la parcelle la plus âgée, les auteurs ont montré une influence du génotype sur un des deux indices de diversité-α mesurés pour les bactéries et les champignons, ainsi que sur la diversité-β mesurée pour les deux groupes de micro-organismes. En revanche, aucune influence du génotype sur la diversité-α et -β n'a été observée dans la jeune parcelle. Les auteurs concluent à un effet du porte-greffe sur la composition du microbiome rhizosphérique, mais suggèrent qu'elle est aussi influencée par l'âge de la plante, les propriétés physico-chimiques du sol et les pratiques culturales. En comparant des échantillons prélevés chez 1103P et RGM greffés avec CS, cultivés en serre dans du sol de zone saine ou dépérissante d'une même parcelle viticole, Darriaut et al. (2022a) ont montré une influence du génotype de porte-greffes sur certains indices de diversité-α et -β mesurés pour les bactéries et les champignons, au sein de la rhizosphère et de l'endosphère racinaire. Dans l'article de Dries et al. (2021a), les auteurs ont comparé les bactéries rhizosphériques de quatre génotypes de porte-greffe, cultivés pendant 5 ans dans des tubes cylindriques, remplis avec le même sol, afin de réduire la variabilité induite par les facteurs environnementaux. Ils ne montrent pas d'effet du porte-greffe sur la diversité-α. En revanche, une influence du génotype de porte-greffe a été reportée sur les trois indices de diversité-β mesurés. De plus, plusieurs taxons bactériens étaient enrichis dans la rhizosphère de chacun des porte-greffes. Les auteurs concluent que le génotype de porte-greffe affecte la composition mais pas la structure de la communauté bactérienne rhizosphérique. Wright et al. (2022) ont étudié la composition bactérienne et fongique des racines de RGM et 3309C greffées avec le cultivar New York Muscat, ainsi que chez le même cépage cultivé franc de pied. Les auteurs ne montrent pas d'influence du génotype de porte-greffe sur la diversité-α pour les deux groupes de micro-organismes. Cependant, un effet du génotype est reporté sur les trois indices de diversité-β mesurés pour les bactéries, et sur deux d'entre eux pour les champignons. Les auteurs concluent à un effet du porte-greffe sur la composition du microbiome du système racinaire. Dans une

autre étude, Swift et al. (2021) ont comparé l'effet du porte-greffe (quatre génotypes), du compartiment de la plante (baies, feuilles, racines et sol) et de l'irrigation (trois modalités), sur la composition des microbiomes bactérien et fongique de la plante, au sein d'une parcelle divisée en 3 blocs. En intégrant tous ces facteurs dans le même modèle, les auteurs ne montrent pas d'influence du génotype de porte-greffe sur la diversité-α et -β du microbiome bactérien *in planta*. En revanche, ils reportent une influence du génotype de porte-greffe, mais aussi de son interaction avec le compartiment, sur la diversité-β des champignons (expliquant uniquement 4,8% de la variance), ainsi que sur un seul des trois indices de diversité-α mesuré pour les champignons. Les auteurs concluent que le génotype de porte-greffe a un effet limité sur la composition de l'ensemble du microbiome de la plante. Enfin, seulement un article étudie l'influence du porte-greffe sur la composition des CMA chez la vigne (Moukarzel et al., 2021a). Les auteurs montrent une différence significative dans la communauté de CMA associée à neuf porte-greffes, greffés ou non avec le Pinot noir, en utilisant des approches d'électrophorèse sur gel en gradient dénaturant (DGGE) et des systèmes de culture en piège (inoculation de plants avec des racines de vigne déjà mycorhizées prélevées en parcelle).

Très récemment, d'autres études se sont intéressées à la potentielle contribution du génotype du greffon sur la composition du microbiome du système racinaire de la vigne. Par une approche de métatranscriptomique, Dries et al. (2023) ont comparé la communauté bactérienne rhizosphérique de cépages de vigne (Mueller-Thurgau et Riesling), greffés ou non, à trois temps de prélèvement. Les auteurs montrent une différence significative au premier temps de prélèvement uniquement pour l'un des deux indices de diversité-α mesurés chez les cépages cultivés franc de pied. Des différences significatives sont aussi observées entre les deux cultivars cultivés franc de pied pour la diversité β à deux des temps de prélèvement. Cependant, ces différences ne furent plus observables lorsque tous ces indices furent comparés entre les deux cépages cultivés greffés. Des différences significatives dépendantes de l'indice de diversité-α et -β et du temps de prélèvement ont aussi été observées entre les cultivars greffés avec les cultivars non greffés, ainsi qu'entre les différents porte-greffes. Ici, les auteurs concluent que les génotypes de porte-greffe et de greffon influencent la structure et la composition des bactéries rhizosphériques. Dans une autre étude, Vink et al. (2021) ont étudié les bactéries rhizosphériques associés à quatre cépages, greffés avec quatre porte-greffes. Les auteurs mettent en évidence un effet du porte-greffe et de la combinaison porte-greffe × greffon sur quatre indices de diversité-α, ainsi que du greffon sur deux d'entre eux. De plus, ils démontrent que le principal facteur influençant la diversité-β de la communauté bactérienne rhizosphérique est le génotype du greffon, suivi de celui du porte greffe avec une contribution moins importante, mais que l'interaction des deux génotypes ne semble pas intervenir dans la structuration de ces bactéries. Enfin,

Introduction

Marasco et al. (2022) ont étudié les communautés bactériennes et fongiques associées au système racinaire de sept combinaisons de porte-greffe × greffon de vigne cultivées dans 10 vignobles différents. Les auteurs ont montré à la fois une influence des génotypes de porte-greffe et de greffon sur la diversité des bactéries et des champignons rhizosphériques et endophytes des racines. Cependant, ils observent aussi un effet de la combinaison des deux génotypes, plus important que celui des deux composants du plant étudiés indépendamment. Les auteurs concluent alors que la combinaison porte-greffe × greffon est derrière le type de sol, un autre facteur déterminant la diversité des bactéries et des champignons associés au microbiome du système racinaire.

Comme nous l'avons vu dans cette partie, il semble admis par la communauté scientifique que le génotype de porte-greffe présente une influence sur la composition du microbiote du système racinaire chez la vigne. Cependant, il s'avère que certains travaux ne démontrent que peu ou pas d'effet du génotype, mais aussi que les résultats obtenus semblent dépendants des expérimentations, des dates de prélèvement, de la parcelle, des compartiments et des micro-organismes étudiés, ainsi que des indicateurs de diversité mesurés. De plus, il apparait que la combinaison porte-greffe × greffon exerce une influence importante mais qui reste encore trop peu prise en compte. Le fait que certains travaux montrent un effet du greffon uniquement lorsqu'il est cultivé franc de pied, ou que d'autres se contredisent à propos de quel composant du plant exerce la plus forte influence sur le microbiote du système racinaire, nécessite de poursuivre l'implémentation des connaissances sur le sujet. Il apparait ainsi compliqué de pouvoir extrapoler les résultats et de comparer les communautés microbiennes entre les différents jeux de données. Enfin, encore trop peu d'études cherchent à caractériser le rôle des micro-organismes du système racinaire de la vigne au sein de leur environnement, ainsi que sur le développement de la plante. Il est donc aujourd'hui capital de coupler les analyses d'identification taxonomique avec des approches permettant de comprendre le rôle des microorganismes du microbiote racinaire dans son environnement et sur la vigne (e.g. phénotypage, tests enzymatiques, profilage physiologique de communautés, LC-MS/MS).

3) Les exsudats racinaires influencent la communauté microbienne rhizosphérique

a) Le rôle des exsudats racinaires dans la rhizosphère

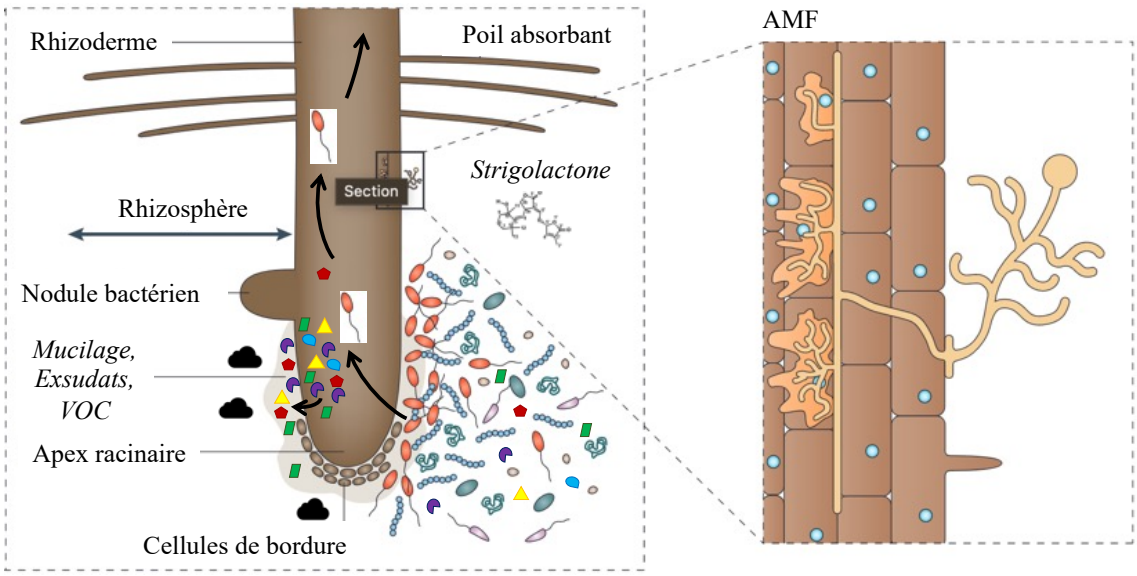


Figure 0-18 : Schéma des interactions complexes entre les racines de la plante et les microbiotes rhizosphériques et racinaires.
(Adapté de : Philippot et al., 2013)

Les racines des plantes sont remarquablement capables de sécréter une vaste gamme de composés dans la rhizosphère. Ce phénomène s'appelle la rhizodéposition et regroupe le relargage du mucilage (i.e. une couche gélatineuse entourant l'extrémité des racines composée de sucres, protéines et phospholipides), des cellules de bordure ou de la coiffe des racines, de composés organiques volatils (COV) et de gaz (e.g. éthylène, CO_2 et H_2), ainsi que d'exsudats (Figure 18). Parmi les exsudats racinaires, on trouve une large diversité de composés de faible poids moléculaire (i.e. acides aminés, acides organiques, sucres, vitamines, composés phénoliques, métabolites secondaires et hormones), ainsi qu'une grosse proportion de composés de poids moléculaire élevé (i.e. sucres complexes composant le mucilage et protéines) (Haichar et al., 2014). La quantité et la composition des rhizodépôts dépendent des caractéristiques de la plante tels que l'espèce, le génotype, l'âge et le stade phénologique, mais aussi de la physiologie de l'organisme, en relation avec les facteurs biotiques et abiotiques environnants (Jamil et al., 2022). Grâce à la rhizodéposition, les plantes modifient les propriétés de la rhizosphère, et par conséquent la composition des communautés microbiennes environnantes. En effet, les rhizodépôts représentent 3 à 25% du carbone fixé par la photosynthèse et peuvent être utilisés en tant que source de carbone par les micro-organismes. L'absorption d'eau et la

respiration des racines affectent la teneur en oxygène du sol, impactant la respiration microbienne. Les plantes vont aussi modifier la disponibilité des nutriments dans le sol, grâce à leur absorption par les racines et la sécrétion de chélateurs (e.g. phytosidérophore). Enfin, certains métabolites secondaires présents dans les exsudats vont être impliqués dans la lutte contre les agents pathogènes ou la mise en place de symbioses (Philippot et al., 2013).

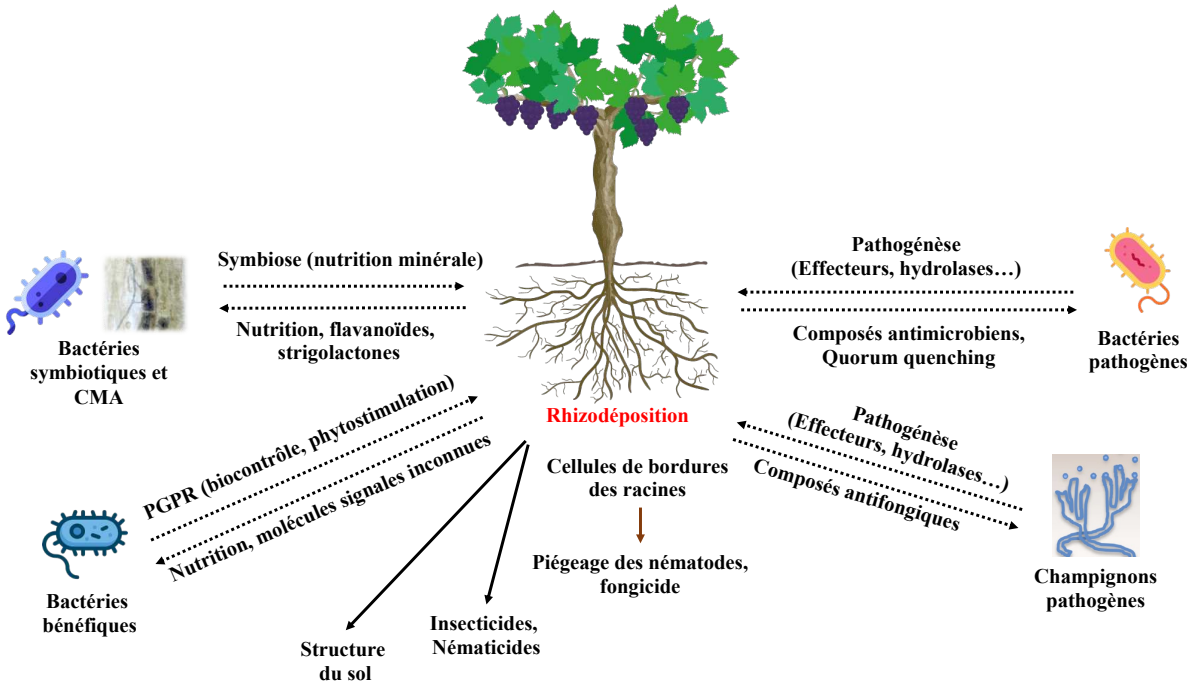


Figure 0-19 : Influence de la rhizodéposition les communautés microbiennes du sol et du système racinaire.
(Adapté de : Haichar et al., 2014).

Certains composés présents dans les exsudats racinaires sont réputés pour lutter contre les agents pathogènes (Figure 19). On retrouve par exemple des composés antimicrobiens (e.g. phytoanticipines ou phytoalexines), ainsi que des protéines de défense (e.g. chitinase, β-1,3-glucanase ou protéases) (Haichar et al., 2014). Il a récemment été proposé que les strigolactones, une classe d'hormone exsudée dans la rhizosphère, impactent négativement le développement de champignons et de bactéries pathogènes (Kaniganti et al., 2022). Les racines libèrent aussi des composés organiques volatiles (COV), qui représentent environ 1 % de l'ensemble des métabolites secondaires des plantes et comprennent des terpenoïdes, des acides gras, des phénylpropanoïdes et des acides aminés. Dans le sol, les COV attirent les agents pathogènes et inhibent leur croissance (Jamil et al., 2022). Certaines bactéries pathogènes possèdent des systèmes de quorum-sensing (QS) qui contrôlent la production et la sécrétion de facteurs de virulence. Le QS est une forme de communication intercellulaire entre

bactéries, médiée par de petites molécules de signalisation diffusibles, qui leur permettent de mener des actions coordonnées inter et intra espèces. Les plantes ont alors développé des mécanismes d'interférence (Quorum Quenching : QQ) de ces signaux, grâce à la synthèse de molécules capables de mimer ou bloquer les ligands impliqués, ainsi que des protéines capables de les dégrader ou d'empêcher leur synthèse (Koh et al., 2013). Enfin, les cellules de bordures et de la coiffe sont programmées pour être libérées de la coiffe et être actives métaboliquement dans la rhizosphère. Elles peuvent attirer et immobiliser les nématodes, attirer les zoospores, synthétiser des composés de défenses en réponse aux attaques de pathogènes, ainsi que repousser les bactéries pathogènes ou se lier avec elles (Haichar et al., 2014).

Il a récemment été suggéré que le remodelage opportun du microbiome des plantes puisse conférer des avantages dans la réponse à certains stress d'ordre biotique et abiotique. En fonction de leur état physiologique, les plantes vont au travers de l'exsudation de certains composés par les racines attirer des micro-organismes bénéfiques (e.g. CMA ou PGPR) pour établir des symbioses mutualistes, conduisant à l'apparition du concept appelé : « Cry for help » (Wang and Song, 2022). Parmi eux, on trouve des flavonoïdes principalement, mais aussi d'autres composés phénoliques, des acides aminés, ainsi que des composés produits par les cellules de bordure des racines, qui sont impliqués dans l'association de la plante avec des bactéries de la famille des *Rhizobiaceae*. Ils vont induire l'expression des gènes *nod* impliqués dans la formation des nodules. Comme pour l'interaction de la plante avec *Rhizobium*, les flavonoïdes et les composés phénoliques sont impliqués dans la mise en place de symbioses avec le genre d'actinomycètes *Frankia* (Haichar et al., 2014). Les strigolactones (SL) sont une classe d'hormones végétales dérivées du métabolisme des caroténoïdes. Elles jouent un rôle clef dans les premières étapes de mise en place de la symbiose mycorhizienne. En effet, elles vont être perçues par les CMA et induirent la germination des spores et la ramification des hyphes (Akiyama et al., 2010; Besserer et al., 2006). La conversion de la forme d'azote relativement peu mobile NH_4^+ en forme très mobile NO_3^- par les bactéries nitrifiantes, influence la nutrition azotée de la plante car la forme mobile est plus susceptible d'être perdue par lessivage ou dénitrification. Les plantes peuvent ralentir ce mécanisme en libérant des inhibiteurs biologiques de la nitrification (IBN) à partir des racines (Subbarao et al., 2007). Enfin, la libération de composés sources de carbone va agir en tant que chimio-attractant chez certaines bactéries (bénéfiques ou non) et augmenter leur capacité de colonisation de la rhizosphère. Il a été reporté que d'autres métabolites exsudés par la plante peuvent jouer le même rôle tels que des sucres, des acides aminés, des acides dicarboxyliques ou des composés phénoliques (Haichar et al., 2014). Par la variabilité des sources de carbone exsudées, elles stimulent aussi la croissance des micro-organismes rhizosphériques et sont intégrées dans la production de

composés bénéfiques pour la plante, tels que des antibiotiques, fongicides, substrats de l'ACC désaminase, hormones végétales, et ainsi accélèrent la décomposition de la matière organique du sol.

b) La caractérisation des exsudats racinaires chez la vigne

Chez la vigne, la composition métabolique et le rôle des exsudats racinaires sur les communautés microbiennes sont très peu étudiés. Contreras et al. (2019) ont caractérisé leur composition chez 1103P, greffé avec le cépage Chardonnay, cultivé en condition hydroponique pendant 60 jours. Les résultats de l'analyse non ciblée montrent que les exsudats sont constitués d'acides organiques (31%), de flavonoïdes (13%), de benzopyrènes (13%), d'alcaloïdes (13%), d'acides aminées (6%), de sucres (6%), d'enzymes (6%), d'esters (6%) et d'aldéhydes (6%). Les auteurs ont identifié des acides organiques tels que les acides 5-dodécénoïque, 4-hydroxyphénylacétique, trans-cinnamique et tartronique, ainsi que des flavonoïdes tels que l'isorhamnétine. Récemment, une autre étude a caractérisé les composés exsudés, mais cette fois-ci par les cellules du bord des racines chez le porte-greffe Beta (Zhang et al., 2022). Les auteurs montrent que la composition est dominée par les lipides (19%), les acides aminés et leurs dérivés (15%), les sucres (12%), les acides organiques (7%), les acides phénoliques (10%), les flavonoïdes (9%) et les quinones (7%). Concernant le rôle des exsudats, ils observent aussi que certains flavonoïdes et tanins inhibent la croissance de *Fusarium solani* cultivé sur milieu PDA. Liu et al. (2022) ont étudié le rôle fonctionnel de l'acide ρ-hydroxybenzoïque (4-HBA), un composé exsudé des racines, grâce à son ajout dans le sol de porte-greffes Beta cultivés en pot. Les auteurs montrent que l'ajout exogène de 4-HBA impacte le profil des autres molécules exsudées par les racines, ainsi que la communauté microbienne rhizosphérique en réduisant l'abondance de bactéries bénéfiques et en augmentant celle de champignons pathogènes. En étudiant la réponse du génotype 140 Ruggeri à la carence en fer ou l'ajout d'engrais contenant cet élément, López-Rayo et al. (2015) ont montré que les acides oxalique, tartrique, malique et ascorbique sont les principaux acides organiques exsudés chez la vigne. En évaluant l'efficacité de l'ajout de P dans le sol pour atténuer l'effet toxique de l'excès de cuivre dans le sol, Baldi et al. (2018) détectent 5 acides organiques dans les racines de 1103P cultivées *in vitro*, mais retrouvent uniquement l'acide citrique dans les exsudats racinaires.

Actuellement, très peu d'études ont comparé la composition des exsudats racinaires entre différents génotypes de porte-greffe. Cançado et al. (2009) ont comparé l'exsudation des acides organiques entre Kober 5BB et 110R, cultivées *in vitro*, en présence de différentes concentrations d'aluminium. Les auteurs observent une exsudation de citrate significativement supérieure chez

Kobber 5BB comparativement à 110R, suggérant une implication de cet acide organique dans la tolérance de Kobber 5BB à l'excès d'aluminium. Marastoni et al. (2020) ont comparé la réponse de la carence en fer chez deux génotypes de porte-greffe tolérants (Ramsey et 140R). L'étude du métabolome des exsudats a montré des stratégies communes pour l'acquisition du Fe telles que la réduction de la concurrence microbienne pour cet élément en limitant l'exsudation d'acides aminés et de sucres, mais aussi grâce à l'augmentation de composés permettant la réduction de l'oxyde de fer. Cependant, ils montrent que les deux porte-greffes réalisent des ajustements spécifiques de leur profil d'exsudation, tels que ceux observés au niveau de certains acides aminés (e.g. enrichissement de la L-tyrosine chez Ramsey contre la L-histidine et la L-méthionine chez 140R). Enfin, nous avons récemment étudié l'exsudation des strigolactones (SL) chez RGM et 1103P cultivés dans un système hydroponique en réponse à la disponibilité en azote (Lailheugue et al., 2023). Dans un premier temps, nous avons identifié deux formes de SL non-canoniques dans les exsudats de RGM grâce à une approche de LC-MS/MS. Nos résultats suggèrent que l'une correspond à l'héliolactone et l'autre à une forme de SL encore inconnue. Nous l'avons donc baptisé « Vitislactone ». Dans un second temps, l'analyse LC-MS/MS a montré que la Vitislactone était exsudée dans des proportions similaires entre les deux génotypes, avec une augmentation significative en condition de carence azoté. Cependant, l'héliolactone a été détectée uniquement chez RGM, principalement en condition de carence azotée. Ces résultats suggèrent que l'héliolactone est spécifiquement produite par RGM ou que ce composé est présent à des niveaux trop faibles pour sa détection chez 1103P. Caractériser le métabolome des racines et de la rhizosphère de différents porte-greffes pourrait représenter une voie prometteuse pour comprendre l'influence qu'il exerce sur la composition microbienne du système racinaire de la vigne. À notre connaissance, aucune étude n'a réalisé la caractérisation des métabolites de la rhizosphère et des racines en parcelle, notamment entre différents génotypes de porte-greffes. Caractériser le métabolome du système racinaire par une approche non ciblée (LC-MS/MS), afin de le relier avec la composition taxonomique des communautés microbiennes qu'il abrite au sein de la rhizosphère et de l'endosphère racinaire, permettrait l'étude plus holistique des interactions entre le microbiote du système racinaire et la plante, et donc du microbiome.

IV) Les objectifs de la thèse

Comprendre les interactions entre la vigne greffée et le microbiote du sol est indispensable pour proposer des techniques innovantes et efficaces pour l'adaptation de la viticulture aux enjeux actuels. Dans ce cadre, l'influence des génotypes du plant greffé, et plus particulièrement celui du porte-greffe, en contact direct avec le sol, revêt une importance fondamentale. En effet, il est nécessaire de comprendre comment le porte-greffe interagit avec ce microbiote afin de définir des stratégies d'amélioration variétale ou de savoir quel génotype interagira le mieux (i.e. attirera un microbiote bénéfique) avec un microbiote existant dans une parcelle, ou avec un consortium de micro-organismes stimulateurs de croissance ou des défenses de la plante. Comme cela a été dit précédemment, les travaux publiés actuellement par différentes équipes internationales semblent montrer une influence du porte-greffe et du greffon. Cependant, l'influence réciproque des deux partenaires n'est pas toujours clairement démontrée. Par ailleurs il est difficile de comparer ces études à cause de différences dans les méthodologies d'analyses employées, les micro-organismes et les compartiments du système racinaire étudiés, les génotypes utilisés, ainsi que les contextes pédoclimatiques des parcelles analysées. De plus, la plupart de ces études se sont concentrées sur l'identification des microorganismes, quand très peu d'entre elles se sont intéressées aux mécanismes impliqués dans la sélection de ces communautés microbiennes, ainsi que leurs rôles sur l'environnement et sur la plante. Enfin, l'influence du génotype de porte-greffe sur la communauté de CMA reste encore très peu étudiée.

Toutes nos expérimentations ont été conduites sur des échantillons prélevés sur le dispositif GreffAdapt. Cette parcelle expérimentale a été mise en place à Villenave d'Ornon (France) en 2015, afin d'étudier la capacité des porte-greffes à s'adapter au réchauffement climatique. Elle contient 55 génotypes de porte-greffe (30 inscrits au catalogue français et 20 étrangers) greffés avec cinq cépages (Cabernet Sauvignon, Grenache, Pinot noir, Syrah and Ugni blanc). La parcelle est divisée en trois blocs, établie selon la résistivité du sol, contenant chacun cinq répétitions des 275 combinaisons porte-greffe × greffon. Pour étudier les effets du porte-greffe sur les microbiotes du système racinaire, nous avons sélectionné six génotypes contrastés en termes d'origine génétique et de profil physiologique (1103P, 3309C, 41B MGt, Nemadex, RGM et SO4), greffés avec le Cabernet Sauvignon (CS). Pour étudier l'influence du greffon, nous avons choisi de travailler sur les cinq cépages de la parcelle, greffés sur RGM.

Introduction

Les objectifs de ma thèse étaient : (i) d'étudier l'influence des deux génotypes du plant greffé de vigne sur la composition du microbiote du système racinaire de la vigne, (ii) comparer la capacité d'association des CMA avec le système racinaire de différentes combinaisons porte-greffe × greffon, (iii) caractériser le rôle fonctionnel des micro-organismes du système racinaire et (iv) de comparer chez les six génotypes de porte-greffe les profils métaboliques des racines et leurs exsudats, afin de potentiellement la relier avec la composition taxonomique de la rhizosphère et de l'endosphère racinaire.

Dans le premier chapitre, nous avons étudié l'influence des génotypes de porte-greffe et de greffons de vigne sur la composition des microbiotes bactériens et fongiques, y compris des CMA, du système racinaire. Pour cela, des échantillons de rhizosphère et de racines ont été prélevés en mai 2021, chez 10 combinaisons de porte-greffe × greffon, présentes sur deux blocs de la même parcelle (i.e. GreffAdapt, blocs 2 et 3). Les communautés microbiennes de la rhizosphère ont alors été analysées grâce des approches de cultivable et de qPCR dans la rhizosphère, ainsi qu'une approche de métabarcoding en ciblant les gènes codant l'ARNr 16S des bactéries, les séquences ITS des champignons et l'ARNr 28S des CMA, dans les deux compartiments du système racinaire. Les fonctions des communautés bactériennes et fongiques ont ensuite été prédites *in silico*. Enfin, nous avons étudié l'existence de corrélations entre les variables mesurées pour caractériser la composition des microbiomes avec le phénotype ou le statut nutritionnel de la plante (Figure 20).

Dans le second chapitre, nous avons souhaité confirmer ou non l'influence des deux composants du plant greffé sur la communauté de CMA présente au sein de l'endosphère racinaire. Pour cela, nous avons prélevé en septembre 2021 des échantillons de racines des 10 mêmes combinaisons de porte-greffe × greffon, cette fois-ci réparties sur le 3ème bloc de la parcelle GreffAdapt (bloc 1). La diversité des CMA a été étudiée par une approche de métabarcoding, en ciblant cette fois-ci le gène codant l'ARNr 18S. En parallèle, la même analyse a été réalisée en ciblant celui codant l'ARNr 28S, seulement chez les six porte-greffes (greffés avec le Cabernet-Sauvignon), afin de comparer les méthodes entre elles, ainsi qu'avec les résultats obtenus lors du premier prélèvement pour l'effet du porte-greffe. De plus, la capacité de mycorhization du système racinaire des 10 combinaisons a été quantifiée par microscopie. Enfin, nous avons établi des corrélations entre la diversité et la quantité de CMA au sein des racines avec le phénotype ou le statut nutritionnel de la plante (Figure 20).

Introduction

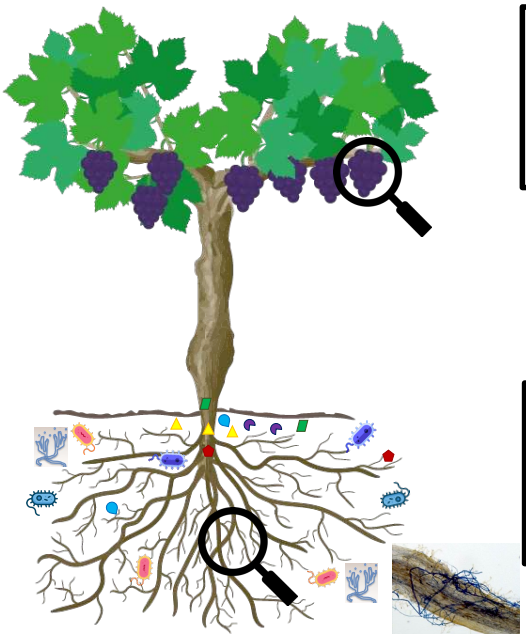
Dans le troisième chapitre, nous nous sommes concentrés exclusivement sur l'effet du porte-greffe sur la composition des bactéries, des champignons et des CMA, associés au sol brut, à la rhizosphère, ainsi qu'à l'endosphère racinaire. Ici, nous avons collecté les échantillons en octobre 2022 chez les six mêmes porte-greffes (greffés avec CS) sur les trois blocs de la parcelle. Les communautés microbiennes ont été quantifiées par qPCR dans le sol et la rhizosphère. La diversité des communautés a été analysée par une approche de métabarcoding dans les deux compartiments du sol et l'endosphère racinaire par une approche de métabarcoding en ciblant trois gènes (i.e., ARNr 16S des bactéries, séquences ITS des champignons et ARNr 28S des CMA), ainsi que par une approche de profilage physiologique des communautés microbiennes (CLPP), uniquement dans la rhizosphère. Dans le but de caractériser le rôle du microbiome rhizosphérique dans les cycles biogéochimiques, nous avons réalisé des tests d'activités enzymatiques clefs dans ces processus (i.e., arylamidase, β-glucosidase et phosphatase). De plus, la capacité de mycorhization des racines des différents génotypes a été à nouveau quantifiée par microscopie. La fonction des communautés microbiennes des trois compartiments étudiés a été prédite *in silico* et le même type de corrélations que dans les deux chapitres précédents a été établie. Dans le but de comprendre de comprendre par quel processus les génotypes de porte-greffe influencent les communautés microbiennes au sein du système racinaire, nous avons étudié la composition métabolique du sol, de la rhizosphère et de l'endosphère racinaire par une approche de LC-MS/MS non ciblée (Figure 20).

Dans une dernière partie, nous ferons la synthèse des résultats acquis pendant la thèse. Nous discuterons ensuite de comment assurer la continuité des travaux réalisés, ainsi que de l'amélioration de l'étude du microbiome racinaire chez la vigne. Enfin, nous ferons une brève conclusion dans laquelle nous discuterons des perspectives de ce travail.

Parcelle GreffAdapt - INRAe Bordeaux

I et II
5 cépages:
- Grenache
- Pinot noir
- Syrah
- Ugni blanc
greffés sur RGM

I, II et III
6 porte-greffes (PG) :
-1103P
- 3309C
- 41B
- Nemadex
- RGM
- SO4
greffés avec CS



I, II, III
Phénotypage:
- Croissance
- Rendement
- qualité
- stress hydrique

I, II, III
Sol:
- Analyses physico-chimiques
- Fosses pédologiques
- Résistivité

Bactéries, Champignons, CMA dans la rhizosphère et les racines	**CMA dans les racines**	**Bactéries, Champignons, CMA dans le sol brut, la rhizosphère et les racines**
I : Influence des génotypes de porte-greffe et de cépage de la vigne sur les microbiotes de la rhizosphère et de l'endosphère racinaire **Mai 2021, Blocs 2 et 3** **Méthodes:** - qPCR / Cultivable - Métabarcoding (16S bactéries, ITS champignons, 28S AMF) + prédiction *in silico* des fonctions microbiennes - Corrélation microbiomes et phénotype/nutrition minérale de la plante **Résultats :** → La rhizosphère et l'endosphère racinaire présentent des communautés microbiennes distinctes. → Le PG et le cépage influence la composition et le rôle des communautés bactériennes des deux compartiments. → Effet PG > Effet cépage → Le porte-greffe influence la composition des CMA de l'endosphère racinaire. → Corrélation microbiomes avec croissance et nutrition de la plante	**II : Influence des génotypes du plant greffé de vigne sur la communauté de CMA des racines** **Octobre 2021, Bloc 1** **Méthodes:** - Métabarcoding: (28S et 18S AMF) - Microscopie **Résultats :** → Pas d'effet du PG et du cépage sur la capacité de mycorhization des racines. → Le choix du gène ciblé en métabarcoding peut impacter les résultats. → Confirmation de l'effet du porte-greffe sur la diversité des CMA de l'endosphère racinaire. → Le greffon exerce peu ou pas d'effet. → Corrélation entre la communauté de CMA des racines et la croissance de la plante	**III : Mécanismes moléculaires des impliqués dans la sélection des microorganismes du sol par le porte-greffe de vigne** **Octobre 2022, Bloc 1, 2 et 3** **Méthodes:** - qPCR - Métabarcoding (16S bactéries, ITS champignons, 28S AMF) + prédiction *in silico* des fonctions microbiennes - Tests enzymatiques / Biolog -LC-MS/MS **Résultats :** → Confirmation de l'effet du PG sur la diversité des bactéries, des champignons et des CMA du système racinaire. → Corrélations composition des microbiotes avec la croissance la plante. → Effet du porte greffe sur l'activité d'enzymes microbiennes impliquées dans plusieurs cycles biogéochimiques. → Différences dans le métabolome du système racinaire entre PG? Corrélation avec la composition des microbiotes?

Figure 0-20 : Schéma récapitulatif des expérimentations menées dans les trois chapitres de la thèse.

Chapitre 1 : Influence des génotypes de porte-greffe et de greffon de la vigne sur la composition des microbiotes de la rhizosphère et de l'endosphère racinaire

Préface

Il est aujourd'hui admis que les microorganismes du sol s'associant avec le système racinaire de la vigne jouent un rôle clef dans la croissance et le développement de la plante, ainsi que son adaptation au contraintes environnementales. Comprendre le rôle des deux composants du plant greffé sur la sélection des microorganismes du sol revêt donc une importance fondamentale. Dans ce premier chapitre, l'objectif était d'étudier l'influence des génotypes de porte-greffe et de greffons de vigne sur la composition des microbiotes bactériens et fongiques, y compris des CMA, du système racinaire. Pour cela, des échantillons de rhizosphère et de racines ont été prélevés en mai 2021, chez 10 combinaisons de porte-greffe × greffon, présentes simultanément sur les blocs 2 et 3 du dispositif GreffAdapt. Pour étudier l'effet du porte-greffe, nous avons travaillé sur six porte-greffes (1103P, 3309C, 41B, Nemadex, RGM, SO4) présentant des origines génétiques distinctes, ainsi que des réponses contrastées dans la tolérance à la sécheresse et à la vigueur conférée au greffon, greffés avec le cépage Cabernet Sauvignon. Pour mettre en évidence l'effet du cépage, nous avons étudié les cinq cépages du dispositif (Cabernet Sauvignon, Grenache, Pinot noir, Syrah et Ugni blanc), greffés sur RGM. Les microorganismes de la rhizosphère alors été quantifiés grâce des approches de cultivable et de qPCR dans la rhizosphère. Nous avons ensuite réalisé une approche de métabarcoding en ciblant les gènes codant l'ARNr 16S des bactéries, les séquences ITS des champignons et l'ARNr 28S des CMA, pour étudier la diversité des communautés microbiennes dans la rhizosphère et l'endosphère racinaire. Les fonctions des communautés bactériennes et fongiques ont ensuite été prédites *in silico*. Enfin, nous avons étudié l'existence de corrélations entre les variables mesurées pour caractériser la composition des microbiomes avec le phénotype ou le statut nutritionnel de la plante. Nos résultats montrent la capacité des génotypes de porte-greffe et de cépage de la vigne à recruter différentes communautés fonctionnelles de micro-organismes, affectant la croissance de l'hôte et son adaptation à l'environnement, avec un effet plus important du génotype de porte-greffe. Après relecture par les co-auteurs et quelques corrections mineures, nous souhaitons publier ce chapitre en tant qu'article au sein de la revue « Environmental Microbiome ».

Chapitre 1

The genotypes of the two components of grafted grapevines influence the rhizosphere and root endophyte microbiomes, with rootstocks having a greater impact

Vincent Lailheugue, Romain Darriaut[1], Joseph Tran, Marine Morel, Elisa Marguerit, Virginie Lauvergeat*

EGFV, Univ. Bordeaux, Bordeaux Sciences Agro, INRAE, ISVV, F-33882 Villenave d'Ornon, France

* corresponding author: virginie.lauvergeat@inrae.fr

[1] Present address : Univ Rennes, CNRS, ECOBIO (Ecosystèmes, biodiversité, évolution) - UMR 6553, F-35000 Rennes, France

Abstract:

Background

Soil microorganisms play an extensive role in the biogeochemical cycles providing the nutrients necessary for plant growth. Root-associated bacteria and fungi, originated from soil, are also known to influence host health. In response to environmental stresses, the plant roots exude specific molecules influencing the composition and functioning of the rhizospheric and root microbiomes. This response is host genotype-dependent and is affected by the soil microbiological and chemical properties. It is essential to unravel the influence of grapevine rootstock and scion genotypes on the composition of this microbiome, and to investigate this relationship with plant growth and adaptation to its environment. Here, the composition and the predicted functions of the microbiome of the root system were studied using metabarcoding on ten grapevine scion × rootstock combinations grown on the same plot, in addition to plant growth and nutrition measurements.

Results

The rootstock genotype significantly influenced the composition of the bacterial and fungal microbiome and its predicted functioning in rhizosphere and root compartments when grafted with the same scion cultivar. Based on β-diversity analyses, 1103P rootstock showed distinct bacterial and fungal communities compared to the five others (RGM, SO4, 41B, 3309C and Nemadex). The influence of the scion genotype was more variable depending on the community and the investigated compartment. Its contribution was primarily observed on the β-diversity measured for bacteria and fungi in both root system compartments, as well as for the AMF in the rhizosphere. Significant

correlations were established between microbial variables and the plant phenotype, as well as with the plant mineral status measured in the petioles and the roots.

Conclusion: These results shed light on the capacity of grapevine rootstock and scion genotypes to recruit different functional communities of microorganisms, which affect host growth and adaptation to the environment. Selecting rootstocks capable of associating with positive symbiotic microorganisms is an adaptation tool that can facilitate the move towards sustainable viticulture and help cope with environmental constraints.

Keywords: Bacteria, Fungi, Arbuscular Mycorrhizal Fungi**,** root system, metabarcoding, PICRUSt2, FUNGuild

Chapitre 1

Background

Grapevine is a cultivated perennial plant of major economic interest. In 2022, the International Organization of Vine and Wine estimated the world vineyard surface area to be 7.3 mha, producing 258 mhl of wine with a world trade volume of 107 mhl, representing €37.6 bn. Since the phylloxera crisis at the end of the 19th century, *Vitis vinifera* has mostly been cultivated by grafting on to species or hybrids of American *Vitis* rootstock (Ollat et al., 2017). Market globalization and the rapid industrialization of agricultural sectors have introduced new requirements for winegrowers. Sustainable agriculture means limiting the use of chemical fertilizers and pesticides, while maintaining yields and berry quality. In addition, global warming is causing higher temperatures and radiation, as well as changes in precipitation patterns, resulting in severe drought periods that have negative impacts on vine development (Van Leeuwen et al., 2019). Viticulture adaptation is currently based on the modification of cultivation practices or of the plant material such as the rootstock or scion genotypes (Bucur and Dejeu, 2022; Cataldo et al., 2021).

Plants closely interact with various microorganisms such as bacteria, fungi, archaea, protists, or viruses, known as plant microbiota. It is now well established that microbial communities play indisputable roles in supporting grapevine health and adaptation to environmental conditions (Darriaut et al., 2022b; Dries et al., 2021). This awareness led to the emergence of the "holobiont" concept, which considers the multicellular host and its associated microbiota as a functional entity (Hassani et al., 2018). In the rhizosphere, defined as the area of soil immediately surrounding the roots, several microorganisms interact, directly or not, with the root system. Some of them can reach the root endosphere through intercellular junctions in the epidermis or wounds on the rhizoplane (Bettenfeld et al., 2022). On one hand, soil microorganisms can be detrimental for grapevine longevity and productivity. For example, pathogenic fungi cause trunk diseases such as Esca complex, Phomopsis, Eutypa or Botryosphaeriae dieback in established vineyards, as well as Petri disease or Black foot in young vineyards (Fontaine et al., 2016). On the other hand, several microorganisms provide benefits to the plant in terms of biofertilization, biostimulation and biocontrol properties. For instance, plant growth promoting rhizobacteria (PGPR) can increase plant nutrient uptake by solubilizing non-assimilable forms of phosphorus into plant-assimilable forms or by fixing atmospheric nitrogen (Sabir et al., 2012). Other PGPR can interfere with phytohormone homeostasis or synthetize pseudo-phytohormones, promoting plant growth and adaptation to environmental stresses (Salomon et al., 2014). Mechanisms used by bacteria to counter pathogens are antibiosis, suppression of virulence factors, niche competition and activation of the plant-induced systemic resistance (Compant et al.,

2013). As reviewed by Trouvelot et al. (2015), viticulture adaptation can benefit from arbuscular mycorrhizal fungi (AMF). They improve grapevine development by improving access to soil nutrients and regulation of plant nutrient transporters, primarily for phosphorus and nitrogen. These root symbionts can increase grapevine tolerance to drought, iron deficiency in calcareous soil, soil salinity or heavy metals. Besides abiotic stresses, AMF also confer tolerance to biotic stressors thanks to the mycorrhiza-induced resistance (MIR) and/or the systemic acquired resistance (SAR) (Trouvelot et al., 2015).

In response to the environment, plant roots exude a wide range of chemical compounds into the rhizosphere, including small molecules (e.g., organic acids, sugar, aliphatic acids, fatty acids, amino acids, flavonoids, and secondary metabolites) and complex molecules (e.g., proteins and mucilage) (Jamil et al., 2022). Rhizodeposits influence the biology of microorganisms in the rhizosphere as a source of carbon, antimicrobial or chemoattractant compounds (Philippot et al., 2013). Plant hormones are also involved in plant × microorganism interactions, such as strigolactones, which have been reported to stimulate hyphal branching in AMF (Yoneyama et al., 2018). The composition of root exudate is mainly influenced by edaphic (properties, nutrients, indigenous microorganisms) and plant factors (species, phenophase, root morphology), including host genotype (Ma et al., 2022). Selecting genotypes with a low capacity for association with pathogenic organisms, or conversely, with high capacity for association with symbiotic organisms, could help overcome some of the challenges facing viticulture.

Few studies have been published in recent years on the effects of grapevine rootstock genotype on root and/or rhizosphere microbiota composition. Analyses of metabarcoding data targeting bacterial communities only (D'Amico et al., 2018; Dries et al., 2021, Marasco et al., 2018) or bacterial and fungal communities (Berlanas et al., 2019; Swift et al., 2021; Marasco et al., 2022; Wright et al., 2022) show that rootstock genotype influences the rhizosphere microbiota diversity and community structure. Marasco et al. (2022) further displayed that this genotype-dependent effect was also present for the bacterial and fungal communities of the root endosphere. In their study, seven graft/stock combinations from ten vineyards in two geographical areas of Italy were analyzed. The results show that while the major factors driving microbial community structure are soil type and cultivation practices, the interaction of the two genotypes is the second driver, even more than each genotype separately. These results confirm those obtained by Vink et al. (2021), who studied bacterial communities in the rhizosphere of four cultivars combined with four rootstocks in the same vineyard. However, given that soil quality is the most significant factor influencing the microbiota of viticultural

soils (Darriaut et al., 2023) and therefore that of the root system, it is very difficult to compare the structure and function of the microbiota of different genotypes between all these studies. Finally, only one study investigated the AMF communities of grapevine roots from three vineyards and nine rootstocks by DGGE and trap cultures (Moukarzel et al., 2021a). The authors demonstrated that the rootstock genotype significantly influenced the AMF community colonizing the roots.

The current aim is to explore the greatest possible genetic variability of grapevine rootstocks to identify those capable of recruiting the most effective functional microbiota in response to environmental constraints, and to test the influence of scion cultivars on these responses. This also requires further knowledge of the links between community structure and biological function, and the potential impact on vine growth and resistance. First, we quantified the level of rhizosphere bacteria and fungi using qPCR and cultivable approaches. Secondly, the communities of bacteria, fungi, and AMF in the rhizosphere and the root endosphere were explored using Illumina sequencing of the 16S rRNA gene, ITS and 28S rRNA gene, respectively. Finally, the functions of bacterial and fungal microbiome were predicted using PICRUSt2 and FUNGuild respectively, and microbial variables measured in both microbiomes were correlated to plant phenotypic traits and mineral nutrition.

Materials and methods

Plot, plant material and phenotyping

The experiment was set up in Bordeaux, France (44°47'26.6"N 0°34'26.7"W), in GreffAdapt plot, a large-scale experimental plot designed with 55 rootstocks grafted with five scions, divided into three blocks of five vines per combination, i.e., 15 vines per combination, distributed randomly within each block (Marguerit et al., 2019). The climate is oceanic, with mild winters and high rainfall. The study was carried out in May 2021. The plot was planted with a density of 6,666 vines/ha and is pruned using the simple Guyot method and trained with a vertical trellis system. A natural cover crop is planted on each row and is mowed according to grass growth. The inter-rows are not tilled, but the area under the vines is tilled mechanically. Fungicide treatments are applied regularly to limit the development of downy and powdery mildew during the vegetative period. Phenotypic monitoring was carried out annually on the vines. This included the number of shoots, fertility (number of bunches per shoot), winter pruning weight and the vigor conferred (pruning weight / number of shoots). The number of bunches, berry yield and $\delta^{13}C$ of berry juice were assessed at the harvest, when the berries from the different scions were at maturity (between August and October). Mineral content in the petioles (collected between the fourth and sixth leaf of the shoot on the cane side) and the roots were assessed by Waypoint Analytical (Virginia, USA). We selected six rootstocks' genotypes, presenting contrasting drought tolerance and vegetative vigor conferred to the scion (Supplementary Table 1), grafted with Cabernet-Sauvignon (CS) clone 169, to study the impact of the rootstock genotype on the rhizosphere and root endophyte microbiomes: 1103 Paulsen (1103P), 3309 Couderc (3309C), 41 B Millardet et de Grasset (41 B), Nemadex Alain Bouquet (Nem), Riparia Gloire de Montpellier (RGM) and Selection Oppenheim 4 (SO4). To evaluate the effect of the scion, we focused on one of these rootstocks (RGM) grafted with the five grape varieties: CS, Grenache (Gre), Pinot noir (PN), Syrah (Syr) and Ugni blanc (UB) (Supplementary Table 1). Six individuals were sampled for each scion × rootstock combination, three on block 2 and three on the block 3. Blocks 2 and 3 correspond to different areas on the plot designed according to the soil resistivity. Aurea Agrosciences (Orléans, France) assessed the soil properties and defined them as sandy gravelly soil in both blocks (Supplementary Table 2).

Sample collection and processing

Roots from different parts of the root system with attached soil particles were collected at a depth of 20-30 cm in sterile tubes containing 40 ml of 0.85% NaCl, placed in a cooler before being processed in the laboratory. To separate the rhizosphere from the roots, the samples were vortexed for 5 min and

then centrifuged at 4000 g for 5 min. The roots were transferred into a new tube before discarding the supernatant to keep only the rhizosphere. One gram of rhizosphere was diluted into 9 ml of physiological solution for the plating approach and the rest was lyophilized and stored at -80°C before DNA extraction. To investigate endophyte microorganisms, root tissues were surface sterilized by soaking in 3% sodium hypochlorite (NaClO) for 1 min, followed by 3% H_2O_2 for 1 min and finally by washing with sterile distilled water five times. Sterilized roots were grounded in 35-ml stainless-steel grinding jars with 20-mm stainless steel balls at 30 oscillations per second for 30 sec with the mixer mill MM400 (Retsch, Haan, Germany), using liquid nitrogen and then stored at -80°C until DNA extraction.

Quantification of cultivable bacteria and fungal colonies in the rhizosphere

The rhizosphere was vortexed, and the supernatant was serially diluted in 0.85% NaCl to 1/100 for the fungi and to 1/10 000 for the bacteria before plating 100 µl of each dilution. Cultivable bacteria were quantified on R2A medium (0.5% yeast extract, 0.5% proteose peptone, 0.5% casamino acids, 0.5% glucose, 0.5% soluble starch, 0.3% sodium pyruvate, 0.3% H_2KO_4P, 0.05% $MgCl_2$, pH 7) supplemented with nystatin (25 mg. l^{-1}). Cultivable fungi were quantified on Potato Dextrose Agar medium (BioKar) supplemented with 500 mg l^{-1} of gentamicin and 50 mg l^{-1} of chloramphenicol. Incubation was done at ambient temperature in the dark and the colony-forming units (CFUs) were counted five and seven days after fungal and bacterial plating, respectively.

DNA extraction from roots and soil samples

DNA of root tissues was extracted from 150 mg of frozen powder using the DNeasy® Plant Mini kit (Qiagen) with a modified protocol adapted from Pouzoulet et al. (2013). At step two, the root powder was incubated for 30 min in 1 ml of CTAB buffer (2% CTAB, 2% PVPP, 1.4 M NaCl, 100 mM Tris, 20 mM EDTA) supplemented with 0.2% β-mercaptoethanol and 0.16% RNase A (100 mg. ml^{-1}). At step three, 325 µl of buffer P3 was used and the incubation step on ice was increased to 10 min. At step four, the lysate was centrifugated at 6500 g for 10 min. At step six, the AW1 buffer was replaced by the AW2 buffer. At step eleven, DNA was eluted in 50 µl of buffer AE and step twelve was deleted. DNA from the rhizosphere was extracted from 250 mg of lyophilized soil using DNeasy® PowerSoil® Pro kit (Qiagen) according to the manufacturer's instructions with some adaptations. The vortex step was replaced by three 30-second runs, each on power 4 m. s^{-1} with the homogenizer FastPrep®-24. At step thirteen, an extra wash was performed using 350 µL of C5 solution. At step sixteen, DNA was eluted twice into a final volume of 80 µL of C6 solution. Extracted DNA was quantified on a Qubit® 3.0 fluorometer (Thermo Fisher Scientific) using the Qubit™ dsDNA HS Assay Kit, and its quality

was checked using a NanoDrop™ 2000/2000c spectrophotometer (Thermo Fisher Scientific). DNA was then stored at -20 °C until further use.

Quantitative PCR (qPCR) amplification of bacterial and archaeal 16S and fungal 18S rRNA genes

Analyses of qPCR were performed on the DNA extracted from the rhizosphere using primers and cycling conditions described in Darriaut et al. (2021). The primer pairs 515R/341F, FR1/FF390 and Arch967F/Arch1060R were used to amplify bacterial 16S rRNA, fungal 18S rRNA and archaeal 16S rRNA genes, respectively. Reactions were carried out in a final volume of 20 µl composed of 10 µl of GoTaq® qPCR Master Mix (Promega), 1 µl of each primer (10 µM), 7 µl of nuclease-free water and 1 µl of extracted DNA (1 ng. μl^{-1}). Standards used for absolute quantification were obtained from amplicons previously subcloned into pGEM®-T easy vector system (Promega) by Darriaut et al. (2021). Each sample was quantified in triplicates using the CFX96 Touch Real-Time PCR Detection System (Bio-Rad Laboratories, France). The efficiencies of the qPCR were between 80% and 99% (R^2 > 0.99). All analyses included PCR negative and positive controls.

Target metabarcoding on bacterial 16S rRNA gene, fungal ITS region and Glomeromycete 28S rRNA gene

The bacterial 16S rRNA gene was amplified using the primer pair 341F/785R, while the fungal ITS1 region was amplified using the ITS1F/ITS2 primer pair. PCR reactions were monitored in a final volume of 25 µl composed of 5 µl of 5X GoTaq® colorless reaction buffer (Promega, France), 0.5 µl of each primer (10 µM), 0.5 µl of dNTPs (10 mM), 0.125 µl of GoTaq® G2 DNA Polymerase (Promega, France), 1 µl (at 1 ng.μl^{-1}) or 2.5 µl (at 5 ng.μl^{-1}) of DNA extracted from roots or soil respectively, and nuclease-free water (q.s.p 25 µl). The fungal 28S rRNA gene was amplified using a nested PCR approach to target the *Glomeromycota* division. A first PCR was performed using the primer pair LR1/NDL22 specific to the eukaryote 28S rRNA gene. The obtained product was diluted to 1/100th and 5 µl were used as template for the second PCR using the primer pair FLR3/FLR4 specific to *Glomeromycota*. All analyses included PCR negative and positive controls. The sequences of the Illumina adapters and the primers, as well as the cycling conditions are listed in Supplementary Table 3. Further steps were carried out at the Plateforme Génome Transcriptome de Bordeaux (Cestas, France). The PCR products were purified with the platform-specific SPRI magnetic beads (1X ratio) and quantified using Quant-iT™ dsDNA assay kit (ThermoFisher, France). MID and Illumina sequencing adapters were added. Libraries were pooled in equimolar amounts using a Hamilton Microlab STAR robot and sequenced on an Illumina MiSeq platform using the MiSeq Reagent Kit v2

(2 × 250 bp). Obtained sequences were demultiplexed with index search at the PGTB facility. The quality of the obtained sequences were first checked with FastQC v.0.11.8 (Andrews, 2010). Sequences were quality filtered, trimmed, denoised, and clustered into Operational Taxonomy Units (OTUs) using FROGS pipeline from Galaxy instance (Escudié et al., 2018; Bernard et al., 2021). This involved assembling raw forward and reverse reads for each sample into paired-ended reads with a minimum overlapping of 50 nucleotides and 0.1 mismatch using the VSEARCH tool (Rognes et al., 2016b). Primers were removed using Cutadapt (Martin, 2011), chimeras were detected and removed with UCHIME (Edgar et al., 2011), and clustering was performed using SWARM (Mahé et al., 2014) in the FROGS pipeline. The minimum sequence abundance proportion was set at $5e^{-5}$ to keep OTUs with a minimum prevalence fixed at 4. Taxonomic assignments of 16S rRNA, ITS, and 28S rRNA-based OTUs were performed using Silva138.1 (Quast et al., 2012), Unite8.2 (Nilsson et al., 2019), and MaarjAM (28S) (Öpik et al., 2010), respectively. For the 16S rRNA gene of bacteria, the sequences "multi-affiliated" at the phylum level were removed, as well as those affiliated to grapevine mitochondrial and chloroplastic16S rRNA sequences. As the proportions of host 16S rRNA sequences were important in the root endosphere, the samples from root and rhizosphere were divided before rarefaction at the number of sequences in the sample containing the fewest ones. Only the samples containing more than 4,000 or 250 sequences were kept for the rhizosphere and the root endosphere, respectively. For the fungal ITS region, the sequences "multi-affiliated" or "unidentified" at the phylum level were removed and only the samples containing more than 4,000 sequences were kept. For the 28S rRNA gene of AMF, the sequences affiliated to "New_clade" at the class level were removed and only the samples containing more than 5,000 sequences were kept.

Metabarcoding data processing and prediction of microbial functions

Bacterial functions and pathways were predicted using phylogenetic investigation of communities by reconstruction of unobserved states (PICRUSt2) (Douglas et al., 2020). The tool was run on the FROGS pipeline installed in a Galaxy instance (Escudié et al., 2018). EPA-ng was used to construct the reference tree with a minimum alignment length of 0.8. Bacterial functions abundance was predicted using KO database with a NSTI cut-off set at 0.5, and an identity and coverage alignment cut-off at 0.9. Obtained abundances of pathways were measured using the KEGG database and the final output tables were normalized (values were divided by the sum of columns, then multiplied by 10^6). Only the "Metabolism" and "Environmental Information Processing" classifications were kept for statistical analyses. Fungal trophic modes and guilds were predicted at the genus level using the "funguild_assign" function from the *FUNGuildR* (0.2.0.9000) package and the FUNGuild database (Nguyen et al., 2016). Only the confidence ranking "probable" and "highly probable" were selected

for statistical analyses. OTUs assigned to more than two trophic modes and more than two guilds were classified as "multi-affiliated". The OTUs "unassigned" were removed before comparisons were made.

Statistical analyses

All the statistical analyses were performed on R (v4.2.1) using RStudio (2022.07.1). Figures were generated with *ggplot2* (v3.4.1) and *ggthemes* (v4.0.4) and arranged with *ggpubr* (v0.4.0). Chao1 and Simson indexes were calculated using the "estimate_richness" function and PCoA based on the Bray-Curtis distance were performed using the "plot_ordination" function, both from *phyloseq* (1.38.0) (McMurdie and Holmes, 2013). Linear Discriminant Analysis Effect Size (LEfSe) was carried out using the "run_lefse" function from *microbiomeMarker* (1.2.2) with data transformation (log10), lda_cutoff fixed at 4, kw_cutoff and wilcoxon_cutoff at 0.05 (Cao et al., 2022). For comparisons of α-diversity metrics between the root system compartments, student t-tests or Wilcoxon tests were performed after checking assumptions for parametric tests with Shapiro (normality) and Bartlett (homogeneity of variance) tests, respectively. Two-way Analysis of Variance (ANOVA) with the genotype and block factors were performed on α-diversity metrics, bacterial predicted pathways, and results obtained with cultivable and qPCR approaches. The genotype × block interaction was tested prior to this test. Assumptions for parametric tests were checked on the residuals with Shapiro (normality) and Bartlett (homoscedasticity) tests. Comparison between genotypes were carried out with "pairwise.t.test" or "pairwise.wilcox.test" functions with Bonferroni correction from the *stats* package (4.2.1). To test the effects of the genotype and block on the Bray-Curtis index, Permutational Analysis of Variance (PERMANOVA) with 999 permutations were performed with the "adonis2" function from *vegan* package (2.6.4). Genotypes were then compared together using the "pairwise.adonis2" function from the *pairwiseAdonis* package (0.4.1). Heatmaps were generated using Euclidian distance to compare the abundances of bacterial metabolic pathways between genotypes using the "pheatmap" function from *pheatmap* (1.0.12). The effect of genotypes on the proportion of trophic modes and guilds were assessed with a chi-squared test using "chisq.test" function from *stats* package. PCA were assessed with "PCA" function from *FactoMineR* (2.8) and plotted using "fviz_pca_ind" function from *factoextra* (1.0.7) to compare predicted bacterial functions between genotypes. Matrices showing only the significant correlations were established using the ggcorrplot function from *ggcorplot* (0.1.4) with the "square" method and *p*-values were calculated using the "cor.mtest" function.

Results

Rhizosphere and root endosphere present distinct microbial communities

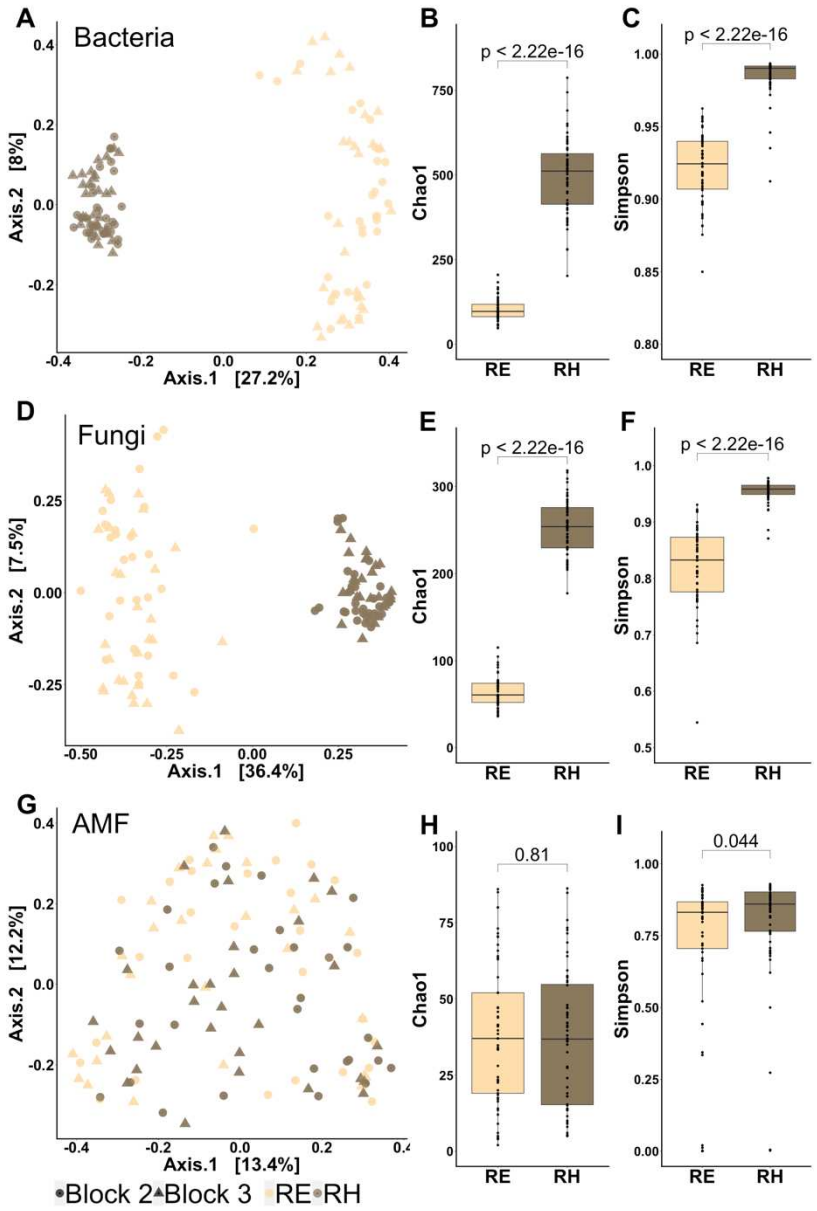


Figure 1-1: Comparison of microbial communities between the root endosphere (RE, light brown) and the rhizosphere (RH, dark brown).
Comparison of β-diversity by principal coordinate analysis (PCoA) of (A) bacterial, (B) fungal and AMF (C) communities based on Bray–Curtis dissimilarity matrices.
Comparison of α-diversity with richness (Chao1) and diversity (Simpson) of bacterial (B, C), fungal (E, F) and AMF communities (H, I). *p*-values were calculated using Student or Wilcoxon tests and were considered as significant when < 0.05 (n=60).

In the root system (rhizosphere and root endosphere), 1450 bacterial OTUs were successfully affiliated to 16 phyla, 41 classes, 85 orders, 115 families, 167 genera and 70 species. The bacterial community associated to the globality of the root system was composed of *Proteobacteria* (43%), *Actinobacteriota* (32%), *Acidobacteriota* (7%), *Chloroflexi* (5%), *Bacteroidota* (3%), *Verrucomicrobiota* (3%), *Firmicutes* (2%), *Myxococcota* (2%), *Planctomycetota* (2%) and other phyla whose proportions were less than 1% (*Dependentiae*, *Desulfobacterota*, *Gemmatimonadota*, *Latescibacterota*, *Methylomirabilota*, *Nitrospirota* and RCP2-54) (Supplementary Figure 1 A). PCoA displayed a strong clustering of the bacterial communities according to the compartments and were primarily differentiated along the first axis (Figure 1 A). A higher dispersion of the individuals was observed in the root endophytes group along the second axis. Bacterial richness (Figure 1 B) and diversity (Figure 1 C), represented by Chao1 and Simpson indexes respectively, were significantly higher in the rhizosphere than in the root endosphere. Bacterial OTUs were primarily exclusives (66%) of the rhizosphere, while 31% were common between the root system compartments and less than 3% were root exclusives (Supplementary Figure 2 A). Root system compartments displayed bacterial dissimilarities at the phylum (Supplementary Figure 1 A) and the class (Supplementary Figure 1 B) levels. The LEfSe detected an enrichment of 7 phyla (*Acidobacteriota*, *Chloroflexi*, *Verrucomicrobiota, Planctomycetota, Firmicutes, Actinobacteriota, Gemmatimonadota*), 10 classes, 16 orders, 17 families, 14 genera and 13 species in the rhizosphere, compared to 3 phyla (*Proteobacteria, Bacteroidota, Dependentiae)*, 5 classes, 8 orders, 14 families, 17 genera, 16 species in the root endosphere (Supplementary Figure 3 A).

Among the fungal community associated with ITS sequencing, 650 OTUs were affiliated with 12 phyla, 31 classes, 69 orders, 115 families, 174 genera and 302 species. The root system community was composed of *Ascomycota* (60%), *Basidiomycota* (22%), *Rozellomycota* (11%), *Mortierellomycota* (5%), *Glomeromycota* (2%) and other phyla whose proportions were less than 1% (*Blastocladiomycota*, *Calcarisporiellomycota*, *Chytridiomycota*, *Kickxellomycota*, *Mucoromycota*, *Olpidiomycota*, *Zoopagomycota*) (Supplementary Figure 1 C). PCoA enabled separation of the fungal community into two groups corresponding to the compartments of the root system, with the same profile as that observed for bacteria (Figure 1D). Fungal richness (Figure 1 E) and diversity (Figure 1 F) were significantly higher in the rhizosphere than in the root endosphere. Amongst the root system compartments, 62% of the fungal OTUs were shared, with 38% and less than 1% specific to the rhizosphere and the root endosphere, respectively (Supplementary Figure 2 A). Dissimilarities were observed at the phyla (Supplementary Figure 1 C) and the class (Supplementary Figure 1 D) levels between the root system compartments. LEfSe showed an enrichment of 2 phyla (*Ascomycota,*

Mortierellomycota), 5 classes, 9 orders, 12 families, 12 genera and 10 species in the rhizosphere. In the root endosphere, 2 phyla (*Glomeromycota, Basidiomycota)*, 5 classes, 7 orders, 9 families, 12 genera and 14 species were enriched (Supplementary Figure 3 B).

In the fungal sub-group of AMF, 230 OTUs were affiliated to 1 phylum, 2 classes, 3 orders, 5 families, 8 genera, and 40 species. The AMF genera were represented by *Glomus* (86%), *Claroideoglomus* (3%), *Paraglomus* (2%), *Scutellospora* (2%), multi-affiliated genera (6%), and other genera whose proportions were less than 1% (*Acaulospora*, *Rhizophagus*, and *Septoglomus*) (Supplementary Figure 1 E). No segregation of the root system compartments was observed with the PCoA (Figure 1 G). Although no significant difference was observed for the Chao1 index (Figure 1 H) between root system compartments, the Simpson index (Figure 1 I) was significatively higher in the rhizosphere than in the roots. Amongst both root and rhizosphere compartments, 88% of AMF OTUs were shared, with 11% and less than 1% specific to the rhizosphere and the root endosphere, respectively (Supplementary Figure 2 A). The abundance graph at the genus level showed different proportions of AMF between root endosphere and rhizosphere compartments (Supplementary Figure 1 E). LEfSe revealed an enrichment of 1 order (*Paraglomerales*), 2 families (*Paraglomeraceae* and *Claroideoglomeraceae*), 2 genera and 2 species in the rhizosphere, compared to 1 order (*Glomerales*) and 1 family (*Glomeraceae*) in the root endosphere (Supplementary Figure 3 C). Although the differences amongst the root system compartments were less evident for the AMF, we decided to separate the root endosphere and the rhizosphere in the following analyses for the three groups of microorganisms.

Chapitre 1

Rootstock and scion genotypes influence the bacterial community of the rhizosphere and the root endosphere

Table 1-1: Influence of the rootstock and the scion genotypes on the α-diversity (richness = Chao1, diversity= Simpson) and the β-diversity metrics (Bray-Curtis dissimilarity) amongst bacteria, fungi and AMF, in the rhizosphere (RH) and the root endosphere (RE).

			Influence of the rootstock								Influence of the scion							
			Chao1			Simpson			Bray-Curtis		Chao1			Simpson			Bray-Curtis	
			p-value		PVE	*p*-value		PVE	*p*-value	PVE	*p*-value		PVE	*p*-value		PVE	*p*-value	PVE
Bacteria		Genotype (G)	**1.69e-08**	***	**73%**	**2.99e-4**	***	**53%**	**0.001**	**50%**	0.574	ns	/	**0.008**	**	**41%**	**0.002**	**25%**
	RH	Block (B)	**0.012**	*	**5%**	0.485	ns	/	**0.003**	**7%**	**0.001**	***	**36%**	0.408	ns	/	**0.019**	**6%**
		G x B	**1.85e-05**	***	**15%**	0.919	ns	/	**0.001**	**17%**	**0.031**	*	**22%**	0.749	ns	/	**0.001**	**33%**
	RE	G	0.663	ns	/	**0.018**	*	**29%**	**0.001**	**42%**	0.469	ns	/	0.632	ns	/	**0.004**	**24%**
		B	0.826	ns	/	**0.002**	**	**19%**	**0.019**	**4%**	0.861	ns	/	0.483	ns	/	**0.044**	**6%**
		G x B	0.644	ns	/	0.512	ns	/	**0.045**	**12%**	0.476	ns	/	0.318	ns	/	**0.001**	**25%**
Fungi	RH	G	0.141	ns	/	**0.007**	**	**40%**	**0.001**	**42%**	0.990	ns	ns	0.232	ns	/	**0.001**	**30%**
		B	**0.008**	**	**18%**	0.590	ns	/	**0.002**	**6%**	0.193	ns	ns	0.754	ns	/	**0.001**	**7%**
		G x B	**7.67e-06**	***	**45%**	0.168	ns	/	**0.001**	**19%**	**1.79e-4**	***	**60%**	**0.045**	*	**30%**	**0.001**	**29%**
	RE	G	**0.001**	**	**49%**	0.052	ns	/	**0.001**	**33%**	0.490	ns	/	0.727	ns	/	**0.002**	**24%**
		B	0.897	ns	/	0.389	ns	/	**0.008**	**5%**	0.558	ns	/	0.318	ns	/	**0.015**	**7%**
		G x B	0.729	ns	/	0.694	ns	/	**0.001**	**19%**	0.279	ns	/	0.136	ns	/	**0.001**	**26%**
AMF	RH	G	0.395	ns	/	0.239	ns	/	**0.001**	**23%**	0.409	ns	/	0.471	ns	/	**0.001**	**22%**
		B	0.373	ns	/	**0.033**	*	**12%**	**0.042**	**4%**	0.284	ns	/	0.489	ns	/	0.438	ns	/
		G x B	0.194	ns	/	0.056	ns	/	**0.006**	**17%**	0.374	ns	/	0.284	ns	/	**0.031**	*	**16%**
	RE	G	**0.007**	**	**41%**	**0.013**	*	**37%**	**0.031**	**19%**	0.191	ns	/	0.516	ns	/	0.137	ns	/
		B	0.385	ns	/	0.210	ns	/	0.523	ns	/	0.997	ns	/	0.174	ns	/	0.299	ns	/
		G x B	0.131	ns	/	0.233	ns	/	0.278	ns	/	0.548	ns	/	0.098	ns	/	**0.002**	**	**24%**

Significances were assessed through a Two-way ANOVA. Asterisks represent significant effects * *p*-value <0.05, ** *p*-value <0.01, *** *p*-value <0.001, PVE : Percentage of variance explainedn ns = non-significant.

When the bacterial communities of the six rootstocks grafted with CS were assessed, no effect of the rootstock genotype was observed on the rhizosphere bacteria level with both cultivable and qPCR methodologies (Supplementary Table 4, Supplementary Figure 4 A). The rootstock genotype, the block, and the factor combinations significantly influenced the bacterial Bray-Curtis index in the rhizosphere compartment with a percentage of variance explained (PVE) of 50, 7, and 17%, respectively (Table 1). In the root endosphere, similar results were obtained with 42, 4, and 12% of PVE, respectively. The Chao1 and Simpson indexes were influenced by the rootstock genotype (73 and 53% of PVE respectively) in the rhizosphere. The Chao1 index was also influenced by the block (5% of PVE) and the factor interactions (15% of PVE). In the root endosphere, only the Simpson index was influenced by the genotype and the block (29 and 19 % of PVE respectively). As the effect of the genotype (expressed as the percentage of variance explained) was always stronger than that of the block or the factor interactions, we kept the genotype factor to compare rootstocks with a suitable number of biological replicates (n = 6). PCoA showed a genotype-dependent clustering of individuals in both rhizosphere (Figure 2 A) and root endosphere (Figure 2 D) compartments. Interestingly, the Bray-Curtis index measured for 1103P rootstock was significantly different from those of all other genotypes in both root system compartments, except for SO4 rootstock in the root endosphere (Supplementary Table 5). Moreover, the Bray-Curtis index of 41B rootstock was significantly different from those of Nemadex and SO4 in the rhizosphere, as well as those of 3309C in both root system compartments. In the rhizosphere, 1103P rootstock had a significantly lower Chao1 index (Figure 2 B) than all the other genotypes, while RGM had the significantly lowest Simpson index (Figure 2 C). In the root endosphere, no significant differences were detected between bacterial richness amongst the rootstock (Figure 2 E), while the Simpson index of 3309C rootstock was significantly lower compared to Nem (Figure 2 F). Between the six different rootstock genotypes, 47% of the rhizospheric OTUs were common, while less than 1% were specific from one genotype (Supplementary Figure 2 B). Inversely in the root endosphere, only 6% of bacterial OTUs were common and 49% were genotype-exclusives. LEfSe detected an enrichment of 4 phyla (*Acidobacteriota* for SO4, *Verrucomicrobiota* for Nemadex, *Planctomycetota* for 3309C and *Proteobacteria* for 1103P- rootstocks), 7 classes, 7 orders, 6 families, 6 genus, 6 species in the rhizosphere amongst the six rootstocks (Figure 3 A). In the root endosphere, 3 classes, 10 orders, 11 families, 16 genus and 17 species were enriched (Figure 3 B).

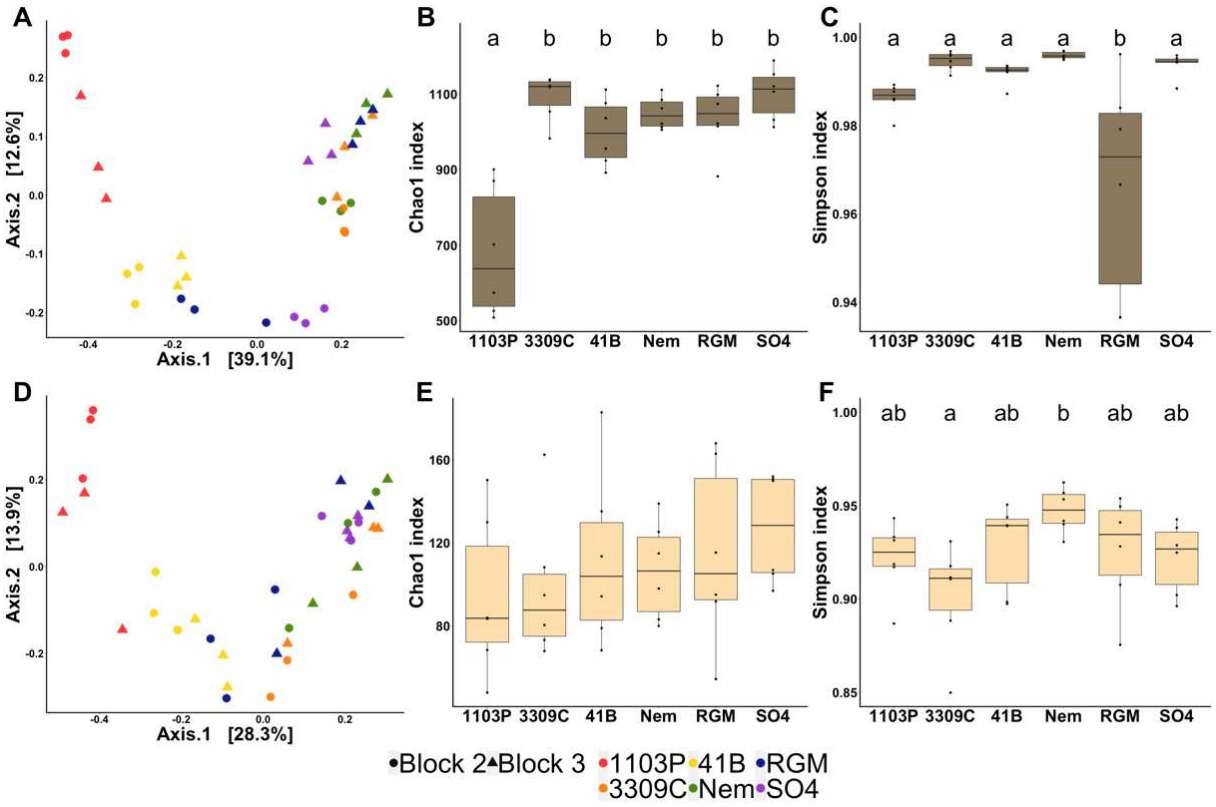


Figure 1-2: Comparison of bacterial communities in the rhizosphere (dark brown, top panel) and the root endosphere (light brown, bottom panel) between the 6 rootstock genotypes grafted onto CS (n=6). Comparison of bacterial communities by principal coordinate analysis (PCoA) based on Bray–Curtis dissimilarity matrices in the rhizosphere (A) and the root endosphere (D). Comparison of bacterial richness (Chao1) and diversity (Simpson) in the (B, C) rhizosphere and the (E, F) root endosphere. *p*-values were calculated using Pairwise-Student tests with Bonferroni correction and were considered as significant when the adjusted *p*-value < 0.05.

Regarding the influence on microbial communities of five scion genotypes grafted onto RGM rootstock, an effect of the scion on the level of bacterial 16S rRNA gene from the rhizosphere was reported (Supplementary Table 4), but no significant difference was observed between groups with the adjusted *p*-values (Supplementary Figure 4 D). In the rhizosphere and the root endosphere, Bray-Curtis index was influenced by the scion genotype (25 and 24% of PVE), the block (6% of PVE) and their interaction (33 and 25% of PVE) (Table 1). Regarding the bacterial α-diversity, the effect of the scion genotype was only reported on the Simpson index in the rhizosphere (41% of PVE). Individuals were not well clustered by scion genotype according to PCoA plot for both rhizosphere (Supplementary Figure 5 A) and root endosphere (Supplementary Figure 5 D) compartments. Only the Bray-Curtis index of UB scion was significantly different from the one of Syrah grafted onto RGM in both root system compartments, as well as the Bray-Curtis indexes of UB and Grenache in the rhizosphere (Supplementary Table 5). Simpson index in the rhizosphere was significantly lower in CS than in Grenache and UB (Supplementary Figure 4 C). Bacterial OTUs were common between scion

genotypes at 78% and less than 1% were genotype exclusive in the rhizosphere, compared to 18% and 40% in the root endosphere (Supplementary Figure 2 C). The LEfSe identified genotype-dependent enrichments of 2 phyla (*Planctomycetota* for UB, *Proteobacteria* for Grenache), 2 classes, 1 order, 1 family, 1 genus and 1 species in the rhizosphere (Supplementary Figure 6 A), compared to 2 phyla (*Acidobacteriota* for UB and *Proteobacteria* for Grenache) 2 orders, 2 families, 5 genera and 6 species in the root endosphere (Supplementary Figure 6 B).

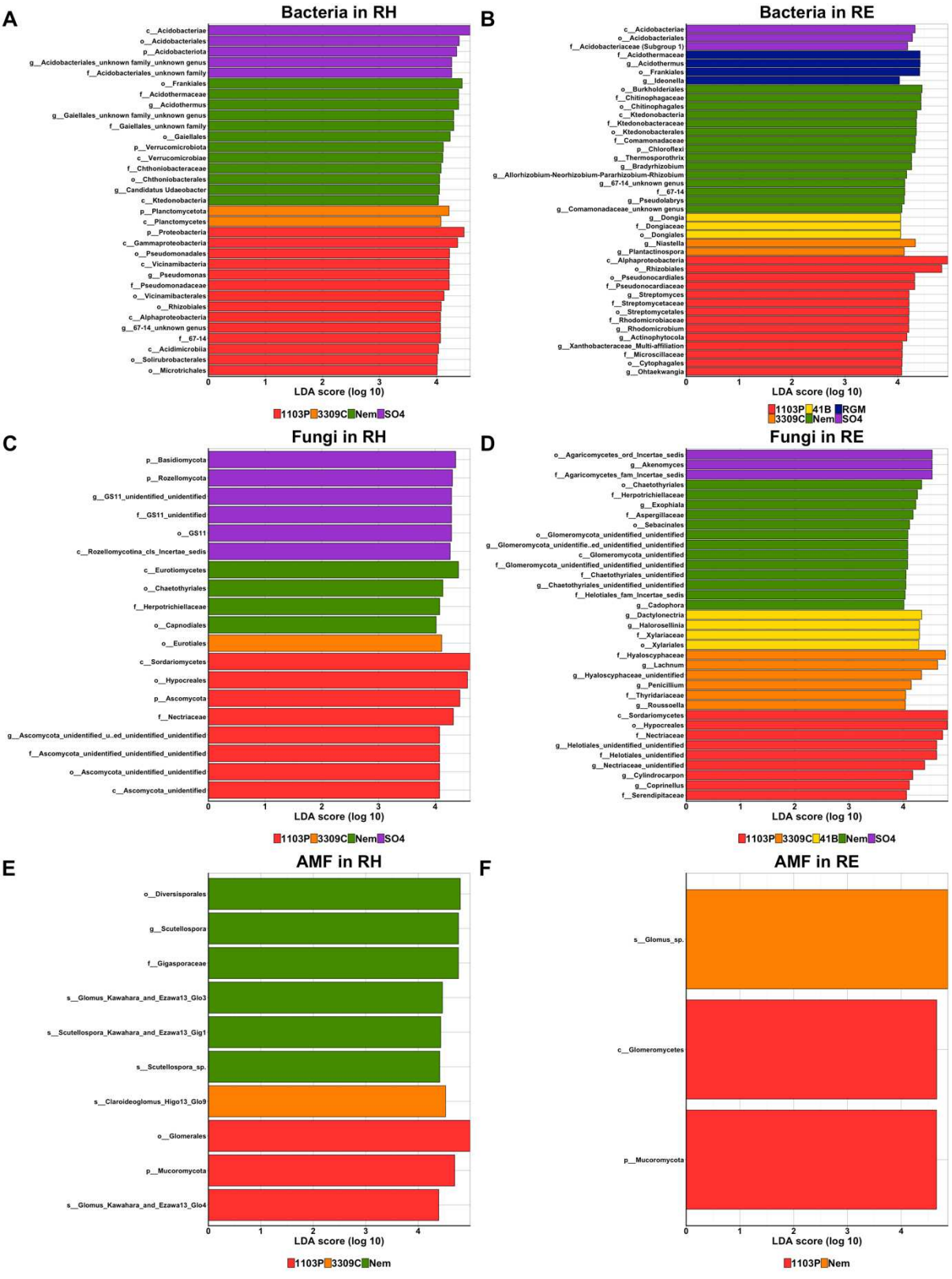


Figure 1-3: Histogram of the linear discriminant analysis (LDA) scores reveals the most differentially abundant taxa of bacteria (A, B), fungi (C, D) and AMF (D, E) in the rhizosphere (RH) and the root endosphere (RE) between rootstock genotypes.

Both genotypes of the grafted plant influence the root-associated fungal community

Quantitative PCR analysis revealed that the rootstock genotype affected the level of the fungal ITS gene from the rhizosphere (Supplementary Table 4) which was significantly higher for SO4 rootstock than for 1103P, 41B and RGM (Supplementary Figure 4 B). In the rhizosphere and the root endosphere, the Bray-Curtis index of fungal communities was influenced by the rootstock genotype (explaining 42 and 33% of PVE), the block (6% and 5% of PVE) and their interaction (19% of PVE) (Table 1). Regarding α-diversity metrics, the Chao1 index in the rhizosphere and the Simpson index in the root endosphere were influenced by the rootstock genotype only (40 and 49% of PVE, respectively). PCoA displayed strong genotype-dependent clustering in the rhizosphere (Figure 4 A). The fungal Bray-Curtis index of 1103P rootstock was significantly different from those of all other genotypes except for 41B (Supplementary Table 6). Other distinct fungal Bray-Curtis indexes were observed between Nemadex and 41B, as well as 3309C and RGM or 41B. The clustering of fungal communities according to rootstock genotype was less evident in the root endosphere (Figure 4 D). The fungal communities were significantly different between 1103P rootstock and Nemadex, 41B, and 3309C, as well as between 41B rootstock and Nemadex and 3309C (Supplementary Table 6). In the rhizosphere, the Simpson index was significantly higher in 1103P rootstock than in Nemadex and SO4 (Figure 4 C). In the root endosphere, the Chao1 index was significantly higher in Nemadex rootstock than in 1103P and 41B (Figure 4 E). In the rhizosphere, fungal OTUs were common and genotype-exclusive at 32% and 10%, respectively, while 7% were common and 34% were genotype-exclusive in the root endosphere (Supplementary Figure 2 B). Three phyla (*Ascomycota* for 1103P, *Basidiomycota* and *Rozellomycota* for SO4), 4 classes, 6 orders, 4 families, 2 genera, 2 species were enriched in the rhizosphere of rootstock genotypes (Figure 3 C). In the root endosphere, 2 classes, 7 orders, 14 families, 17 genera and 19 species were enriched (Figure 3 D).

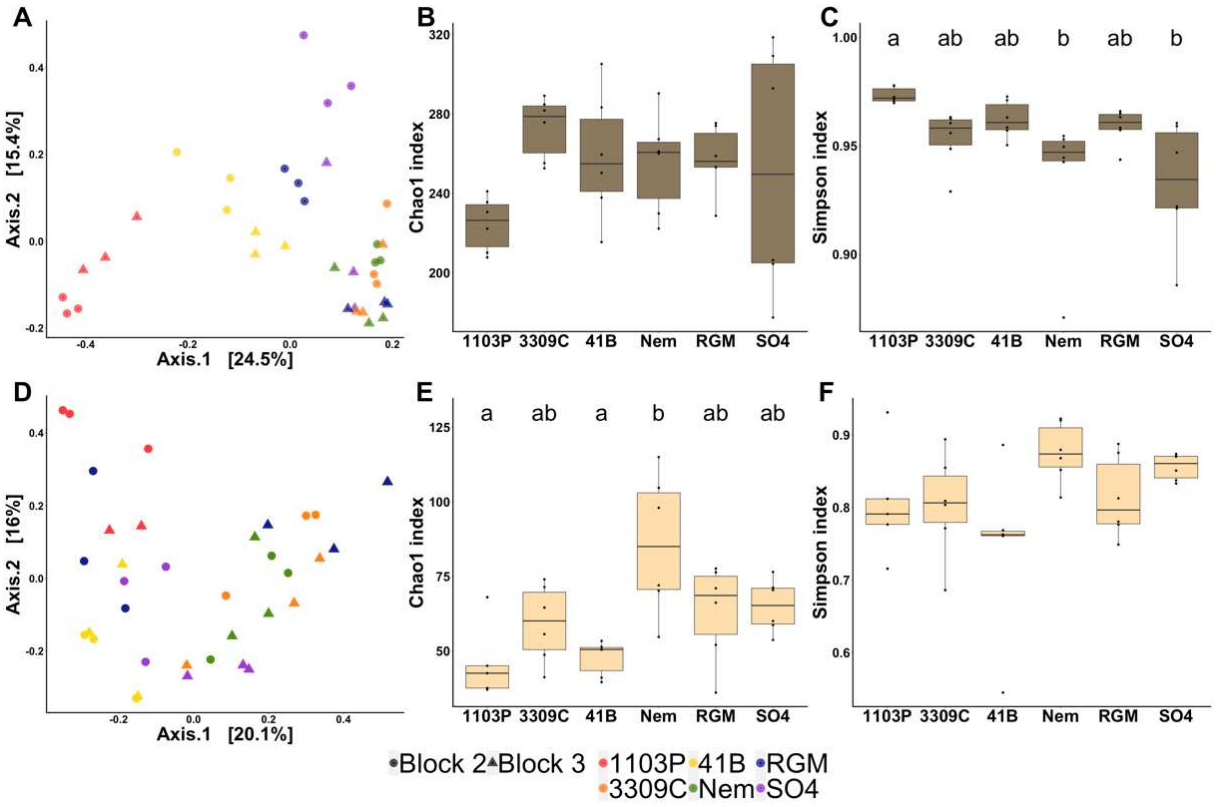


Figure 1-4: Comparison of fungal communities in the rhizosphere (top panel, dark brown) and the root endosphere (bottom panel, light brown) between the 6 rootstock genotypes grafted with CS (n=6). Comparison of fungal communities by principal coordinate analysis (PCoA) based on Bray–Curtis similarity matrices in the rhizosphere (A) and the root endosphere (D). Comparison of fungal richness (Chao1) and diversity (Simpson) in the rhizosphere (B, C) and the root endosphere (E, F). *p*-values were calculated using pairwise-Student tests with Bonferroni correction and were considered as significant when the adjusted *p*-value < 0.05.

Despite the reported effect of the scion on the level of fungal 18S rRNA gene from the rhizosphere (Supplementary Table 4), no significant differences were observed between scion genotypes using the adjusted *p*-values (Supplementary Figure 4 E). In the rhizosphere and the root endosphere, the fungal Bray-Curtis index was influenced by the scion genotype (30% and 24% of PVE), the block (7% of PVE) and their interaction (29% and 26% of PVE) (Table 1). None of the fungal α-diversity metrics were influenced by the scion genotype or the block. However, effects of their interaction were reported on the richness and the diversity of the rhizosphere (60% and 30% of PVE, respectively) (Table 1). According to PCoA, individuals were not clustered by genotypes in both rhizosphere (Supplementary Figure 7 A) and root endosphere (Supplementary Figure 7 D) compartments. The fungal Bray-Curtis index measured for UB was significantly different from those of PN, Syr and Gre in the rhizosphere, and from those of PN in the root endosphere (Supplementary Table 6). In the rhizosphere, 40% of fungal OTUs were common and 11% were genotype-exclusive, while 17% were common and 33% were genotype-exclusive in the root endosphere. LEfSe analysis

detected enrichments in 3 scion genotypes of 2 classes, 3 orders, 2 families, 2 genera and 2 species in the rhizosphere (Supplementary Figure 6 C), while enrichments of 3 classes, 2 orders, 2 families, 2 genera and 2 species were detected in the root endosphere (Supplementary Figure 6 D).

Rootstock genotypes drive the AMF community in the root endosphere

The Bray-Curtis index measured for AMF was influenced by the rootstock genotype, the block, and the interaction in the rhizosphere (23%, 4%, and 17% of PVE, respectively), as well as by the genotype in the root endosphere (19% of PVE) (Table 1). However, Chao1 and Simpson indexes were influenced by the genotype only in the root endosphere (41% and 37% of PVE). PCoA failed to cluster individuals according to rootstock genotypes in both rhizosphere (Figure 5 A) and root endosphere (Figure 5 D) compartments. Only the Bray-Curtis index of 3309C rootstock was significantly distinct from the indexes of 1103P and 41B in the rhizosphere (Table S7). In the root endosphere, the Chao1 index was significantly higher in RGM than in 1103P and 41B (Figure 5 E). Likewise, the Simpson index was higher in RGM and Nemadex than in 41B (Figure 5 F). In the rhizosphere, 12% of the AMF OTUs were common between the rootstocks while 26% were genotype exclusive (Supplementary Figure 2 B). In the root endosphere, 20% were common and 30% were exclusive. LEfSe detected an enrichment of 2 orders, 1 family, 1 genus and 5 species in the rhizosphere (Figure 3 F), compared to 1 phylum, 1 class and 1 species in the root endosphere (Figure 3 E).

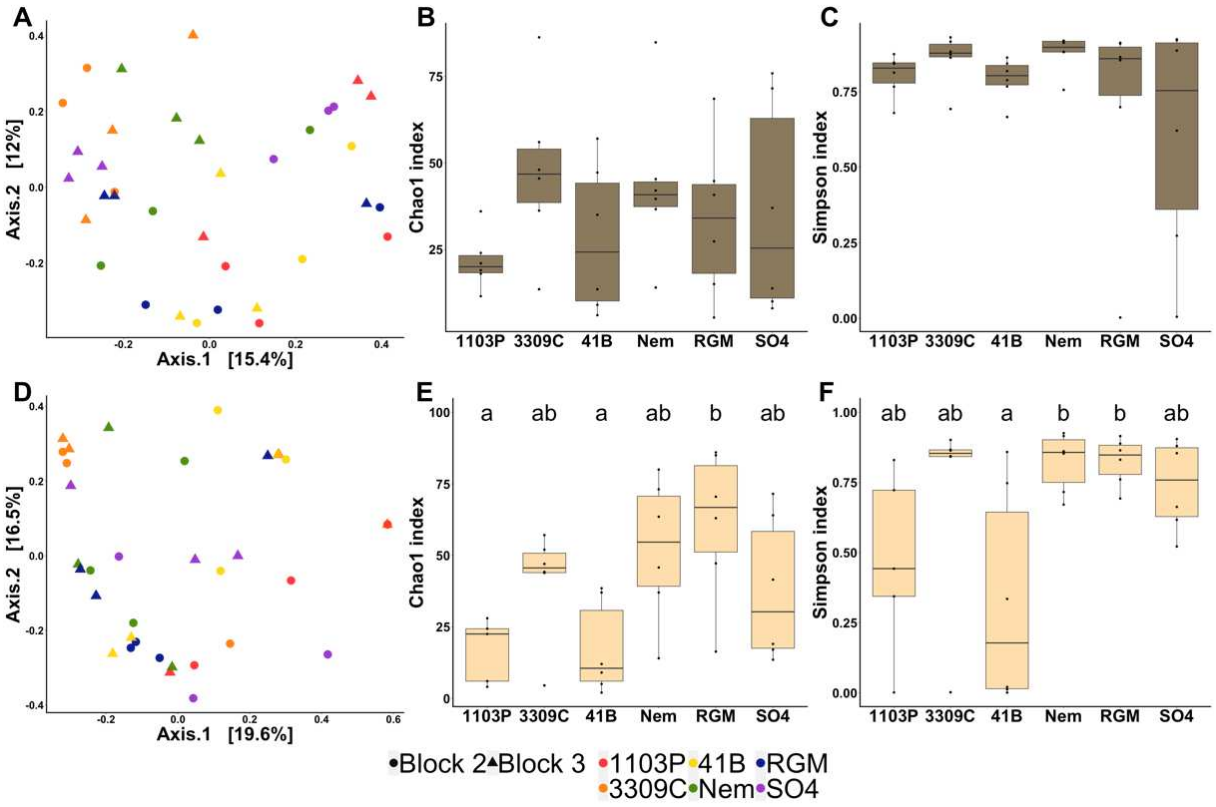


Figure 1-5: Comparison of AMF communities in the rhizosphere (top panel) and the root endosphere (bottom panel) between the 6 rootstock genotypes grafted with CS (n=6).
Comparison of AMF communities by principal coordinate analysis (PCoA) based on Bray–Curtis similarity matrices in the rhizosphere (A) and the root endosphere (D). Comparison of AMF richness (Chao1) and diversity (Simpson) in the rhizosphere (B, C) and the root endosphere (E, F). *p*-values were calculated using Pairwise-Student tests with Bonferroni correction and were considered as significant when the adjusted *p*-value < 0.05.

In addition to rootstock, a scion genotype effect was reported on AMF communities, the Bray-Curtis index was influenced by both the genotype and its interaction with the block in the rhizosphere (22 and 16% of the PVE, respectively), as well as by the factor interactions in the root endosphere (24% of PVE) (Table 1). However, the α-diversity indices did not detect any effects of the scion genotype in either of the root system compartments. According to PCoA, individuals were not clustered by genotype in either the rhizosphere (Supplementary Figure 8 A) or the root endosphere (Supplementary Figure 8 D) compartments. No AMF communities were significantly distinct between the scion genotypes with the Bray-Curtis index in either of the root system compartments (Supplementary Table 7). In the rhizosphere, 14% of the AMF OTUs were common between scion genotypes, while 27% were exclusive, while in the root endosphere, 20% were common and 28% were genotype exclusive (Supplementary Figure 2 C). LEfSe detected an enrichment of 1 phylum, 1 genus

and 4 species in the rhizosphere (Supplementary Figure 6 E), compared to 1 phylum, 1 class and 2 species in the root endosphere (Supplementary Figure 6 F).

Predicted functions of the bacterial and fungal microbiomes and impact of the root system microbiomes on plant phenotypic traits

Bacterial potential metabolic pathways were predicted using PICRUSt2. All the abundances of pathways were significantly higher in the rhizosphere than in the root endosphere, except for the lipid metabolism and the xenobiotic biodegradation and metabolism (Supplementary Table 8). PCA performed with the 119 predicted functions showed high clustering dependent on the root system compartment (Figure 6 D), suggesting that the function of the bacterial microbiomes depends on their environment. An effect of the rootstock genotype was reported on the abundances of all the predicted bacterial metabolic pathways in the rhizosphere (Supplementary Table 9). Several biosynthetic pathways were very abundant in the rhizosphere of certain rootstock genotypes, such as the amino acid metabolism for 1103P, the carbohydrate metabolism for Nemadex, the signaling molecules interaction for 41B, and the xenobiotics biodegradation and metabolism for RGM (Figure 6 A). According to PCAs, the predicted functions of the rhizospheric bacterial community for 1103P rootstock were distinct from those of 3309C and Nemadex (Figure 6 E). In the root endosphere, the rootstock genotype influenced only the metabolisms of amino acids and lipids, the membrane transport, and the signal transduction of bacteria (Supplementary Table 9, Figure 6 B). However, according to PCA, a slight segregation was detected between Nemadex and 41B (Figure 6 F). The abundances of six predicted bacterial metabolic pathways in the rhizosphere were influenced by the scion genotype (metabolism of carbohydrate, energy and lipid, membrane transport, signal transduction and xenobiotics biodegradation and metabolism), while the abundance of three and four pathways was influenced by the block and the factor combinations, respectively (Supplementary Table 9, Figure 6 C). According to PCA, no genotype-dependent clustering of bacterial functions was observed in either the rhizosphere (Supplementary Figure 9 A) or root endosphere (Supplementary Figure 9 B) compartments. Here, the influence of the scion on the bacterial metabolic pathways is weaker than that of the rootstock.

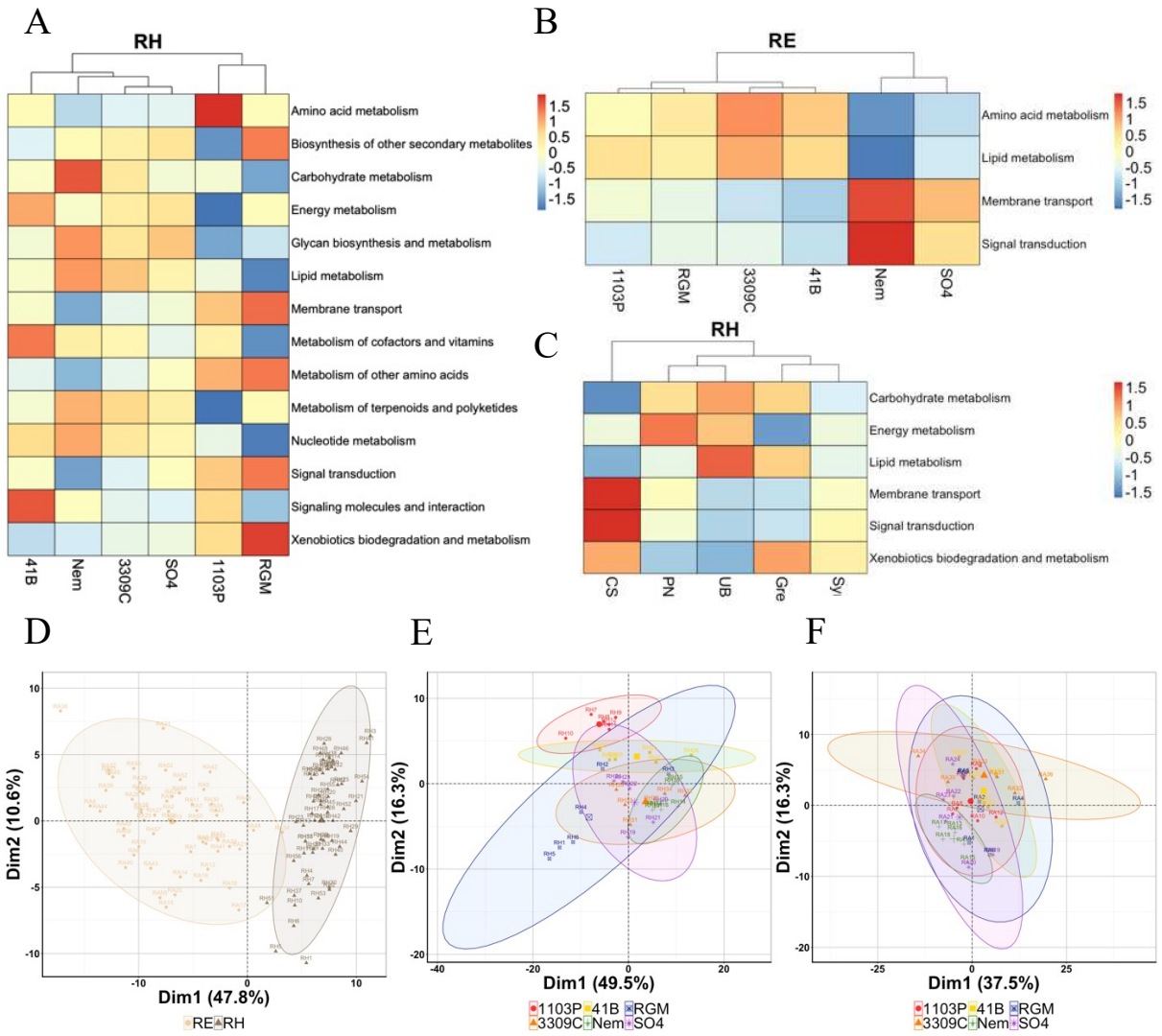


Figure 1-6: PICRUSt inference of bacterial metabolic pathways and functions.
Heatmap showing the abundance of bacterial metabolic pathways which were significantly influenced by the rootstock genotype in (A) the rhizosphere and (B) the root endosphere, and by (C) the scion genotypes in the rhizosphere (n = 6). PCA to compare the predicted functions of bacteria (119 variables) between (D) roots system compartments (n = 60), and rootstock genotypes in (E) the rhizosphere and (F) the root endosphere (n = 6).

Fungal trophic modes and guilds, predicted using the FUNGuild database, were successfully affiliated with 33% of fungal OTUs from the rhizosphere and 42% from the root endosphere. An effect of the root system compartments on the proportions of fungal trophic modes (Figure 7 A) and guilds (Figure 7 C) was reported (Chi Squared test: *p*-values < 2.2e-16). Fungi were mainly saprotroph in both root system compartments, even though a significant number of multi-trophic modes were observed in the rhizosphere. The highest proportions of pathotroph and plant pathogen were observed in the rhizosphere, whereas the highest proportions of symbiotroph or arbuscular mycorrhizal were observed in the roots. Rootstock genotype influenced the proportions of fungal trophic modes (Figure

7 B) and guilds (Figure 7 D) in both root system compartments (Chi Squared test: *p*-values < 2.2e-16). Interestingly, 1103P had over 3 times more pathogenic fungi than any other genotype in the root endosphere. Moreover, the highest proportion of AMF in roots was observed for Nemadex rootstock. An effect of the scion was also detected on the proportions of trophic modes and guilds in both root system compartments (Chi Squared test: *p*-values < 2.2e-16, Supplementary Figure 10). The root system of RGM grafted with UB had over twice as much AMF in the roots than other scion genotypes.

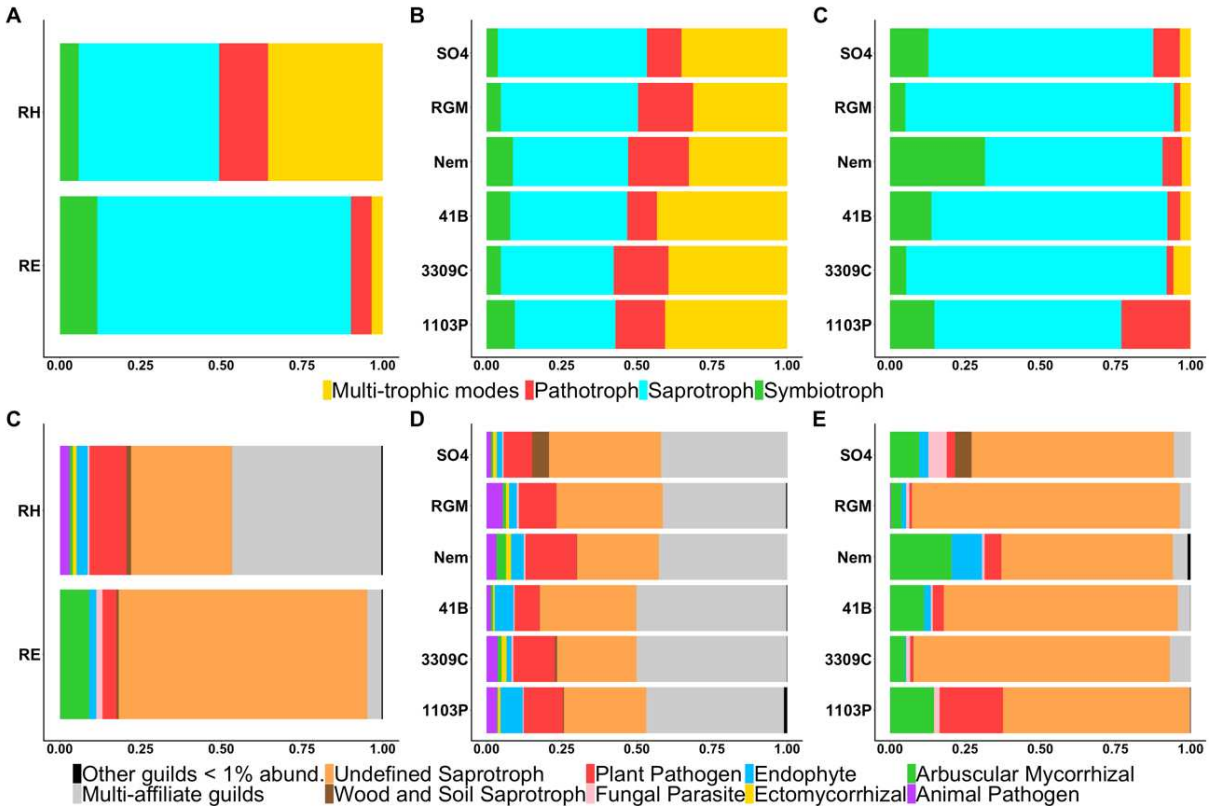


Figure 1-7: Comparisons of the predicted trophic modes and guilds between the root system compartments (A, C) or the rootstock genotypes in the rhizosphere (B, D) and the root endosphere (C, E)

To study the impacts of microbial communities on plant phenotypic traits, and mineral content in the roots and petioles, correlation matrices were established with the microbial variables (cultivable, qPCR and metabarcoding approaches). Between the root system microbiomes and the plant phenotypic traits, 21 significant correlations were established, with r values ranging from -0.49 to 0.45. The strongest correlations (*p*-values < 0.05) were obtained between the number of shoots and AMF richness in the rhizosphere (r = -0.45); the number of bunches and the cultivable fungi (r = -0.4) and the AMF richness in the rhizosphere (r = 0.41); the bunch pruning weight and the rhizosphere archaeal level measured by qPCR (r = 0.45); the $\delta^{13}C$ and the rhizosphere archaeal level (r = -0.49) and the bacterial

richness in the rhizosphere (r = 0.44) (Figure 8 A). In addition, 39 microbial variables were significantly correlated to mineral dosage in the petiole, with r values ranging from -0.44 to 0.45. The strongest correlations were obtained between the sulfur content and the AMF diversity in the roots (r = 0.45); the richness of rhizosphere bacteria and the calcium content (r = -0.46) and the manganese content (r = 0.43) (Figure 8 B). Finally, 29 microbial variables were significantly correlated to mineral content in the roots, ranging from -0.48 to 0.4. Interestingly, the calcium content was negatively correlated with the richness of bacteria (r = - 0.42), fungi (r = - 0.48), and AMF (r = - 0.42) in the rhizosphere. The manganese was also correlated with the AMF diversity (r = 0.4) and richness (r = 0.37) in the roots (Figure 8 C).

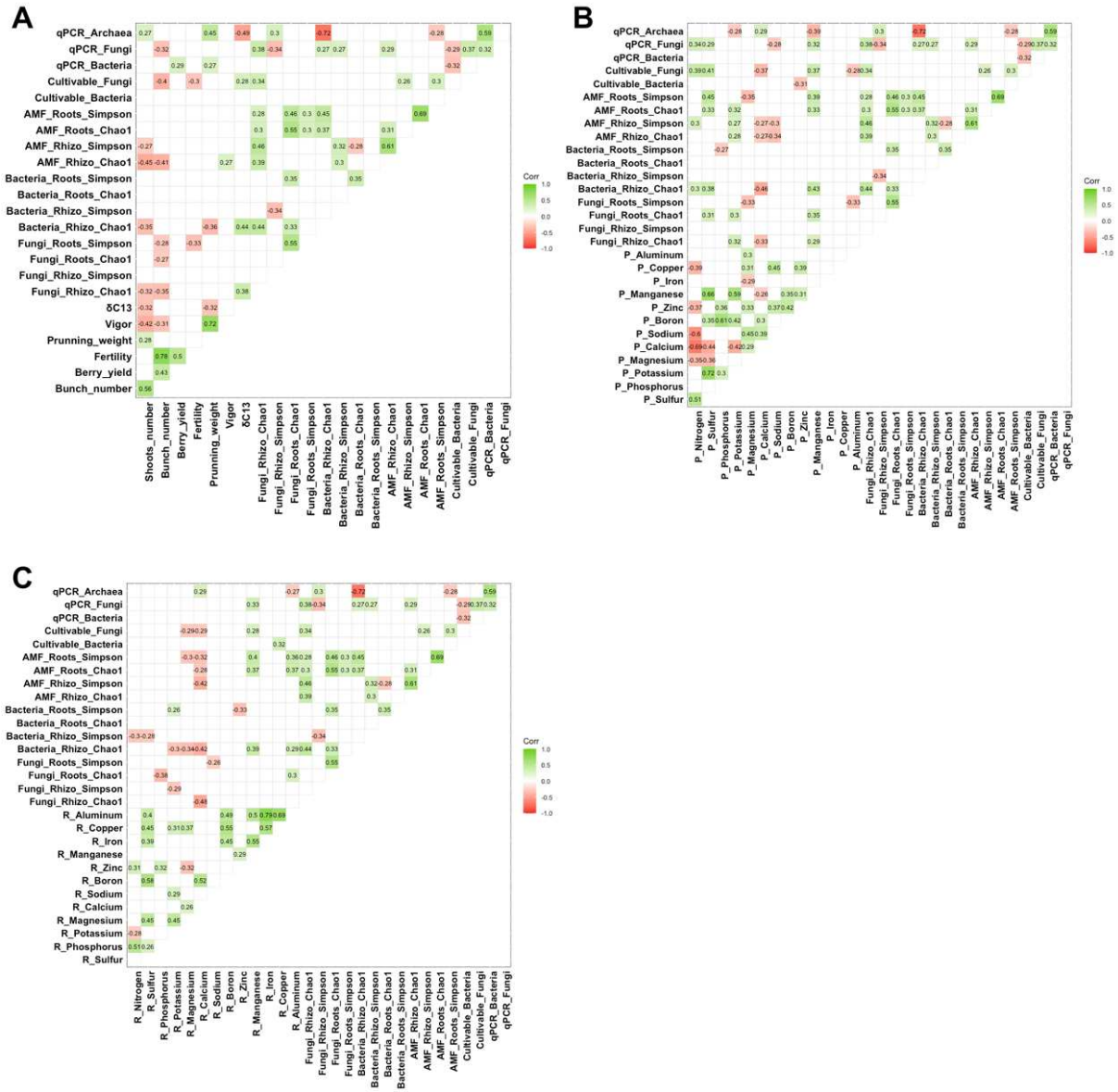


Figure 1-8: Matrices showing significant correlations established between the variables measured to characterize the root system microbiomes and the plant phenotype (A), the mineral status of petioles (B) and the mineral status of roots (C).

Discussion

The root compartments have distinct microbial communities which play different functions

Grapevine bacterial microbiome was largely composed of *Proteobacteria* and *Actinobacteria*. *Proteobacteria* are related to a wide range of functions involved in carbon, nitrogen, and sulfur cycling (Zhang et al., 2022). *Actinobacteria* are known for their production of secondary metabolites, degradation of organic substances and contribution to plant fitness by acting as PGPR or biocontrol agents (Hazarika and Thakur, 2020). Relatively similar proportions of bacterial phyla were found in other studies (Marasco et al., 2022; Darriaut et al., 2022a; Deyett and Rolshausen, 2020). Interestingly, some studies found a greater abundance of *Acidobacteria* than *Actinobacteriota*, and observed several phyla such as *Armatimonadetes*, *Deinococcus-Thermus*, *Rokubacterua*, or *Synergistetes,* which were not detected in the GreffAdapt plot (Swift et al., 2021; Vink et al., 2021). Fungal microbiome was primarily dominated by *Ascomycota (Sordariomycetes, Dothideomycetes, Eurotiomycetes and Leotiomycetes)* and *Basidiomycota (Agaricomycetes, Tremellomycetes)*. These phyla have diverse ecological roles, such as ectomycorrhizae, plant pathogens and saprotrophic fungi, and are involved in nutrient acquisition, decomposition, and carbon sequestration (Challacombe et al., 2019; Kjøller and Rosendahl, 2014). Several studies have found the same major fungal phyla and classes in a relatively similar proportion depending on the class (Darriaut et al., 2022a; Marasco et al., 2022; Swift et al., 2021). Investigation of AMF community using 28S rRNA gene sequencing displayed a clear dominance of the *Glomus* genera in the rhizosphere and the root endosphere, which is consistent with other studies (Massa et al., 2020; Schreiner, 2020). Together, these results show that a core of bacteria and fungi is always recruited by grapevine root system compartments regardless of different environmental conditions. The highly dependent segregation of bacterial and fungal communities according to root system compartments, the enrichment of several taxa in both compartments, as well as the higher diversity and richness in the rhizosphere confirmed the plant's ability to recruit only certain strains that will be able to reach the root endosphere (Marasco et al., 2022). Interestingly, the abundances of bacterial metabolic pathways necessary for plant development were significantly higher in the root endosphere, such as lipid metabolism, other amino acid metabolism and xenobiotics biodegradation and metabolism. Moreover, the fungal proportion of symbiotroph (such as arbuscular mycorrhizal) increased in the root endosphere, while that of pathotroph decreased (e.g., plant pathogen). These observations are consistent with the "cry for help" hypothesis, suggesting that the plant interacts with its surrounding microbial communities to alleviate different stresses by natural microbiome selection of specialized strains (Rodriguez and Durán, 2020). These differences could be

explained by environmental conditions, such as temperature, humidity, and incidence of light, within both root endosphere and rhizosphere compartments, which result in different selection pressures for microorganisms (Bettenfeld et al., 2022).

Rootstock genotype drives the microbial communities in the root system

The level of fungi and archaea measured in the rhizosphere by qPCR is dependent on the rootstock genotype. Archaea offer promising applications for agriculture due to their important role in nutrient cycling, their various plant growth-promoting attributes, and their enhancement of tolerance to various abiotic stresses (Naitam and Kaushik, 2021). Despite the existence of a core microbiome between rootstocks, the genotype influenced at least one of the two α-diversity metrics and the Bray-Curtis index measured for bacteria and fungi in both root system compartments. Several studies found the same effects, depending on the diversity indicator examined (Berlanas et al., 2019 ; Marasco et al., 2022; Vink et al., 2021). The enrichment of several taxa of bacteria and fungi in each rootstock genotype in the rhizosphere and the root endosphere suggested that rootstock associates preferentially with certain microbial composition, leading to various inferred metabolic functions. We can hypothesize that rhizodeposit composition varies between genotypes and that they recruit different microorganisms (Philippot et al., 2013). In grapevines, root exudates are still poorly characterized. Marastoni et al., (2020) unveiled common and specific responses in root exudate composition between Ramsey and 140R rootstocks subjected to iron deficiency. Concerning AMF communities, all the α-diversity metrics were influenced by the rootstock genotype in the root endosphere. In terms of β-diversity, it was difficult to draw any conclusions about the effect of the genotype. The Bray-Curtis index was significantly dependent on the rootstock genotype in both root system compartments and PCoA did not detect any clustering related to rootstock. Finally, few AMF taxa were enriched in several genotypes. These results confirms those obtained by Moukarzel et al. (2021) who showed, using denaturing gradient gel electrophoresis (DGGE) and trap cultures, that rootstock genotypes drive AMF community in the root system. Previous work suggested differential production of strigolactones between RGM and 1103P (Cochetel et al., 2018). We have just recently characterized the chemical structure of two non-canonical strigolactones in the exudates of these two rootstocks grown on nitrogen depleted medium (Lailheugue et al., 2023). Interestingly, RGM and 1103P exuded a similar concentration of vitislactone, whereas a heliolactone-like compound was detected exclusively in the root exudates of RGM. We can hypothesize that genotypes regulate the AMF community through the quantity and the types of strigolactones exuded into the rhizosphere. Finally, even if the soil physicochemical parameters were similar between the two sampled areas, an effect of the block was

reported on several diversity indicators measured on bacterial, fungal and AMF communities. However, its contribution was generally lower than that of the genotype. Indeed, soil properties such as texture, structure, mineral content, and acidity affect microbial communities (Seaton et al., 2020; Schreiner and Mihara, 2009), and are known to be one of the most important factors influencing microbial communities (Darriaut et al., 2023; Marasco et al., 2022).

Scion genotype is involved in the selection of root system bacterial and fungal communities but with a smaller contribution than that of the rootstock

Studies have shown that the scion genotype influences the development of the rootstock root system (Tandonnet et al. 2009) and that several signaling molecules are exchanged between the two components of the chimeric plant (Ollat et al., 2017). We therefore decided to study the effect of the scion genotype on the root system microbial communities with five scions grafted onto RGM. An effect of the scion genotype was reported on the level of bacteria, fungi and archaea measured in the rhizosphere. Among the α-diversity metrics measured for the three groups of microorganisms, the scion genotype influenced the Simpson index measured for the bacteria in the rhizosphere only. Moreover, several microbial taxa were enriched in the root system of RGM grafted with different scion genotypes, and all the Bray-Curtis indexes were influenced by the scion genotype, with the exception of those measured for AMF in the root endosphere. Marasco et al. (2022) similarly found a contribution of the scion genotype towards the β-diversity of bacteria and fungi in the rhizosphere and the root tissue. In addition, Vink et al. (2021) detected a scion effect on the Simpson and Faith's PD indexes measured for bacterial community in the rhizosphere. Dries et al. (2023) has just recently uncovered significant differences in α- and β-diversities between the scion genotypes Riesling and Mueller-Thurgau when cultivated ungrafted but were no longer observed when the scion were compared grafted. Together, these results suggest that the scion genotype is involved in the selection of root system microbiomes. The scion is responsible for the production of sugars through photosynthesis and for their allocation to the rootstock (Ollat et al., 2017). If fewer sugars reach the rootstock, this could interfere with the sugar composition and quantity released into the rhizosphere, which undoubtedly mediate the functional and taxonomic diversity of microbial communities. In this case, the contribution of the scion genotype was less important than that of the rootstock genotype on the shaping of microbial communities. Finally, our experimental design does not allow us to compare the contribution of the rootstock and the scion genotypes on the root system microbial communities together. However, the number of diversity metrics or bacterial pathways significantly influenced by the genotype with the associate PVE, as well as the number of microbial taxa enriched between the scion genotypes,

suggest a lower involvement of the scion genotype than rootstock in the recruitment of microbial communities in the root system.

Upgrading the study of grapevine microbiome and prospects

Instead of targeting one microbial community, multiplex sequencing of 3 amplicons provides a good alternative for a more global view of a microbial environment (Darriaut et al., 2023). The use of the primers pair 341F/785R is well suited to study soil bacteria. However, it amplifies a large proportion of host mitochondrial and chloroplastic 16S rRNA genes when studying plant tissues. Results on the root endosphere bacteria must be interpreted carefully because of the low sequencing depth obtained after removing host sequences and data rarefaction. Using pPNA and mPNA clamps to reduce host chloroplasts and mitochondria amplification is recommended for this type of study (Fitzpatrick et al., 2018; Deyett and Rolshausen, 2020). In our case, the use of the nested PCR could affect AMF community analysis, resulting in a decrease of taxa and diversity (Yu et al., 2015). The comparisons between this method and classic PCR, as well as finding optimal primer pairs, must be carried out to arrive at a consensus on the method to analyze AMF community (Suzuki et al., 2020). Quantifying AMF colonization of plant roots by microscopy or qPCR would have been interesting to compare the mycorrhization capacity of the root system between genotypes (Bodenhausen, 2021; Phillips and Hayman, 1970).

Although metabarcoding data cannot be used to study the role of microbiomes, it is possible to obtain an overview of microbial functions using taxonomy-based function prediction methods. These methods are based on the association of taxonomic clades with known functional guilds, or with metabolic functions or pathways obtained from public databases of annotated genomes (Fournier et al., 2022). Even though we were satisfied with PICRUSt2 results, the FUNGuild tool needs to be improved because more than half of the sequences obtained were not affiliated.

To our knowledge, this work is the first to explore correlations between microbial variables and plant phenotypic traits or mineral nutrition in grapevines, confirming the role of the root system microbiomes in grapevine development. It would be interesting to supplement these functional analyses in the rhizosphere by measuring the activities of microbial enzymes involved in soil biogeochemical cycling or by using community-level physiological profiling approach such as Biolog EcoPlate™ (Caldwell, 2005; Gryta and Fr, 2014). Investigating another scion grafted onto all the rootstock genotypes studied would enable us to explore the influence of the rootstock × scion

interaction on the belowground microbiomes, especially as it has been suggested that the rootstock × scion combination results were more significant than the two components taken alone (Marasco et al., 2022). Finally, coupling microbiome studies with biochemical analysis of the rhizosphere and the root endosphere could provide new insights into the understanding of plant-microorganism interactions.

Conclusion

Our results confirm that rootstock genotypes drive the composition and the structure of bacteria and fungi microbiomes in the rhizosphere and the root endosphere. We showed that the scion genotypes have an influence on these communities, but to a lesser extent than the rootstock. We have also demonstrated that the different microbial communities observed between cultivars (i.e., rootstock or scion genotypes) may have different roles in their ecosystems. Moreover, this is the first study based on a metabarcoding approach, which displays the rootstock genotype's influence on the AMF community of grapevine root system, primarily in the root endosphere, while the involvement of the scion genotype remains disputable, depending on the diversity metrics observed (α or β). Finally, we have highlighted correlations between the composition of the root system microbiomes and the phenotype and the mineral status of the plant, confirming the important role of these microorganisms in grapevine development.

Supplementary tables

Table S1: Rootstocks and scion cultivars used in this study.

	Name	Genetic backgrounds	Characteristics	
			Conferred vigour	Waterdeficit tolerance
Rootstocks grafted with Cabernet Sauvignon	Selection Oppenheim 4 (SO4)	*V. berlandieri* × *V. riparia*	High	Medium to good
	3309 Couderc (3309C)	*V. riparia* × *V. rupestris*	Low to medium	Weak in top soil
	41 B MGt (41B)	*V. berlandieri* × *V. vinifera*	Medium to high	Medium to high
	1103 Paulsen (1103P)	*V. berlandieri* × *V. rupestris*	High	Good
	Riparia Gloire de Montpellier (RGM)	*V. riparia*	Very low to low	Weak
	Nemadex AB	*V. berlandieri* × *V. Muscadinia* × *V. vinifera* × *V. rupestris*	Low	Weak
Scion cultivars grafted on RGM			Berry color	
	Cabernet-Sauvignon clone 169	*V. vinifera*	Red	
	Syrah clone 524	*V. vinifera*	Red	
	Grenache clone 362	*V. vinifera*	Red	
	Pinot noir clone 113	*V. vinifera*	Red	
	Ugni blanc clone 481	*V. vinifera*	White	

Table S2: Soil analysis carried out on the blocks 2 and 3 in the GreffAdapt plot.

	Block 2	Block 3
Depth (cm)	0-35	0-30
Coarse elements (%)	31	33.6
Fine Clay (%)	5.2	4.5
Fine silt (%)	6.5	6.2
Coarse silt (%)	4.0	3.2
Fine sand (%)	8.2	12.0
Coarse sand (%)	76.1	73.8
Given texture	Sandy	Sandy
Organic matter (%)	2.2	1.2
Total nitrogen (%)	0.109	0.049
C/N	11.5	14.7
Water pH	7.2	6.7
Absorbed complex		
Potassium ($cmol^+$/ kg)	0.06	0.15
Magnesium ($cmol^+$/ kg)	0.33	0.30
Calcium ($cmol^+$/ kg)	6.28	2.57
CEC ($cmol^+$/ kg)	5.3	3

Table S3: List of primers and PCR conditions used for the metabarcoding approaches.

Target genes	Primers	Sequences (5'-3')	Initial denaturation	Nulmber of cycles	Denaturation	Annealing	Extension	Final extension	Sources
Bacterial 16S rRNA gene V3-V4 regions	341F 785R	CCTACGGGNGGCWGCAG GACTACHVGGGTATCTAATCC	95°C/5min	25	95°C/30s	55°C/30s	72°C/30s	72°C/5min	Klindworth et al., 2013
Fungal ITS1 region (highly variable)	ITS1F ITS2	CTTGGTCATTTAGAGGAAGTAA GCTGCGTTCTTCATCGATGC	95°C/5min	30	95°C/30s	55°C/30s	72°C/45s	72°C/7min	Gardes and Bruns, 1993 White et al., 1990
Eurayote 28S rRNA gene	LR1 NDL22	GCATATCAATAAGCGGAGGA TGGTCCGTGTTTCAAGACG	95°C/5min	30	95°C/30s	58°C/30s	72°C/30s	72°C/5min	van Tuinen et al., 1998
AMF 28S rRNA gene	FLR3 FLR4	TTGAAAGGGAAACGATTGAAGT TACGTCAACATCCTTAACGAA	98°C/30s	30	95°C/30s	55°C/30s	72°C/45s	72°C/7min	Gollotte et al. 2004
Specific overhang Illumina adapters	Forward Reverse	TCGTCGGCAGCGTCAGATGTGTATAAGAGACAG GTCTCGTGGGCTCGGAGATGTGTATAAGAGACAG							PGTB

Table S4: Quantification of the rhizospheric bacteria and fungi using plating method, and the rhizospheric bacteria, fungi and archaea using qPCR approach. Significances were assessed through two-way ANOVA. Significant *p*-values (< 0.05) are highlighted in bold, ns = non significant.

		Cultivable						**qPCR**								
		Bacteria			**Fungi**			**Bacteria**			**Fungi**			**Archaea**		
		***p*-value**		**PVE**	***p*-value**		**PVE**	***p*-value**		**PVE**	***p*-value**		**PVE**	***p*-value**		**PVE**
Rootstock	**Genotype (G)**	0.296	ns	/	0.118	ns	/	0.218	ns	/	0.004	**	**41%**	**8.96e-04**	***	**46%**
	Bloc (B)	0.145	ns	/	0.179	ns	/	0.432	ns	/	0.065	ns	/	0.054	ns	/
	G x B	0.341	ns	/	**0.0172**	*	**30%**	0.342	ns	/	0.052	ns	/	**3.28e-05**	***	**32%**
Scion	**G**	0.109	ns	/	0.135	ns	/	**0.007**	**	**39%**	**0.0357**	*	**31%**	**0.016**	*	**30%**
	B	0.465	ns	/	0.645	ns	/	0.067	ns	/	0.0821	ns	/	**0.003**	**	**22%**
	G x B	0.566	ns	/	0.287	ns	/	0.465	ns	/	0.1479	ns	/	**0.002**	**	**27%**

Table S5: Pairwise Adonis comparisons of the Bray-Curtis index measured for bacterial community between the genotypes of rootstock or scion in the rhizosphere and the root endosphere. Significant adjusted *p*-values (< 0.05) are highlighted in bold.

		Bacteria											
		Rhizosphere						**Root endosphere**					
		Df	**SumsOfSqs**	**F.Model**	**R2**	***p*-value**	***p*-adjusted**	**Df**	**SumsOfSqs**	**F.Model**	**R2**	***p*-value**	***p*-adjusted**
Rootstock	**1103P vs Nem**	1	1.373	17.56	0.637	0.002	**0.03**	1	1.379	9.45	0.486	0.001	**0.015**
	1103P vs SO4	1	1.132	12.44	0.554	0.002	**0.03**	1	1.322	9.96	0.499	0.005	0.075
	1103P vs RGM	1	0.969	8.46	0.458	0.003	**0.045**	1	0.921	5.35	0.346	0.002	**0.03**
	1103P vs 41B	1	0.468	5.49	0.355	0.002	**0.03**	1	0.600	4.47	0.309	0.003	**0.045**
	1103P vs 3309C	1	1.329	16.71	0.626	0.002	**0.03**	1	1.295	8.65	0.464	0.003	**0.045**
	Nem vs SO4	1	0.202	2.10	0.174	0.042	0.63	1	0.273	1.97	0.165	0.009	0.135
	Nem vs RGM	1	0.361	3.02	0.232	0.013	0.195	1	0.350	1.96	0.164	0.028	0.42
	Nem vs 41B	1	0.860	9.53	0.488	0.001	**0.015**	1	0.749	5.34	0.348	0.005	0.075
	Nem vs 3309C	1	0.122	1.45	0.126	0.099	1	1	0.414	2.66	0.210	0.008	0.12
	SO4 vs RGM	1	0.230	1.739	0.148	0.113	1	1	0.296	1.79	0.152	0.043	0.645
	SO4 vs 41B	1	0.545	5.30	0.346	0.003	**0.045**	1	0.691	5.44	0.352	0.007	0.105
	SO4 vs 3309C	1	0.137	1.41	0.123	0.149	1	1	0.350	2.45	0.197	0.007	0.105
	RGM vs 41B	1	0.486	3.84	0.277	0.015	0.225	1	0.304	1.83	0.155	0.025	0.375
	RGM vs 3309C	1	0.275	2.28	0.186	0.02	0.3	1	0.209	1.15	0.103	0.319	1
	41B vs 3309C	1	0.749	8.19	0.450	0.003	**0.045**	1	0.569	3.95	0.283	0.003	**0.045**
Scion	**CS vs PN**	1	0.165	1.12	0.101	0.241	1,000	1	0.181	0.95	0.087	0.489	1
	CS vs UB	1	0.323	2.77	0.217	0.013	0.13	1	0.233	1.33	0.117	0.178	1
	CS vs Syr	1	0.198	1.37	0.120	0.238	1	1	0.307	1.79	0.152	0.058	0.58
	CS vs Gre	1	0.295	2.21	0.181	0.074	0.74	1	0.254	1.46	0.140	0.143	1
	PN vs UB	1	0.286	2.65	0.210	0.01	0.1	1	0.433	2.71	0.213	0.009	0.09
	PN vs Syr	1	0.146	1.07	0.097	0.344	1	1	0.135	0.87	0.080	0.551	1
	PN vs Gre	1	0.172	1.38	0.121	0.126	1	1	0.130	0.83	0.084	0.597	1
	UB vs Syr	1	0.440	4.17	0.294	0.004	**0.04**	1	0.633	4.46	0.308	0.003	**0.03**
	UB vs Gre	1	0.364	3.88	0.279	0.003	**0.03**	1	0.471	3.33	0.270	0.022	0.22
	Syr vs Gre	1	0.222	1.81	0.153	0.105	1	1	0.176	1.28	0.125	0.221	1

Table S6: Pairwise Adonis comparisons of the Bray-Curtis index measured for fungal community between the genotypes of rootstock or scion in the rhizosphere and the root endosphere. Significant adjusted *p*-values (< 0.05) are highlighted in bold.

		Fungi											
		Rhizosphere						Root endosphere					
		Df	SumsOfSqs	F.Model	R2	*p*-value	*p*-adjusted	Df	SumsOfSqs	F.Model	R2	*p*-value	*p*-adjusted
Rootstock	1103P vs Nem	1	0.973	8.44	0.458	0.001	**0.015**	1	0.943	3.46	0.278	0.002	**0.03**
	1103P vs SO4	1	0.964	7.32	0.423	0.003	**0.045**	1	0.938	3.89	0.302	0.004	0.06
	1103P vs RGM	1	0.839	7.13	0.416	0.002	**0.03**	1	0.594	2.03	0.184	0.054	0.81
	1103P vs 41B	1	0.574	4.81	0.325	0.004	0.06	1	0.848	3.80	0.297	0.001	**0.015**
	1103P vs 3309C	1	0.987	10.00	0.500	0.003	**0.045**	1	1.022	4.07	0.311	0.003	**0.045**
	Nem vs SO4	1	0.380	2.90	0.225	0.02	0.3	1	0.322	1.54	0.133	0.128	1
	Nem vs RGM	1	0.190	1.62	0.140	0.095	1	1	0.400	1.56	0.135	0.098	1
	Nem vs 41B	1	0.495	4.18	0.295	0.003	**0.045**	1	0.764	3.94	0.283	0.003	**0.045**
	Nem vs 3309C	1	0.156	1.59	0.137	0.013	0.195	1	0.353	1.62	0.139	0.093	1
	SO4 vs RGM	1	0.312	2.34	0.190	0.032	0.48	1	0.528	2.31	0.187	0.032	0.48
	SO4 vs 41B	1	0.416	3.08	0.235	0.008	0.12	1	0.419	2.53	0.202	0.01	0.15
	SO4 vs 3309C	1	0.303	2.64	0.209	0.051	0.765	1	0.453	2.38	0.192	0.036	0.54
	RGM vs 41B	1	0.343	2.84	0.221	0.005	0.075	1	0.734	3.45	0.256	0.004	0.06
	RGM vs 3309C	1	0.263	2.62	0.208	0.001	**0.015**	1	0.334	1.41	0.123	0.19	1
	41B vs 3309C	1	0.471	4.62	0.316	0.001	**0.015**	1	0.891	5.09	0.337	0.002	**0.03**
Scion	CS vs PN	1	0.181	1.65	0.141	0.104	1	1	0.409	1.79	0.151	0.114	1
	CS vs UB	1	0.243	2.37	0.192	0.011	0.11	1	0.317	1.42	0.136	0.198	1
	CS vs Syr	1	0.284	2.18	0.179	0.02	0.2	1	0.334	1.39	0.122	0.208	1
	CS vs Gre	1	0.213	1.77	0.150	0.063	0.63	1	0.295	1.25	0.121	0.266	1
	PN vs UB	1	0.314	3.38	0.252	0.002	**0.02**	1	0.546	3.19	0.262	0.002	**0.02**
	PN vs Syr	1	0.376	3.11	0.237	0.007	0.07	1	0.340	1.75	0.149	0.049	0.49
	PN vs Gre	1	0.235	2.12	0.175	0.006	0.06	1	0.191	1.04	0.103	0.367	1
	UB vs Syr	1	0.445	3.91	0.281	0.003	**0.03**	1	0.541	2.94	0.246	0.006	0.06
	UB vs Gre	1	0.321	3.11	0.237	0.001	**0.01**	1	0.381	2.20	0.216	0.022	0.22
	Syr vs Gre	1	0.371	2.83	0.221	0.005	**0.05**	1	0.272	1.38	0.133	0.159	1

Table S7: Pairwise Adonis comparisons of the Bray-Curtis index measured for AMF community between the genotypes of rootstock or scion in the rhizosphere and the root endosphere. Significant adjusted *p*-values (< 0.05) are highlighted in bold.

		AMF											
		Rhizosphere						Root endosphere					
		Df	SumsOfSqs	F.Model	R2	*p*-value	*p*-adjusted	Df	SumsOfSqs	F.Model	R2	*p*-value	*p*-adjusted
Rootstock	1103P vs Nem	1	0.750	1.99	0.166	0.011	0.165	1	0.541	1.62	0.153	0.075	1
	1103P vs SO4	1	0.636	1.56	0.135	0.071	1	1	0.299	0.83	0.085	0.615	1
	1103P vs RGM	1	0.534	1.46	0.127	0.162	1	1	0.512	1.68	0.157	0.064	0.96
	1103P vs 41B	1	0.532	1.45	0.126	0.14	1	1	0.478	1.13	0.112	0.257	1
	1103P vs 3309C	1	1.047	3.35	0.251	0.002	**0.03**	1	0.587	1.80	0.167	0.118	1
	Nem vs SO4	1	0.387	1.01	0.091	0.427	1	1	0.312	1.03	0.093	0.421	1
	Nem vs RGM	1	0.455	1.32	0.117	0.187	1	1	0.216	0.85	0.079	0.623	1
	Nem vs 41B	1	0.657	1.90	0.160	0.014	0.21	1	0.569	1.59	0.137	0.067	1
	Nem vs 3309C	1	0.563	1.94	0.163	0.026	0.39	1	0.264	0.97	0.089	0.442	1
	SO4 vs RGM	1	0.490	1.31	0.116	0.151	1	1	0.279	1.01	0.092	0.488	1
	SO4 vs 41B	1	0.574	1.53	0.132	0.061	0.915	1	0.322	0.84	0.078	0.594	1
	SO4 vs 3309C	1	0.431	1.34	0.119	0.15	1	1	0.452	1.53	0.132	0.163	1
	RGM vs 41B	1	0.325	0.97	0.089	0.52	1	1	0.563	1.69	0.144	0.048	0.72
	RGM vs 3309C	1	0.708	2.54	0.202	0.004	0.06	1	0.548	2.22	0.182	0.037	0.555
	41B vs 3309C	1	0.938	3.34	0.250	0.003	**0.045**	1	0.665	1.89	0.159	0.032	0.48
Scion	CS vs PN	1	0.452	1.22	0.108	0.215	1				nd		
	CS vs UB	1	0.466	1.33	0.117	0.185	1				nd		
	CS vs Syr	1	0.782	2.79	0.218	0.013	0.13				nd		
	CS vs Gre	1	0.315	0.90	0.082	0.554	1				nd		
	PN vs UB	1	0.688	1.77	0.150	0.011	0.11				nd		
	PN vs Syr	1	0.866	2.72	0.213	0.014	0.14				nd		
	PN vs Gre	1	0.473	1.21	0.108	0.21	1				nd		
	UB vs Syr	1	0.930	3.13	0.238	0.009	0.09				nd		
	UB vs Gre	1	0.482	1.31	0.116	0.163	1				nd		
	Syr vs Gre	1	0.455	1.52	0.132	0.109	1				nd		

Table S8: Comparison of the bacterial metabolic pathways predicted with PICRUSt2 between the rhizosphere and the root endosphere.
Asterisks represent significant differences between the root system compartments using Student test or Wilcoxon test (n=60): *p-value<0.05, ** p-value <0.01, *** p-value <0.001.

Metabolic pathways	Rhizosphere		Root endosphere		p -value	
	mean	sd	mean	sd		
Amino acid metabolism	132939	2008	131251	2278	**3.72e-05**	***
Biosynthesis of other secondary metabolites	26355	1888	23129	1858	**5.923e-16**	***
Carbohydrate metabolism	135468	2329	130675	1864	**2.438e-16**	***
Energy metabolism	50142	910	45456	1894	**< 2.2e-16**	***
Glycan biosynthesis and metabolism	24839	1135	22280	2688	**7.392e-08**	***
Lipid metabolism	57421	1571	65740	4302	**< 2.2e-16**	***
Membrane transport	17916	1438	15387	1517	**8.05e-16**	***
Metabolism of cofactors and vitamins	110981	2650	101894	5369	**< 2.2e-16**	***
Metabolism of other amino acids	49166	1735	49682	2586	**0.004209**	**
Metabolism of terpenoids and polyketides	92957	3598	91588	4873	**0.01689**	*
Nucleotide metabolism	13917	371	12766	548	**< 2.2e-16**	***
Signal transduction	4844	586	3898	313	**6.131e-16**	***
Signaling molecules and interaction	7	6	3	8	**5.289e-07**	***
Xenobiotics biodegradation and metabolism	83738	7064	124334	11289	**< 2.2e-16**	***

Table S9: Comparison of the bacterial metabolic pathways predicted with PICRUSt2 between rootstock or scion genotypes in the rhizosphere or the root endosphere.
Significances were assessed through a Two-way ANOVA. Asterisks represent significant effects * *p*-value <0.05, ** *p*-value <0.01, *** *p*-value <0.001.

		Influence of the rootstock						Influence of the scion					
		Rhizosphere			Root endosphere			Rhizosphere			Root endosphere		
		p -value		PVE	*p* -value		PVE	*p* -value		PVE	*p* -value		PVE
Amino acid metabolism	Genotype (G)	**8.00e-10**	***	**80%**	**0.002**	**	**46%**	0.088	ns	/	0.917	ns	/
	Block (B)	0.101	ns	/	0.493	ns	/	0.891	ns	/	0.247	ns	/
	G x B	0.194	ns	/	0.144	ns	/	0.103	ns	/	**0.029**	*	**38%**
Biosynthesis of other secondary metabolites	G	**4.40e-04**	***	**49%**	0.996	ns	/	0.278	ns	/	0.337	ns	/
	B	0.073	ns	/	0.597	ns	/	0.198	ns	/	0.051	ns	/
	G x B	0.114	ns	/	0.971	ns	/	0.928	ns	/	0.477	ns	/
Carbohydrate metabolism	G	**3.89e-04**	***	**51%**	0.396	ns	/	**0.037**	*	**33%**	0.115	ns	/
	B	0.230	ns	/	0.414	ns	/	0.719	ns	/	0.111	ns	/
	G x B	0.170	ns	/	0.284	ns	/	**0.048**	*	**24%**	0.440	ns	/
Energy metabolism	G	**0.016**	*	**18%**	0.528	ns	/	**0.039**	*	**28%**	0.267	ns	/
	B	**1.64e-07**	***	**51%**	0.811	ns	/	**0.023**	*	**14%**	0.269	ns	/
	G x B	**0.018**	*	**13%**	0.520	ns	/	**0.004**	**	**30%**	0.889	ns	/
Glycan biosynthesis and metabolism	G	**1.33e-05**	***	**58%**	0.380	ns	/	0.075	ns	/	0.949	ns	ns
	B	**0.016**	*	**8%**	0.243	ns	/	0.367	ns	/	**0.014**	*	**23%**
	G x B	0.360	ns	/	0.630	ns	/	0.109	ns	/	**0.006**	**	**39%**
Lipid metabolism	G	**4.81e-06**	***	**64%**	**0.013**	*	**38%**	**0.008**	**	**42%**	0.805	ns	/
	B	0.15	ns	/	0.670	ns	/	0.467	ns	/	0.253	ns	/
	G x B	0.340	ns	/	0.709	ns	/	0.074	ns	/	**0.006**	**	**45%**
Membrane transport	G	**2.47e-04**	***	**51%**	**0.002**	**	**46%**	**0.026**	*	**36%**	0.530	ns	/
	B	0.075	ns	/	0.721	ns	/	0.625	ns	/	0.778	ns	/
	G x B	0.306	ns	/	0.381	ns	/	0.119	ns	/	**0.047**	*	**34%**
Metabolism of cofactors and vitamins	G	**0.016**	*	**31%**	0.870	ns	/	0.119	ns	/	0.690	ns	/
	B	**0.005**	**	**17%**	0.743	ns	/	0.077	ns	/	0.075	ns	/
	G x B	0.230	ns	/	0.198	ns	/	**0.013**	*	**31%**	**0.008**	**	**40%**
Metabolism of other amino acids	G	**5.52e-04**	***	**47%**	0.498	ns	/	0.056	ns	/	0.112	ns	/
	B	**0.019**	*	**9%**	0.335	ns	/	0.465	ns	/	0.332	ns	/
	G x B	0.123	ns	/	0.668	ns	/	0.151	ns	/	**0.013**	*	**33%**
Metabolism of terpenoids and polyketides	G	**3.28e-04**	***	**42%**	0.089	ns	/	0.137	ns	/	0.690	ns	/
	B	**3.40e-04**	***	**21%**	0.089	ns	/	**0.0220**	*	**16%**	**0.021**	*	**19%**
	G x B	0.051	ns	/	0.267	ns	/	0.421	ns	/	**0.007**	**	**37%**
Nucleotide metabolism	G	**0.002**	**	**39%**	0.966	ns	/	0.069	ns	/	0.842	ns	/
	B	**0.003**	**	**16%**	0.461	ns	/	0.407	ns	/	0.095	ns	/
	G x B	0.460	ns	/	0.400	ns	/	0.061	ns	/	**0.019**	*	**38%**
Signal transduction	G	**1.50e-04**	***	**53%**	**3.67e-05**	***	**60%**	**0.030**	*	**35%**	0.379	ns	/
	B	0.080	ns	/	0.846	ns	/	0.680	ns	/	0.164	ns	/
	G x B	0.222	ns	/	0.257	ns	/	0.119	ns	/	0.698	ns	/
Signaling molecules and interaction	G	**0.002**	**	**42%**	0.681	ns	/	0.078	ns	/	0.574	ns	/
	B	**0.023**	*	**10%**	0.217	ns	/	0.837	ns	/	0.553	ns	/
	G x B	0.062	ns	/	0.454	ns	/	**0.002**	**	**40%**	0.451	ns	/
Xenobiotics biodegradation and metabolism	G	**0.013**	*	**25%**	0.484	ns	/	**0.020**	*	**33%**	0.167	ns	/
	B	**4.94e-05**	***	**33%**	0.764	ns	/	**0.028**	*	**12%**	0.147	ns	/
	G x B	0.296	ns	/	0.562	ns	/	0.050	ns	/	0.104	ns	/

Supplementary figures

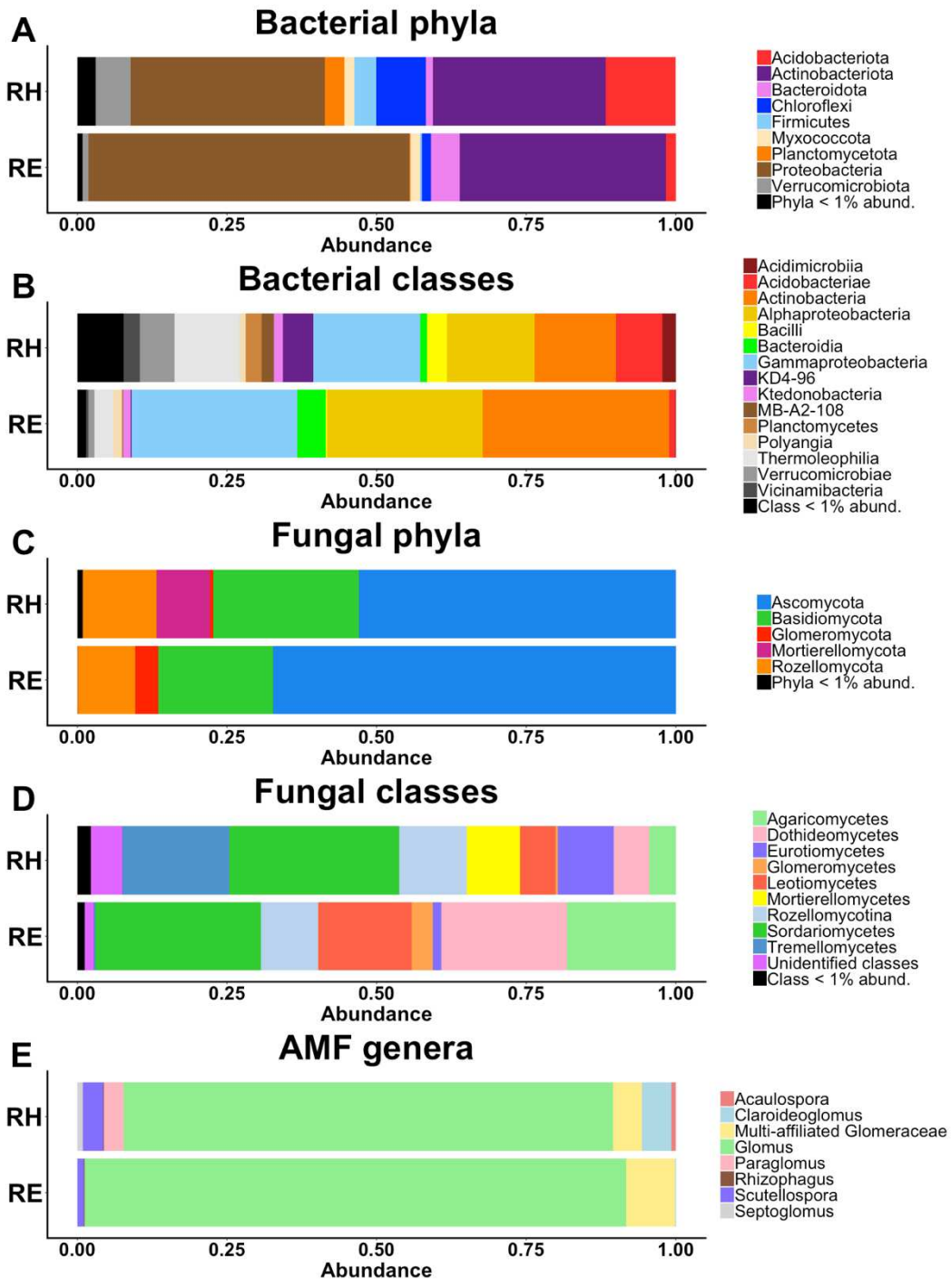


Figure S1: Comparison of the relative abundances of (A, B) bacterial phyla and classes, (C, D) fungal phyla and classes, and (E) AMF genera between the root endosphere and the rhizosphere.

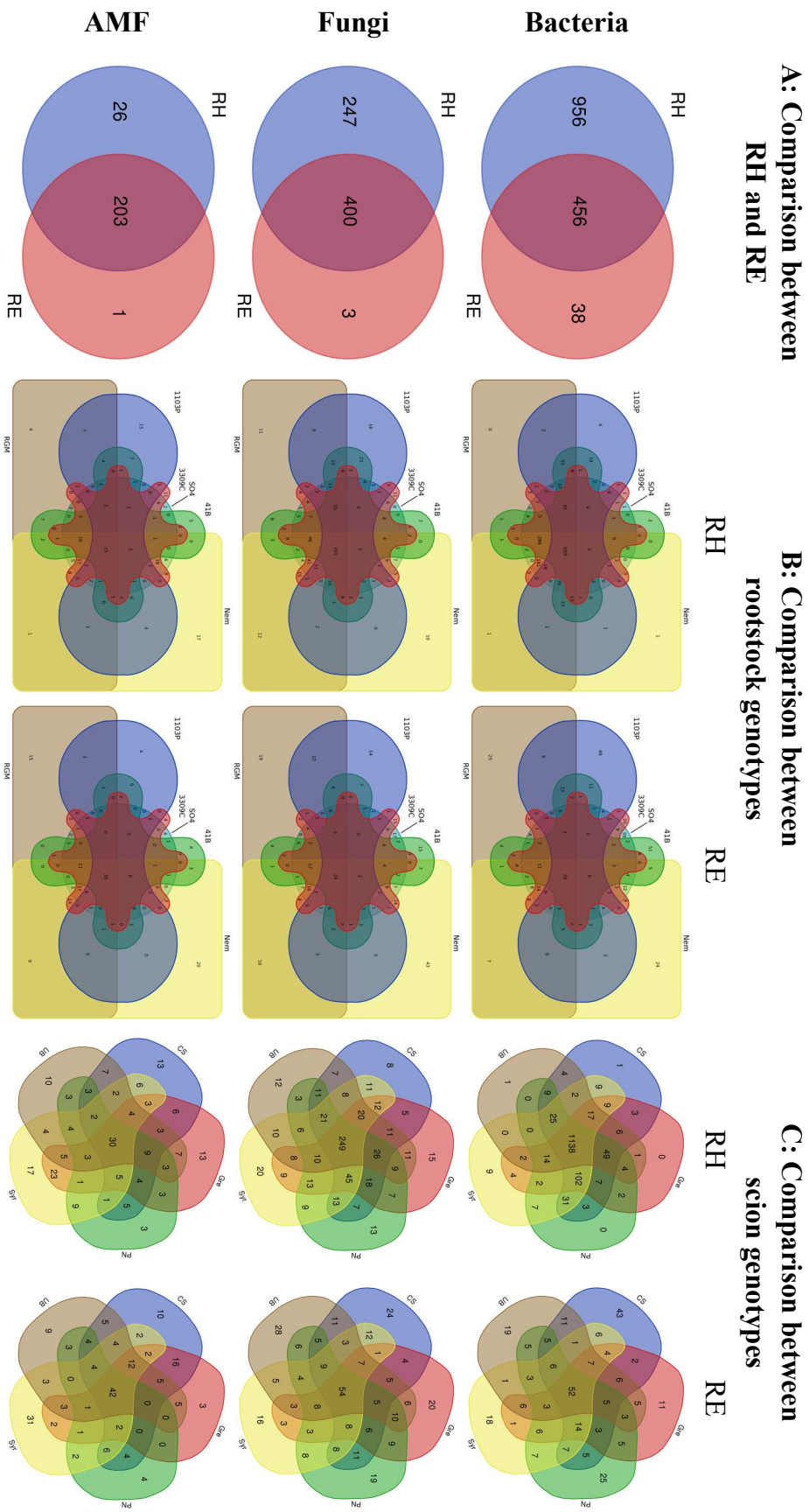


Figure S2: Venn diagrams showing common and specific OTUs of bacteria, fungi and AMF, between (A) root compartments, (B) rootstock and (C) scion genotypes.

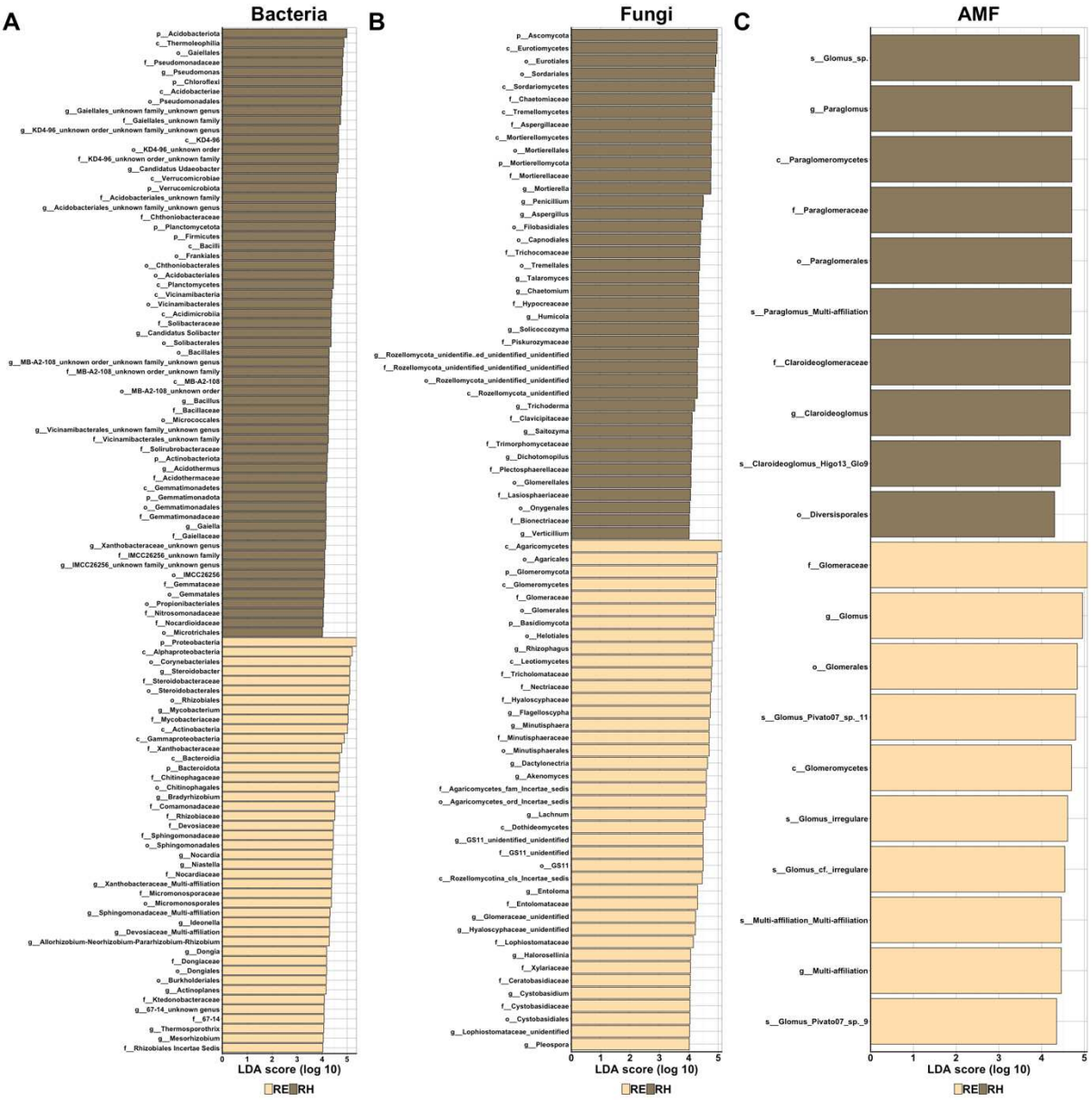


Figure S3: Histograms of the linear discriminant analysis (LDA) scores (> 4) reveal the most differentially abundant taxa of (A) bacteria, (B) fungi and (C) AMF among the rhizosphere (dark brown) and the root endosphere (light brown).

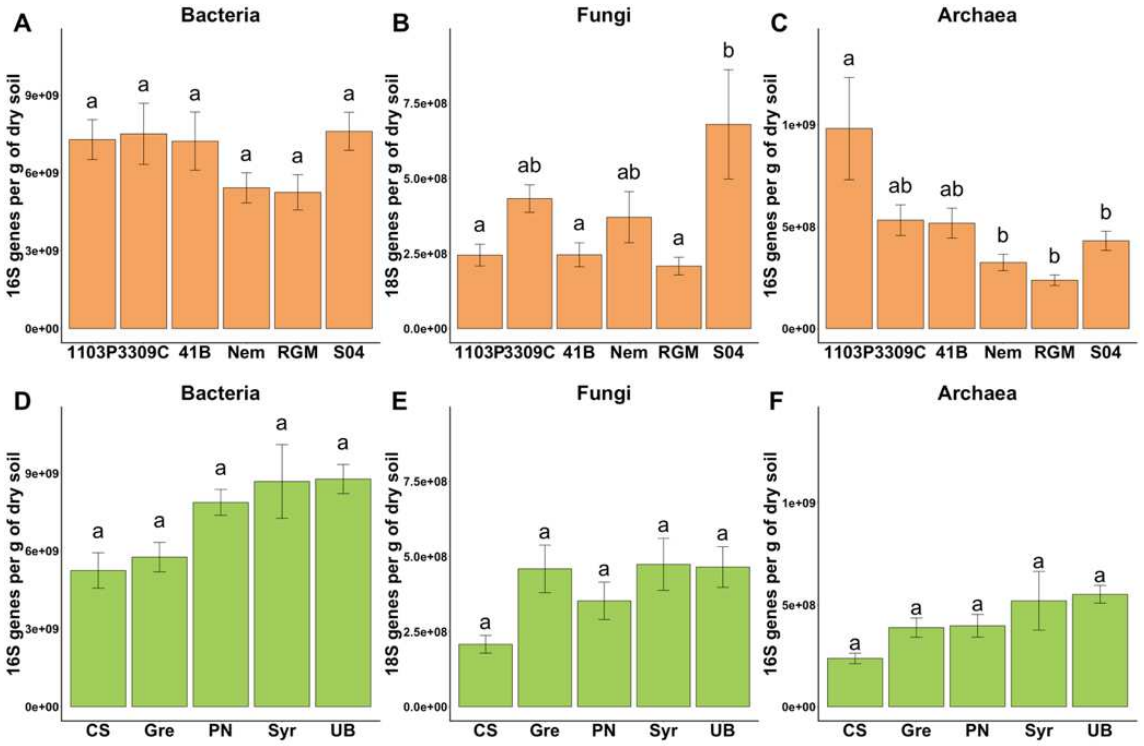


Figure S4: Comparison of the levels of rhizosphere bacteria, fungi and archaea measured by qPCR between the rootstock (A, B and C, respectively, orange) or the scion genotypes (D, E and F, respectively, green).
Data are represented as mean ± SE, for the comparisons between rootstocks (orange, n = 6) or scion genotypes (green, n = 5). P-values were calculated using pairwise-Student tests with Bonferroni correction and letters indicate significant differences when the adjusted *p*-value < 0.05.

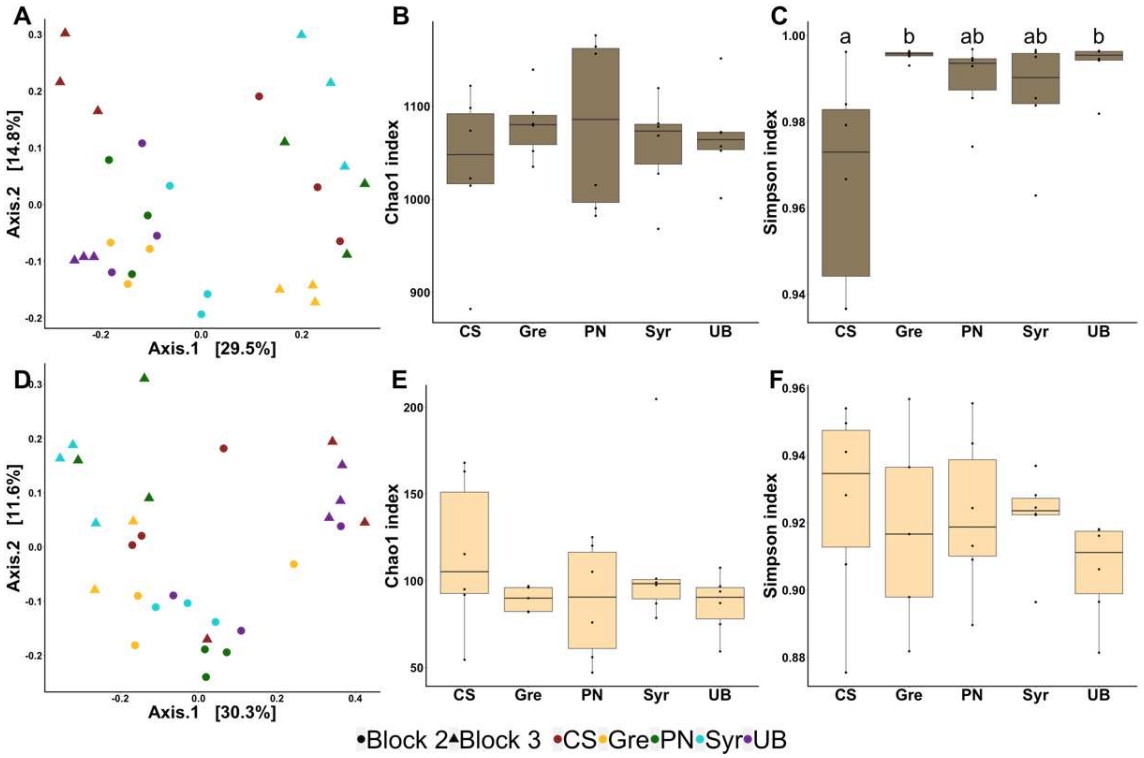


Figure S5: Comparison of bacterial communities in the rhizosphere (dark brown, top panel) and the root endosphere (light brown, bottom panel) between the five scion genotypes grafted onto RGM (n=6).
Comparison of bacterial communities by principal coordinate analysis (PCoA) based on Bray–Curtis dissimilarity matrices in the rhizosphere (A) and the root endosphere (D). Comparison of bacterial richness (Chao1) and diversity (Simpson) in the (B, C) rhizosphere and the (E, F) root endosphere. *p*-values were calculated using Pairwise-Student tests with Bonferroni correction and were considered as significant when the adjusted *p*-value < 0.05.

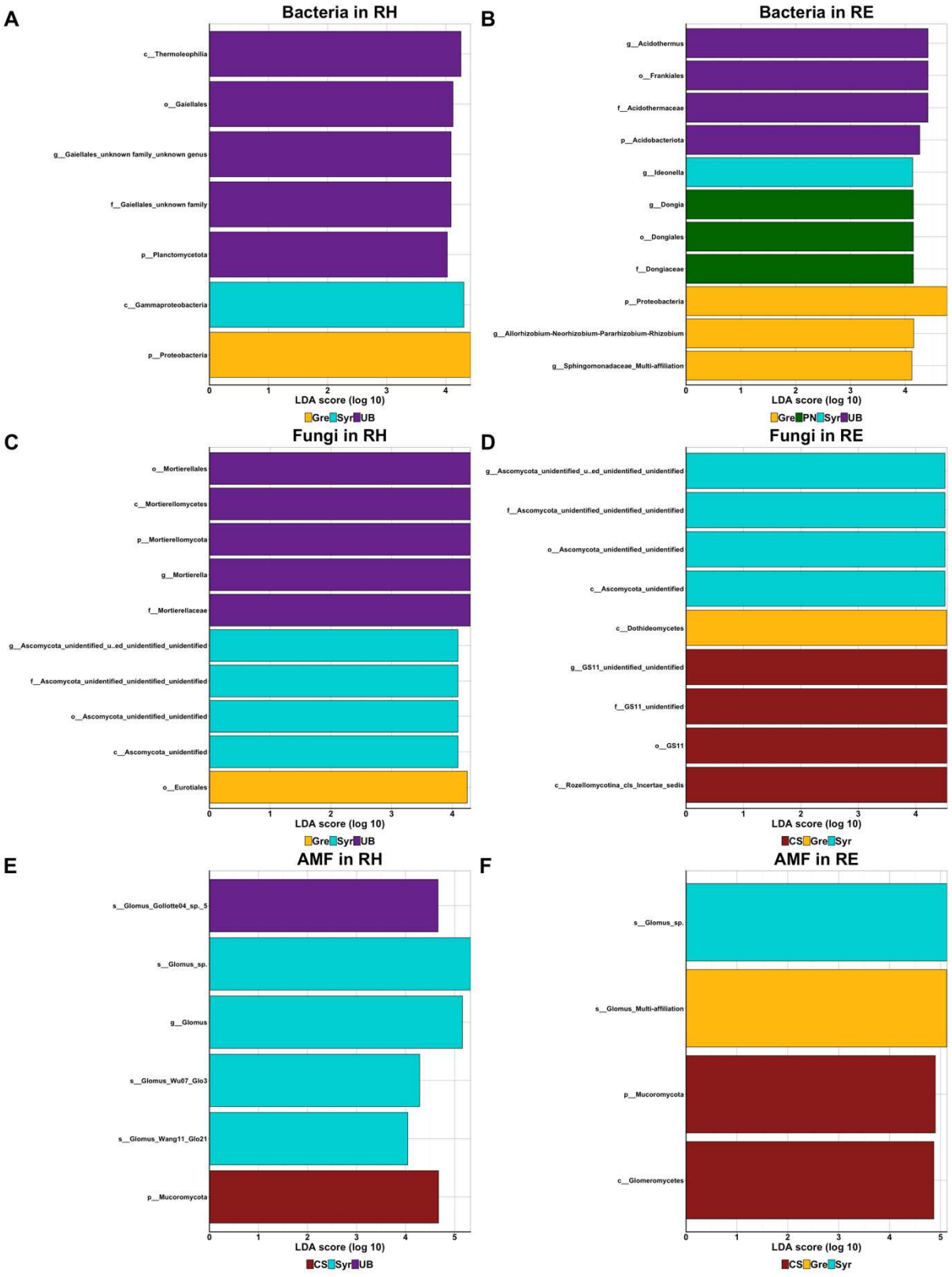


Figure S6: Histogram of the linear discriminant analysis (LDA) scores reveals the most differentially abundant taxa of bacteria in the rhizosphere (A) and the root endosphere (B) between scion genotypes.

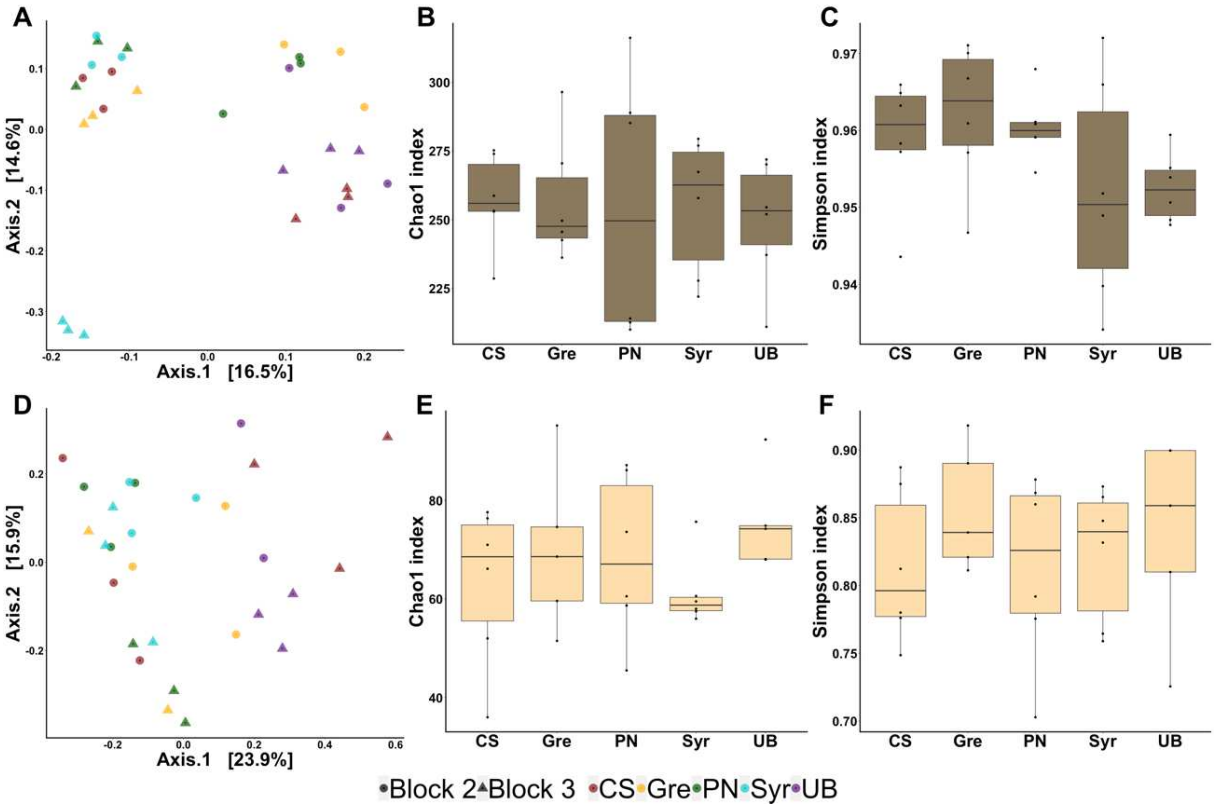


Figure S7: Comparison of fungal communities in the rhizosphere (dark brown, top panel) and the root endosphere (light brown, bottom panel) between the five scion genotypes grafted onto RGM (n=6). Comparison of fungal communities by principal coordinate analysis (PCoA) based on Bray-Curtis dissimilarity matrices in the rhizosphere (A) and the root endosphere (D). Comparison of fungal richness (Chao1) and diversity (Simpson) in the (B, C) rhizosphere and the (E, F) root endosphere. *p*-values were calculated using Pairwise-Student tests with Bonferroni correction and were considered as significant when the adjusted *p*-value < 0.05.

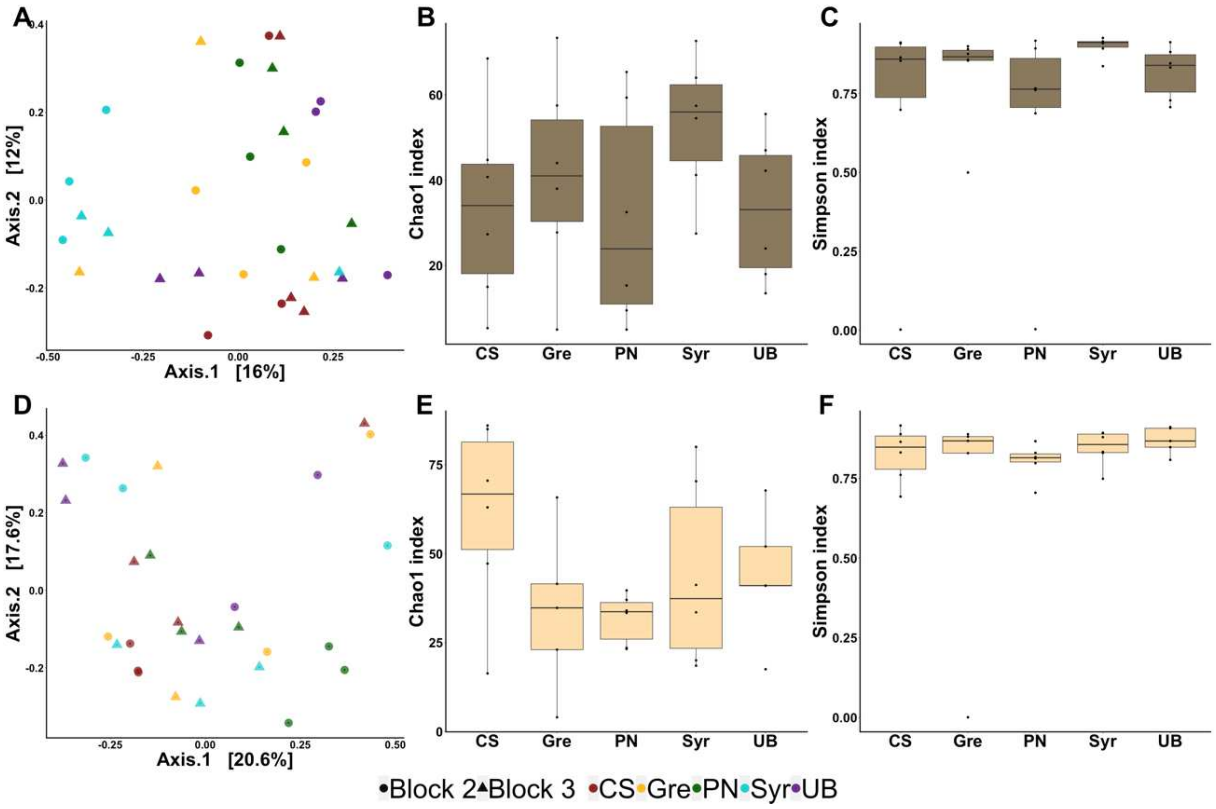


Figure S8: Comparison of AMF communities in the rhizosphere (dark brown, top panel) and the root endosphere (light brown, bottom panel) between the five scion genotypes grafted onto RGM (n=6). Comparison of AMF communities by principal coordinate analysis (PCoA) based on Bray-Curtis dissimilarity matrices in the rhizosphere (A) and the root endosphere (D). Comparison of AMF richness (Chao1) and diversity (Simpson) in the (B, C) rhizosphere and the (E, F) root endosphere. *p*-values were calculated using Pairwise-Student tests with Bonferroni correction and were considered as significant when the adjusted *p*-value < 0.05.

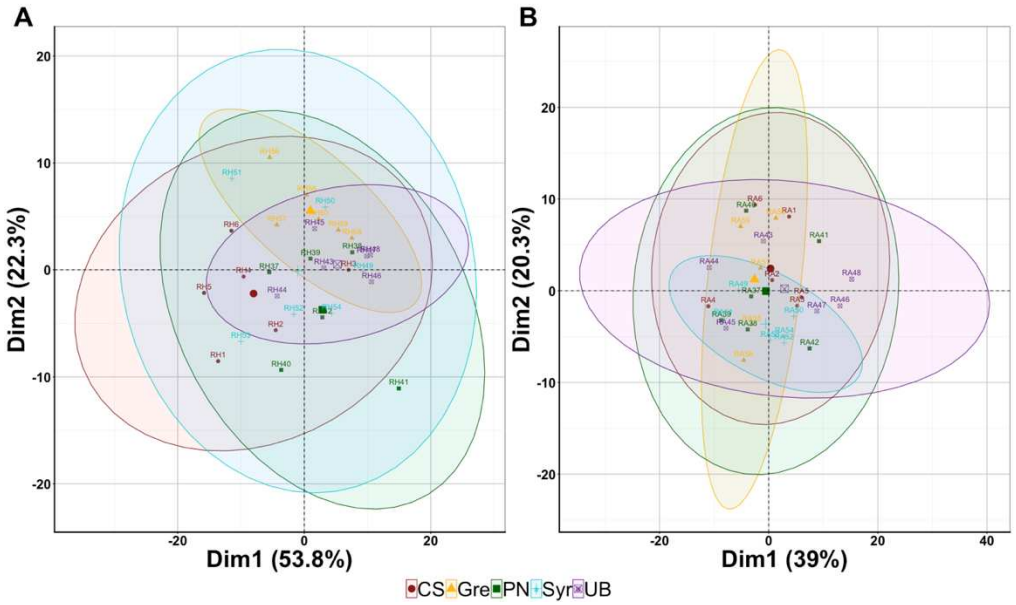


Figure S9: PCA analysis of the predicted functions of bacteria (119 variables) between scion genotypes in the rhizosphere (A) and the root endosphere (B).

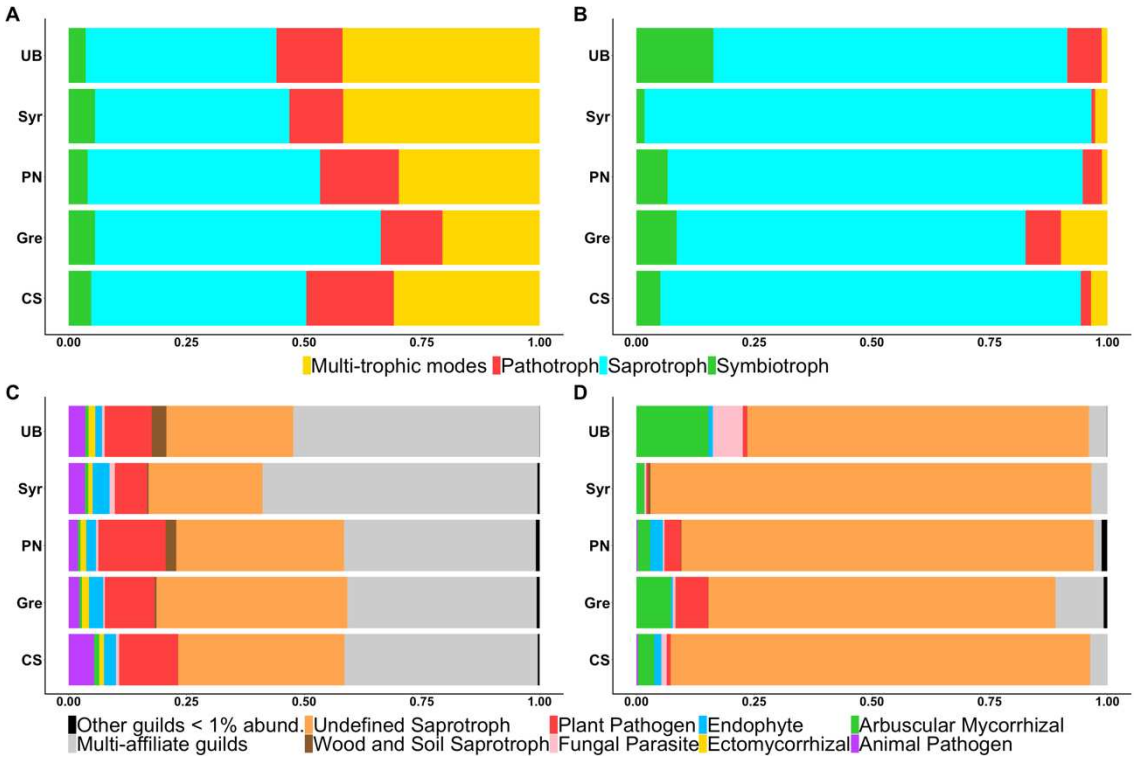


Figure S10: Comparison between scion genotypes of the trophic mode (A, B) and the guild (C, D) in the rhizosphere and the root endosphere.

Chapitre 2 : Influence des génotypes du plant greffé de vigne sur la communauté des champignons mycorhiziens arbusculaires des racines

Préface

Précédemment, nous avons vu que les deux génotypes du plant greffé de vigne impactent significativement la composition des microbiotes bactériens et fongiques de la rhizosphère et de l'endosphère racinaire, y compris les champignons mycorhiziens arbusculaires, avec une contribution plus forte du porte-greffe. Comme les CMA sont prometteurs pour la viticulture et qu'une seule étude précédente démontrait un effet du porte-greffe sur cette communauté, nous avons souhaité ici confirmer l'influence des deux composants du plant greffé sur la diversité des CMA de l'endosphère racinaire. Pour cela, nous avons prélevé en septembre 2021 des échantillons de racines des 10 mêmes combinaisons de porte-greffe × greffon, cette fois-ci réparties uniquement sur le bloc 1 de la parcelle GreffAdapt, afin de réduire la variabilité biologique liée aux différents paramètres pédologiques des blocs. La diversité des CMA a été étudiée par une approche de métabarcoding, en ciblant cette fois-ci le gène codant l'ARNr 18S. En parallèle, la même analyse a été réalisée en ciblant celui codant l'ARNr 28S, seulement chez les six génotypes porte-greffes (greffés avec le Cabernet-Sauvignon), afin de comparer les méthodes entre elles, ainsi qu'avec les résultats obtenus lors du premier prélèvement pour l'effet du porte-greffe. De plus, le degré de colonisation du système racinaire des 10 combinaisons a été quantifiée par microscopie. Enfin, nous avons établi des corrélations entre la diversité et la quantité de CMA au sein des racines avec le phénotype de la plante. Nos résultats d'analyse microscopique montrent que les deux génotypes ne semblent pas impacter la capacité d'association des racines avec les CMA. En revanche, l'impact du PG sur la diversité des CMA est à nouveau démontré avec les deux approches de métabarcoding, quand celui du cépage reste faible ou inexistant. Enfin, l'observation de corrélations positives entre les variables utilisées pour caractériser les CMA des racines et le phénotype du plant souligne les actions bénéfiques de ces champignons sur la plante. Ce chapitre est présenté sous format d'article qui sera retravaillé avant soumission à une revue.

Chapitre 2

Influence of grapevine rootstock and scion genotypes on the structure and composition of arbuscular mycorrhizal fungi associated with the root system

Vincent Lailheugue, Romain Darriaut[1], Joseph Tran, Marine Morel, Elisa Marguerit, Virginie Lauvergeat*

EGFV, Univ. Bordeaux, Bordeaux Sciences Agro, INRAE, ISVV, F-33882 Villenave d'Ornon, France

* corresponding author: virginie.lauvergeat@inrae.fr

[1] Present address : Univ Rennes, CNRS, ECOBIO (Ecosystèmes, biodiversité, évolution) - UMR 6553, F-35000 Rennes, France

Abstract:

Background:

The contribution of Arbuscular Mycorrhizal fungi (AMF) to better resilience of the grapevine in the face of climate change but also to the need to reduce the use of pesticides and fertilizers is an increasingly relevant question. Characterizing the effects of rootstock and scion genotypes on the association with native AMF communities, as well as the roles of AMF on grapevine development, could provide new avenues for adapting viticulture to these current problematics. As several methodologies exist to study the efficiency of the mycorrhization with AMF, we first evaluated the root colonization of ten scion × rootstock combinations using microscopy after ink staining of young roots. Then, AMF community structure in roots were analyzed using metabarcoding approach using the 18S rRNA gene sequencing. A second gene (28S rRNA gene) was targeted for some combinations to compare the results and evaluate the effect of the targeted gene in metabarcoding approaches.

Results

The root colonization indexes were not significantly different between the grapevine scion or rootstock genotypes. Metabarcoding analyses show an effect of the rootstock genotype on the β-diversity and the enrichment of several AMF genera in each of the rootstocks with the two targeted genes, as well as an effect on the Chao1 index with the 18S rRNA gene. No significant differences were found between scion genotypes for the α- and β-diversity metrics and very few taxa were found to be enriched in the root system of RGM grafted with the different cultivars. Finally, several correlations were established between AMF community and plant phenotype, such as the Simpson index with the yield, the bunch number, or the shoot numbers of grapevine.

Conclusion

These results confirm that vine rootstocks do not recruit the same functional communities of AMF when subjected to the same pedoclimatic conditions. The scion has little or no effect on the AMF community associated with the root system of the RGM rootstock. AMF are promising for viticulture, as observed with the significant correlations observed between AMF community and grapevine phenotype, suggesting the need for a consensus method for studying these beneficial micro-organisms.

Keywords: Arbuscular Mycorrhizal Fungi, Root system, Illumina sequencing, Microscopy.

Chapitre 2

Background

Nowadays, about 80% of land plants form intimate symbiotic associations with a class of ubiquitous soil microorganisms called arbuscular mycorrhizal fungi (AMF) in a wide range of terrestrial environments (Smith and Read, 2010). Fossilized AMF-type hyphae and spores from the Ordovician period suggest that AM symbiosis appeared 460 million years ago and played a key step in the evolution of terrestrial plants. AMF are obligate biotrophs which provide mineral nutrients to the host plant in exchange of 4 to 23% of photosynthetically fixed carbon (Salmeron-Santiago et al., 2021). Within the rhizosphere, defined as the area of soil stuck to the roots, AM symbiosis is achieved by chemical communication between both partners. AMF release Myc factors that are perceived by plant receptors, inducing a common signaling pathway leading to the establishment of the symbiosis (Wang et al., 2021). Strigolactones (SL) constitute a class of plant hormone derived from the carotenoid biosynthetic pathway, which are known to be exuded by the roots, mainly in response to N and P starvation (Yoneyama et al., 2018). SL are known to induce the germination of AMF spores, as well as the growth of hyphae until they reach the root surface to form hyphopodia. The epidermal cells of plant roots undergo a series of reprogramming events to form a prepenetration apparatus that guides the hyphae through the root epidermal cells. Hyphae develop in the cortical cells of the root, forming highly branched structures called arbuscules, surrounded by a periarbuscular membrane that provides a wide interface for the exchange of nutrients (Wang et al., 2017).

Currently, around 300 AMF species have been described. Even if AMF phylogeny still controversy, Redecker et al. (2013) proposed a consensus classification of the Glomeromycetes division into four orders (*Diversisporales*, *Glomerales*, *Archaeosporales* and *Paraglomerales*) subdivided into 11 families. Quantification of AMF community in soil and roots has traditionally been performed by microscopic methods such as spore density (Gerdemann and Nicolson, 1963) and root colonization (Phillips and Hayman, 1970). Alternatively, lipid biomarker analysis can be used to measure AMF population density (Sharma and Buyer, 2015). Very recently, molecular methods were developed to estimate mycorrhization intensity by qPCR (Bodenhausen, 2021) and RT-qPCR (Duret et al., 2022). Finally, sequencing of AMF ribosomal Internal Transcribed Spacers (ITS), 18S rRNA or 28S rRNA genes provided deeper insights about AMF diversity (Suzuki et al., 2020).

Viticulture adaptation to sustainable agriculture and climate change can take benefit of AMF (Torres et al., 2018). AMF are particularly known to improve grapevine mineral uptake (especially in

phosphorus) by increasing soil exploration surface and activating plant transport proteins for P, N and other elements (Schreiner, 2005; Trouvelot et al., 2015; Moukarzel et al., 2023). Moreover, AMF increase grapevine tolerance to biotic stresses such as diseases caused by pathogenic fungi (Cruz-Silva et al., 2021; Moukarzel et al., 2022) or viruses (Gaši et al., 2023). Several roles in mitigating abiotic stresses such as salt stress, drought, or copper toxicity were also reported in grapevine (Gazioglu Sensoy, 2022; Aguilera et al., 2022; Brunetto et al., 2023). They increase the soil structural stability and quality (Trouvelot et al., 2015). Finally, mycorrhizal symbiosis has been proposed to improve berry quality (Torres et al., 2018). In this context, finding rootstock genotypes with a high capacity of association with AMF, as well as discovering new AMF species that are better adapted to wine-growing terroirs, could be levers for adapting to the problems of the wine industry.

Since the Phylloxera crisis, *V. vinifera* is grafted on hybrid of American Vitis naturally tolerant to the soil-born aphid. Many signaling and regulating molecules, such as hormones, are exchanged between partners (Ollat et al., 2017). Darriaut et al. (2022a) showed that RGM rootstock presented a significatively higher intensity of mycorrhization, as well as a higher relative abundance of Glomeromycota sequences than 1103P when grown in symptomatic vineyard soil. These results are consistent with previous works (Cochetel et al., 2018; Lailheugue et al., 2023) which suggest that RGM produce more strigolactones than 1103P when subjected to N depletion in the nutritive solution. A recent study based on denaturing gradient gel electrophoresis and trap cultures shows an effect of the rootstock genotype on the AMF community composition (Moukarzel et al., 2021a). In a previous study, we investigated the effect of the rootstock and the scion genotypes on the rhizosphere and the root endosphere microbiomes (Chapter 1). In the root samples harvested in May 2021, the Glomeromycota community was analyzed using Illumina sequencing of the *Glomeromycota* 28S rRNA gene. We identified significant differences of the α- and β-diversity indexes (Chao1, Simpson and Bray-Curtis indexes) between the six rootstocks grafted with the same scion. In the present study, we performed a second experiment on the same combinations grown in another area of the same plot and young white roots were harvested in September 2021. Furthermore, to confirm the differences previously observed between rootstocks, we used three approaches: microscopy, and Illumina sequencing of two different genes involving or not nested PCR. The correlation between the resulting variables and the phenotypic traits of the plants were investigated.

Material and methods

Site, plant material and sample collection

The experiment was conducted in September 2021 in the GreffAdapt plot, located near Bordeaux, France (44°47'26.6"N 0°34'26.7"W). The plot was previously described in a previous experiment (Chapter 1). The soil was analyzed by Aurea Agrosciences (Orléans, France) and its nature is sandy and gravely (Supplementary Table 1). To study the ability of different rootstock genotypes to associate with AMF, root samples were collected from six rootstocks: 1103 Paulsen (1103P), 3309 Couderc (3309C), 41 B Millardet et de Grasset (41 B), Nemadex Alain Bouquet (Nem), Riparia Gloire de Montpellier (RGM) and Sélection Oppenheim 4 (SO4), grafted with a Cabernet-Sauvignon (CS) scion. To evaluate the effect of the scion, samples of RGM roots grafted with Grenache (Gre), Pinot noir (PN), Syrah (Syr) and Ugni blanc (UB) were also collected. For each combination, roots' samples were collected on five plants per genotype at a depth of 20-30 cm. For microscopic analyses, the smallest, young, and white roots were collected in Falcon tube containing 50 ml of ethanol 10% and transferred to 4°C before being processed. Roots of all sizes were rinsed with sterile water and transferred in empty tubes, frozen using liquid nitrogen and stored at -80°C before DNA extraction.

Staining and quantification of root mycorrhiza by microscopy

The staining protocol was adapted from the method of Phillips and Hayman (1970). Briefly, the roots were incubated in 40 ml KOH 10% during 30 min at 95°C. After this step, 500 µl of H_2O_2 30% were added and left to react for 5 minutes at ambient temperature. The roots were then rinsed 3 times with distilled water, drained and transferred to the staining solution (5% of Sheaffer black ink 94231 and 8% of FLUKA acetic acid 4574) for 5 min at 90°C. The roots were rinsed 3 times with distilled water, incubated in acetic acid 8% at ambient temperature during 15min and rinsed one last time with distilled water. The mycorrhization rate was estimated using the method of Trouvelot et al. (1986), based on the assignment of 6 classes graded from 0 to 5, dependent of the level of mycelium present in each root fragments. Thirty root fragments per individual were observed per microscopy (LEICA DM750) and the mycorrhization frequency (F%), the overall mycorrhization intensity (M%) and the mycorrhization intensity of mycorrhized fragments (m%) were calculated using the Mycocalc program (INRAe, Dijon).

DNA extraction from the roots

Roots were ground in 35-ml stainless-steel grinding jar with 20-mm stainless steel balls at 30 oscillations per second during 30 seconds with the mixer mill MM400 (Retsch, Haan, Germany), using

liquid nitrogen and then stored at -80°C until processing. DNA was extracted from 150 mg of frozen root powder using the protocol of Berger et al. (2022). Extracted DNA was quantified on a Qubit® 3.0 fluorometer (Thermo Fisher Scientific) using the Qubit™ dsDNA HS Assay Kit, and its quality was checked with a NanoDrop™ 2000/2000c spectrophotometer (Thermo Fisher Scientific). DNA was then stored at –20 °C until further use.

Amplification of the glomeromycotan 18S and 28S rRNA genes

The glomeromycotan 18S rRNA gene was amplified by PCR using the primer pair AMV4.5NF/AMDGR. The glomeromycotan 28S rRNA gene was amplified using a Nested PCR using the same methodology as in Chapter 1. A first PCR was performed with the primer pair LR1/NDL22 to amplify the Eucaryote 28S rRNA gene. The product has been diluted 100-fold and used as template for the second PCR using the primer pair FLR3/FLR4 to amplify the Glomeromycotan 28S rRNA gene. All the PCR reactions were monitored in a final volume of 25 µl composed of 5 µl of 5X GoTaq® colorless reaction buffer (Promega, France), 0.5 µl of each primer (10 µM), 0.5 µl of dNTPs (10mM), 0.125 µl of GoTaq® G2 DNA Polymerase (Promega, France), 1 µl of DNA extracted (1 ng. μl^{-1}) or 5 µl of the PCR product, and nuclease-free water (qsp. 25 µl). The sequence and the sources of the primers used and the cycling condition are presented in the Supplementary Table 2. Further steps were carried out at the Plateforme Génome Transcriptome de Bordeaux (Cestas, France). The PCR products were purified with the platform-specific SPRI magnetic beads (1X ratio) and quantified using Quant-iT^{TM} dsDNA assay kit (ThermoFisher, France). MID and Illumina sequencing adapters were added. Libraries were pooled in equimolar amounts using a Hamilton Microlab STAR robot and sequenced on an Illumina MiSeq platform using the MiSeq Reagent Nano Kit V2 (2 × 250 bp).

Metabarcoding data processing

Obtained sequences were demultiplexed with index search at the PGTB facility. The quality of the obtained sequences were first checked with FastQC v.0.11.8 (Sharma and Buyer, 2015). Sequences were quality filtered, trimmed, denoised, and clustered into Operational Taxonomy Units (OTUs) using FROGS pipeline from Galaxy instance (Escudié et al., 2018; Bernard et al., 2021). This involved assembling raw forward and reverse reads for each sample into paired-ended reads with a minimum overlapping of 50 nucleotides and 0.1 mismatch using the VSEARCH tool (Rognes et al., 2016). Primers were removed using Cutadapt (Martin, 2011), chimeras were detected and removed with UCHIME (Edgar et al., 2011), and clustering was performed using SWARM (Mahé et al., 2014) in the FROGS pipeline. The minimum sequence abundance proportion was set at $5e^{-5}$, with a minimum prevalence fixed at 4 to keep OTUs. Taxonomic assignments of 18S and 28S rRNA genes were

performed against MaarjAM database (Öpik et al., 2010). For the 28S rRNA gene, the sequences affiliated to "New_clade" at the class level were removed and one sample containing less than 5000 sequences was excluded before rarefying to the number of sequences in the sample containing the fewest sequences using the phyloseq "rarefy_even_depth" function. For the 18S rRNA gene, the sequences "#N/A" at the phylum level were removed and one sample containing less than 5000 sequences was excluded before rarefying in the same way as above.

Statistical analyses

All the statistical analyses were performed on R (v4.2.1) using RStudio (2022.07.1). Figures were generated with *ggplot2* (v3.4.1) and *ggthemes* (v4.0.4) and arranged with *ggpubr* (v0.4.0). Chao1 and Simson indexes were calculated using the "estimate_richness" function and PCoA based on the Bray-Curtis distance were done using the "plot_ordination" function, both from *phyloseq* (1.38.0) (McMurdie and Holmes, 2013). Linear Discriminant Analysis Effect Size (LEfSe) has been carried out using the "run_lefse" function from *microbiomeMarker* (1.2.2) with data transformation (log10), lda_cutoff fixed at 4, kw_cutoff and wilcoxon_cutoff at 0.05 (Cao et al., 2022). The effects of the genotypes on the α-diversity metrics and the variables measured by microscopy were tested with One-Way ANOVA or Kruskal-Wallis' test, depending on whether the assumptions of the parametric tests were met. Normality and heteroscedasticity were checked on residuals with Shapiro and Bartlett tests, respectively. Comparisons between genotypes were realized with "pairwise.t.test" or "pairwise.wilcox.test" functions with Bonferroni correction from the *stats* package (4.2.1). To test the effect of the genotype on the Bray-Curtis index, Permutational Analysis of Variance (PERMANOVA) with 999 permutations was done with the "adonis2" function from *vegan* package (2.6.4). Genotypes were then compared together using the "pairwise.adonis2" function from *pairwiseAdonis* (0.4.1). Venn diagrams showing common and exclusive OTUs were generated with the following tool: http://bioinformatics.psb.ugent.be/webtools/Venn/. Correlation matrix were established by using the "ggcorrplot" function from *ggcorplot* (0.1.4) with the "square" method and the *p*-values were calculated using the "cor.mtest" function.

Results

Rootstock and scion genotypes do not influence the intensity of the root colonization by AMF

Table 2-1: Effects of the genotype of rootstock or scion on the root colonization by AMF, assessed by measuring the mycorrhization frequency (F%), the overall mycorrhization intensity (M%) and the mycorrhization intensity of mycorrhized fragments (m%).

	Rootstock			Scion		
	p-value		PVE	p-value		PVE
F%	0.272	ns	/	0.212	ns	/
M%	**0.032**	*	**38%**	0.329	ns	/
m%	**0.039**	*	**37%**	0.328	ns	/

Significances were assessed through ANOVA. Asterisks represent significant effects * *p*-value <0.05, ** *p*-value <0.01, *** *p*-value <0.001, PVE: Percentage of variance explained, ns = non-significant.

The quantification of the mycorrhization frequency (F%) shows that all the studied plants were naturally mycorrhized in the GreffAdapt plot (Figure 1). ANOVA shows no effect of the rootstock genotype on this parameter (F%) (Table 1, Figure 1 A). An effect of the genotype was reported on the overall mycorrhization intensity (M%), but no significant differences were observed between rootstock genotypes using pairwise t-test with Bonferroni correction (Table 1, Figure 1 B). Same result was obtained for the mycorrhization intensity of mycorrhized fragments (m%) (Table 1). Together, these results suggest a slight or no influence of the rootstock genotype on the root system colonization by AMF. When the five scions grafted on RGM were studied, no effect of the genotype was reported on the three parameters (F%, M%, and m%), suggesting no contribution of the scion genotype on the root system colonization by AMF (Table 1, Figure 1).

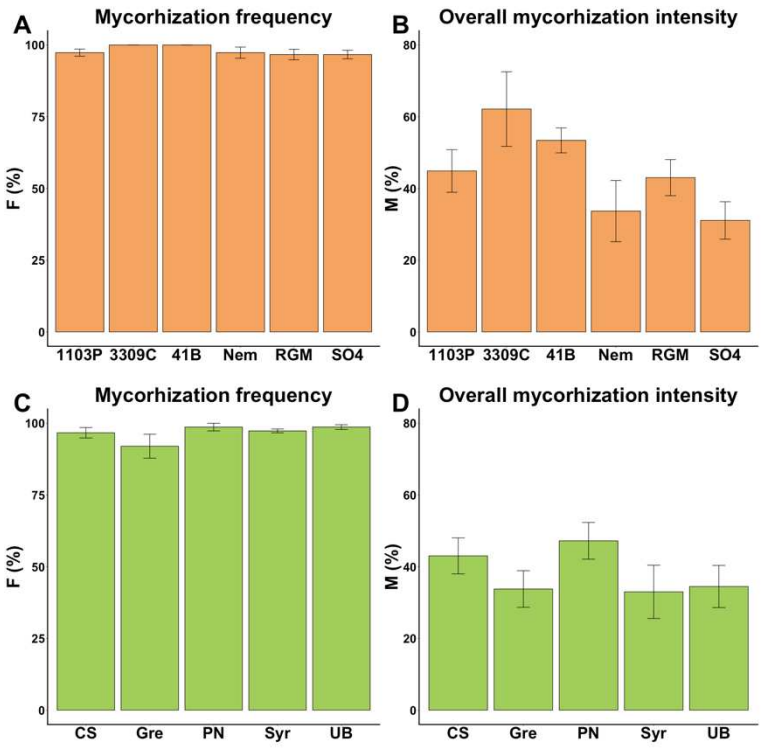


Figure 2-1: Comparison of the mycorrhization frequency (F%), the overall mycorrhization intensity (M%) and the mycorrhization intensity of mycorrhized fragments (m%) between genotypes of rootstock (A, B) or scion (C, D).
Data are represented as mean ± SE, n=5. No significant differences (*p*-value < 0.05) were observed between genotypes using pairwise-t-test with Bonferroni correction.

Comparison of rootstock AMF community by 28S rRNA gene sequencing

Table 2-2: Effects of the genotype of rootstock or scion on α-diversity (Chao1, Simpson) and β-diversity metrics.

Method	Factor	Chao1			Simpson			Bray-Curtis		
		p-value		PVE	p-value		PVE	p-value		PVE
28S rRNA gene	**Rootstock**	0.209	ns	/	0.065	ns	/	**0.001**	***	**47%**
18S rRNA gene	**Rootstock**	**0.020**	*	**46%**	0.574	ns	/	**0.001**	***	**39%**
	Scion	0.577	ns	/	0.349	ns	/	**0.016**	*	**31%**

Significances were assessed through ANOVA or PERMANOVA for α- or β-diversity metrics, respectively. Asterisks represent significant effects * *p*-value <0.05, ** *p*-value <0.01, *** *p*-value <0.001, PVE: Percentage of variance explained, ns = non-significant.

Comparison of the root AMF community assessed by 28S rRNA gene sequencing between rootstock genotypes shows dissimilar proportions of genera between genotypes (Figure 2A). *Glomus* was the main genera in the roots of all genotypes (ranging from 81 to 97% of abundance). Interestingly, several genera were genotype exclusive such as *Acaulospora* in 1103P (representing 7.5% of abundance) or *Gigaspora* (representing 0.5% of abundance) in SO4. Nineteen OTUs were common

between all the genotypes but others were exclusives of certain genotypes (6 OTUs in 1103P, 1 in SO4, Nemadex and 41B) (Supplementary Figure 1 A). An effect of the genotype was reported on the Bray Curtis index, explaining 47% of variance (PVE) (Table 2). The Bray-Curtis index of SO4 was significatively different from those of 1103P and 3309C (Supplementary Table 3). PCoA analyses based on this index didn't show a clear genotype-dependent clustering of individuals (Figure 2 B). No effects of the genotype were observed on both measured α-diversity metrics (Chao1 for richness and Simpson for diversity) (Table 1, Figure 2 C/D). LEfSe analyses show enrichments of AMF taxa in both genotype (1103P: 1 order, 2 genera, 2 families and 2 species; 3309C: 1 genus and 1 species; 41B: 1 genus, 1 family and 2 species; Nemadex: 2 species; RGM: 1 specie; SO4: 2 species) (Figure 2 E). Although α-diversity metrics were not influenced by rootstock genotypes, these results suggest an influence of the rootstock in the structure of the root system AMF community.

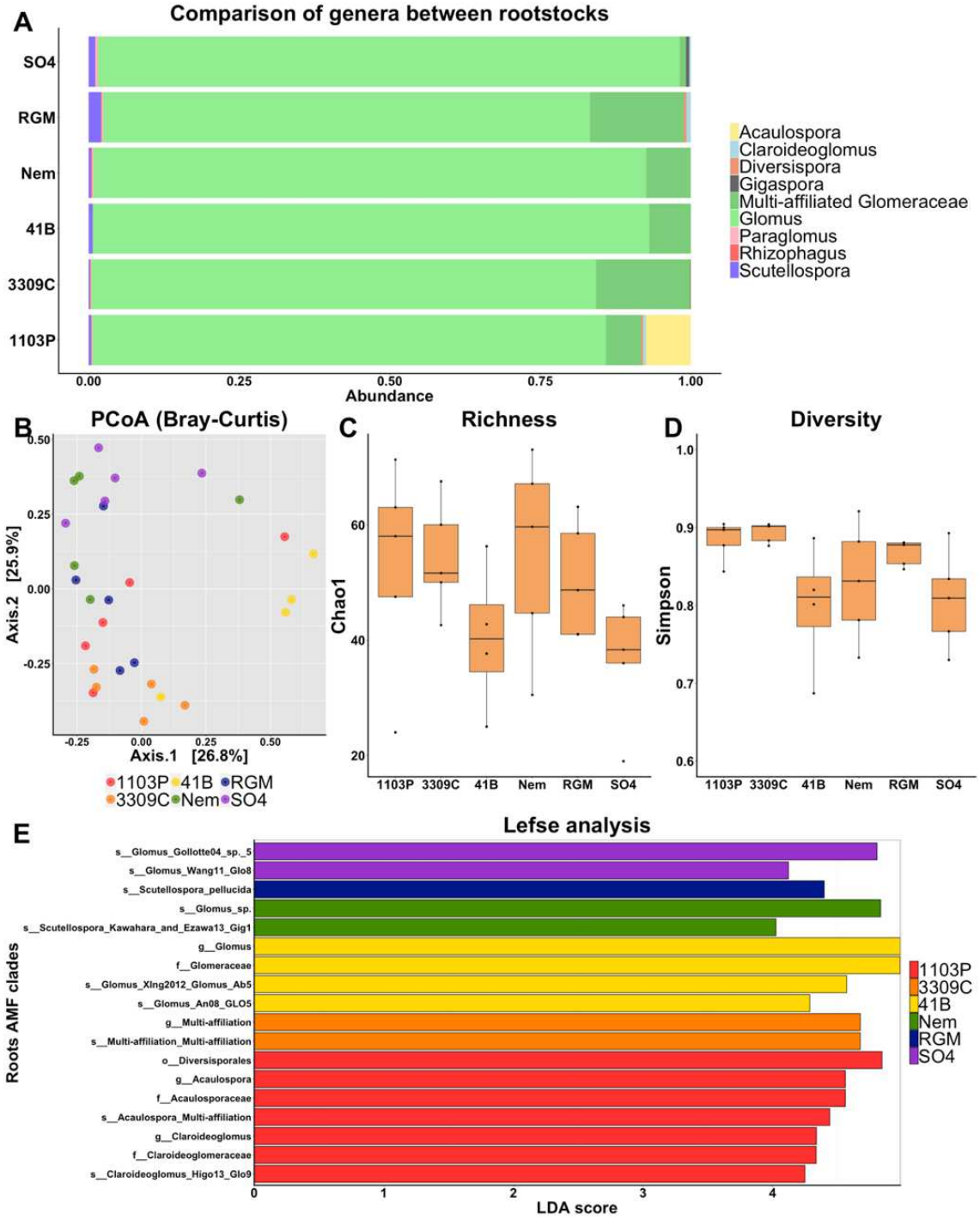


Figure 2-2: Comparison of AMF community assessed with the 28S rRNA gene between rootstocks. Comparison of the proportion of AMF genera (A). Comparison of the β-diversity by principal coordinate analysis (PCoA) based on Bray-Curtis similarity matrices (B). Comparison of the α-diversity with the Chao1 (C) and the Simpson (D): indexes. *p*-value were calculated using Pairwise-Student tests with Bonferroni correction and were considered as significant when the adjusted *p*-value <0.05 (n=5). Histogram of the linear discriminant analysis (LDA) scores reveals the most differentially abundant taxa of AMF (E).

Comparison of AMF community between rootstock and scion genotypes by 18S rRNA gene sequencing

Differences of AMF genera proportions were also observed between rootstock genotypes with the 18S rRNA gene sequencing approach. The *Glomus* still the main genera observed in the roots (ranging from 88 to 99%) (Figure 3 A). Only 9 OTUs were common between all the rootstock genotypes, but 2 OTUs were specific of 3309C and 1 OTU from 41B and Nemadex (Supplementary Figure 1 B). An effect of the rootstock genotype was shown on the Bray-Curtis index, explaining 39% of the variance (Table 2). However, after adjustment of the *p*-value, Bray-Curtis index was significatively different between SO4 and 3309C only (Supplementary Table 4). PCoA analysis didn't show a well genotype dependent clustering with distinct communities of AMF (Figure 3 B). Concerning α-diversity, the rootstock genotype influenced the Chao1 index only (46% of PVE) (Table 2). This index was significatively higher in 1103P than in 41B (Figure 3 C). LEfSe analyses show enrichments of several taxa in both genotype (1103P: 1 family, 1 genus and 3 species; 3309C: 2 specie; 41B: 1 order, 1 family and 1 genus; Nemadex: 1 order, 1 family, 1 genus and 2 species; RGM: 1 specie; SO4: 1 order, 1 family, 1 genus and 1 specie) (Figure 3 E). Together, these results confirm an effect of the rootstock genotype on the root AMF community.

When the AMF communities of the five scions grafted on RGM were studied, slight dissimilarities were observed in the abundance of genera between genotypes. *Aucolospara* was specific from the root system of RGM grafted with UB, as well as *Diversispora* of those of RGM grafted with CS (Figure 4 A). Fourteen OTUs were commons between the scion genotypes and 5 were specific to UB, 3 to Syrah, 4 to CS and PN (Supplementary Figure 1 C). Even if an effect of the scion was observed on the Bray-Curtis index (explaining 31% of variance), no significant differences were found between genotypes (Supplementary Table 5). This result is consistent with the PCoA analysis showing no genotype-dependent clustering (Figure 4 B). Moreover, both α-diversity metrics were not influenced by the scion (Table 2, Figure 4 C/D). LEfSe analyses show the enrichment of 1 family, 1 genus and 1 specie in Grenache, as well as 1 specie in PN and UB (Figure 4 E). Taken together, these results show that the scion genotype contributes little or nothing to the structuring of the root AMF community.

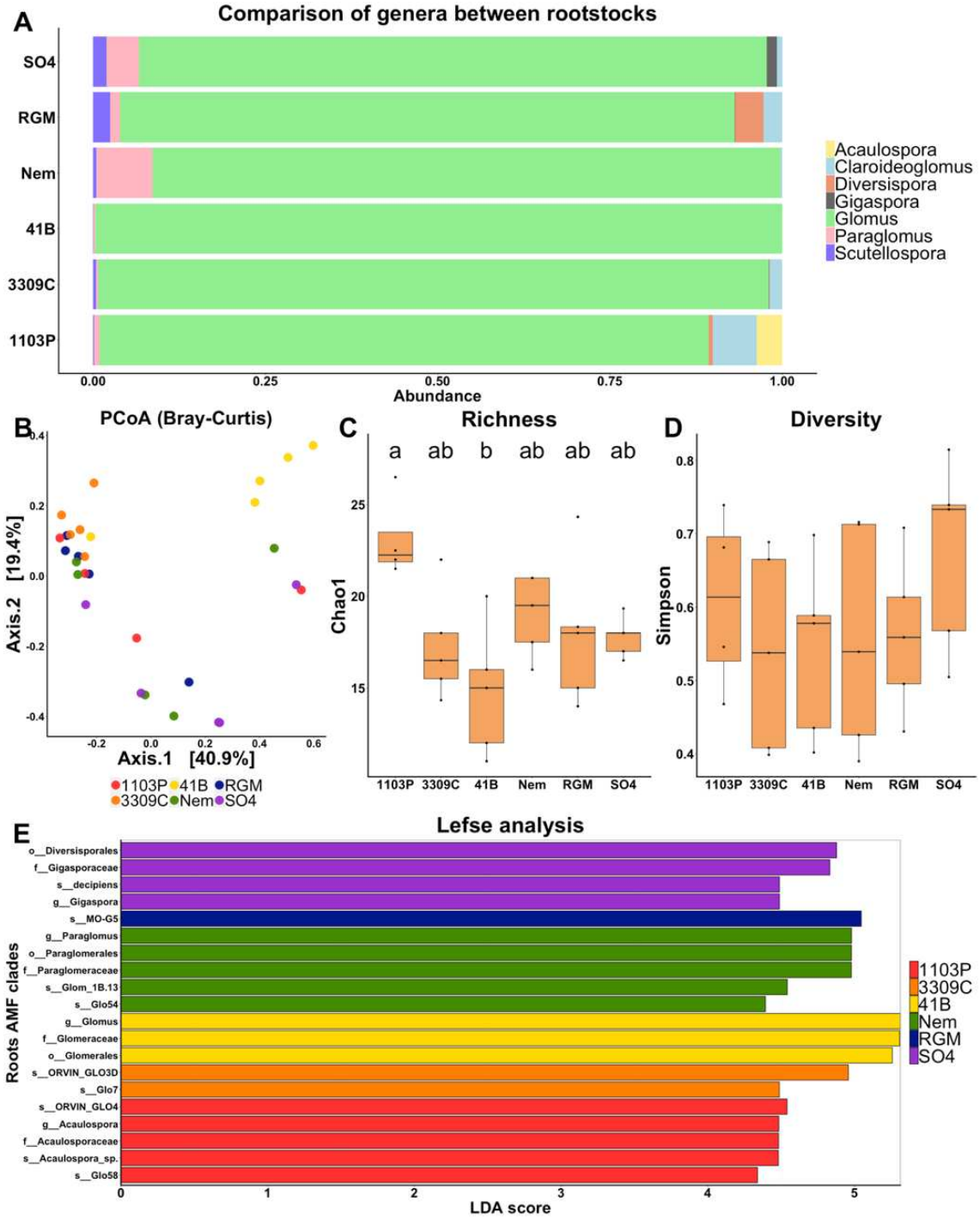


Figure 2-3: Comparison of AMF community assessed with the 18S rRNA gene between the rootstock genotypes.
Comparison of the proportion of AMF genera (A). Comparison of the β-diversity by principal coordinate analysis (PCoA) based on Bray-Curtis similarity matrices (B). Comparison of the α-diversity with the Chao1 (C) and the Simpson (D) indexes. *p*-value were calculated using Pairwise-Student tests with Bonferroni correction and were considered as significant when the adjusted *p*-value <0.05 (n=5). Histogram of the linear discriminant analysis (LDA) scores reveals the most differentially abundant taxa of AMF (E).

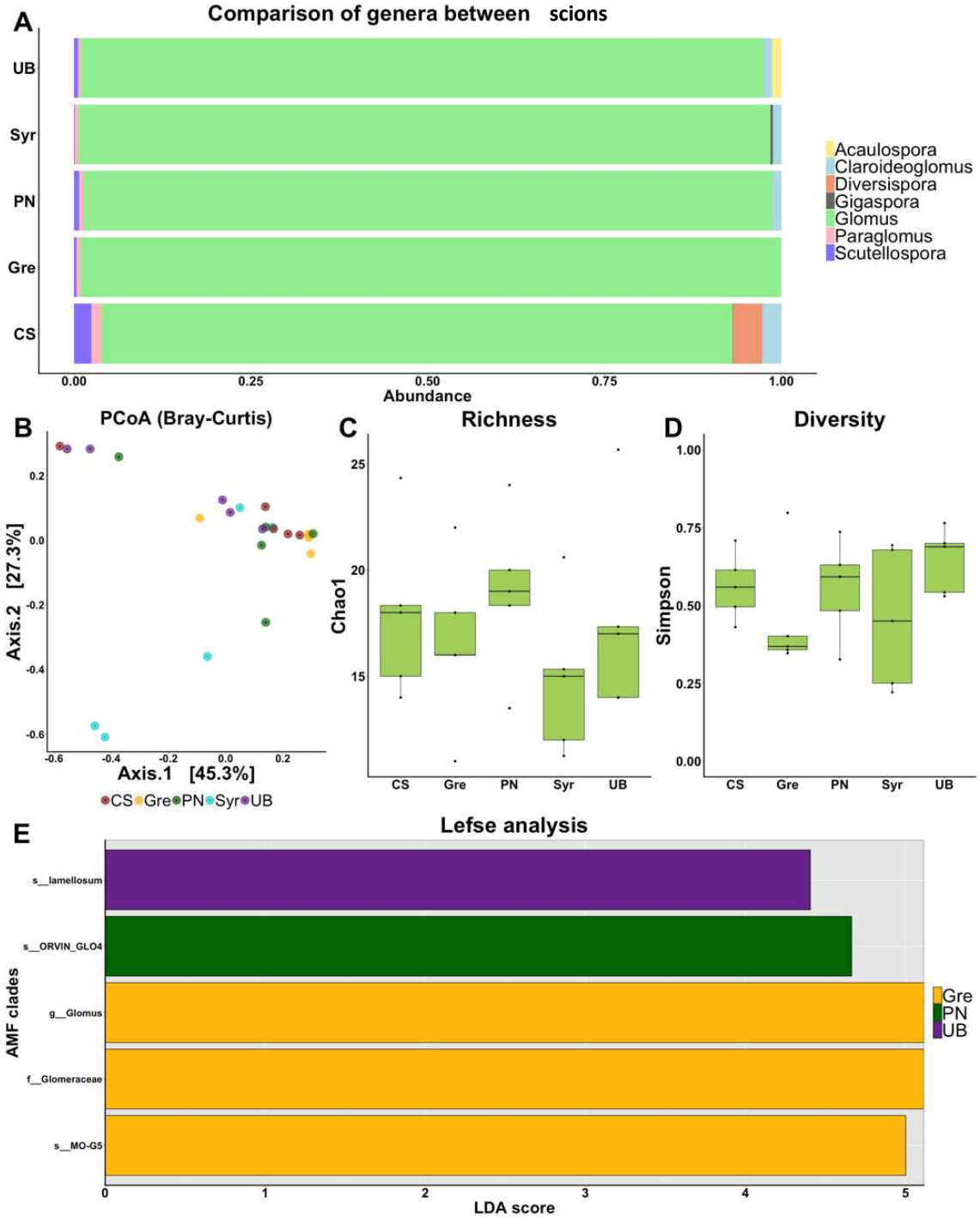


Figure 2-4: Comparison of AMF community assessed with the 18S rRNA gene between the scion genotypes.
Comparison of the proportion of AMF genera (A). Comparison of the β-diversity by principal coordinate analysis (PCoA) based on Bray-Curtis similarity matrices (B). Comparison of the α-diversity with the Chao1 (C) and the Simpson (D) indexes. *p*-value were calculated using Pairwise-Student tests with Bonferroni correction and were considered as significant when the adjusted *p*-value <0.05 (n=5). Histogram of the linear discriminant analysis (LDA) scores reveals the most differentially abundant taxa of AMF (E).

Influence of AMF community on grapevine phenotypic traits

AMF variables assessed by microscopy and sequencing of the 18S rRNA gene in the ten rootstock × scion combinations were correlated to plant phenotypic traits. Ten significant Person's correlations (*p*-values < 0.05) were established between AMF variables and plant phenotypic traits, ranging from -0.36 to 0.44 (Figure 5). The richness (Chao1) was correlated with the $\delta^{13}C$ (r = -0.31) and the shoots number (r = 0.44). The diversity (Simpson) was correlated to the yield (r = 0.33), the bunches number (r = 0.37) and the shoots number (r = 0.31). The mycorrhization frequency (F%) was negatively correlated to the $\delta^{13}C$ (r = -0.31). Finally, the overall mycorrhization intensity (M) and the mycorrhization intensity of mycorrhized fragments (m%) were correlated to the vigor (r = 0.29) and the pruning weight (r = 0.32 and r = 0.31, respectively). Together, these results suggest that AMF community influence grapevine development.

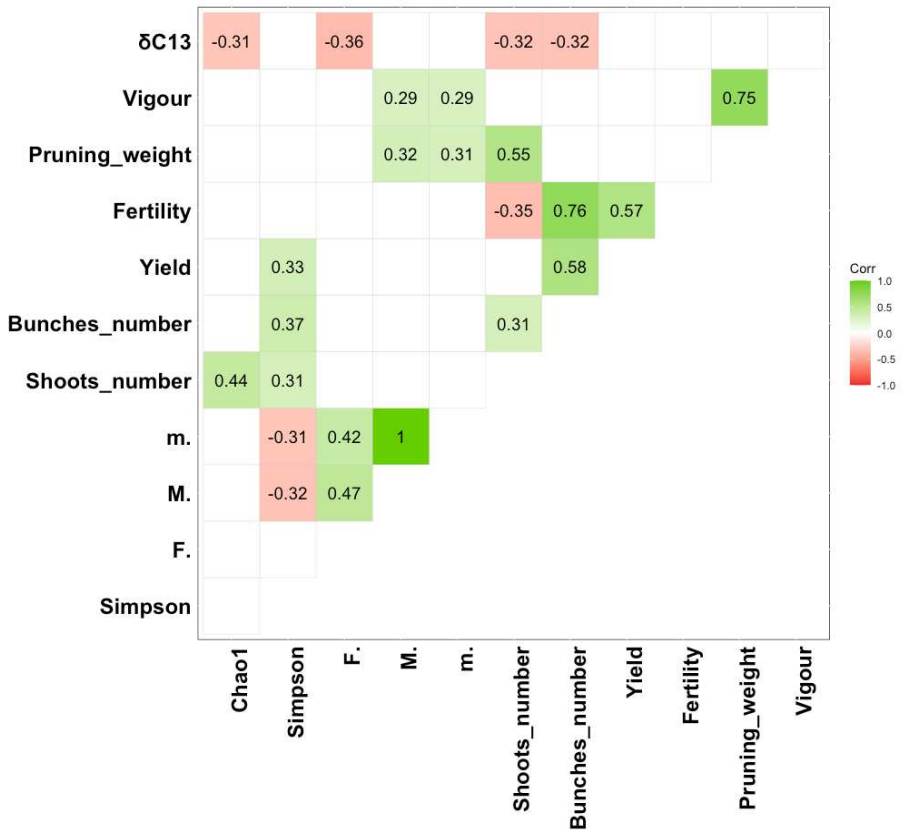


Figure 2-5: Matrix showing significant Pearson correlations between AMF community assessment variables and plant phenotypic traits measured in the 10 rootstock combinations (p-value < 0.05).

Chapitre 2

Comparison of 18S or 28S rRNA gene approaches to study AMF community

Using the Glomeromycotan 28S rRNA gene allows to identify 170 OTUs affiliated to 3 orders (*Diversisporales*, *Glomerales* and *Paraglomerales*), 6 families (*Acaulosporaceae*, *Claroideoglomeraceae*, *Diversisporaceae*, *Gigasporaceae*, *Glomeraceae* and *Paraglomeraceae*), 8 genera and 30 species. With the 18S rRNA gene, 72 OTUs were successfully affiliated to the same orders and families as above but subdivided into 7 genera and 25 species. Abundance graphs show that the relative abundances of AMF genera were similar between methodologies. However, 9% of total sequences were classified in "multi-affiliated *Glomeraceae*" with the 28S rRNA gene. The genera *Rhizophagus* was detected with the 28S rRNA gene only representing less than 1% of total sequences. Both approaches show an effect of the rootstock genotype on the Bray-Curtis index, but significant differences between rootstocks were repeated (SO4 vs 3309C) or not (1103P vs 41B). No significant Pearson correlations were found between α-diversity metrics measured by sequencing of 18S and 28S rRNA genes (Figure 6). Amongst the different rootstocks, LEfSe showed the enrichment of 18 and 20 taxa with the 28S and the 18S rRNA genes, respectively. Even if certain enrichments of order, families and genera were observed with both technics (e.g., the *glomus* genus and the *glomeraceae* family in 41B or the genus *Acaulospora* and the family *Acaulosporaceae* in 1103P), others were not, especially at the specie level. When the correlation matrices between α-diversity metrics and plant phenotypic traits measured in the 6 rootstocks grafted with CS were assessed with the 28S rRNA gene, Chao1 index was significatively correlated (p-values < 0.05) to the shoots number (r = 0.44), the fertility (r = -0.54) and the $\delta^{13}C$ (r = -0.38), but Simpson index didn't correlate with any phenotypic traits (Supplementary Figure 2 A). When the correlations were established with α-diversity metrics measured with the 18S rRNA methodology on the same individuals, the Chao1 index was significatively correlated (p-values < 0.05) to the vigour (r = -0.38), whereas the Simpson index was correlated to the $\delta^{13}C$ (r = -0.38) (Supplementary Figure 2 B). Interestingly, the α-diversity metrics obtained with the 28S rRNA gene were significatively correlated together (r = 0.58).

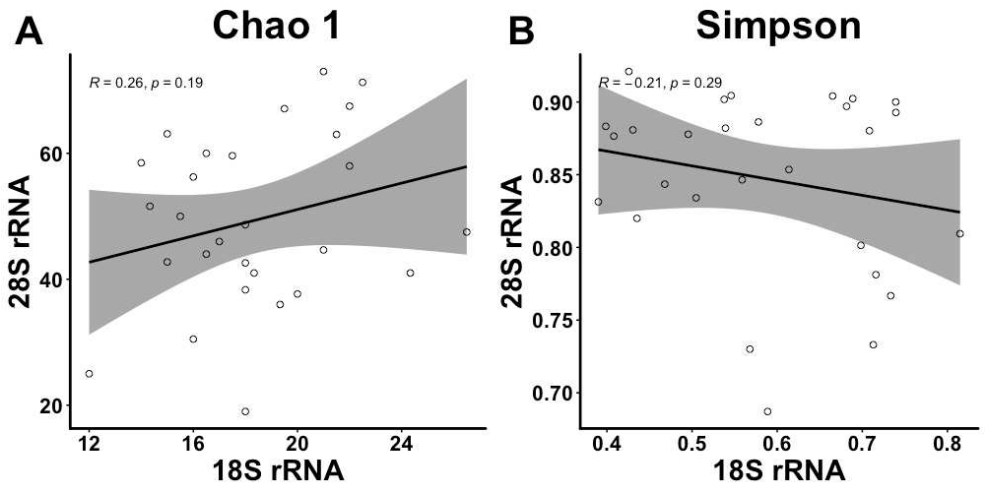


Figure 2-6: Pearson correlations of α-diversity metrics measured by sequencing 18S and 28S rRNA genes.

Discussion

The rootstock and scion genotypes do not influence the root mycorrhization capacity.

Traditionally, AMF structures in the roots are stained with trypan blue (Landi et al., 2021; Gaši et al., 2023). However, this product is classified as carcinogenic and may therefore present risks for the operator. For this reason, we used the Shaeffer black ink as a safe alternative which provide good results to stained AM structures (Duret et al., 2022; Vierheilig et al., 1998). The arbuscular mycorrhiza colonization rate was evaluated using the method of Trouvelot et al. (1986). No effect of the rootstock or the scion genotypes were observed on the frequency of mycorrhization (F%) which was closed to 100% in all the individuals tested. A recent study shows the same frequency in three vineyards of central-eastern Italy (Landi et al., 2021). Taken together, these results suggest that grapevine associate with natural populations of AMF in the soil, even if the cep were not inoculated before planting. Our overall mycorrhization intensity was 42% with values ranging from 14 to 81% which is consistent with the ones observed in several studies (Landi et al., 2021). Similar result was obtained for the mycorrhization intensity of mycorrhized fragments (m = M*100/F) because F was closed of 100% in all rootstock genotypes. Even if the arbuscular abundance (A%) provide by the Mycocalc program is an interesting parameter to study AMF community, we decided not to take it into account. Indeed, when the score of the semi-quantitative scale used to quantify the mycorrhization reaches 4 or 5, the large number of hyphae and vesicles prevents accurate observation of the arbuscules for their quantification. Our microscopy analyses suggest that the choice of rootstock and scion genotypes do not influence the mycorrhization capacity of the root system.

Metabarcoding analyses of the 28S rRNA gene show that rootstock genotype influences the AMF community of the root system.

In this study, our analyses were carried out on the root system of vines located on the block 1 of the GreffAdapt plot. Among the diversity metrics measured with the 28S rRNA methodology, the rootstock genotype significantly influenced the Bray-Curtis index only. Indeed, the AMF community of SO4 was significatively distinct from those of 1103P and 3309C. Several AMF taxa were enriched in the root system of the six rootstock genotypes. In a previous work, we carried out the same analysis on samples collected in May 2021 from the same rootstock genotypes grafted with CS in the blocks 2 and 3 of the same plot (Chapter 1). In the root endosphere, Bray-Curtis index was also influenced by the rootstock genotype but no significant differences were found between genotypes with pairwise

Adonis comparisons. The rootstock genotype influenced both Chao1 and Simpson metrics, but only 3 taxa were enriched in 1103P and Nemadex rootstocks. These differences of results between the two experiments can be explained in part by the season of sampling. We hypothesize that the season may have an impact on various environmental and physiological factors of the plant, and consequently on its rhizodeposition in term of compounds quantity and quality, as reviewed by (Ma et al., 2022). The nature of plant rhizodeposition (i.e., root exudate, mucilage, root border cells, dead root cap cells) is known to influence the microbiome of the root system, including AMF communities (Philippot et al., 2013). However, this hypothesis is in contradiction with the results of Schreiner and Mihara (2009) which observed similar AMF phylotypes between the phenological stages of bloom and véraison in Pinot noir. Even if the soil analysis were relatively similar between blocks, differences were found in the structure of the block 1, such as a higher percentage of coarse elements and a lower one of fine soil. It is already known that soil properties influence AMF diversity (Darriaut et al., 2023; Schreiner and Mihara, 2009). Although certain results differ between the two experiments, which may be due to the characteristics of the soil and the sampling season, we affirm that rootstock genotype influences the AMF community composition in the root endosphere.

Assessment of the AMF diversity by sequencing 28S rRNA gene confirms an influence of the rootstock but shows a small or no contribution of the scion.

As for the gene encoding the 28S rRNA gene, the metabarcoding analysis of the 18S rRNA gene showed an effect of the rootstock genotype on the Bray-Curtis index which was significantly different between SO4 and 3309C. In addition, this analysis shows an effect of the genotype on the Chao1 index which was significantly higher in 1103P than in 41B. Finally, several taxa of AMF were enriched in the roots of the six rootstock genotypes with the 18S rRNA gene, common or not with those observed with the 28S rRNA gene. Even if differences are observed between the results of the two approaches, using two target genes confirm that rootstock genotype drives the AMF community of the root system in grapevine, as proposed in our previous work (Chapter 1). These differences could be explained by the primers selection of the amplification region which can affect fungal community composition analyses (Suzuki et al., 2020), as well as the use of the nested PCR to amplify the 18S rRNA genes which could result in a decrease of AMF taxa and diversity (Yu et al., 2015). The lack of an AMF consensus analysis method makes it very difficult to reuse data acquired from different studies to achieve meta-analysis. Our results are consistent with those of Moukarzel et al. (2021) who were the first authors to demonstrate that rootstock genotype determines the root-colonizing AMF community, based on the analysis of grapevine roots from three vineyards and nine rootstocks by

DGGE, and the use of the roots in trap cultures for AMF recovery. Other studies carried out on other grafted fruit trees have shown an influence of the rootstock genotype on the AMF composition of the root system, such as in lemon (Song et al., 2020) or apple (Van Horn et al., 2021) trees. The plant genotype is also a factor influencing the rhizodeposition that may explain the differences of root AMF community between rootstock genotypes (Ma et al., 2022). Indeed, it has already been shown in grapevine that the composition of root exudates can vary between different rootstock genotypes such as organic acids (Cançado et al., 2009), amino-acids (Marastoni et al., 2020) or strigolactones (Lailheugue et al., 2023).

Concerning the effect of the scion, similar proportions of AMF genera were observed in the root system of RGM grafted with the five scions. Even if an effect of the scion genotype was reported on the Bray-Curtis index, none of the cultivars were significantly different with pairwise Adonis comparisons. Finally, no effect of the scion was reported on α-diversity metrics and few enriched taxa were detected in RGM roots grafted with the different cultivars. These results are consistent with those obtained in May 2021, using 28S rRNA methodology, which show no effect of the scion genotype on both α- and β-diversity metrics measured in the roots (and the rhizosphere) (Chapter 1). Together, these experiments show that the scion genotype has little or no influence on the AMF community of the grapevine root system, compared with that of the rootstock. Interestingly, Song et al. (2020) reported no effect of the scion genotype on several α-diversity metrics in citrus. However, PCoA based on the OTU abundance indicated that AMF community's composition was impacted by both scion and rootstock genotypes, even if samples were mainly clustered according to rootstock genotype rather than the scion. The authors conclude that rootstock genotype might exert a greater impact on the AMF community than scion genotype, as observed in grapevine.

The AMF community of the root system provides benefits to grapevine.

In this work several correlations were established between AMF variables and plant phenotypic traits. The M (%) and m (%) were positively correlated to vegetative growth-related traits (vigour and pruning weight), as well as the richness and the diversity which were correlated to the shoot number. Indeed, several reports have already shown that AMF improve the growth of grapevine aerial parts (Moukarzel et al., 2023). The F (%) and the AMF richness (Chao1) were negatively correlated to the $\delta^{13}C$, suggesting that mycorrhizal symbiosis is more important when the water status is less constraining. This is consistent with other studies showing that AMF improved grapevine water status and alleviate drought stress (Torres et al., 2021). AMF diversity (Simpson) was positively correlated

to the plant productivity (yield and bunches number). Even if no reports investigated the effect of the AMF diversity on grapevine yield, several reports propose that grapevine inoculation with AMF improve it (Trouvelot et al., 2015). Interestingly, the AMF diversity was negatively correlated to m (%) and M (%), suggesting that competition between species occur during the colonization of the root system, as proposed by Moukarzel et al. (2023). In a previous work, no significant correlations were found between plant phenotype and α-diversity metrics measured for AMF. This may be explained by the differences of soil properties between blocs or the choice of the target genes used, as we observed here by comparing the correlation matrices obtained with the 18S rRNA and the 28S rRNA.

Conclusion

This study shows that the colonization of the grapevine root system by AMF is not dependent of the rootstock and the scion genotypes. However, we demonstrate with two methods of metabarcoding (i.e., 28S and 18S rRNA genes) that different rootstock genotypes, subjected to the same pedoclimatic conditions, drive the AMF community of the root system. We also show that the choice of method for analyzing AMF diversity can have an impact on the results, underlining the need for a consensus method for future research. Analyses of the 28S rRNA gene confirm that the scion genotype exerts a poor or no contribution on the AMF diversity of the root system, as proposed in a previous work. Finally, several parameters measured to quantify the AMF community in the root system using microscopy and metabarboding approaches were correlated with the plant phenotype, highlighting the beneficial roles of AMF in vine development and adaptation to environmental conditions.

Supplementary tables

Table S1: Soil analysis carried out on the sampled block of the GreffAdapt plot.

	Block 1
Depth (cm)	0-35
Coarse elements (%)	47.6
Fine soil (%)	52.4
Coarse sands (‰)	725
Fine sands (‰)	110
Coarse silts (‰)	14
Fine silts (‰)	73
Clay (‰)	79
Texture given	Sand
Organic matter (%)	2.3
Total nitrogen (%)	0.103
C / N	12.8
Water pH	6.5
Absorbent complex	
Potassium (g / 100g)	0.71
Magnesium (g / 100g)	1.29
Calcium (g / 100g)	16
C.E.C. (cmol+ / kg)	6.2
Saturation (%)	105.3

Table S2: List of primers and PCR conditions used for the metabarcoding approaches.

Target genes	Primers	Sequences	Initial denaturation	Nulmber of cycles	Denaturation	Annealing	Extension	Final extension	Sources
Eurayote 28S rRNA gene	LR1 NDL22	GCATATCAATAAGCGGAGGA TGGTCCGTGTTTCAAGACG	95°C/5min	30	95°C/30s	58°C/30s	72°C/30s	72°C/5min	van Tuinen et al., 1998
AMF 28S rRNA gene	FLR3 FLR4	TTGAAAGGGAAACGATTGAAGT TACGTCAACATCCTTAACGAA	98°C/30s	30	95°C/30s	55°C/30s	72°C/45s	72°C/7min	Gollotte et al. 2004
AMF 18S rRNA gene	AMV4.5NF AMDGR	AAGCTCGTAGTTGAATTTCG CCCAACTATCCCTATTAATCAT	95°C/5min	35	95°C/45s	58°C/45s	72°C/1min	72°C/7min	Sato et al. 2005
Specific overhang Illumina adapters	Forward Reverse	TCGTCGGCAGCGTCAGATGTGTATAAGAGACAG GTCTCGTGGGCTCGGAGATGTGTATAAGAGACAG							PGTB

Table S3: Comparison of the Bray-Curtis index between rootstock genotypes assessed by sequencing of 28S rRNA gene.

pairs	Df	SumsOfSqs	F.Model	R2	p.value	p.adjusted	sig
RGM vs 1103P	1	0.696	2.803	0.259	0.017	0.255	ns
RGM vs Nem	1	0.412	2.054	0.204	0.06	0.9	ns
RGM vs SO4	1	0.527	2.548	0.242	0.032	0.48	ns
RGM vs 41B	1	0.984	4.460	0.389	0.005	0.075	ns
RGM vs 3309C	1	0.392	1.923	0.194	0.107	1	ns
1103P vs Nem	1	0.802	3.864	0.326	0.009	0.135	ns
1103P vs SO4	**1**	**1.101**	**5.143**	**0.391**	**0.003**	**0.045**	*
1103P vs 41B	1	0.881	3.849	0.355	0.068	1	ns
1103P vs 3309C	1	0.795	3.768	0.320	0.012	0.18	ns
Nem vs SO4	1	0.208	1.253	0.135	0.348	1	ns
Nem vs 41B	1	1.075	6.181	0.469	0.024	0.36	ns
Nem vs 3309C	1	0.942	5.781	0.419	0.008	0.12	ns
SO4 vs 41B	1	1.191	6.563	0.484	0.011	0.165	ns
SO4 vs 3309C	**1**	**1.288**	**7.603**	**0.487**	**0.003**	**0.045**	*
41B vs 3309C	1	0.777	4.367	0.384	0.032	0.48	ns

Table S4: Comparison of the Bray-Curtis index between rootstock genotypes assessed by sequencing of 18S rRNA gene.

pairs	Df	SumsOfSqs	F.Model	R2	p.value	p.adjusted	sig
RGM vs 1103P	1	0.242	1.263	0.153	0.284	1	ns
RGM vs Nem	1	0.316	1.757	0.180	0.064	0.96	ns
RGM vs SO4	1	0.539	2.547	0.242	0.063	0.945	ns
RGM vs 41B	1	1.000	4.838	0.377	0.016	0.24	ns
RGM vs 3309C	1	0.154	1.295	0.139	0.294	1	ns
1103P vs Nem	1	0.331	1.564	0.183	0.267	1	ns
1103P vs SO4	1	0.510	2.055	0.227	0.124	1	ns
1103P vs 41B	1	0.693	2.861	0.290	0.063	0.945	ns
1103P vs 3309C	1	0.328	2.315	0.249	0.056	0.84	ns
Nem vs SO4	1	0.258	1.125	0.123	0.391	1	ns
Nem vs 41B	1	0.827	3.691	0.316	0.019	0.285	ns
Nem vs 3309C	1	0.485	3.569	0.309	0.005	0.075	ns
SO4 vs 41B	1	0.842	3.286	0.291	0.024	0.36	ns
SO4 vs 3309C	**1**	**0.930**	**5.529**	**0.409**	**0.003**	**0.045**	*
41B vs 3309C	1	0.993	6.083	0.432	0.027	0.405	ns

Table S5: Comparison of the Bray-Curtis index between rootstock genotypes assessed by sequencing of 18S rRNA gene.

pairs	Df	SumsOfSqs	F.Model	R2	p.value	p.adjusted	sig
UB vs Syr	1	0.502	2.701	0.252	0.114	1	ns
UB vs Gre	1	0.557	4.709	0.371	0.037	0.37	ns
UB vs CS	1	0.270	1.701	0.175	0.175	1	ns
UB vs PN	1	0.391	2.321	0.225	0.15	1	ns
Syr vs Gre	1	0.584	3.911	0.328	0.06	0.6	ns
Syr vs CS	1	0.497	2.620	0.247	0.055	0.55	ns
Syr vs PN	1	0.422	2.114	0.209	0.116	1	ns
Gre vs CS	1	0.164	1.345	0.144	0.315	1	ns
Gre vs PN	1	0.153	1.156	0.126	0.293	1	ns
CS vs PN	1	0.095	0.549	0.064	0.568	1	ns

Supplementary figures

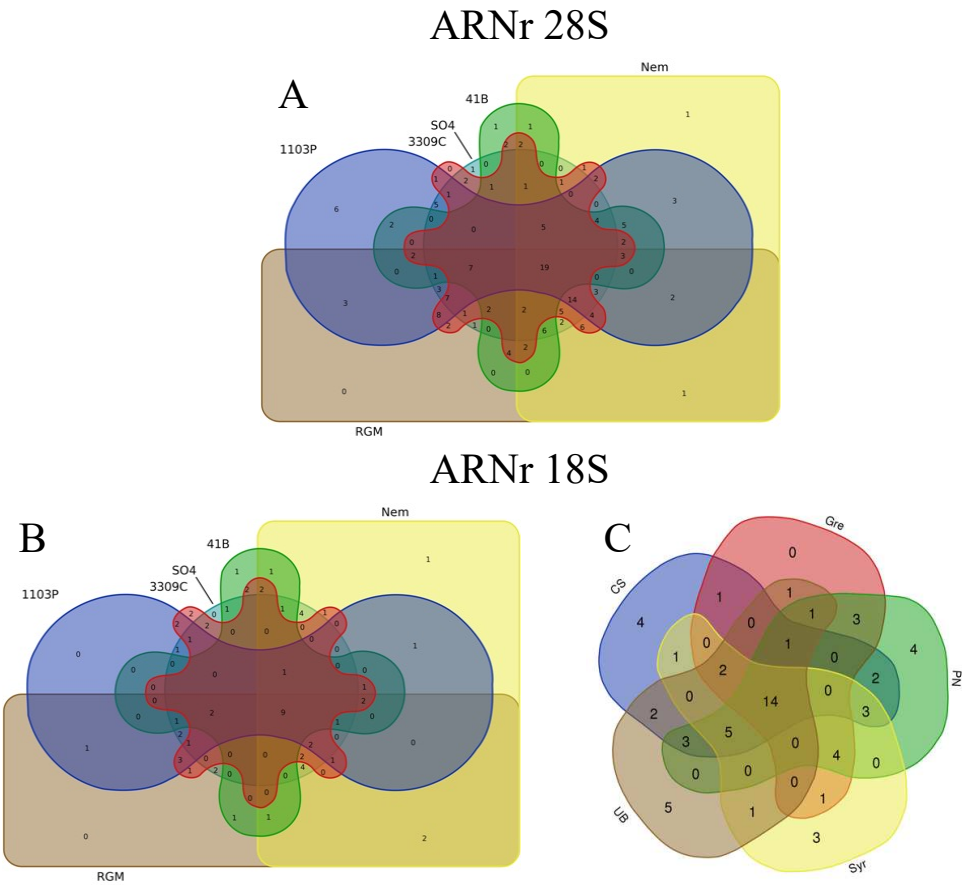


Figure S1: Venn diagram showing common and exclusives OTUs between rootstock genotype with the 28S rRNA (A) or the 18S rRNA gene (B), and scion genotypes with the 18S rRNA gene (C).

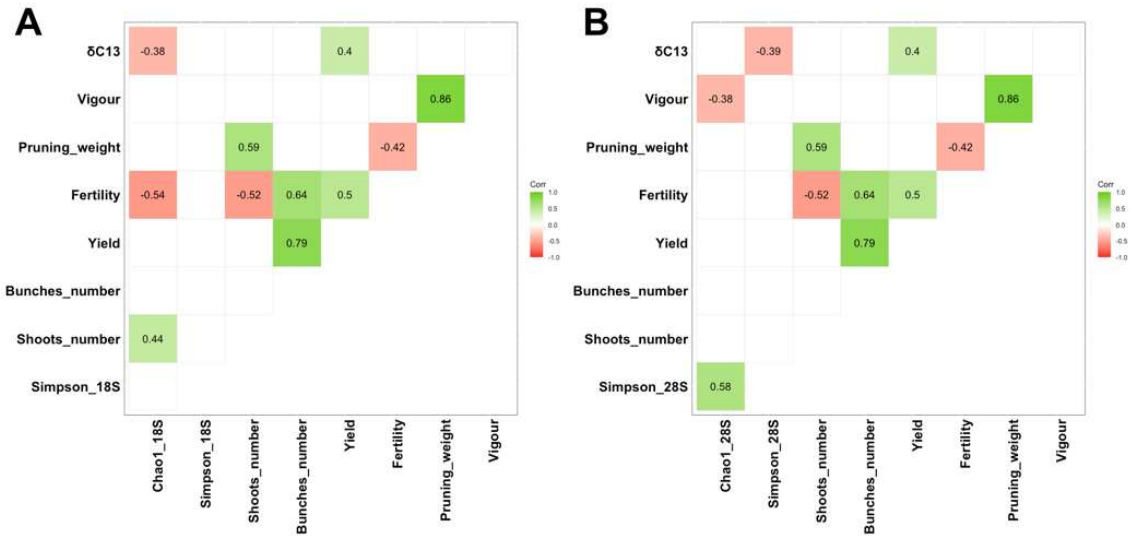


Figure S2: Matrix showing significant Pearson correlations between AMF community assessment variables and plant phenotypic traits measured in the 5 rootstocks grafted with CS with the 18S (A) and the 28S (B) rRNA genes approaches.

Chapitre 3 : Mécanismes moléculaires induits par le porte-greffe dans la sélection des microorganismes du système racinaire

Préface

Dans les chapitres précédents, nous avons démontré que les deux génotypes du plant greffé de vigne exerçaient une influence sur la composition et les fonctions des bactéries, des champignons et des CMA, au sein de la rhizosphère et de l'endosphère racinaire. De plus, nos résultats suggéraient que la contribution du génotype de porte-greffe serait plus importante que celle du cépage. Nous avons aussi établi des corrélations entre les variables utilisées pour caractériser la composition du microbiote du système racinaire avec le phénotype et la nutrition minérale des plants en parcelle, confirmant le rôle clef de ces communautés microbiennes sur le développement de la vigne. Dans ce dernier chapitre, l'objectif sera de comprendre une partie des mécanismes moléculaires induis par les génotypes de porte-greffe dans la sélection des microorganismes du système racinaire.

En octobre 2022, nous avons mené une dernière campagne de prélèvement du système racinaire (rhizosphère et racine) des six porte-greffes (1103P, 3309C, 41B, Nemadex, RGM, SO4), greffés avec le cépage Cabernet Sauvignon (CS). Pour tous les porte-greffes, trois réplicas biologiques du système racinaire (i.e., rhizosphère et racines) ont été prélevés sur chacun des trois blocs du dispositif GreffAdapt. Nous avons aussi prélevé du sol brut à proximité des racines. Nous avons comparé la composition des microorganismes associés aux trois compartiments entre les génotypes, grâce aux méthodologies employées dans les chapitres précédents. Nous avons quantifié par qPCR la quantité de bactéries, de champignons et d'archées dans le sol brut et la rhizosphère. La diversité des microorganismes a ensuite été analysée au sein des trois compartiments grâce au séquençage du gène de l'ARNr 16S des bactéries, des séquences ITS des champignons et du gène de l'ARNr 18S des CMA. Pour les bactéries du système racinaire, nous avons ajouté des sondes de type PNA (Peptide Nucleic Acid) afin de bloquer l'amplification des séquences de l'ARNr 16S des organites de l'hôte et gagner en profondeur de séquençage. La diversité des bactéries de la rhizosphère a aussi été analysée par une approche de CLPP, grâce au système Biolog Ecoplate^{TM}. La capacité de colonisation des racines par les CMA a été évaluée par microscopie. Pour comprendre le rôle des communautés microbiennes, nous avons à nouveau prédit les fonctions bactériennes et fongiques à l'aide des outils PICRUSt2 et FUNGuild. De plus, nous avons mesurés dans la rhizosphère les activités de trois enzymes

microbiennes (arylamidase, β-glucosidase, phosphatase) impliquées dans les cycles des nutriments. Nous avons ensuite cherché des corrélations entre la composition du microbiome du système racinaire de la vigne et le phénotype de la plante. Enfin, nous avons extrait et quantifié les métabolites du sol brut de la rhizosphère et des racines par LC-MS/MS en mode non ciblé, afin d'essayer de comprendre comment les porte-greffes recrutent différentiellement les microorganismes du sol au sein de leur système racinaire.

Grâce aux différentes méthodes de caractérisation du microbiome du système racinaire utilisés ici, cette expérimentation plus robuste en termes de nombre de méthodes d'analyse du microbiome et de réplicas biologiques, confirment que le génotype de porte-greffe influence la composition et les fonctions des microorganismes du système racinaire. De plus, ils suggèrent que l'influence du porte-greffe pourrait s'étendre au-delà de la rhizosphère. Comme nous n'avons pas encore reçu les résultats de LC-MS/MS, ce travail n'est pas encore achevé. Pour respecter la logique du manuscrit, ce dernier sera présenté sous le format d'un article. Cependant, il sera réécrit pour sa publication, après le traitement des données de métabolomique, ainsi que leur intégration avec les données de métarcoding.

Chapitre 3

Molecular mechanisms of rootstocks involved in the selection of rhizosphere and root endosphere microbiomes

Vincent Lailheugue, Joseph Tran, Marine Morel, Elisa Marguerit, Virginie Lauvergeat*

EGFV, Univ. Bordeaux, Bordeaux Sciences Agro, INRAE, ISVV, F-33882 Villenave d'Ornon, France

* corresponding author: virginie.lauvergeat@inrae.fr

Abstract

Background

The soil micro-organisms play undeniably a fundamental role on the growth, the development, and the adaptation of vines to environmental constraints by interacting with the root system. Currently, it is well established that rootstock genotype drives the microbial communities of the root system. Therefore, it is necessary to understand the molecular mechanisms involved to advance knowledge for rootstock breeding or the development of methods to enhance plant interactions with beneficial microorganisms. Here, we characterized the composition and functions of microorganisms in soil, rhizosphere, and root endosphere of six rootstock genotypes (1103P, 3309C, 41B, Nemadex, RGM and SO4) grafted with *Vitis* cv. Cabernet-Sauvignon, using several methods. In addition, we correlated the plant phenotypic traits with the variables measured by qPCR, metabarcoding, CLPP, microscopy, and enzyme activity assays. Finally, we used LC-MS/MS to analyze the metabolome of the root system in relation to its microbial taxonomic composition.

Results

Quantitative PCR analyses showed different concentrations of bacteria, fungi, and AMF, in the rhizosphere of the six rootstocks. The metabarcoding approach has shown that the diversity and the structure of bacteria, fungi, and AMF, were significantly influenced by the rootstock genotype in the rhizosphere and the root endosphere. CLLP analyses of the rhizosphere bacterial community confirmed these results. Significant differences were also observed between genotypes in the bulk soil. As shown by bioinformatics tools or enzymatic assays, the roles of root system microbial communities on the environment and the plant change significantly across genotypes. We established several correlations between the variables used to characterize the root system microbiome and the plant

phenotypic traits. We already extracted the metabolites from the samples, but we are still waiting for the LC-MS/MS data from the analysis platform.

Conclusion

We confirmed with several approaches that grapevine rootstock genotypes drive the root system composition of bacteria, fungi, AMF, and therefore the associated functions of these microorganisms. Furthermore, we suggest that this influence could extend beyond the rhizosphere. We observed several correlations between the plant phenotype and its microbiome, underlining the need to continue researching on understanding the roles of root system microbial communities. Although the metabolomic data has not yet been processed, they represent, in combination with the metabarcoding data, a promising resource for highlighting the mechanisms induced by the rootstock in the selection of soil micro-organisms.

Chapitre 3

Background

Viticulture is a major economic sector and a cultural heritage in many regions of the world, which requires rapid adaptation to the current constraints of climate change, as well as a reduction in the use of chemical fertilizers and pesticides, in order to guarantee its long-term survival (Bucur and Dejeu, 2022; Cataldo et al., 2021). In vineyard, the soil is acts as a reservoir of microorganisms, such as bacteria and fungi, which can colonize the plant to form its microbiota (Gobbi et al., 2022; Zarraonaindia et al., 2015). In the rhizosphere and the root endosphere compartments, these micro-organisms directly or indirectly influence the plant's development and its adaptation to environmental constraints in different ways (i.e., neutral, beneficial, detrimental) (Philippot et al., 2013). The indirect mechanisms by which micro-organisms influence plant development are linked to the modification of soil structure, the completion of biogeochemical cycles (carbon, nutrients and water) and competition for the ecological niche between microbial taxa (Smith et al., 2015; Hartmann and Six, 2022; Shah et al., 2021). Direct mechanisms of microorganisms which influence plant development involved the modulation of phytohormone levels (e.g., cytokinins, gibberellins, indole acetic acid, and ethylene), production of antibiotic compounds, solubilization of nutrients (including zinc, potassium, and phosphorus), fixation of atmospheric nitrogen, and uptake of iron through chelating compounds such as siderophores (Orozco-Mosqueda et al., 2022; Shah et al., 2021). Several authors suggest that rhizosphere engineering could be a solution to adapt viticulture to today's challenges (Bettenfeld et al., 2022; Darriaut et al., 2022b). In this context, Plant Growth Promoting Rhizobacteria (PGPR) or Arbuscular mycorrhizal fungi (AMF) act as a promising resource by increasing plant growth and tolerance to biotic and abiotic stresses (Álvarez-Pérez et al., 2017; Erdogan et al., 2018; Moukarzel et al., 2022; Moukarzel et al., 2023).

Within the dynamic spot of rhizosphere, plants influence soil microbial communities through rhizodeposition. This mechanism includes the release of root exudates (i.e., sugars, amino acids, organic acids, hormones, volatile organic compounds (VOC), secondary metabolites, mucilage (polymerized sugars), root border cells and dead root cap cells (Philippot et al., 2013). Some of these compounds act as a source of carbon for micro-organisms, while others are directly involved in the establishment of symbioses or in the fight against pathogens and parasites (Haichar et al., 2014). For example, strigolactone, a plant hormone derived from the carotenoid pathway, is involved in the first stage of the establishment of arbuscular mycorrhizal symbiosis by stimulating the branching of fungal hyphae close to the host's roots (Yoneyama and Brewer, 2021). The quantity and the quality of plant

roots exudates are influenced by several biotic and abiotic factors, including plant genotype (Jamil et al., 2022). In grapevine, several studies demonstrated an influence of the rootstock genotype on the community of bacteria, fungi and AMF in the rhizosphere and/or the root endosphere (Marasco et al., 2022; Moukarzel et al., 2021a; Vink et al., 2021). Some studies have shown qualitative or quantitative differences between root exudates composition from different rootstock genotypes grown *in vitro* (Cançado et al., 2009; Lailheugue et al., 2023; Marastoni et al., 2020). We hypothesized that differences in root exudates nature could explain the differences observed between rootstock genotypes in the composition of the rhizosphere and the root endosphere microbiota (Chapter 1, Chapter 2). However, no studies have yet been carried out to characterize the root and rhizosphere metabolomes in different rootstock genotypes grown in the field, to understand how different genotypes influence the composition of micro-organisms in the root system.

In a previous work, we studied the influence of the rootstock genotype on grapevine root system microbiota (Chapter 1). In May 2021, we sampled the root system from 6 rootstock genotypes (i.e., 1103P, 3309C, 41B, Nem, RGM and SO4) grafted with Cabernet Sauvignon (CS), on the blocs 2 and 3 of the GreffAdapt plot. Six individuals were sampled for each scion × rootstock combination, three in block 2 and three in block 3. We showed that rootstock genotypes drive the composition and the structure of bacterial and fungal microbiomes in the rhizosphere and the root endosphere, as well as their putative functions, predicted *in silico*. In addition, this work was the first study based on a metabarcoding approach to show an influence of rootstock genotype on the AMF community of the grapevine root system, mainly in the root endosphere. Finally, we have highlighted correlations between the composition of root system microbiomes and the phenotype or mineral status of the plant. Before us, only the work of Moukarzel et al. (2021a) showed with other methods (i.e., PCR-DGGE, trap cultures) an influence of the rootstock genotype on AMF community of grapevine root system. To confirm our results, we decided to reanalyze the AMF diversity of the root sampled from the same rootstock genotypes grafted with CS, distributed on the block 1 of the GreffAdapt plot (n=5), by metabarcoding approaches with two target genes (28S and 18S rRNA genes) (Chapter 2). Even if microscopic analysis showed similar root colonization by AMF between rootstocks, we confirmed the influence of the genotype on the diversity and the structure of AMF community. Moreover, we established significant correlations between variables used to characterize AMF community and grapevine phenotypic traits.

Today, the aim is to understand how rootstock genotypes interact differently with the soil microbiota. The first objective of this work was to study the influence of the rootstock genotype on the

microbial communities (i.e., bacteria, fungi, AMF) of the rhizosphere (RH) and the root endosphere (RE), but also to see whether the effect of the rootstock can be extended to the bulk soil (BS) in the vicinity of the root system. We quantified by qPCR the quantities of bacterial 16S rRNA gene, fungal 18S rRNA gene and archaeal 16S rRNA genes in BS and RH. In the three compartments, we analyzed the diversity of bacteria, fungi, and AMF by Illumina sequencing of the 16S rRNA gene, the ITS region and the 18S rRNA gene, respectively. Bacterial diversity of the rhizosphere was also evaluated by Community-Level Physiological Profiling (CLPP) and the ability of rootstocks to associate with AMF was quantified by microscopy. The second aim was to characterize the molecular composition of these ecological niches to elucidate the rootstock mechanisms involved. The metabolites from BS, RH and RE were extracted and analyzed by LC-MS/MS in non-targeted mode. The last aim was to highlight the functional role of these microorganisms on plant development. We predicted the ecological roles of bacterial and fungal microbiomes *in silico*, using PICRUSt2 and FUNGuild, respectively. We evaluated the activity of microbial enzymes involved in biogeochemical cycles (i.e., nitrogen, carbon, phosphorus) in RH. Finally, we searched correlations between the variables measured to characterize the root system microbiome and the plant phenotype. Our analyses were conducted on samples taken from six rootstock genotypes (1103P, 3309C, 41B, Nem, RGM, SO4) grafted with the CS cultivar, sampled in triplicates on the three blocks of the GreffAdapt plot.

Material and methods

Site, plant material and phenotyping

The experiment was set up in Bordeaux, France (44°47'26.6"N 0°34'26.7"W), in the GreffAdapt plot, a large-scale experimental plot designed with 55 rootstocks grafted with 5 scions, divided into 3 blocks of 5 vines per combination, i.e., 15 vines per combination, distributed randomly within each block (Marguerit et al., 2019). The soil and climate conditions, as well as the viticultural practices carried out on the plot, were the same as those described in our previous work (Chapter 1). Phenotypic monitoring was carried out annually on the vines. This included the number of shoots, fertility (number of bunches per shoot), winter pruning weight and the vigor conferred (pruning weight / number of shoots). The number of bunches, berry yield and $\delta^{13}C$ of berry juice were assessed at the harvest in september, when the berries from the Cabernet Sauvignon (CS) were at maturity. Mineral contents in the petioles (collected between the fourth and sixth leaf of the shoot on the cane side) were assessed by Waypoint Analytical (Virginia, USA). Microbial analyses were performed on the same rootstock genotypes as those studied in our previous works (Chapter 1 and 2), i.e., 1103 Paulsen (1103P), 3309 Couderc (3309C), 41 B Millardet et de Grasset (41 B), Nemadex Alain Bouquet (Nem), Riparia Gloire de Montpellier (RGM) and Selection Oppenheim 4 (SO4), grafted with CS clone 169. The root system of the different rootstocks was sampled in triplicates on each of the three blocks of the GreffAdapt plot, designed according to soil resistivity. Aurea Agrosciences (Orléans, France) assessed the soil properties and defined them as sandy gravelly soil in both blocks (Supplementary Table 1).

Sample collection and processing

Roots with attached soil particles were collected in October 2022 from a depth of 20-30 cm in sterile bags and placed in a cooler before being processed in the laboratory. The rhizosphere was separate from the roots using a brush under a sterile hood and sieved to 2 mm to remove large soil particles and homogenize the samples. The rhizosphere destinated to metabarcoding and metabolomic analyses was stored at -80°C, but a small fraction was kept at 4°C for enzymatic assays and the CLPP approach. Roots intended for the metabarcoding approach were transferred to a new tube and surface sterilised to eliminate epiphytic micro-organisms by soaking in 3% sodium hypochlorite (NaClO) for 1 min, followed by 3% H_2O_2 for 1 min and finally by washing with sterile distilled water five times (Chapter 1). Sterilized roots were then stored at -80°C. For metabolic analysis of the roots, a part of the root system was briefly rinsed with sterile water in the plot, then transferred to a 50 ml Falcon tube which was immediately frozen in liquid nitrogen before being stored at -80°C. All the roots' samples were ground in 35-ml stainless-steel grinding jar with 20-mm stainless steel balls at 30 oscillations per

second for 30 sec with the mixer mill MM400 (Retsch, Haan, Germany), using liquid nitrogen and then stored at -80°C until DNA or metabolites extraction. Bulk soil was taken from beneath the plants at the same depth as the rhizosphere, placed in a cooler, sieved to 2 mm and then stored at -80°C until further analysis. For microscopic analysis, the finest young white roots were collected in a Falcon tube containing 50 ml of 10% ethanol and transferred to 4°C before processing.

DNA extraction from roots, rhizosphere, and bulk soil

DNA from sterilized root tissues was extracted from 150 mg of frozen powder using the protocol of Berger et al. (2022). DNA from rhizosphere and bulk soil was extracted from 250 mg of lyophilized soil with the DNeasy® PowerSoil® Pro kit (Qiagen), using the manufacturer recommendations with some adaptations, as described in a previous work (Chapter 1). Extracted DNA was quantified on a Qubit® 3.0 fluorometer (Thermo Fisher Scientific) using the Qubit™ dsDNA HS Assay Kit, and its quality was checked with a NanoDrop™ 2000/2000c spectrophotometer (Thermo Fisher Scientific). DNA was then stored at -20°C until further use.

Quantitative PCR (qPCR) amplification of bacterial and archaeal 16S and fungal 18S rRNA genes

The quantities of bacteria, fungi and archaea in the rhizosphere and the bulk soil were quantified by quantitative Polymerase Chain Reaction (qPCR), using the same methodology as in Chapter 1. The primer pairs 515R/341F, FR1/FF390 and Arch967F/Arch1060R, were used to amplify bacterial 16S rRNA, fungal 18S rRNA and archaeal 16S rRNA genes, respectively. Reactions were done in a final volume of 20 µl composed of 10 µl of GoTaq® qPCR Master Mix (Promega), 1 µl of each primer (10 µM), 7 µl of nuclease-free water and 1 µl of extracted DNA (1 ng. μl^{-1}). Standards used for absolute quantification were obtained from amplicons previously subcloned into pGEM®-T easy vector system (Promega) by Darriaut et al. (2021). Each sample was quantified in triplicates using the CFX96 Touch Real-Time PCR Detection System (Bio-Rad Laboratories, France). The efficiencies of the qPCR were ranging from 80% to 99% ($R^2 > 0.99$).

Staining and quantification of root mycorrhiza by microscopy

The root staining protocol was adapted from the method of Phillips et Hayman (*1970*), described in the Chapter 2. The method of Trouvelot et al (1986) was then used to quantify the rate of root colonization by AMF. Thirty root fragments per individual were observed under a microscope (LEICA DM750) and the mycorrhization frequency (F%), the overall mycorrhization intensity (M%) and the

mycorrhization intensity of mycorrhized fragments (m%) were calculated using the Mycocalc program (INRAe, Dijon).

Determination of phosphatase, β-glucosidase and arylamidase activities in the rhizosphere

Alkaline phosphatase and β-glucosidase activities were measured using a method adapted from (Tabatabai and Bremner, 1969). The methods are based on the colorimetric estimation of the p-nitrophenol released by enzyme activity. Briefly, 0.5g of rhizosphere (sieved < 2mm) was incubated in 2 ml of Modified Universal Buffer (MUB) pH 6.5, 0.125 ml of toluene and 0.5 ml (0.025M) of the enzyme substrates (p-Nitrophényl-B-D-glucopyranoside (0.025 M) or disodium p-nitrophenyl phosphate tetrahydrate (0.115 M) for β-glucosidase or phosphatase, respectively) and left to react 1 hour at 37°C, under agitation at 200 rpm. Next, 0.5 ml of $CaCl_2$ 0.5M were added to stop the reaction and revelation was done with the addition of 2 ml of Tris 0.1M pH12 or NaOH 0.5M for β-glucosidase or phosphatase, respectively. A centrifugation at 8000 g was realized before filtration at 0.2 µm. Then, 80 µl of the filtrate were used to measure the absorbance in triplicates at 400 nm with the EPOCH2 microplate reader (BioteK). For the negative controls, the enzyme substrates were added after the incubation step. The p-nitrophenol content was calculate using a reference graph obtained with standards containing 0, 10, 20, 30, 40 and 50 µg of p-nitrophenol, as prepared in Tabatabai and Bremner (1969). Finally, the enzyme activities were measured using the following equation:

Activity ($\mu g_{p\text{-}nitrophenol}\ g_{soil}^{-1}\ dwt\ h^{-1}$) = $\mu g_{p\text{-}nitrophenol}\ ml^{-1}$ * V * fw * t / dw; where V is a reaction volume (ml), t is the incubation time (1 hour), fw is the sample fresh weight (0.5g) and dw is the sample dry weight.

Arylamidase activity was measured using a method adapted from Acosta-Martinez and Tabatabai (2000). This method involves the colorimetric determination of β-naphthylamine released by enzyme activity. Briefly, 0.5 g of rhizosphere (sieved < 2mm) was incubated in 1.5 ml of 0.1M THAM buffer (pH 8.0) and 0.5 mL of 8.0 mM L-leucine p-naphthylamide hydrochloride (8 mM) and left to react 1 hour at 37°C under agitation at 200 rpm. Next, 3 ml of ethanol (95%) were added to stop the reaction. The solution was mixed and centrifugated for 1 min at 17 000g. Next, 0.5 ml of the supernatant was transferred to a new tube and the revelation was done with the addition of 0.5 ml ethanol (100%), 1 ml of acidified ethanol (0.26 M HC1), and 1 ml of p-dimethylaminocinnamaldehyde. The solution was mixed, and the absorbance was measured in triplicates at 540 nm. For the negative controls, the enzyme substrate was added after the incubation step. The β -naphthylamine content was calculate using a reference graph obtained with standards containing 0, 5, 10, 15, 20 and 25 µg of β-naphthylamine ml-

[1], as prepared in Acosta-Martinez and Tabatabai (2000). Finally, the enzyme activities were measured using the following equation:

Arylamidase activity ($\mu g_{\beta\text{-naphthylamine}}\ g_{soil}^{-1}\ dwt\ h^{-1}$) = $\mu g_{\beta\text{-naphthylamine}}\ ml^{-1}$ * V * fw * t / dw; where V is a reaction volume (ml), t is the incubation time (1 hour), fw is the sample fresh weight (0.5g) and dw is the sample dry weight.

Potential metabolic diversity (PMD) of cultivable bacteria from the rhizosphere

PMD of the rhizosphere was evaluated using Biolog Ecoplate™ system, containing 3 repetitions of 32 wells containing 31 carbon sources and a control well. Briefly, one gram of rhizosphere (sieved < 2mm) was transferred into sterile 0.85% NaCl, vortexed, incubated for 10 min at 300 rpm under ambient temperature, left to settle for 10 min and the supernatant was serially diluted to 1/1000 with sterile water. For each individual, the 32 Eco-Plate wells were filled with 120 µL of this diluted supernatant, incubated at ambient temperature in the dark and subsequently, their absorbance at 590 nm was measured every 24 hours for 7 days. The absorbance value of each carbon source was corrected by subtracting the absorbance value of the well containing only water and the negative values were set to zero. Average Well Color Development (AWCD) was calculated by summing the absorbance values of the corrected wells divided by the number of wells. The substrate richness was calculated by adding the number of wells for which the corrected absorbance was higher than 0.25. Finally, the Simpson index was calculated according to Németh et al. (2021).

Target metabarcoding on bacterial 16S rRNA gene, fungal ITS region and Glomeromycete 28S rRNA gene

The bacterial 16S rRNA gene was amplified using the primer pair 341F/785R with PNA clamps (mPNA and pPNA) to reduce the amplification of host chloroplast and mitochondria (Fitzpatrick et al., 2018; Deyett and Rolshausen, 2020). PCR reactions were monitored in a final volume of 25 µl composed of 5 µl of 5X GoTaq® colorless reaction buffer (Promega, France), 1 µl of each primer (10 µM), 0.5 µl of dNTPs (10 mM), 0.125 µl of GoTaq® G2 DNA Polymerase (Promega, France), 1.25 µl of mPNA blocker (5 µM), 1.25 µl of pPNA blocker (5 µM), 1 µl (at 1 $ng.\mu l^{-1}$) or 2.5 µl (at 5 $ng.\mu l^{-1}$) of DNA extracted from roots or soil compartments, respectively, and nuclease-free water (q.s.p 25 µl). The fungal ITS gene was amplified using the primer pair ITS1F/ITS2, while the glomeromycotan 18S rRNA gene region was amplified using the AMV4.5NF/AMDGR one. Both PCR reaction were monitored in a final volume of 25 µl composed of 5 µl of 5X GoTaq® colorless reaction buffer (Promega, France), 0.5 µl of each primer (10 µM), 0.5 µl of dNTPs (10 mM), 0.125 µl of GoTaq® G2 DNA Polymerase (Promega, France), 1 µl (at 1 $ng.\mu l^{-1}$) or 2.5 µl (at 5 $ng.\mu l^{-1}$) of DNA extracted from

roots or soil respectively, and nuclease-free water (q.s.p 25 µl). The sequence of primers, PNA clamp and Illumina adapters, as well as the cycling condition, are presented in Supplementary Table 2. Further steps were carried out at the Plateforme Génome Transcriptome de Bordeaux (Cestas, France). The PCR products were purified with the platform-specific SPRI magnetic beads (1X ratio) and quantified using Quant-iT^{TM} dsDNA assay kit (ThermoFisher, France). MID and Illumina sequencing adapters were added. Libraries were pooled in equimolar amounts using a Hamilton Microlab STAR robot and sequenced on an Illumina MiSeq platform using the MiSeq Reagent Kit v2 (2 × 250 bp) for bacteria and fungi in multiplex, and the MiSeq Reagent Nano Kit V2 (2 × 250 bp) for AMF. Obtained sequences were demultiplexed with index search at the PGTB facility. The quality of the obtained sequences were first checked with FastQC v.0.11.8 (Andrews, 2010). Sequences were quality filtered, trimmed, denoised, and clustered into Operational Taxonomy Units (OTUs) using FROGS pipeline from Galaxy instance (Escudié et al., 2018). This involved assembling raw forward and reverse reads for each sample into paired-ended reads with a minimum overlapping of 50 nucleotides and 0.1 mismatch using the VSEARCH tool (Rognes et al., 2016). Primers were removed using Cutadapt (Martin, 2011), chimeras were detected and removed with UCHIME (Edgar et al., 2011), and the clustering was performed using SWARM method (Mahé et al., 2014). The minimum sequence abundance proportion was set at 5e^{-5} to keep OTUs with a minimum prevalence fixed at 4. Taxonomic assignments of 16S rRNA, ITS, and 28S rRNA-based OTUs were performed against Silva138.1 (Quast et al., 2012), Unite8.2 (Nilsson et al., 2019), and MaarjAM (Öpik et al., 2010), respectively.

Prediction of bacterial and fungal functions

The bacterial function and pathways were predicted using phylogenetic investigation of communities by reconstruction of unobserved states (PICRUSt2) (Douglas et al., 2020), run on the FROGS pipeline integrated within the Galaxy instance (Escudié et al., 2018). Fungal trophic modes and guilds were predicted at the genus level using the "funguild_assign" function from the *FUNGuildR* (0.2.0.9000) package and the FUNGuild database (Nguyen et al., 2016). The methods used for *in silico* prediction of bacterial and fungal functions were the same as those described in the Chapter 1.

Metabolite extraction from the roots and the soil compartments

Metabolite extraction was realized from 20 mg of lyophilized roots powder in 300 µl of solvent (80% ethanol, 0.1% formic acid, 250 µg.ml^{-1} methyl vanillate), using a robotized method developed at Bordeaux Metabolome Facility (https://metabolome.cgfb.u-bordeaux.fr/en, Villenave d'Ornon, France). The robot was used to pipette solvents, mix, cool and centrifuge racks of micronics. The extraction of 400 mg of soil samples (BS and RH) was carried out using the same method, but manually

to overcome the limitations of robotic work with such a large quantity of material. Untargeted metabolic profiling by UHPLC-LTQ-Orbitrap mass spectrometry (LCMS) was performed with the platform method using an Ultimate 3000 ultra-high-pressure liquid chromatography (UHPLC) system coupled to an LTQ-Orbitrap Elite mass spectrometer interfaced with an electrospray (ESI) ionisation source (ThermoScientific, Bremen, Germany), as detailed in Luna et al. (2020).

Results

Comparisons of the quantities of bacteria, fungi, and archaea between rootstock genotypes in the bulk soil (BS) and the rhizosphere (RH) measured by qPCR

Table 3-1: Influence of the rootstock genotype and the block on the quantity of bacteria, fungi, and archaea in the bulk soil (BS) and the rhizosphere (RH).

		Copy of bacterial 16S rRNA gene			Copy of fungal 18S rRNA gene			Copy of archaeal 16S rRNA gene		
		p-value		PVE	*p*-value		PVE	*p*-value		PVE
BS	Rootstock (R)	0.907	ns	/	**0.027**	*	**21%**	**9.56e-05**	***	**35%**
	Block (B)	**3.52e-04**	***	**29%**	0.057	ns	/	**7.81e-04**	***	**17%**
	R * B	**0.005**	**	**33%**	**0.003**	**	**34%**	**3.38e-08**	***	**36%**
RH	R	**1.99e-04**	***	**33%**	**0.006**	**	**25%**	**2.45e-07**	***	**47%**
	B	**9.31e-04**	***	**18%**	**0.010**	*	**14%**	**1.57e-04**	***	**17%**
	R * B	0.084	ns	/	**1.29e-04**	***	**36%**	**2.31e-13**	***	**32%**

Asterisks represent significant effects with Two-way ANOVA: * *p*-value < 0.05, ** *p*-value <0.01, *** *p*-value < 0.001, PVE = percentage of variance explained, ns = non-significant.

The number of copies of bacterial 16S, fungal 18S and archaeal 16S rRNA genes, measured by qPCR were compared between the soil compartments. Student t-test showed a significantly higher number of copies of bacterial (Figure 1 A) and archaeal (Figure 1 G) 16S rRNA genes in RH than in BS. No significant difference was found between the soil compartments for the fungal 18S rRNA gene (Figure 1 D). We then investigated the effect of rootstock genotype on the quantities of microbial genes in the soil compartments near (RH) and far (BS) from the root system. In BS, Two-way ANOVA reported effects of the block and its interaction with the genotype on the quantity of bacterial 16S rRNA gene, explaining 29 and 33% of variance explained (PVE), respectively (Table 1). In RH, the quantity of bacterial 16S rRNA gene was influenced by the rootstock genotype (PVE = 33%) and the block (PVE = 18%) (Table 1). Even if no differences between genotypes were found in BS (Figure 1 B), the quantity of bacterial 16S rRNA gene in RH was significantly higher in 1103P than in Nem, RGM and SO4 (Figure 1 C). The amount of fungal 18S rRNA gene was influenced in both soil compartments by the rootstock genotype (PVE ranging from 21% in BS to 25% RH) and the factors interaction (PVE ranging from 34% in BS to 36% in RH), as well as by the block in RH (PVE = 14%) (Table 1). Paired t-test using Bonferroni correction showed no significant differences in the amount of fungal 18S rRNA gene between rootstock genotypes in BS (Figure 1 E). In RH, SO4 presented a significantly higher number of fungi than 41B (Figure 1 F). The quantity of archaeal 16S rRNA gene in both soil compartments were influenced by the rootstock genotype (PVE ranging from 35% in BS to 47% in RH), the block (PVE = 17% in BS and RH), and the factors interaction (PVE ranging from 32% in RH to 36% in BS) (Table 1). The amount of archaeal 16S rRNA gene was significantly higher in 1103P than in all other genotypes in both soil compartments, at the exception of 41B in BS (Figure

1 H/I). Together, these results show that rootstock genotype influence the level of microorganisms from both kingdom in RH, as well as the one of archaea in BS.

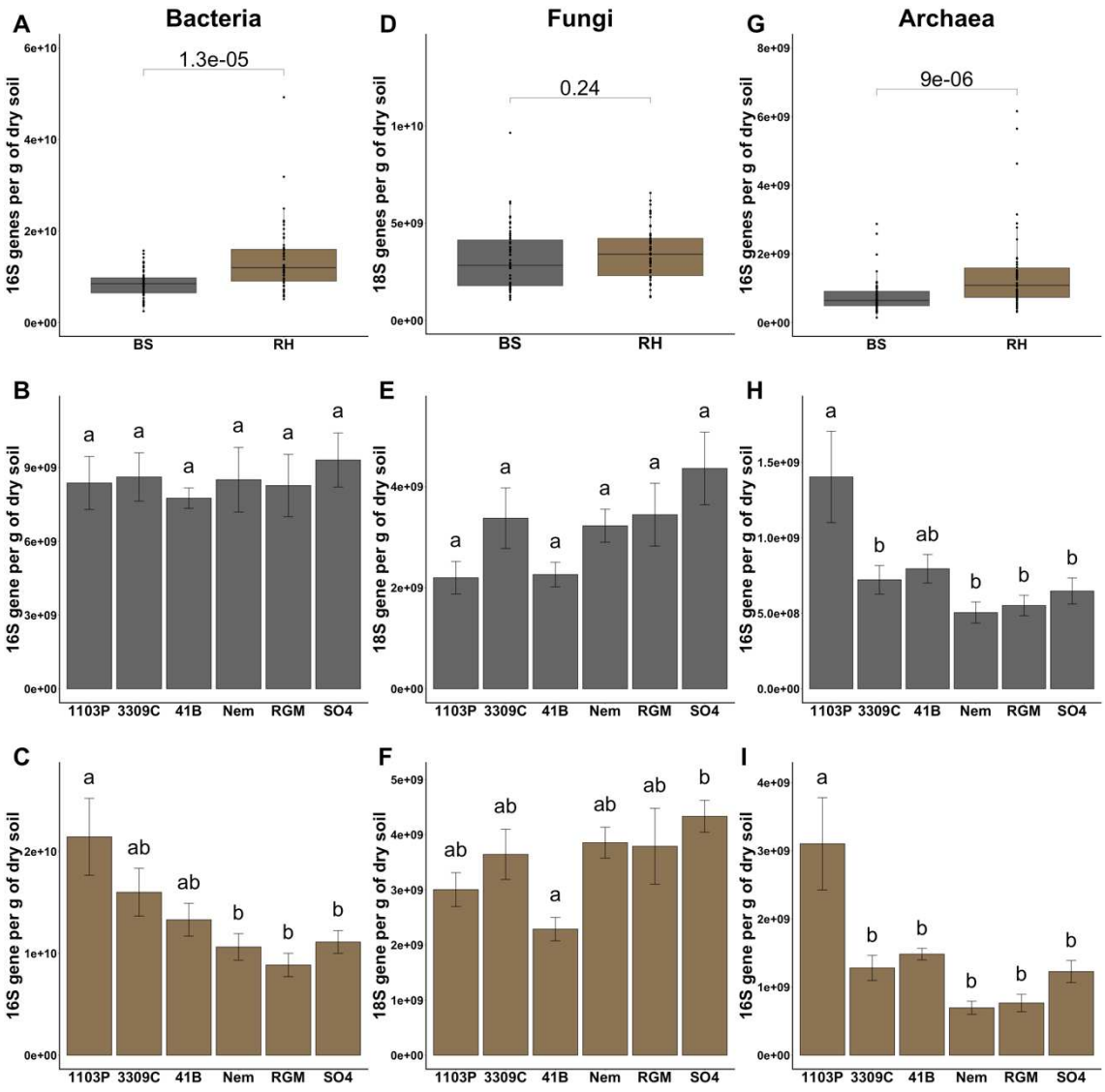


Figure 3-1: Comparison of the number of copies of bacterial 16S rRNA, fungal 18S rRNA and archaeal 16S rRNA genes between soil compartments (A, D, G) or rootstock genotypes in BS (B, E, H, dark grey) and RH (C, F, I, dark brown).
Data are represented as mean ± SE. Comparison between soil compartments were realized with t-test using Bonferroni correction (n=54). Comparison between rootstock genotypes were realized with paired t-test using Bonferroni correction (n=9). Letters indicate significant differences between groups (p-value < 0.05)

Comparison of the microbial communities (bacteria, fungi, AMF) between the bulk soil (BS), the rhizosphere (RH) and the root endosphere (RE)

Table 3-2: Influence of the studied compartment (BS, RH and RE) on the α-diversity (richness = Chao1, diversity= Simpson) and the β-diversity metrics (Bray-Curtis dissimilarity) measured for bacteria, fungi and AMF.

	Chao1			Simspon			Bray-Curtis		
	p-value		PVE	*p*-value		PVE	*p*-value		PVE
Bacteria	< 2e-16	***	94%	<2e-16	***	81%	0.001	***	45%
Fungi	<2e-16	***	94%	<2e-16	***	52%	0.001	***	35%
AMF	<2e-16	***	74%	<2e-16	***	64%	0.001	***	20%

Effects on Chao1 and Simpson indexes were evaluated with ANOVA (n = 54), while the effect on the Bray-curtis index was evaluated with PERMANOVA using 999 permutations (n = 54), PVE = percentage of variance explained, ns = non-significant.

Amongst the bulk soil (BS), the rhizosphere (RH), and the root endosphere (RE), 2593 bacterial OTUs were successfully affiliated to 22 phyla, 49 classes, 103 orders, 141 families, 253 genera and 144 species, after data rarefaction. An influence of the compartment was reported on Chao1, Simpson and Bray-Curtis metrics measured for bacteria, explaining 94, 81 and 45% of PVE, respectively (Table 2). PCoA based on Bray-Curtis distance (Figure 2 A) showed a clear separation of RE samples from those of BS and RH along the first axis. Samples from the soil compartments seemed to be grouped along this axis. Along the second axis, a higher dispersion of the individuals was observed in both soil compartments than in RE. Pairwise Adonis comparisons of the Bray-Curtis index showed that RE was significantly different from BS and RE (Supplementary Table 3). Chao1 (Figure 2 B) and Simpson (Figure 2 C) indexes were significantly lower in RE than in BS and RH, but no significant differences were found between soil compartments. Abundance graph at the phyla level (Figure 2 D) showed a clear dominance of *Actinobacteriota* (ranging from 30% in RE to 35% in RH) and *Proteobacteria* (ranging from 22 % in soil compartments to 51% in RE). LEfSe analysis of bacteria (Supplementary Figure 1 A) showed enrichments at the phyla level of *Acidobacteriota*, *Chloroflexi* and *Gemmatimonadota* in BS; *Actinobacteriota*, *Planctomycetota* and *Firmicutes* in RH; as well as *Proteobacteria*, *Bacteroidota* and *Patescibacteriota* in RE. Other bacterial taxa were also enriched at every taxonomic levels. Finally, Venn diagram showed that 48% bacterial OTUs were common between the three compartments, 50% were exclusively common between BS and RH, and less than 1% were exclusive from RE (Supplementary Figure 2 A).

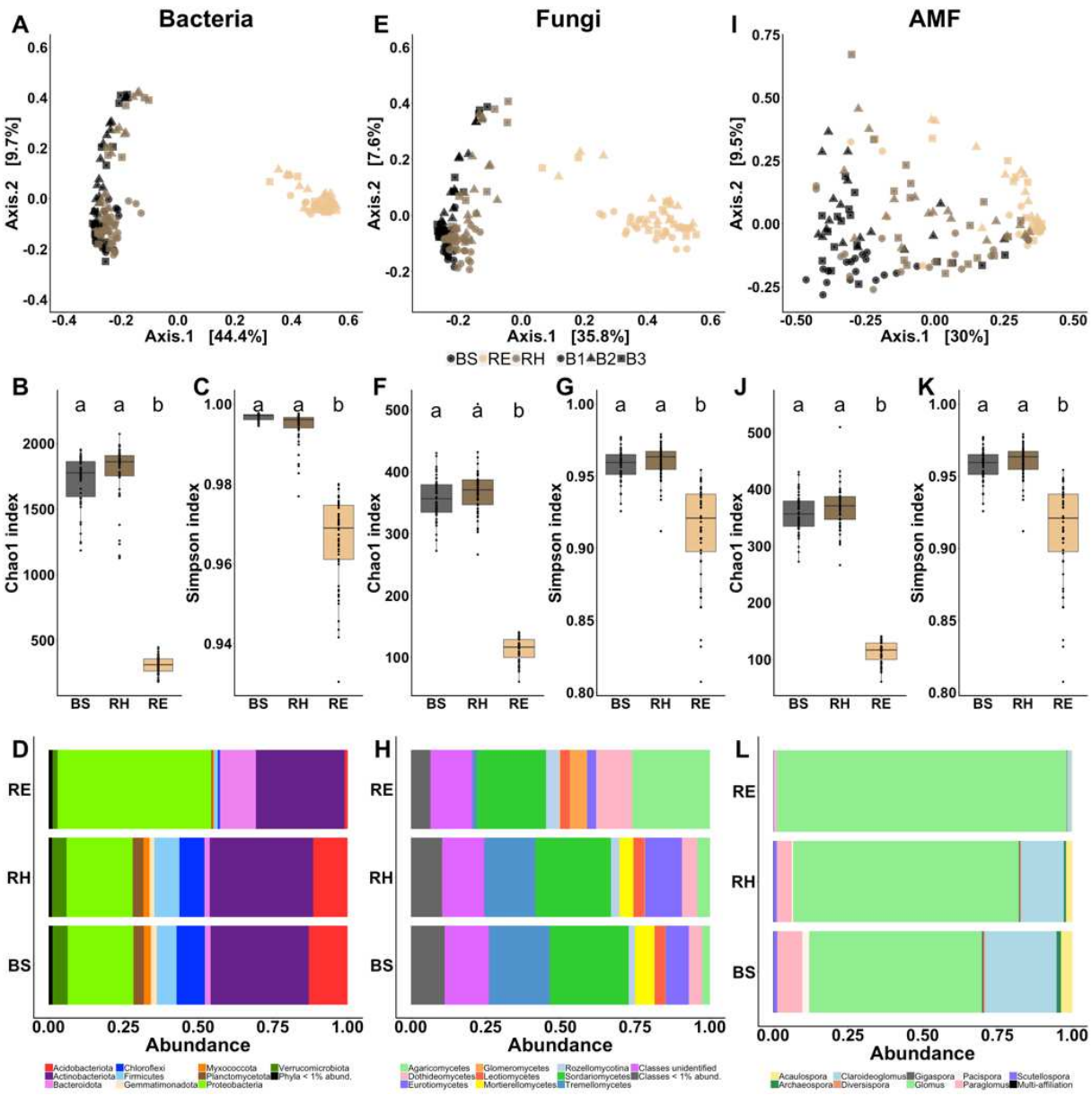


Figure 3-2: Comparison of microbial communities between the bulk soil (grey), the rhizosphere (dark brown) and the root endosphere (RE, light brown) (n=54).
Comparison of β-diversity by principal coordinate analysis (PCoA) of (A) bacterial, (E) fungal and (I) AMF communities based on Bray–Curtis dissimilarity matrices.
Comparison of α-diversity with Chao1 and Simpson indexes measured for bacterial (B and C), fungal (F, G) and AMF communities (J, K). *p*-values were calculated using Paired-Student or -Wilcoxon tests and were considered as significant when < 0.05.
Abundance graphs showing the abundances of bacterial phyla (D), fungal classes (H) and AMF genera (L) within compartments.

Among both compartments, 757 fungal OTUs were successfully affiliated to 15 phyla, 31 classes, 68 orders, 121 families, 174 genera and 299 species. Effects of the root system compartment were reported on Chao1, Simpson and Bray-Curtis metrics measured for fungi, explaining 94, 52 and 35% of PVE, respectively (Table 2). PCoA based on Bray-Curtis distance (Figure 2 E) showed a well separation between RE and soil compartments. In comparison to bacteria, we observed for fungi a slight segregation of samples from BS and RH along the first axis, as well as a reduce segregation between samples from soil compartments and RE. The Bray-Curtis index measured for fungi was significantly distinct between BS, RH and RE (Supplementary Table 3). All the α-diversity indexes (Figure 2 F/G) were significantly lower in RE than in BS and RH. Abundance graph at the class level (Figure 2 H) showed a dominance of *Sordariomycetes* in both compartments (ranging from 23% in RE and BS to 25% in RH), followed by *Tremellomycetes* in soil compartments (14%) or *Agaricomycetes* in RE (26%). LEfSe analysis of fungi (Supplementary Figure 1 B) showed enrichments at the class level of *Sordariomycetes*, *Mortierellomycetes* and *Tremellomycetes* in BS; *Eurotiomycetes* in RH; as well as *Agaricomycetes*, *Glomeromycetes*, *Dothideomycetes* and an unidentified class of *Ascomycota* in RE. Finally, 72% of fungal OTUs were common between the three compartments, 23% were exclusively common between BS and RH, and less than 1% were exclusive from RE or RH (Supplementary Figure 2 E).

When the AMF community was investigated, 261 OTUs were successfully affiliated to 1 phylum, 3 classes, 4 orders, 8 families, 10 genera and 53 species. Effects of the compartment were reported on Chao1, Simpson and Bray-Curtis indexes, explaining 74%, 64% and 20% of PVE, respectively (Table 2). PCoA analyses based on Bray-Curtis index (Figure 2 I) showed a well separation of all the compartments along the first axis, with individuals from RH in the midst of those from BS and RE. A high dispersion of the individuals was observed in both compartments along the second axis. The Bray-Curtis index was significantly different between BS, RH and RE (Supplementary Table 3). The Chao1 (Figure 2 J) and the Simpson (Figure 2 K) indexes were significantly lower in RE than in both soil compartments. Abundance graph at the genera level (Figure 2 L) show a clear dominance of *Glomus* in both compartments (ranging from 58 % in BS to 96% in RE), as well as an important proportion of *Claroideoglomus* in soil compartments (ranging from 14% in RH to 24% in BS). LEfSe analysis of AMF (Supplementary Figure 1 C) showed enrichments at the genus level of *Claroideoglomus*, *Paraglomus*, *Acaulospora*, *Archaeospora* and *Pacispora* in BS; as well as *Glomus* in RE. Finally, 32% of AMF OTUs were common between the three compartments, 61% were common between BS and RH, and 2 % were exclusives to BS or RH (Supplementary Figure 2 H).

Influence of rootstock genotype on the bulk soil (BS), the rhizosphere (RH) and the root endosphere (RE) bacterial community

Table 3-3: Influence of the rootstock genotype and the block on the α-diversity (richness = Chao1, diversity= Simpson) and the β-diversity metrics (Bray-Curtis dissimilarity) measured for bacteria.

			Chao1			Simspon			Bray-Curtis		
			p-value		PVE	*p*-value		PVE	*p*-value		PVE
Bacteria	BS	Genotype (G)	1.46e-04	***	39%	1.17e-04	***	41%	0.001	***	18%
		Block (B)	0.202	ns	/	0.800	ns	/	0.001	***	21%
		G * B	1.55e-11	***	48%	6.02e-11	***	10%	0.001	***	33%
	RH	G	2.41e-07	***	52%	0.002	**	32%	0.001	***	25%
		B	0.031	*	7%	0.640	ns	/	0.001	***	17%
		G * B	1.18e-12	***	35%	8.62e-06	***	43%	0.001	***	30%
	RE	G	3.58e-04	***	36%	0.005	**	29%	0.001	***	25%
		B	0.098	ns	/	0.214	ns	/	0.001	***	10%
		G * B	0.001	**	30%	0.024	*	27%	0.001	***	23%

Effects on Chao1 and Simpson indexes were evaluated with ANOVA, while the effect on the Bray-curtis index was evaluated with PERMANOVA using 999 permutations. * *p*-value < 0.05, ** *p*-value <0.01, *** *p*-value < 0.001, ns = non-significant, PVE = percentage of variance explained.

When we investigated the bacterial communities of BS, RH and RE, the Bray-Curtis index was influenced by the rootstock genotype (PVE ranging from 18% in BS to 25% in RH and RE), the block (PVE ranging from 10% in RE to 21% in BS) and their interaction (PVE ranging from 23% in RE to 33% in BS) (Table 3). In both compartments, the Chao1 index was influenced by the rootstock genotype (PVE ranging from 36% in RE to 52% in RH) and the factors interaction (PVE ranging to 30% in RE to 48% in BS). The block also influenced the Chao1 index measured in RH (PVE = 7%). The Simpson index was influenced by the rootstock genotype (PVE ranging from 29% in RE to 41% in BS) and the factors interaction (PVE ranging from 10% in BS to 43% in RH) in both compartments. In BS (Figure 3 A), RH (Figure 3 B) and RE (Figure 3 C), PCoA based on Bray-Curtis distance shows a clustering that is highly dependent on the genotype and sometimes also on the block. Pairwise-Adonis comparison of this index showed that the bacterial community of 1103P was significantly distinct from those of 3309C in BS (Supplementary Table 4 A). In RH, the one of 1103P was significantly distinct from those of 3309C and SO4, as well as the one of 3309C which was distinct from those of 41B (Supplementary Table 4 B). In RE, the bacterial community of 1103P was significantly distinct from those of 3309C, Nem, RGM and SO4, the one of 3309C was distinct from those of 41B and Nem, and the one of Nem was distinct from those of 41B and SO4 (Supplementary Table 4 C). The Chao1 index of 1103P was significantly lower than those of all other genotypes except 41B in BS (Figure 3 D), all other genotype in RH (Figure 3 E), as well as 41B, Nem and SO4 in RE (Figure 3 F). The Simpson index of 1103P was significantly lower than those of 3309C, RGM and SO4 in BS (Figure 3 G), as well as those of 3309C and RGM in RH (Figure 3 H). In RE, the Simpson

index was significantly lower in 3309C than in SO4 (Figure 3 I). Abundance graphs show slight dissimilarities of phyla in BS (Figure 3 J), which becomes more pronounced the closer we get to the root endosphere (Figure 3 K/L). In BS, LEfSe analysis showed enrichments of 3 taxa in 2 genotypes, such as at the phyla level the *Acidobacteriota* in 3309C and the *Proteobacteria* in Nemadex (Figure 4 A). In RH, 6 taxa were enriched in 3 genotypes, such as the *Actinobacteriota* in 1103P or the *Acidobacteriota* in 3309C (Figure 4 B). In RE, 24 taxa were enriched in 5 genotypes, such as the *Bacteroidota* in RGM, the *Verrucomicrobiota* in Nemadex, the *Proteobacteria* in 3309C, as well as the *Actinobacteriota* in 1103P (Figure 4 C). In soil compartments, OTUs were mainly common between rootstock genotypes (82% in BS and 81% in RH), whereas a few were genotype-exclusives (3% in BS and 2% in RH, respectively) (Supplementary Figure 2 B/C). In RE, 26% were common were common between genotypes, while 36% exclusives (Supplementary Figure 2 D).

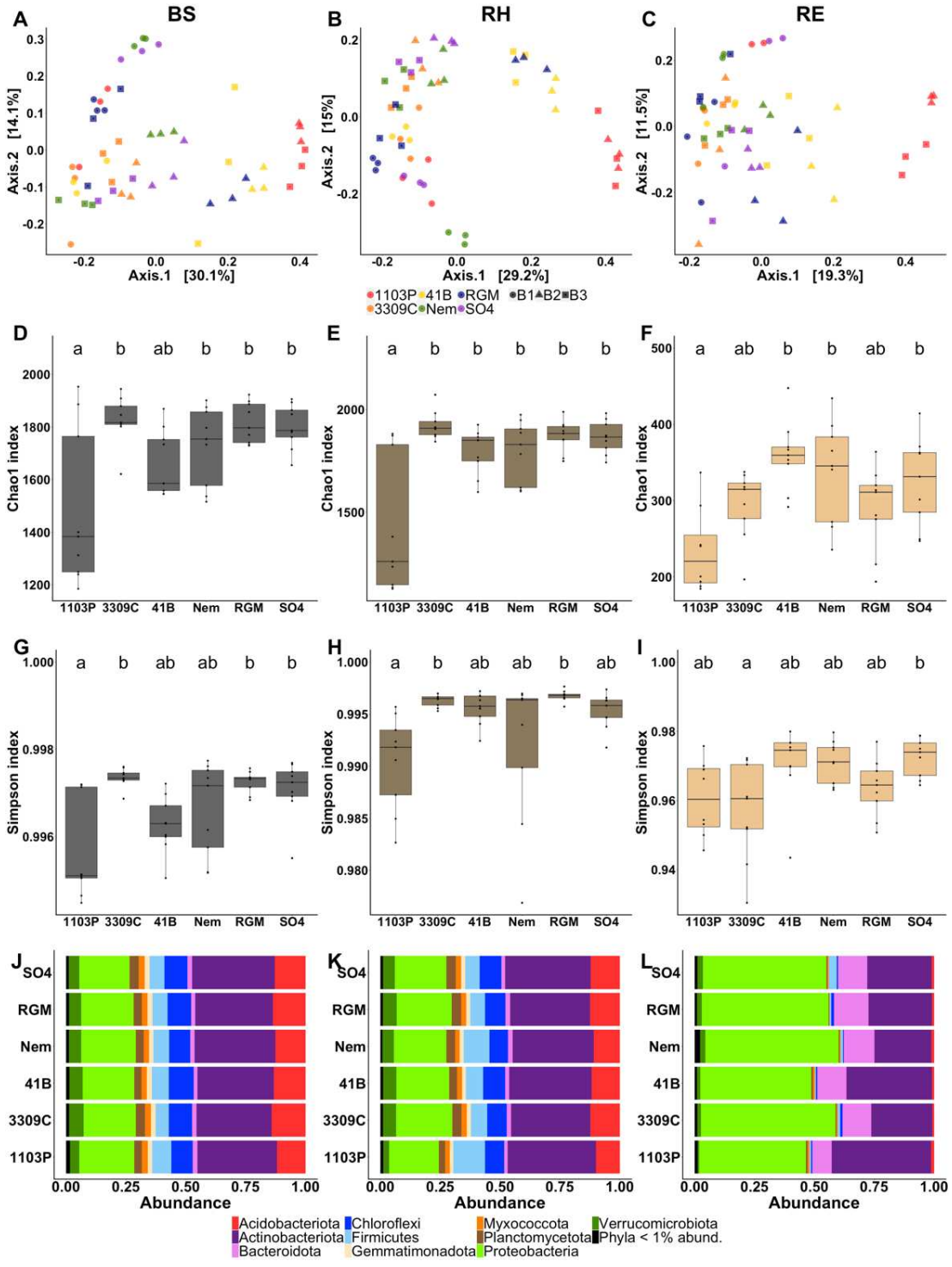


Figure 3-3: Comparison of bacterial communities between the rootstock genotypes in the bulk soil (grey), the rhizosphere (dark brown) and the root endosphere (RE, light brown) (n=9).
Comparison of β-diversity by principal coordinate analysis of bacterial communities based on Bray–Curtis dissimilarity matrices in BS (A), RH (B) and RE (C). Comparison of α-diversity metrics measured for bacteria (richness = Chao1, diversity = Simpson) between rootstock genotypes in BS (D and G), RH (E and H) and RE (F and I). Letters indicate significant differences between groups (p-value < 0.05), which were calculated using paiwise Student test with Bonferroni correction. Abundance graphs showing the abundance of bacterial phyla in BS (J), RH (K) and RE (L).

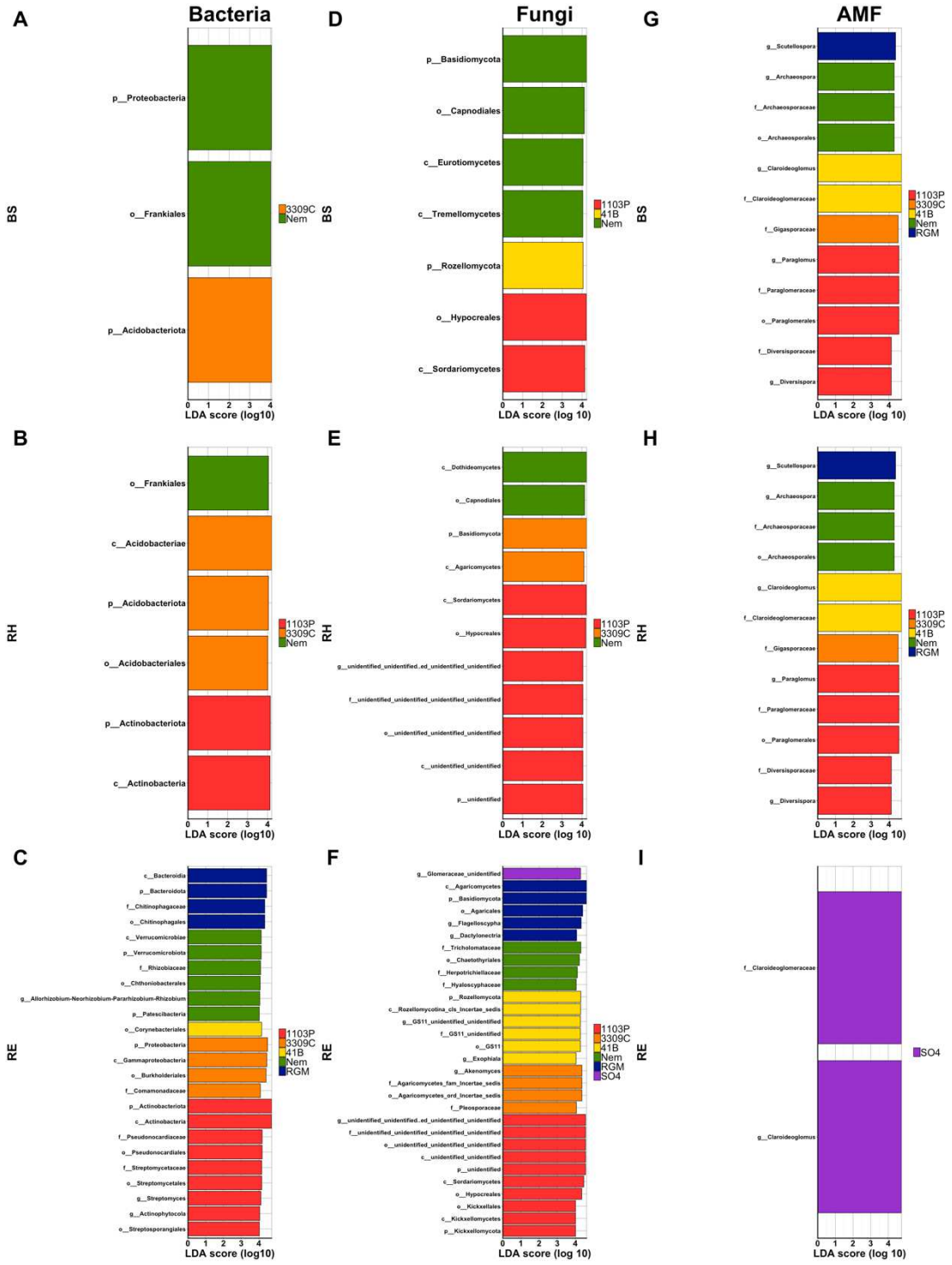


Figure 3-4: Histogram of the linear discriminant analysis (LDA) scores reveals the most differentially abundant taxa of bacteria (A, B and C), fungi (D, E and F) and AMF (G, H and I) within the bulk soil, the rhizosphere and the root endosphere.
For bacteria and fungi, LDA was realized at the phylum, class, order, and family levels.
For AMF, LDA was realized at order, family, genus, and species levels.

Influence of rootstock genotype on the bulk soil (BS), the rhizosphere (RH) and the root endosphere (RE) fungal community

Table 3-4: Influence of the rootstock genotype and the block on the α-diversity (richness = Chao1, diversity= Simpson) and the β-diversity metrics (Bray-Curtis dissimilarity) measured for fungi.

			Chao1			Simspon			Bray-Curtis		
			p-value		PVE	*p*-value		PVE	*p*-value		PVE
Fungi	BS	Genotype (G)	0.069	ns	/	**2.18e-04**	***	**39%**	**0.001**	***	**24%**
		Block (B)	0.083	ns	/	0.414	ns	/	**0.001**	***	**18%**
		G * B	**5.02e-05**	***	**34%**	**7.88e-04**	***	**32%**	**0.001**	***	**30%**
	RH	G	0.099	ns	/	0.371	ns	/	**0.001**	***	**25%**
		B	0.061	ns	/	0.873	ns	/	**0.001**	***	**17%**
		G * B	0.126	ns	/	0.186	ns	/	**0.001**	***	**29%**
	RE	G	0.428	ns	/	**0.045**	*	**22%**	**0.001**	***	**19%**
		B	0.378	ns	/	0.412	ns	/	**0.001**	***	**12%**
		G * B	**0.002**	**	**45%**	0.833	ns	/	**0.001**	***	**28%**

Effects on Chao1 and Simpson indexes were evaluated with ANOVA, while the effect on the Bray-curtis index was evaluated with PERMANOVA using 999 permutations. * *p*-value < 0.05, ** *p*-value <0.01, *** *p*-value < 0.001, ns = non-significant, PVE = percentage of variance explained.

When we investigated the fungal communities of the three compartments, the Bray-Curtis index was influenced by the rootstock genotype (PVE ranging from 19% in RE to 25% in RH), the block (PVE ranging from 12% in RE to 18% in BS) and their interaction (PVE ranging from 28% in RE to 30% in BS) (Table 4). No effect of the rootstock genotype was found on the Chao1 index in both compartments, but an influence of the factor's interaction was reported in BS (PVE = 34%) and RE (PVE = 45%) (Table 4). The Simpson index was influenced by the rootstock genotype in BS (PVE = 39%) and RE (PVE = 22%), as well as by the factor's interaction in BS (PVE = 32%) (Table 4). As for bacteria, PCoA based on Bray-Curtis distance showed for fungi a clustering that is highly dependent on the genotype and sometimes also on the block in both compartments (Figure 5 A/B/C). Pairwise-Adonis comparisons showed in BS that 41B fungal community was significantly distinct from those of all other genotype except 1103P, and that the one of 3309C was distinct from those of 1103P (Supplementary Table 5 A). In RH, the fungal community of 41B was distinct from those of 3309C, Nem and SO4, and the one of 1103P was distinct from those of 3309C and SO4 (Supplementary Table 5 B). In RE, the fungal community of 1103P was significantly distinct from those of all other genotypes (Supplementary Table 5 C). No significant differences were observed between rootstock genotypes for the Chao1 index in both compartments (Figure 5 D/E/F). In BS, the Simpson index of 1103P was significantly higher than in 3309C, Nem and SO4 (Figure 5 G). Even if an effect of the rootstock genotype was reported on the Simpson index measured in RE, no significant differences were found between rootstock genotypes with Paired-Student tests using Bonferroni correction (Figure 5 I). The abundance graphs showed a similar distribution of fungal class between BS and RE, with slight dissimilarities between rootstock genotypes in both soil compartments (Figure 5 J/K). These

dissimilarities appeared to be even greater in RE (Figure 5 L). LEfSe analysis showed enrichments in BS of 7 taxa in 3 genotypes, such as at the class level the *Eurotiomycetes* and *Tremellomycetes* in Nem, or *Sordariomycetes* in 1103P (Figure 4 D). In RH, 11 taxa were enriched in 3 genotypes, such as the *Dothideomycetes* in Nem, the *Agaricomycetes* in 3309C, or the *Sordariomycetes* in 1103P (Figure 4 E). In RE, 30 taxa were enriched in all the rootstock genotypes, such as *Agaricomycetes* in RGM, *Rozellomycotina* in 41B or the *Sordariomycetes* and the *Kickxellomycetes* in 1103P (Figure 4 F). In soil compartments, OTUs were mainly common between rootstock genotypes (57% in BS and 53% in RH), while a small percentage of them were genotype-exclusives (9% in BS and 5% in RH, respectively) (Supplementary Figure 2 F/G). In RE, 20% were common and 25% were genotype-exclusives (Supplementary Figure 2 H).

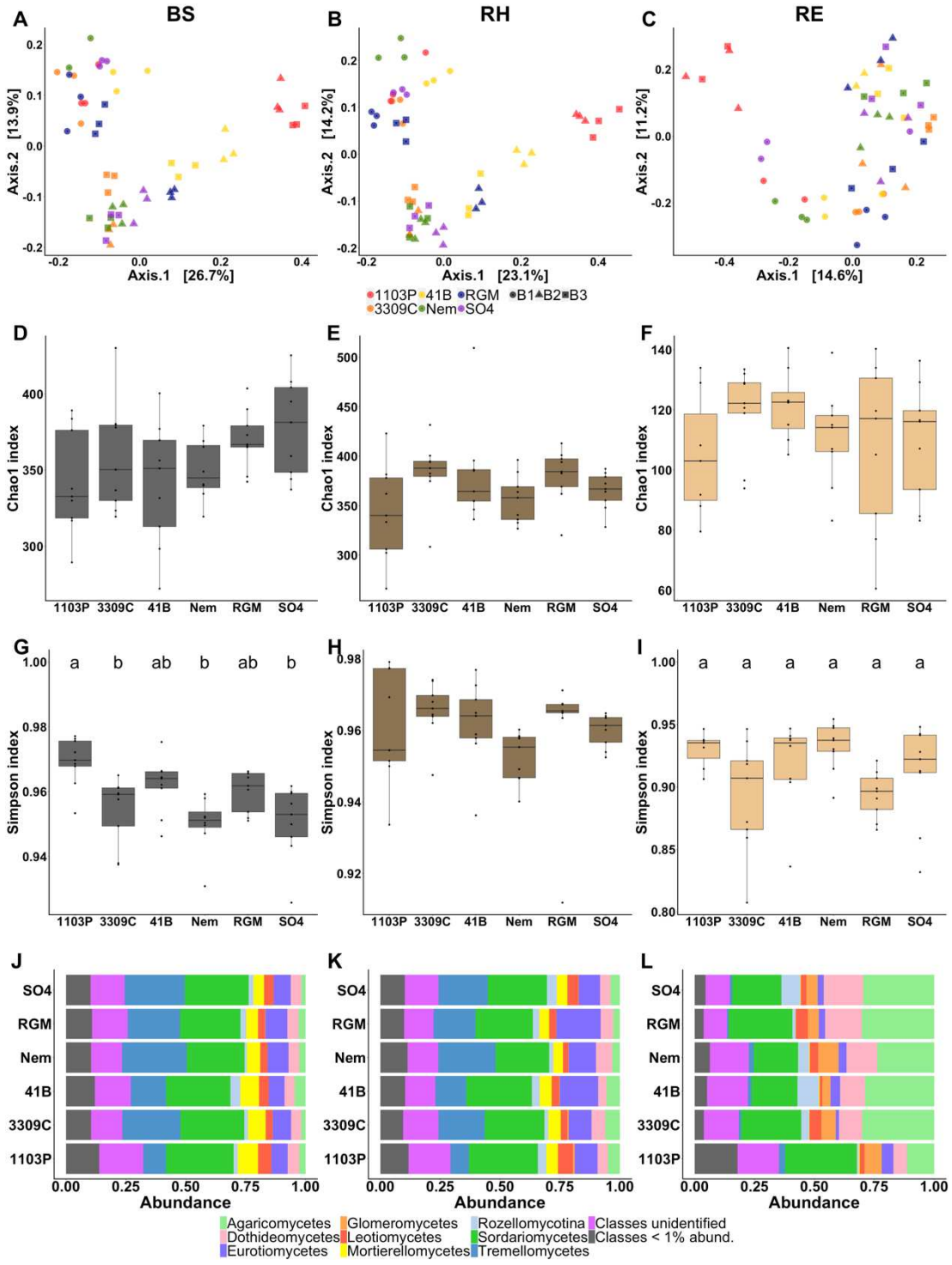


Figure 3-5: Comparison of fungal communities between the rootstock genotypes in the bulk soil (grey), the rhizosphere (dark brown) and the root endosphere (RE, light brown) (n=9).
Comparison of β-diversity by principal coordinate analysis of fungal communities based on Bray-Curtis dissimilarity matrices in the bulk soil (A), the rhizosphere (B) and the root endosphere (C). Comparison of α-diversity metrics measured for fungi (richness = Chao1, diversity = Simpson) between rootstock genotypes in BS (D and G), RH (E and H) and RE (F and I). Letters indicate significant differences between groups (p-value < 0.05), which were calculated using pairwise Student test with Bonferroni correction. Abundance graphs showing the abundance of fungal classes in BS (J), RH (K) and RE (L).

Influence of rootstock genotype on the bulk soil (BS), the rhizosphere (RH) and the root endosphere (RE) AMF community

Table 3-5: Influence of the rootstock genotype and the block on the α-diversity (richness = Chao1, diversity= Simpson) and the β-diversity metrics (Bray-Curtis dissimilarity) measured for AMF.

			Chao1			Simpson			Bray-Curtis		
			p-value		PVE	*p*-value		PVE	*p*-value		PVE
AMF	BS	Genotype (G)	0.438	ns	/	0.701	ns	/	**0.001**	***	**19%**
		Block (B)	**0.003**	**	**21%**	0.237	ns	/	**0.001**	***	**10%**
		G * B	0.143	ns	/	0.165	ns	/	**0.001**	***	**27%**
	RH	G	**5.41e-05**	***	**42%**	**5.82e-07**	***	**54%**	**0.001**	***	**22%**
		B	0.204	ns	/	0.894	ns	/	**0.003**	**	**8%**
		G * B	0.319	ns	/	0.254	ns	/	**0.001**	***	**31%**
	RE	G	0.251	ns	/	**0.006**	**	**29%**	**0.005**	**	**18%**
		B	0.787	ns	/	0.355	ns	/	0.075	ns	/
		G * B	0.081	ns	/	**0.007**	**	**33%**	**0.001**	***	**41%**

Effects on Chao1 and Simpson indexes were evaluated with ANOVA, while the effect on the Bray-curtis index was evaluated with PERMANOVA using 999 permutations. * *p*-value < 0.05, ** *p*-value <0.01, *** *p*-value < 0.001, ns = non-significant, PVE = percentage of variance explained.

Firstly, we assessed the root colonization by AMF in the different rootstock genotypes using three parameters measured by microscopy. ANOVA showed no effect of the rootstock genotype or the block on the mycorrhization frequency (F%), the overall mycorrhization intensity (M%) and the mycorrhization intensity of mycorrhized fragments (m%) (Supplementary Table 6, Supplementary Figure 3). Only the factors' interaction influenced both parameters (PVE ranging from 32% for F% to 41% for m%). However, sequencing of the glomeromycotan 18S rRNA gene showed that the Bray-Curtis index was influenced in all the studied compartments by the rootstock genotype (PVE ranging from 18% in RE to 22% in RH) and the factors interaction (PVE ranging from 27% in BS to 41% in RE) (Table 5). Effects of the block were also reported on the Bray-Curtis index in BS (PVE = 10%) and RH (PVE = 8%) (Table 5). The Chao 1 index was influenced by the block in BS (PVE = 21%) and by the rootstock genotype in RH (PVE = 42%) (Table 5). The Simpson index was influenced by the rootstock genotype in RH (PVE = 54%) and RE (PVE = 29%), as well as by the factor interaction in RE (PVE = 33%) (Table 5). PCoA analyses of AMF community in BS (Figure 6 A) and RH (Figure 6 B) show that individuals were clustered by genotype, even if the individuals from one block are sometimes distant from those of others. In RE, no apparent clustering according to rootstock genotype was observed (Figure 6 C). Pairwise-Adonis comparisons in BS showed that AMF community of 3309C was significantly distinct from those of 41B, 1103P and SO4, the one of 41B was distinct from Nem, and the one of 1103P was distinct from SO4 (Supplementary Table 7 A). In RH, the community of 3309C was distinct from those of all other genotypes except 1103P, and the one of 1103P was also distinct from those of Nem and SO4 (Supplementary Table 7 B). In RE, the community of 41B was

distinct from those of 3309C and Nem, and the one of SO4 was distinct from 3309C (Supplementary Table 7 C). No significant differences of Chao1 index were observed between rootstock genotype in BS (Figure 6 D) and RE (Figure 6 F). In RH, the Chao1 index was significantly lower in 1103P than in Nem, RGM and SO4, as well as significantly lower in 41B than in SO4 (Figure 6 E). Even if no significant differences were observed for the Simpson index between rootstock genotypes in BS (Figure 6 G), this index was significantly lower in 1103P and 3309C than in all other genotypes in RH (Figure 6 H), as well as significantly higher in 41B than in Nem in RE (Figure 6 I). The abundance graph showed dissimilarities in the abundance of AMF genera in both compartments, which seems more marked in BS (Figure 6 J) than in RH (Figure 6 K) and RE (Figure 6 L). LEfSe analysis showed enrichments in BS of 12 taxa in 5 genotypes, such as at the genera level the *Scutellospora* in RGM, *Archaeospora* in Nem, *Claroideoglomus* in 41B, or *Paraglomus* and *Diversispora* in 1103P (Figure 4 G). In RH, same result was obtained (Figure 4 H). In RE, 2 taxa were enriched in SO4, such as the *Claroideoglomus* (Figure 4 I). In soil compartments, the proportions of OTUs common (17% in BS and 13% in RH) between genotypes or exclusives (19% in BS and RH) were similar (Supplementary Figure 2 I/J). In the roots, 4% and 35% of OTUs were common or exclusives, respectively (Supplementary Figure 2 K).

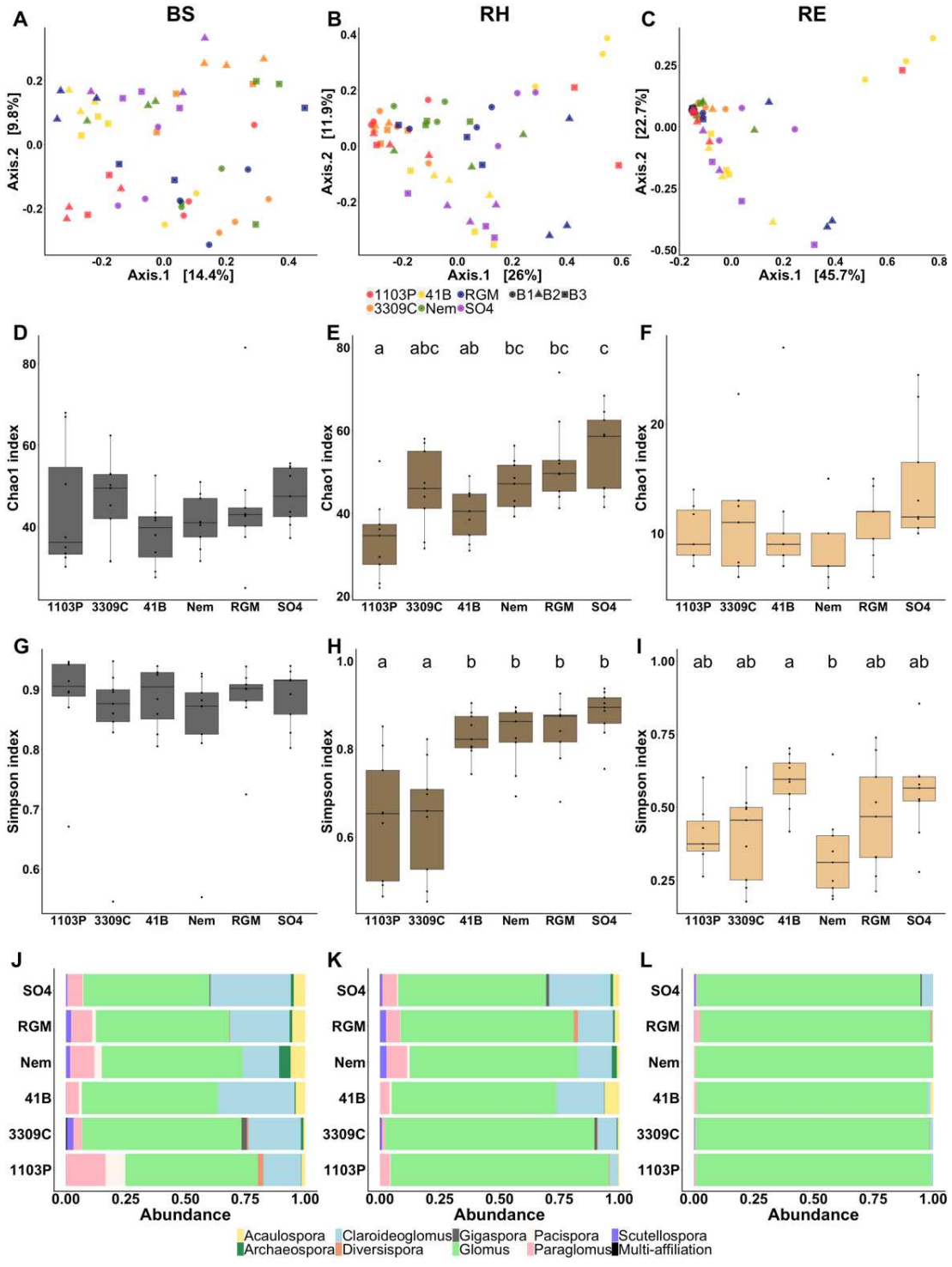


Figure 3-6: Comparison of AMF communities between the rootstock genotypes in the bulk soil (grey), the rhizosphere (dark brown) and the root endosphere (RE, light brown) (n=9).
Comparison of β-diversity by principal coordinate analysis of AMF communities based on Bray–Curtis dissimilarity matrices in the bulk soil (A), the rhizosphere (B) and the root endosphere (C). Comparison of α-diversity metrics measured for AMF (richness = Chao1, diversity = Simpson) between rootstock genotypes in BS (D and G), RH (E and H) and RE (F and I). Letters indicate significant differences between groups (p-value < 0.05), which were calculated using pairwise Student test with Bonferroni correction. Abundance graphs showing the abundance of AMF genera in BS (J), RH (K) and RE (L).

Predicted functions of bacterial and fungal microbiomes

Fungal trophic modes and guilds, predicted using the FUNGuild tool, were successfully affiliated to 23% of fungal OTUs from BS, as well as 25% from RH and RE. After removing the unassigned OTUs, Chi-Squared tests showed significant differences in the abundance of trophic modes (Figure 7 A) and guilds (Figure 7 E) between compartments (*p*-values < 2.2e-16***). The proportions of OTUs pathotroph (ranging from 21% in BS to 7% in RE) or multi-trophic (ranging from 39% in BS to 7% in RE) tend to decrease the closer you get to the root system, while those classified as symbiotroph (ranging from 3% in BS to 19% in RE) and saprotroph (ranging from 37% in BS to 67% in RE) increase (Figure 7 A). These results are consistent with the guilds affiliation which showed that the proportion of "Arbuscular Mycorrhizal" (ranging from less than 1% in soil compartments to 18% in RE) and "Undefined saprotroph" (ranging from 30% in BS to 64% in RE) increase in the root endosphere, while the ones of "Plant Pathogen" (ranging from 6% in RE to 14% in BS) and "Multi-affiliate guilds" (ranging from 9% in RE to 45% in BS) decrease (Figure 7 E). Chi-Squared tests showed significant differences (*p*-values < 2.2e-16***) in the abundances of trophic modes and guilds between rootstock genotypes in BS (Figure 7 B/F), RH (Figure 7 C/G) and RE (Figure 7 D/H). Concerning the abundance of guilds in BS, the proportion of "Undefined Saprotroph" ranged from 26% in 1103P to 34% in 41B, while the one of "Plant Pathogen" ranged from 6% in 41B to 19% in 3309C (Figure 7 F). In RH, the proportion of "Undefined Saprotroph" ranged from 31% in 3309C to 51% in 41B, while the one of "Plant Pathogen" ranged from 7% in 41B to 18% in Nem (Figure 7 G). In RE, the proportions of "Undefined Saprotroph" ranged from 55% in 3309C to 74% in 41B, "Arbuscular Mycorrhizal" ranged from 7% in 41B to 25 % in Nem, while the proportion of "Plant Pathogen" was closed between rootstock genotype (ranging from 5% in 41B and Nem to 7% in RGM) (Figure 7 H). Finally, Chi-Squared tests showed significant differences (*p*-values < 2.2e-16***) in the abundance of trophic modes and guilds between blocks in BS, RH and RE (Supplementary Figure 4). Taken together, these results show that the rootstock genotype and the block influence the ecological roles of fungi in all the compartments studied.

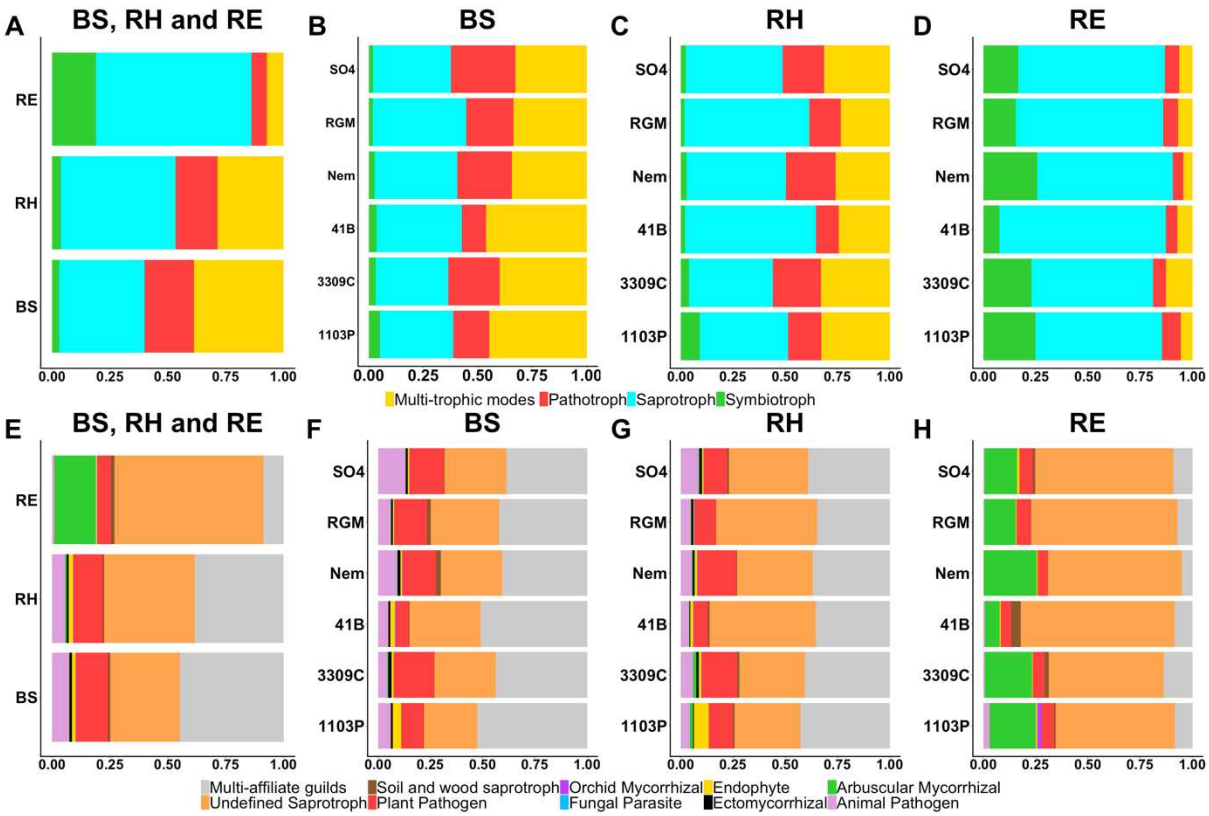


Figure 3-7: Comparison of the trophic modes and the guilds of fungi between compartments (A and E) (n=54), and rootstock genotypes within the bulk soil (B and F), the rhizosphere (C and G) and the root endosphere (D and H) (n=9).

Bacterial metabolic pathways were predicted using PICRUSt2. First, ANOVA showed an effect of the studied compartment on all the metabolic pathways except the "Membrane transport", with PVE ranging from 7% for "Signal transduction" to 89% for "Nucleotide metabolism" (Supplementary Table 8). Slight differences in the activities of the bacterial metabolic pathways were observed between BS and RH, but RE was the most different compartment (Figure 8 A). Indeed, the "Glycan biosynthesis and metabolism", the "Lipid metabolism", the "Metabolism of other amino acids", the "Signal transduction" and the "Xenobiotics biodegradation and metabolism" were highly abundant in RE compared to soil compartments, whereas other pathways were very low. These results were confirmed with the PCA carried out with the 121 predicted functions, which separate individuals of RE from those of BS and RH along the first axis (Supplementary Fig 5 A). In BS, 9 metabolic pathways were influenced by the rootstock genotypes (PVE ranging from 13 to 34%), 9 by the block (PVE ranging from 14 to 51%) and all of them by the factors' interaction (PVE ranging from 19% to 42%) (Supplementary Table 8). Several metabolic pathways were highly abundant depending on the rootstock genotype in BS (Figure 8 B), such as the "Membrane transport" and the "Signaling molecules

and interaction" in 1103P, as well as the "Energy metabolism", the "Metabolism of cofactors and vitamins" and the "Nucleotide metabolism" in 41B, or the "Metabolism of other amino acids" in Nem. In RH, all the 14 bacterial metabolic pathways abundances were influenced by the rootstock genotype (PVE ranging from 12 to 48%) and the factors interaction (PVE ranging from 19 to 48%), while 11 were influenced by the block (PVE ranging from 10 to 46%) (Supplementary Table 8). Several metabolic pathways were highly expressed in RH of certain rootstock genotypes (Figure 8 C), such as the "Amino acid metabolism" and the "Carbohydrate metabolism" in 1103P, the "Metabolism of cofactors and vitamins" and the "Nucleotide metabolism" in 41B, as well as the "Metabolism of terpenoids and polyketides" in SO4. In RE, 6 bacterial metabolic pathways were influenced by the rootstock genotype (PVE ranging from 22 to 30%), 2 by the block (10% of PVE) and 2 by the factors' interaction (PVE ranging from 29 to 31%) (Supplementary Table 8). Interestingly, all the abundances of metabolic pathways were low in 1103P, at the exception of the "Signaling molecules and interaction" (Figure 8 D). Together, these results show that rootstock genotypes have distinct bacterial microbiomes which play different roles within BS, RH and RE.

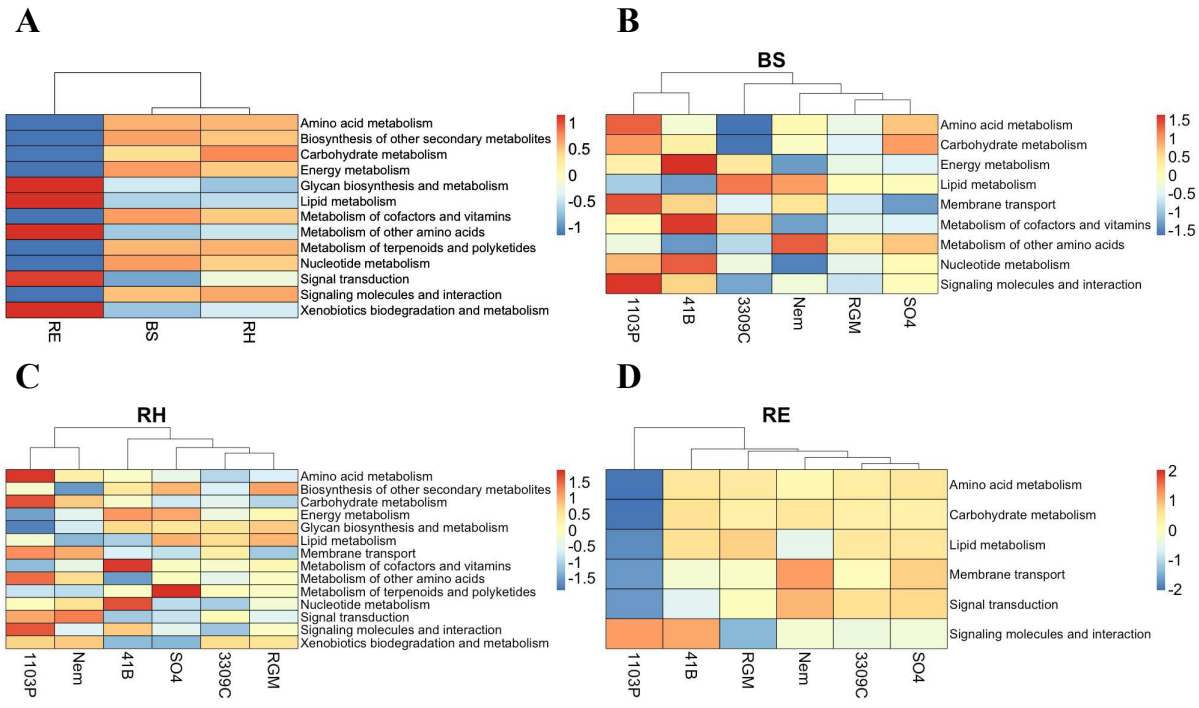


Figure 3-8: Heatmap showing the abundance of bacterial metabolic pathways which were significantly influenced by the compartments (A) (n = 18), or the rootstock genotype in the bulk soil (B), the rhizosphere (C) and the root endosphere (D) (n = 9).

Determination of enzymatic activities involved in rhizosphere nutrient cycles

In the rhizosphere, we investigated the effect of the rootstock genotype on the activities of microbial enzymes involved in the biogeochemical cycles of nitrogen (arylamidase), carbon (β-glucosidase), and phosphorus (phosphatase). ANOVA showed effects of the rootstock genotype and the block on the arylamidase (20% and 28% of PVE, respectively), the β-glucosidase (30% and 10% of PVE, respectively) and the phosphatase (44% and 6% of PVE, respectively) activities (Supplementary Table 9). Even if an effect of the rootstock genotype was reported on the arylamidase activity, no significant differences were observed between rootstock genotypes with Paired-Student test using Bonferroni correction (Figure 9 A). However, the activities of the β-glucosidase (Figure 9 B) and the phosphatase (Figure 9 C) were significantly higher in 3309C than in all other genotypes at the exception of 41B. The phosphatase activity was also significantly higher in 41B than in Nem, RGM and SO4. These results show that rootstock genotype influence the activities of microbial enzymes involved in rhizosphere biogeochemical cycles.

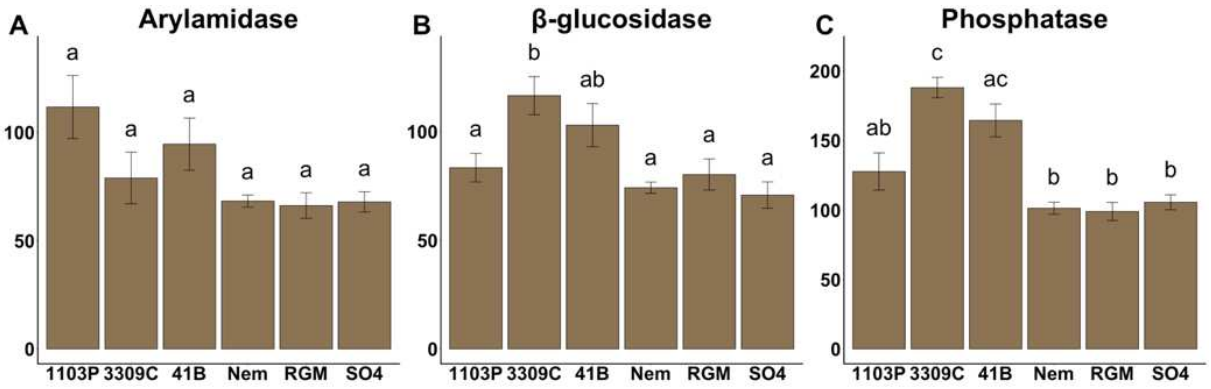


Figure 3-9: Comparison of the activities of the arylamidase (A), the β-glucosidase (B) and the phosphatase (C) in the rhizosphere between rootstock genotypes (n = 9).
Letters indicate significant differences between groups (p-value < 0.05), which were calculated using pairwise Student test with Bonferroni correction.

Community-level physiological profiling of the bacteria in the rhizosphere

Community-level physiological profiling of the rhizosphere was assessed using Biolog EcoPlate™. During each of the 7 days post-inoculation (d.p.i), an influence of the rootstock genotype was reported on the AWCD (PVE ranging from 19% at 1 d.p.i to 40% at 7 d.p.i) (Supplementary Table 10). AWCD was also influenced by the block at 1 d.p.i (PVE = 10%) and by the factors' interaction at 1 and 2 d.p.i (35% and 27% of PVE, respectively). Along the 7 d.p.i, the maximal values of AWCD

were observed for 3309C, followed by Nem and 1103P (Figure 10 A). At 4 d.p.i, the AWCD was significantly higher in 3309C than in 41B and RGM, as well as significantly higher in Nem than in 41B and RGM (Figure 10 B). At 4 d.p.i, the substrate richness and the Simpson index were influenced by the rootstock genotype (19 and 28% of PVE, respectively) and the block (5 and 8% of PVE, respectively) (Supplementary Table 10). The richness was significantly higher in 3309C than in 41B and SO4, as well as significantly higher in Nem than in 41B (Figure 10 C). The Simpson index was significantly higher in 3309C than in 41B, RGM and SO4, as well as significantly higher in Nem than in 41B and SO4 (Figure 10 D). Together, these results confirm an influence of the rootstock genotype on bacterial diversity and functionality in the rhizosphere.

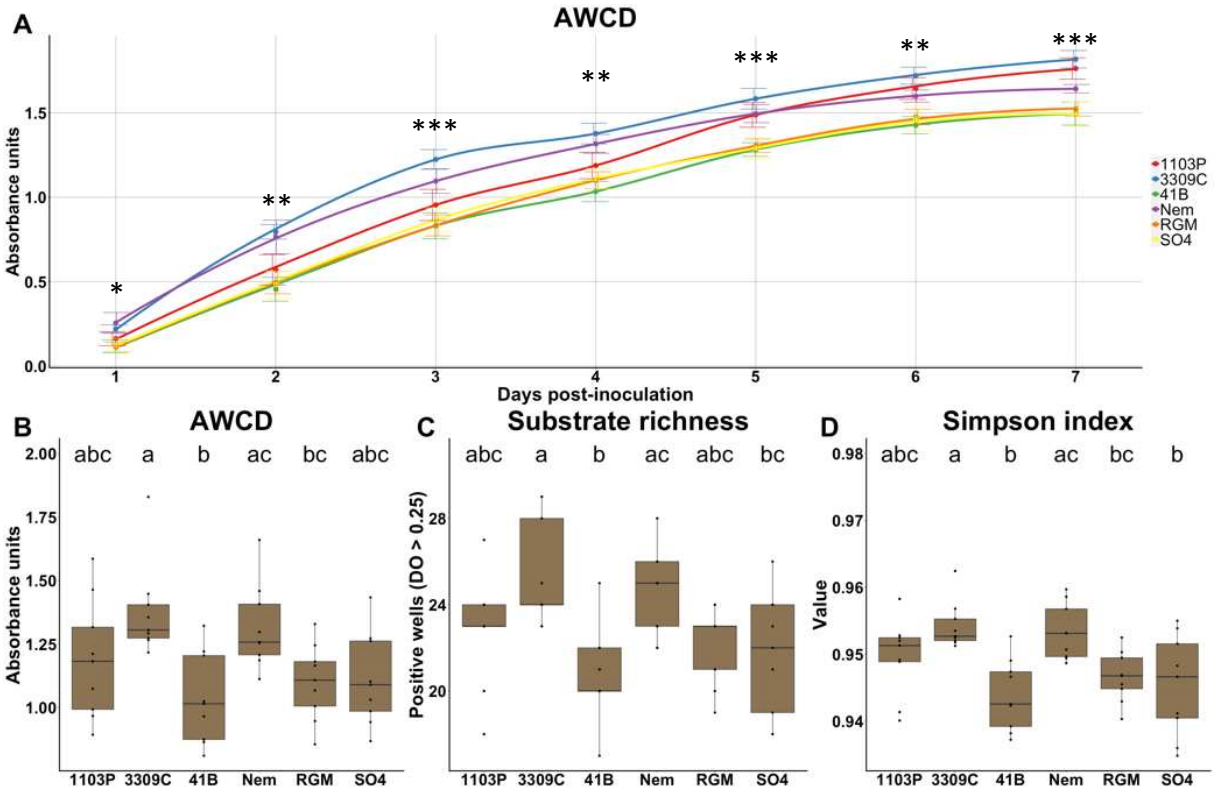


Figure 3-10: Comparison of the parameters measured by community-level physiological profiling (CLPP) using Biolog Ecoplate™ between rootstock genotypes (n = 9).
Comparison of the AWCD during the 7 days post-inoculation (A). Asterisks represent significant effect of the rootstock genotype measured with ANOVA, *p-value<0.05, ** p-value <0.01, *** p-value <0.001. Comparison of the AWCD (B), the substrate richness (C) and the Simpson index (D) at 4 days post-inoculation. Letters indicate significant differences calculated using pairwise Student test with Bonferroni correction between rootstock genotypes (p-value < 0.05).

Correlations between variables used to characterize root system microbiome and plant phenotypic traits

We researched correlations between all the variables used to characterize the microbial community (qPCR, microscopy, metabarcoding and CLPP) in both compartments (BS, RH and RE), the activities of enzymes involved in rhizosphere biogeochemical cycles, and the plant phenotypic traits, measured the same year. In this work, 8 significant correlations were found (*p*-values < 0.05). The pruning weight was positively correlated to the quantity of archaea measured by qPCR in BS (r = 0.39) and RH (r = 39), as well as with the arylamidase activity in RH (r = 0.41). The pruning weight was also negatively correlated to the bacterial Chao1 (r = -0.37) and Simpson (- 0.29) indexes in BS, as well as with the bacterial Chao1 index in RH (r = - 0.33). The shoot number was negatively correlated to the bacterial Simson index in RH (r = - 0.36) and the berry yield was significantly correlated to the quantity of fungi measured by qPCR in BS (r = 0.43).

Our results also showed that 104 microbial variables used to characterize root system microbiomes were significantly correlated together (*p*-value < 0.05), with r-values ranging from - 0.75 between the Chao1 index of bacteria in and the quantity of archaea measured in by qPCR in RH, to 0.99 between the variables used to quantify the root colonization by AMF, m (%) and M (%). The microorganisms' quantities from several kingdoms measured by qPCR in soil compartment were significantly correlated, such as the level of bacteria in BS with those of fungi (r = 0.55) and archaea (r = 0.5). Several other strong correlations were found, such as the level of archaea measured by qPCR and the bacterial Chao1 index in BS (r = - 0.6) or RH (r = - 0.75). Bacterial Chao1 index was correlated with those of fungi in BS (r = 0.55), RH (r = 0.48) and RE (r = 0.57), as well with the one of AMF in BS (r = 0.39). Fungal Chao1 index was also correlated with the one of AMF in BS (r = 0.49).

Finally, 26 significant correlations (*p*-value < 0.05) were established between the variables used to characterize the microbial community and the activity of enzymes involved in rhizosphere biogeochemical cycles. The arylamidase activity was correlated with several variables measured in RH such as the levels of archaea (r = 0.86) and bacteria (r = 0.66) measured by qPCR, the bacterial Chao1 (r = - 0.83) and Simpson (r = - 0.49) indexes, the fungal Chao1 index (r = - 0.35), as well as AMF Chao1 (r = - 0.4) and Simpson (r = - 0.29) indexes. The glucosidase activity in RH was correlated to the levels of bacteria (r = 0.59) and archaea (r = 0.47) measured by qPCR, the Biolog AWCD (r = 0.3), as well as AMF Chao1 (r = - 0.34) and Simpson (r = - 0.5) indexes. The phosphatase activity was correlated to the fungal Chao1 index (r = 0.32) and the AMF Simpson index (r = - 0.56). Interestingly,

the β-glucosidase activity was correlated to those of the arylamidase (r = 0.6) and the phosphatase (r = 0.41).

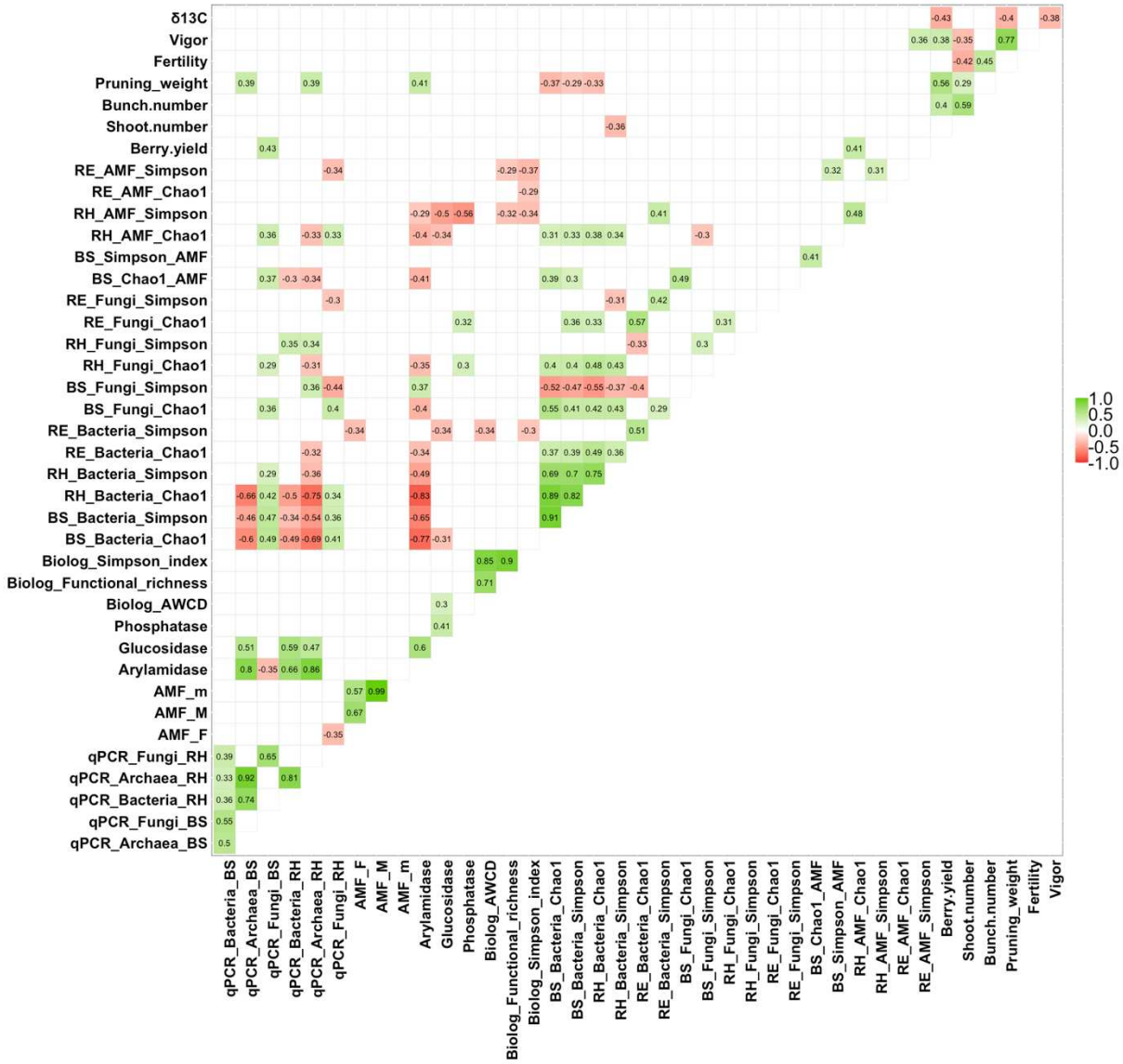


Figure 3-11: Matrices showing significant correlations between the variables used to characterize the root system microbiomes (qPCR, metabarcoding, Biolog, microscopy) and the plant phenotype or the activity of enzymes involved in biogeochemical cycles (n = 54).

Chapitre 3

Discussion

Rhizosphere act as an interface for microorganisms between the soil and the root endosphere

The higher levels of bacteria and archaea measured by qPCR in RH than in BS suggest that the root system of grapevine attract the soil procaryote communities. Even if the highest level of fungi was also observed in RH, difference between soil compartments was not significant. These results are consistent with the fact that RH contains a higher concentration of compounds derived from plant rhizodeposition, which are known to attract soil microbial communities (Dries et al., 2021; Philippot et al., 2013). However, this observation does not seem to apply to the entire plant kingdom. Indeed, Uroz et al. (2016) showed in beech and spruce that the quantity of fungi was significantly lower in RH than in BS, whereas no statistical differences were observed between soil compartments for bacteria and archaea. Indeed, different plant species do not have the same microbiota, which can be explained by differences in the composition and quantity of root exudates (Jamil et al., 2022). The α-diversity of bacteria, fungi and AMF (measured with Chao1 and Simpson indexes) were only significantly lower in RE than in both soil compartments. This is consistent with our previous work which show the same results between RE and RH for the three groups of microorganisms (Chapter 1). Marasco et al. (2022) observed reduced α-diversity in RE compared to soil compartments. The authors also showed significant differences between RH and BS, such as higher richness and Shannon index for bacteria in BS, as well as a higher fungal Shannon index in RH. In this work, all the groups of microorganisms were significantly distinct between compartments in term of β-diversity based on bray Bray-Curtis distance, as observed between RH and RE in the Chapter 1, as well as in all compartments by Marasco et al. (2022). Interestingly, PCoA analyses and abundance graph suggest that the rhizosphere acts as a transition zone for microorganisms, between the soil and the plant's root system, mainly marked for fungal and AMF communities. Finally, the predicted functions of bacterial and fungal microbiomes were also significantly different between the 3 compartments. These differences were even more marked between RE and the soil compartments than between RH and BS. As observed in the Chapter 1, the abundance of the bacterial pathways such as the lipid metabolism, the metabolism of other amino acids and the xenobiotics biodegradation and metabolism were higher in RE than in RH. Moreover, the fungal proportion of symbiotroph (such as arbuscular mycorrhizal) increases the closer you get to the roots, while the proportion of pathogens decreases (such as plant pathogen). Differences in microbial composition between soil compartments may be due to the enrichment of plant rhizodeposits in RH, corresponding to source of nutrients for microorganisms, chemoattractant and antimicrobial compounds, and which modify the soil structure (Dries et al., 2021; Philippot

et al., 2013). The differences between the root compartments depend on the ability of the microorganisms to cross the rhizoplane and overcome the plant's defense mechanisms, as well as the selection pressures linked to the physicochemical parameters of the two environments (Bettenfeld et al., 2022; Darriaut et al., 2022b).

The rootstock genotype drives the bacterial community of the root system

Significant differences were found between rootstock genotypes in the quantity of bacteria and archaea in RH, suggesting that rootstock genotype influences the quantity of all prokaryotes in this compartment. In May 2021 (Chapter 1), an effect of genotype was also reported on the quantity of archaea in RH, with 1103P containing the most, as shown here. It would be interesting here to study the influence of the rootstock genotype on archaea. Indeed, archaea are beneficial for plant by playing important roles in nutrient cycling, promoting plant growth, and increasing tolerance to various abiotic stresses (Naitam and Kaushik, 2021). Regarding bacterial α- / β-diversity metrics, abundance of classes, PCoA and LEfSe analyses, rootstock genotype determines the bacterial community of the root system, as well as their putative functions. Assessment of bacterial diversity using the CLPP technique in RH confirms the effect of the rootstock genotype observed by 16S rRNA gene sequencing. The differences of results obtained with both approaches can be explained by the fact that one method targets all bacteria, unlike the other considers a small proportion of bacteria, which can develop on the culture media of the plate (Basu et al., 2015). Significant differences of α- and β-diversity metrics between rootstock genotypes in BS suggest that the rootstock influence on bacteria could extend beyond the rhizosphere. However, the block is also a factor determining the composition of these bacterial communities, influencing particularly the beta diversity. The significant effects of the factors interraction on diversity parameters underline the fact that rootstocks of the same genotype can influence root system bacterial communities differentially, depending on the physicochemical parameters of the block. These results confirm those obtained in our previous study (Chapter 1), which were somewhat less clear. Indeed, significant differences between rootstock genotypes were dependent on the diversity metrics and the compartment studied, even if more bacterial taxa were enriched in both compartments of the root system in the different genotypes. Few enriched bacterial taxa were found in common to both studies, such as the orders of *Frankiales* in RH of Nem or *Pseudonocardiales* and *Strepomycetales* in RE of 1103P. Interestingly, 1103P genotype presented once again the most different bacterial community in its root system in terms of β-diversity. We hypothesize that the differences between experiments may be explained by the addition of the block 1 analysis in which the soil structure varies from that of the other blocks, as well as by the sampling year and season

(Darriaut et al., 2023; Gobbi et al., 2022; Oyuela Aguilar et al., 2020). In addition, we did not use the same collection method for the rhizosphere between studies. Taken together, these results show that rootstocks influence the quantity and diversity of bacteria in the vine root system. This is consistent with the results of previous studies showing an influence of rootstock genotype on bacterial community in RH (D'Amico et al., 2018; Berlanas et al., 2019; Dries et al., 2021; Vink et al., 2021; Wright et al., 2022) or in RH and RE (Darriaut et al., 2022; Marasco et al., 2018; Marasco et al., 2022).

The rootstock genotype drives the fungal community of the root system.

The significant differences observed between rootstock genotypes for fungal community analyzed by qPCR and Illumina sequencing of the ITS sequences, confirm that rootstocks drive the fungal community of grapevine root system. However, rootstock effects were mainly observed on β-diversity, whereas no significant differences were observed for α-diversity metrics, in both root system compartments. Interestingly, we also observed an effect of the rootstock genotype on Bray-Curtis index in BS. Several diversity metrics were also influenced by the block or the factors interaction, suggesting that soil properties also drive fungal communities and that the effect of the genotype may be block-dependent. In May 2021 (Chapter 1), an effect of the rootstock was detected on α-diversity metrics in both root system compartments. Moreover, 1103P seemed to be the most different rootstock for fungi in term of β-diversity, as observed here. Even if the results of the LEfSe are difficult to compare between the two studies, we observed common enriched taxa of fungi, such as the orders of *Capnodiales* in RH and *Chaetothyriales* in RE of Nem, or the *Hypocreales* in RH and RE of 1103P. Here, FUNGuild prediction confirm that rootstock influence the ecological roles of the root system fungi, as observed in our previous work. Together, these experiments confirm the role of the rootstock genotype as a determinant factor of the fungal microbiome associated to the root system. Differences between experiments can be explained by the same reasons as proposed for bacteria, also known to influence soil and root system fungi (Darriaut et al., 2022; Hernandez and Menéndez, 2019; Oyuela Aguilar et al., 2020). Together, our experiments confirm that rootstock genotype drive the fungal community of the root system, as observed in other works (Berlanas et al., 2019; Darriaut et al., 2022; Wright et al., 2022; Marasco et al., 2022).

The rootstock genotype drives the AMF community of the root system.

Microscopic analysis showed similar colonization of the roots by AMF between genotypes, as observed in our previous study, carried out on the block 1 of the GreffAdapt plot in September 2021

(Chapter 2). Here, α-diversity metrics were influenced by the rootstock genotype in both root system compartments, at the exception of the Chao1 index in RE. The influence of the rootstock genotype on β-diversity was reported in all the studied compartments. No effect of the block was reported on both α-/ β- diversity metrics measured in the root system compartments, at the exception of the Bray-Curtis index in RH, suggesting its poor involvement in structuring AMF community in the roots. However, the factors interaction influenced the β-diversity of AMF in the three compartments and the Simpson index in RE. In our previous work (Chapter 1), the β-diversity of AMF was influenced by the rootstock genotype in both root system compartments, as well as the Simpson index in RH and the Chao1 index in RE. The results obtained between experiments are difficult to compare because the 28S rRNA gene was used previously to study the AMF community in two blocs, whereas the 18S rRNA gene was used here to study them on the three blocks. Indeed, we have shown that the methodology used to study the AMF community using a metabarcoding approach has an impact on the interpretation of the results. (Chapter 2). We suggested that the observed differences were due to the targeted gene, as well as the use of the nested PCR to amplify the 28S rRNA gene, as proposed in other studies (Yu et al., 2015; Suzuki et al., 2020). In September 2021, Illumina sequencing of the 18S rRNA gene in the roots of individuals sampled from the block 1 showed an influence of the rootstock genotype on the Chao1 and the Bray-Curtis metrics (Chapter 2). Interestingly, very few taxa were enriched in the roots here, compared with the experiment carried out in September 2021. Differences between experiments may also be explained by the differences in the soil structure of the sampled blocks and the season, known to influence AMF community (Schreiner and Mihara, 2009; Schreiner, 2020). Altogether, our experiments confirm that rootstock genotype drives the AMF community of grapevine root system, as demonstrated by Moukarzel et al. (2021) by DGGE and trap culture.

The microbial communities of the root system are involved in plant growth and development

In this work, several correlations were established between plant phenotypic traits and variable measured to characterize grapevine root system microbiota. Although we found fewer significant correlations than in our previous work (Chapter 1), several of them were common to both studies such as the pruning weight which correlated positively with the quantity of archaea in the rhizosphere, as well as negatively with the bacterial Chao1 index in RH. Together, these results confirm the role of these microbial communities on grapevine growth and development (Kumar and Dubey, 2020; Orozco-Mosqueda et al., 2022). For example, archaea improved plant growth and tolerance to abiotic stresses by playing roles in soil nutrient cycling of carbon, nitrogen, sulfur and other minerals (Naitam and Kaushik, 2021). The pruning weight was also positively correlated with the arylamidase activity

in RH. This enzymatic process increases NH_4^+ availability to the plant by catalyzing the hydrolysis of an N-terminal amino acid from peptides, amides or arylamides. (Acosta-Martinez and Tabatabai, 2000). Nitrogen is a macro-element involved in most plant physiological processes, such as photosynthesis and nucleic acids or proteins synthesis (Shah et al., 2021). In our previous work (Chapter 1), we also correlated the composition of root system microbiomes with plant nutrient levels measured in roots and petioles. Here, the same measurements were carried out by a specialist company, but unfortunately, we have not yet received the results. Finally, the numerous correlations observed between the variables measured to characterize the microbiota of BS, RH and RE, confirm the existence of close interactions between microbial communities. In fact, microorganisms can interact positively, either intra- or inter-specifically, through quorum sensing, or compete for access to resources and the ecological niche by antibiosis (Jamil et al., 2022; Compant et al., 2013).

Conclusion

Several methods of microbiome analyses confirmed that the rootstock genotype strongly determined the structure and diversity of bacteria, fungi, and AMF in the root system. The rootstock genotype also affected the microorganisms' roles in their environment and their host. Moreover, the influence of the rootstock genotype could extend beyond the rhizosphere. We observed several correlations between plant phenotype and its microbiome, confirming the crucial importance of these communities, as well as the fundamental need to continue studying them. After obtaining the metabolomic data, we plan to compare the metabolome of the different compartments between several rootstock genotypes using the Metaboanalyst tool (https://www.metaboanalyst.ca). We expect to find some metabolites common to all rootstocks in terms of quality and quantity, but we also hope to identify other metabolites produced differentially according to the genotype, mainly in the rhizosphere and the root endosphere. We will then attempt to correlate the metabarcoding data with the metabolomic data to elucidate some of the molecular mechanisms involved in the selection of soil microorganisms by the rootstock genotype. The DIABLO tool from the "mixOmics" R package appears to be suitable for integrating data obtained by both methods (Rohart et al., 2017). We also plan to correlate metabarcoding and plant phenotype data with more powerful tools such the "TITAN2 R" (Baker., 2015). These results will provide knowledges for varietal improvement programs, or the development of methods to enhance beneficial associations between vines and soil microorganisms.

Supplementary tables

Table S1: Soil analysis carried out on the three blocks of the GreffAdapt plot.

	Block 1	Block 2	Block 3
Depth (cm)	0-35	0-35	0-30
Coarse elements (%)	47.6	31	33.6
Fine soil (%)	52.4	69	66.4
Coarse sands (‰)	725	761	738
Fine sands (‰)	110	82	120
Coarse silts (‰)	14	40	36
Fine silts (‰)	73	65	62
Clay (‰)	79	52	45
Texture given	Sand	Sand	Sand
Organic matter (%)	2.3	2.2	1.2
Total nitrogen (%)	0.103	0.109	0.049
C / N	12.8	11.5	14.7
Water pH	6.5	7.2	6.7
Absorbent complex			
Potassium (g / 100g)	0.71	0.28	0.71
Magnesium (g / 100g)	1.29	0.67	0.61
Calcium (g / 100g)	16	1.76	7.2
C.E.C. (cmol+ / kg)	6.2	5.3	3
Saturation (%)	105.3	127.1	102.4

Table S2: Sequences of primers, PNA clamp, Illumina adapters and cycling conditions used for the metabarcoding analyses.

Target genes	Primers	Sequences (5'-3')	Initial denaturation	Nulmber of cycles	Denaturation	Annealing	Extension	Final extension	Sources
Bacterial 16S rRNA gene V3-V4 regions	341F 785R	CCTACGGGNGGCWGCAG GACTACHVGGGTATCTAATCC	95°C/5min	25	95°C/30s	55°C/30s	72°C/30s	72°C/5min	Klindworth et al., 2013
Fungal ITS1 region (highly variable)	ITS1F ITS2	CTTGGTCATTTAGAGGAAGTAA GCTGCGTTCTTCATCGATGC	95°C/5min	30	95°C/30s	55°C/30s	72°C/45s	72°C/7min	Gardes and Bruns, 1993 White et al., 1990
AMF 18S rRNA gene	AMV4.5NF AMDGR	AAGCTCGTAGTTGAATTTCG CCCAACTATCCCTATTAATCAT	95°C/5min	35	95°C/45s	58°C/45s	72°C/1min	72°C/7min	Sato et al. 2005
Grapevine 16S rRNA gene V3-V4 regions	mPNA	GGCAAGTGTTCTTCGGA							Fitzpatrick et al., 2018
	pPNA	GGCTCAACCCTGGACAG							Fitzpatrick et al., 2018
Specific overhang Illumina adapters	Forward Reverse	TCGTCGGCAGCGTCAGATGTGTATAAGAGACAG GTCTCGTGGGCTCGGAGATGTGTATAAGAGACAG							PGTB

Table S3: Comparisons of the Bray-Curtis index measured for bacteria (A), fungi (B) and AMF (C) between the bulk soil (BS), the rhizosphere (RH) and the root endosphere (RE).

A	**Bacteria**						
pairs	**Df**	**SumsOfSqs**	**F.Model**	**R2**	***p*-value**	***p*-adjusted**	**sig**
BS vs RE	**1**	**15.08**	**93.26**	**0.47**	**0.001**	**0.003**	**
BS vs RH	1	0.44	3.15	0.03	0.004	0.012	ns
RE vs RH	**1**	**13.84**	**86.62**	**0.45**	**0.001**	**0.003**	**
B	**Fungi**						
pairs	**Df**	**SumsOfSqs**	**F.Model**	**R2**	***p*-value**	***p*-adjusted**	**sig**
BS vs RE	**1**	**10.49**	**58.3**	**0.36**	**0.001**	**0.003**	**
BS vs RH	**1**	**0.43**	**3.88**	**0.04**	**0.001**	**0.003**	**
RE vs RH	**1**	**8.97**	**47.81**	**0.32**	**0.001**	**0.003**	**
C	**AMF**						
pairs	**Df**	**SumsOfSqs**	**F.Model**	**R2**	***p*-value**	***p*-adjusted**	**sig**
BS vs RE	**1**	**8.03**	**36.39**	**0.26**	**0.001**	**0.003**	**
BS vs RH	**1**	**2.23**	**8.02**	**0.07**	**0.001**	**0.003**	**
RE vs RH	**1**	**2.58**	**14.31**	**0.12**	**0.001**	**0.003**	**

Asterisks represent significant differences between groups using Pairwise Adonis comparisons (n = 9): * *p*-value < 0.05, ** *p*-value <0.01, *** *p*-value < 0.001, ns = non-significant.

Table S4: Pairwise Adonis comparisons of the Bray-Curtis index measured for bacterial community between the genotypes of rootstock in the bulk soil (A), the rhizosphere (B) and the root endosphere (C).

Bacteria							
A				**BS**			
pairs	**Df**	**SumsOfSqs**	**F.Model**	**R2**	***p*-value**	***p*-adjusted**	**sig**
1103P vs 3309C	**1**	**0.76**	**6.4**	**0.29**	**0.003**	**0.045**	*
1103P vs 41B	1	0.30	2.14	0.12	0.087	1	ns
1103P vs Nem	1	0.58	4.18	0.21	0.013	0.195	ns
1103P vs RGM	1	0.44	3.36	0.17	0.033	0.495	ns
1103P vs SO4	1	0.53	4.28	0.21	0.014	0.21	ns
3309C vs 41B	1	0.40	3.41	0.18	0.013	0.195	ns
3309C vs Nem	1	0.20	1.78	0.1	0.06	0.9	ns
3309C vs RGM	1	0.19	1.83	0.1	0.051	0.765	ns
3309C vs SO4	1	0.20	2.02	0.11	0.027	0.405	ns
41B vs Nem	1	0.37	2.74	0.15	0.017	0.255	ns
41B vs RGM	1	0.21	1.66	0.09	0.115	1	ns
41B vs SO4	1	0.29	2.38	0.13	0.021	0.315	ns
Nem vs RGM	1	0.14	1.12	0.07	0.299	1	ns
Nem vs SO4	1	0.12	1.01	0.06	0.392	1	ns
RGM vs SO4	1	0.12	1.1	0.06	0.306	1	ns
B				**RH**			
pairs	**Df**	**SumsOfSqs**	**F.Model**	**R2**	***p*-value**	***p*-adjusted**	**sig**
1103P vs 3309C	**1**	**0.8**	**7.41**	**0.32**	**0.001**	**0.015**	*
1103P vs 41B	1	0.4	3.22	0.17	0.012	0.18	ns
1103P vs Nem	1	0.59	4.56	0.22	0.008	0.12	ns
1103P vs RGM	1	0.62	4.82	0.23	0.005	0.075	ns
1103P vs SO4	**1**	**0.77**	**6.36**	**0.28**	**0.001**	**0.015**	*
3309C vs 41B	**1**	**0.35**	**3.61**	**0.18**	**0.002**	**0.03**	*
3309C vs Nem	1	0.16	1.57	0.09	0.138	1	ns
3309C vs RGM	1	0.18	1.75	0.1	0.064	0.96	ns
3309C vs SO4	1	0.16	1.76	0.1	0.037	0.555	ns
41B vs Nem	1	0.35	2.97	0.16	0.007	0.105	ns
41B vs RGM	1	0.25	2.14	0.12	0.062	0.93	ns
41B vs SO4	1	0.31	2.82	0.15	0.009	0.135	ns
Nem vs RGM	1	0.19	1.59	0.09	0.107	1	ns
Nem vs SO4	1	0.18	1.64	0.09	0.106	1	ns
RGM vs SO4	1	0.15	1.34	0.08	0.166	1	ns
C				**RE**			
pairs	**Df**	**SumsOfSqs**	**F.Model**	**R2**	***p*-value**	***p*-adjusted**	**sig**
3309C vs 41B	**1**	**0.4**	**2.89**	**0.15**	**0.002**	**0.03**	*
3309C vs 1103P	**1**	**1.06**	**6.43**	**0.3**	**0.001**	**0.015**	*
3309C vs Nem	**1**	**0.28**	**2.37**	**0.13**	**0.003**	**0.045**	*
3309C vs RGM	1	0.20	1.31	0.08	0.182	1	ns
3309C vs SO4	1	0.28	1.86	0.1	0.017	0.255	ns
41B vs 1103P	1	0.58	3.34	0.18	0.005	0.075	ns
41B vs Nem	**1**	**0.36**	**2.93**	**0.15**	**0.001**	**0.015**	*
41B vs RGM	1	0.36	2.27	0.12	0.014	0.21	ns
41B vs SO4	1	0.26	1.64	0.09	0.039	0.585	ns
1103P vs Nem	**1**	**0.96**	**6.4**	**0.3**	**0.001**	**0.015**	*
1103P vs RGM	**1**	**0.91**	**4.9**	**0.25**	**0.001**	**0.015**	*
1103P vs SO4	**1**	**0.82**	**4.41**	**0.23**	**0.001**	**0.015**	*
Nem vs RGM	1	0.29	2.1	0.12	0.011	0.165	ns
Nem vs SO4	**1**	**0.29**	**2.15**	**0.12**	**0.003**	**0.045**	*
RGM vs SO4	1	0.27	1.62	0.09	0.067	1	ns

Table S5: Pairwise Adonis comparisons of the Bray-Curtis index measured for fungal community between the genotypes of rootstock in the bulk soil (A), the rhizosphere (B) and the root endosphere (C).

Fungi							
A				**BS**			
pairs	**Df**	**SumsOfSqs**	**F.Model**	**R2**	***p*-value**	***p*-adjusted**	**sig**
3309C vs 41B	**1**	**0.31**	**3.72**	**0.19**	**0.001**	**0.015**	*
3309C vs 1103P	**1**	**0.55**	**5.85**	**0.27**	**0.002**	**0.03**	*
3309C vs Nem	1	0.07	0.99	0.06	0.393	1	ns
3309C vs RGM	1	0.12	1.72	0.10	0.064	0.96	ns
3309C vs SO4	1	0.09	1.29	0.07	0.233	1	ns
41B vs 1103P	1	0.26	2.26	0.12	0.039	0.585	ns
41B vs Nem	**1**	**0.33**	**3.61**	**0.19**	**0.001**	**0.015**	*
41B vs RGM	**1**	**0.24**	**2.72**	**0.15**	**0.003**	**0.045**	*
41B vs SO4	**1**	**0.25**	**2.84**	**0.15**	**0.002**	**0.03**	*
1103P vs Nem	1	0.51	5.05	0.25	0.005	0.075	ns
1103P vs RGM	1	0.43	4.44	0.22	0.014	0.21	ns
1103P vs SO4	1	0.43	4.47	0.22	0.009	0.135	ns
Nem vs RGM	1	0.11	1.46	0.09	0.123	1	ns
Nem vs SO4	1	0.08	1.10	0.07	0.347	1	ns
RGM vs SO4	1	0.09	1.23	0.07	0.249	1	ns
B				**RH**			
pairs	**Df**	**SumsOfSqs**	**F.Model**	**R2**	***p*-value**	***p*-adjusted**	**sig**
3309C vs 41B	**1**	**0.35**	**4.03**	**0.20**	**0.001**	**0.015**	*
3309C vs 1103P	**1**	**0.62**	**5.65**	**0.26**	**0.001**	**0.015**	*
3309C vs Nem	1	0.15	1.98	0.11	0.037	0.555	ns
3309C vs RGM	1	0.17	2.05	0.11	0.016	0.24	ns
3309C vs SO4	1	0.11	1.46	0.08	0.122	1	ns
41B vs 1103P	1	0.37	2.89	0.15	0.005	0.075	ns
41B vs Nem	**1**	**0.38**	**3.94**	**0.20**	**0.001**	**0.015**	*
41B vs RGM	1	0.28	2.78	0.15	0.006	0.09	ns
41B vs SO4	**1**	**0.31**	**3.35**	**0.17**	**0.001**	**0.015**	*
1103P vs Nem	1	0.58	4.93	0.24	0.004	0.06	ns
1103P vs RGM	1	0.53	4.33	0.21	0.004	0.06	ns
1103P vs SO4	**1**	**0.54**	**4.67**	**0.23**	**0.002**	**0.03**	*
Nem vs RGM	1	0.15	1.62	0.09	0.091	1	ns
Nem vs SO4	1	0.13	1.57	0.09	0.126	1	ns
RGM vs SO4	1	0.13	1.47	0.08	0.119	1	ns
C				**RE**			
pairs	**Df**	**SumsOfSqs**	**F.Model**	**R2**	***p*-value**	***p*-adjusted**	**sig**
3309C vs 41B	1	0.32	1.49	0.09	0.088	1	ns
3309C vs Nem	1	0.34	1.57	0.09	0.067	1	ns
3309C vs 1103P	**1**	**1.12**	**5.05**	**0.27**	**0.002**	**0.03**	*
3309C vs RGM	1	0.25	1.11	0.07	0.307	1	ns
3309C vs SO4	1	0.35	1.52	0.09	0.059	0.885	ns
41B vs Nem	1	0.29	1.27	0.08	0.210	1	ns
41B vs 1103P	**1**	**0.77**	**3.27**	**0.20**	**0.001**	**0.015**	*
41B vs RGM	1	0.33	1.40	0.09	0.144	1	ns
41B vs SO4	1	0.21	0.86	0.05	0.619	1	ns
Nem vs 1103P	**1**	**0.79**	**3.4**	**0.20**	**0.001**	**0.015**	*
Nem vs RGM	1	0.44	1.87	0.10	0.032	0.48	ns
Nem vs SO4	1	0.31	1.26	0.07	0.196	1	ns
1103P vs RGM	**1**	**1.04**	**4.26**	**0.23**	**0.001**	**0.015**	*
1103P vs SO4	**1**	**0.82**	**3.22**	**0.19**	**0.002**	**0.03**	*
RGM vs SO4	1	0.29	1.16	0.07	0.257	1	ns

Table S6: Effects of the genotype and the block on the root colonization by AMF assessed by measuring the mycorrhization frequency (F%), the overall mycorrhization intensity (M%) and the mycorrhization intensity of mycorrhized fragments (m%).

	F (%)			M (%)			m (%)		
	p-value		PVE	*p*-value		PVE	*p*-value		PVE
Genotype (G)	0.246	ns	/	0.104	ns	/	0.111	ns	/
Block (B)	0.144	ns	/	0.467	ns	/	0.591	ns	/
G * B	**0.0280**	*	**32%**	**0.004**	**	**38%**	**0.002**	**	**41%**

Significances were assessed using ANOVA. Asterisks represent significant effects *p-value <0.05, ** p-value <0.01, *** p-value <0.001, PVE = percentage of variance explained, ns = non-significant.

Table S7: Pairwise Adonis comparisons of the Bray-Curtis index measured for AMF community between the genotypes of rootstock in the bulk soil (A), the rhizosphere (B) and the root endosphere (C).

AMF							
A				**BS**			
pairs	**Df**	**SumsOfSqs**	**F.Model**	**R2**	***p*-value**	***p*-adjusted**	**sig**
3309C vs 41B	**1**	**0.94**	**3.26**	**0.18**	**0.001**	**0.015**	*
3309C vs 1103P	**1**	**0.89**	**3.08**	**0.17**	**0.001**	**0.015**	*
3309C vs Nem	1	0.42	1.62	0.09	0.087	1	ns
3309C vs RGM	1	0.51	1.78	0.10	0.04	0.6	ns
3309C vs SO4	**1**	**0.69**	**2.73**	**0.15**	**0.001**	**0.015**	*
41B vs 1103P	1	0.70	2.14	0.13	0.005	0.075	ns
41B vs Nem	**1**	**0.74**	**2.50**	**0.14**	**0.003**	**0.045**	*
41B vs RGM	1	0.55	1.71	0.10	0.026	0.39	ns
41B vs SO4	1	0.57	1.99	0.12	0.008	0.12	ns
1103P vs Nem	1	0.61	2.08	0.12	0.008	0.12	ns
1103P vs RGM	1	0.54	1.67	0.10	0.046	0.69	ns
1103P vs SO4	**1**	**0.78**	**2.73**	**0.15**	**0.002**	**0.03**	*
Nem vs RGM	1	0.37	1.25	0.07	0.188	1	ns
Nem vs SO4	1	0.46	1.79	0.10	0.029	0.435	ns
RGM vs SO4	1	0.36	1.27	0.07	0.197	1	ns
B				**RH**			
pairs	**Df**	**SumsOfSqs**	**F.Model**	**R2**	***p*-value**	***p*-adjusted**	**sig**
3309C vs 41B	**1**	**0.93**	**5.03**	**0.24**	**0.001**	**0.015**	*
3309C vs 1103P	1	0.35	2.16	0.12	0.019	0.285	ns
3309C vs Nem	**1**	**0.43**	**3.32**	**0.17**	**0.001**	**0.015**	*
3309C vs RGM	**1**	**0.84**	**4.92**	**0.24**	**0.001**	**0.015**	*
3309C vs SO4	**1**	**0.93**	**6.46**	**0.29**	**0.001**	**0.015**	*
41B vs 1103P	1	0.58	2.27	0.12	0.054	0.81	ns
41B vs Nem	1	0.45	2.00	0.11	0.041	0.615	ns
41B vs RGM	1	0.37	1.38	0.08	0.185	1	ns
41B vs SO4	1	0.36	1.50	0.09	0.119	1	ns
1103P vs Nem	**1**	**0.53**	**2.63**	**0.14**	**0.003**	**0.045**	*
1103P vs RGM	1	0.65	2.68	0.14	0.024	0.36	ns
1103P vs SO4	**1**	**0.77**	**3.57**	**0.18**	**0.002**	**0.03**	*
Nem vs RGM	1	0.37	1.76	0.10	0.051	0.765	ns
Nem vs SO4	1	0.40	2.18	0.12	0.011	0.165	ns
RGM vs SO4	1	0.35	1.54	0.09	0.086	1	ns
C				**RE**			
pairs	**Df**	**SumsOfSqs**	**F.Model**	**R2**	***p*-value**	***p*-adjusted**	**sig**
3309C vs 41B	**1**	**0.54**	**4.04**	**0.20**	**0.001**	**0.015**	*
3309C vs Nem	1	0.01	0.33	0.02	0.913	1	ns
3309C vs 1103P	1	0.10	1.47	0.09	0.07	1	ns
3309C vs RGM	1	0.15	2.15	0.12	0.128	1	ns
3309C vs SO4	**1**	**0.28**	**3.71**	**0.19**	**0.001**	**0.015**	*
41B vs Nem	**1**	**0.56**	**4.05**	**0.20**	**0.003**	**0.045**	*
41B vs 1103P	1	0.32	1.75	0.11	0.153	1	ns
41B vs RGM	1	0.23	1.37	0.08	0.243	1	ns
41B vs SO4	1	0.27	1.56	0.09	0.209	1	ns
Nem vs 1103P	1	0.09	1.18	0.08	0.2	1	ns
Nem vs RGM	1	0.15	2.02	0.11	0.124	1	ns
Nem vs SO4	1	0.27	3.35	0.17	0.004	0.06	ns
1103P vs RGM	1	0.07	0.65	0.04	0.602	1	ns
1103P vs SO4	1	0.21	1.74	0.11	0.081	1	ns
RGM vs SO4	1	0.07	0.62	0.04	0.651	1	ns

Table S8: Comparison of the bacterial metabolic pathways predicted using PICRUSt2 between the compartments (n = 54), or the rootstock genotypes in the bulk soil (BS), the rhizosphere (RH) and the root endosphere (RE) (n = 9).

Predicted pathways	Factor	P value		PVE	Factors	BS			RH			RE		
						P value		PVE	P value		PVE	P value		PVE
Amino acid metabolism	Compartment (C)	7.97e-04	***	9%	Genotype (G)	0.016	*	24%	8.41e-05	***	41%	0.013	*	26%
					Block (B)	0.169	ns	ns	0.27	ns	/	0.514	ns	/
					G x B	6.09e-04	***	38%	1.49e-11	***	47%	0.332	ns	/
Biosynthesis of other secondary metabolites	C	<2e-16	***	50%	G	0.083	ns	/	0.008	**	22%	0.295	ns	/
					B	0.159	ns	/	7.39e-04	***	21%	0.260	ns	/
					G x B	4.4e-04	***	42%	3.31e-04	***	32%	0.254	ns	/
Carbohydrate metabolism	C	<2e-16	***	56%	G	0.008	**	27%	7.07e-06	***	48%	0.005	**	29%
					B	0.341	ns	/	0.843	ns	/	0.336	ns	/
					G x B	0.008	**	32%	5.65e-06	***	34%	0.017	*	29%
Energy metabolism	C	<2e-16	***	70%	G	0.050	*	16%	0.003	**	20%	0.304	ns	/
					B	0.001	**	21%	8.84e-07	***	36%	0.166	ns	/
					G x B	0.001	**	33%	8.75e-04	***	23%	0.110	ns	/
Glycan biosynthesis and metabolism	C	<2e-16	***	44%	G	0.156	ns	/	0.001	**	32%	0.363	ns	/
					B	0.447	ns	/	0.112	ns	/	0.796	ns	/
					G x B	1.21e-07	***	60%	6.14e-09	***	48%	0.300	ns	/
Lipid metabolism	C	<2e-16	***	57%	G	0.009	**	13%	0.007	**	22%	0.003	**	30%
					B	1.06e-09	***	51%	1.96e-04	***	24%	0.204	ns	/
					G x B	3.18e-04	***	20%	0.001	**	28%	0.704	ns	/
Membrane transport	C	0.191	ns	/	G	0.001	**	34%	3.19e-05	***	40%	0.030	*	22%
					B	0.246	ns	/	0.013	*	10%	0.128	ns	/
					G x B	2.4e-04	***	36%	4.82e-04	***	27%	0.014	*	31%
Metabolism of cofactors and vitamins	C	<2e-16	***	79%	G	0.025	*	16%	0.019	*	14%	0.647	ns	/
					B	1.31e-05	***	32%	2.52e-07	***	41%	0.346	ns	/
					G x B	5.31e-04	***	28%	0.002	**	22%	0.147	ns	/
Metabolism of other amino acids	C	<2e-16	***	74%	G	0.044	*	17%	0.019	*	16%	0.439	ns	/
					B	9.44e-04	***	22%	6.85e-06	***	34%	0.391	ns	/
					G x B	0.001	**	32%	2.54e-04	***	28%	0.159	ns	/
Metabolism of terpenoids and polyketides	C	6.14e-06	***	14%	G	0.181	ns	ns	7.74e-05	***	34%	0.524	ns	/
					B	0.017	*	14%	4.19e-04	***	19%	0.386	ns	/
					G x B	1.09e-04	***	43%	0.022	*	19%	0.583	ns	/
Nucleotide metabolism	C	<2e-16	***	89%	G	0.008	**	16%	0.047	*	14%	0.357	ns	/
					B	1.35e-07	***	42%	1.6e-05	***	33%	0.345	ns	/
					G x B	0.009	**	19%	0.003	**	26%	0.183	ns	/
Signal transduction	C	0.003	**	7%	G	0.441	ns	ns	0.003	**	20%	0.007	**	26%
					B	7.16e-07	***	43%	3.11e-07	***	38%	0.032	*	10%
					G x B	6.55e-05	***	31%	5.2e-04	***	23%	0.138	ns	/
Signaling molecules and interaction	C	7.31e-06	***	14%	G	0.001	**	27%	6.96e-04	***	27%	0.007	**	27%
					B	3.6e-04	***	21%	3.34e-05	***	26%	0.032	*	10%
					G x B	4.26e-04	***	29%	9.17e-06	***	30%	0.161	ns	/
Xenobiotics biodegradation and metabolism	C	<2e-16	***	83%	G	0.111	ns	ns	0.031	*	12%	0.329	ns	/
					B	0.001	**	21%	3.87e-08	***	46%	0.495	ns	/
					G x B	0.003	**	32%	0.010	**	19%	0.311	ns	/

Significances were assessed using ANOVA. Asterisks represent significant effects *p-value <0.05, **p-value <0.01, ***p-value <0.001, PVE = percentage of variance explained, ns = non-significant.

Table S9: Effect of the rootstock genotype and the block on the enzyme activities in the rhizosphere

	Arylamidase			β-glucosidase			Phosphatase		
	p-value		PVE	*p*-value		PVE	*p*-value		PVE
Genotype (G)	**0.003**	**	**20%**	**3.52e-04**	***	**30%**	**1.37e-06**	***	**44%**
Block (B)	**1.1e-05**	***	**28%**	**0.016**	*	**10%**	**0.048**	*	**6%**
G * B	0.179	ns	/	0.633	ns	/	0.061	ns	/

Significances were assessed using ANOVA. Asterisks represent significant effects * *p*-value <0.05, ** *p*-value <0.01, *** *p*-value <0.001. PVE = percentage of variance explained, ns = non-significant.

Table S10: Effects of the rootstock genotype and the block on the parameters measured by community-level physiological profiling of the rhizosphere using Biolog Ecoplate™.

	Factor	*p*-value		PVE		Factor	*p*-value		PVE
AWCD Day 1	**Rootstock (R)**	**0.047**	*	**19%**	**AWCD Day 6**	**R**	**0.002**	**	**32%**
	Block (B)	**0.045**	*	**10%**		**B**	0.404	ns	/
	B*R	**0.003**	**	**35%**		**R*B**	0.102	ns	/
AWCD Day 2	**R**	**0.005**	**	**28%**	**AWCD Day 7**	**R**	**8.58e-05**	***	**40%**
	B	0.147	ns	ns		**B**	0.100	ns	/
	R*B	**0.024**	*	**27%**		**R*B**	0.059	ns	/
AWCD Day 3	**R**	**8.29e-04**	***	**34%**	**Substrate richness Day4**	**R**	**4.68e-04**	***	**34%**
	B	0.116	ns	/		**B**	**0.045**	*	**5%**
	R*B	0.328	ns	/		**R*B**	0.154	ns	/
AWCD Day 4	**R**	**0.001**	**	**33%**	**Simpson diversity Day4**	**R**	**9.57e-05**	***	**39%**
	B	0.223	ns	/		**B**	**0.048**	*	**8%**
	R*B	0.645	ns	/		**R*B**	0.290	ns	/
AWCD Day 5	**R**	**6.48e-04**	***	**36%**					
	B	0.388	ns	/					
	R*B	0.444	ns	/					

Significances were assessed using ANOVA. Asterisks represent significant effects *p-value <0.05, ** *p*-value <0.01, *** *p*-value <0.001. PVE = percentage of variance explained, ns = non-significant.

Supplementary figures

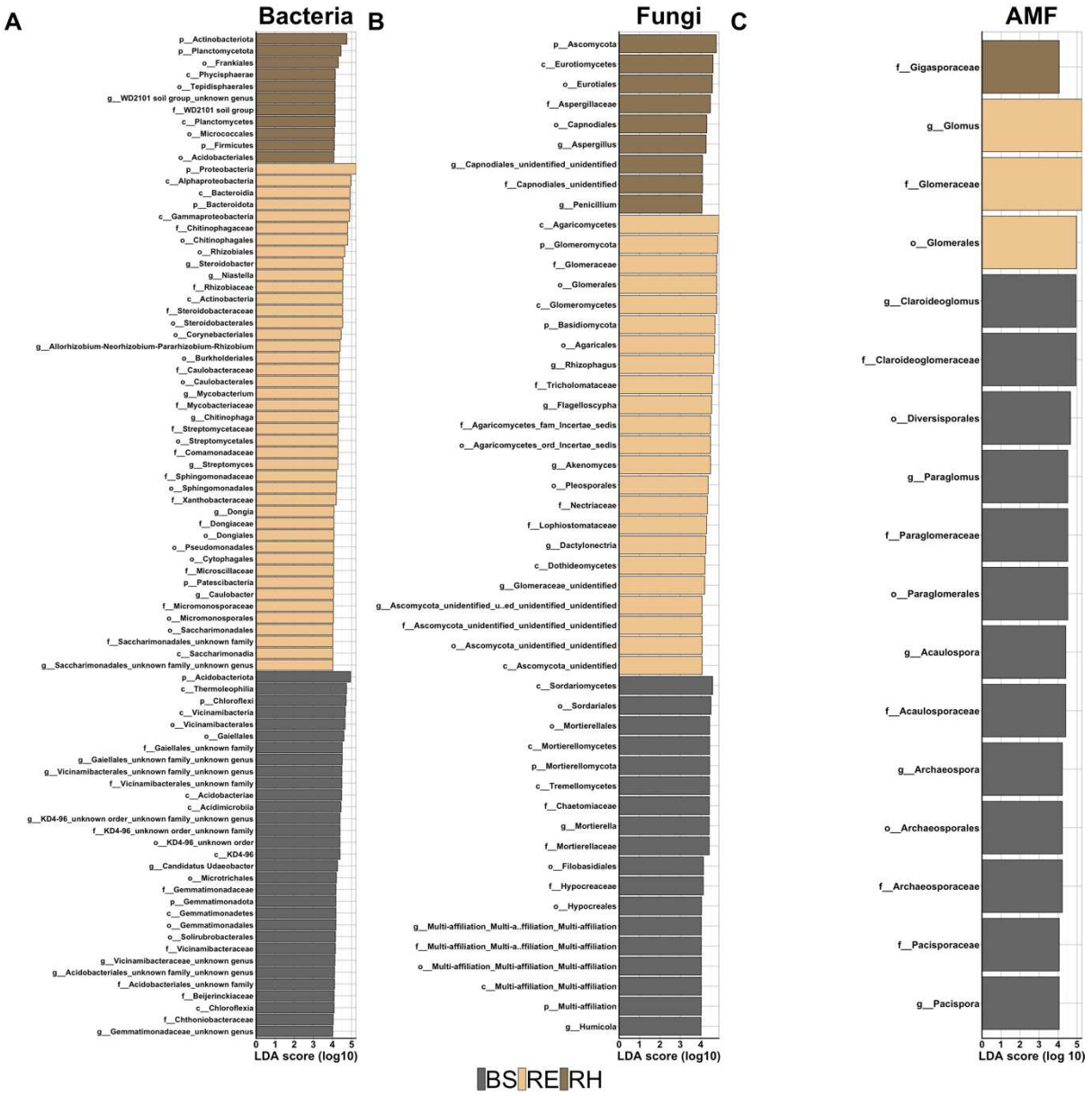


Figure S1: Histogram of the linear discriminant analysis (LDA) scores reveals the most differentially abundant taxa of bacteria (A), fungi (B) and AMF (C) among the bulk soil (grey), the rhizosphere (dark brown) and the root endosphere (pale brown).

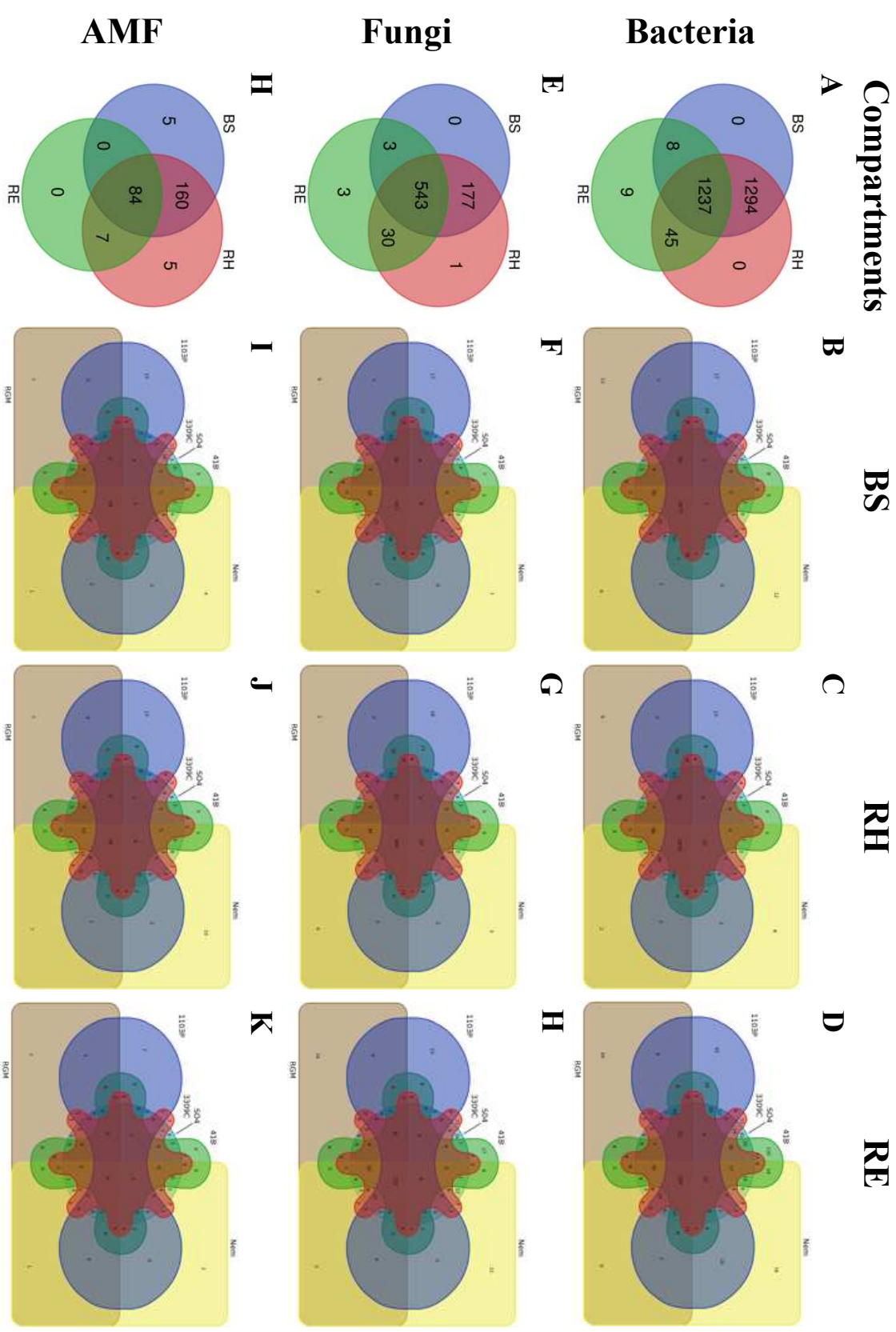


Figure S2: Venn diagrams showing common and exclusives OTUs of bacteria (A, B, C, D), fungi (D, E, F, G) and AMF (H, I, K, K) within compartments, BS, RH and RE.

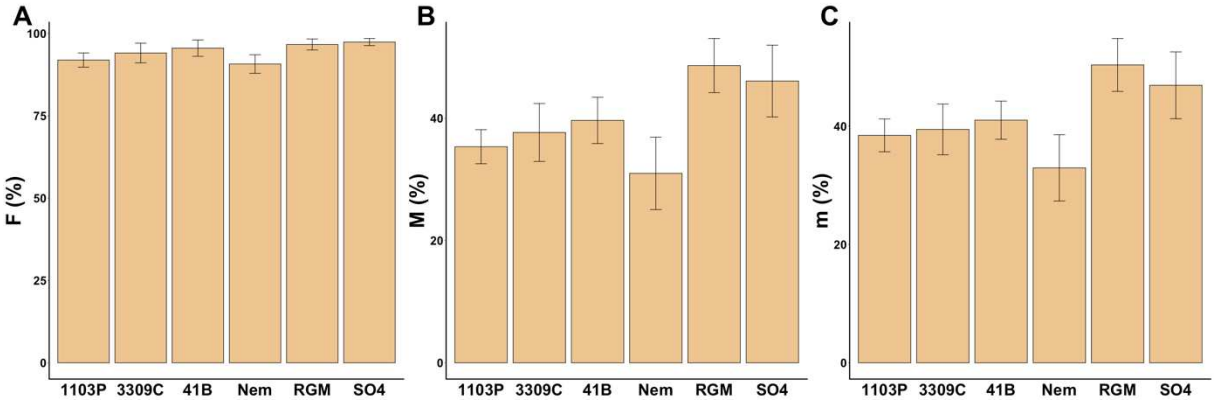


Figure S3: Comparison of the mycorrhization frequency F% (A), the overall mycorrhization intensity M% (B) and the mycorrhization intensity of mycorrhized fragments m% (C) between genotypes of rootstock. Data are represented as mean ± SE, n=5. Letters indicate significant differences between genotype using paired t-test with Bonferroni correction (*p*-value < 0.05).

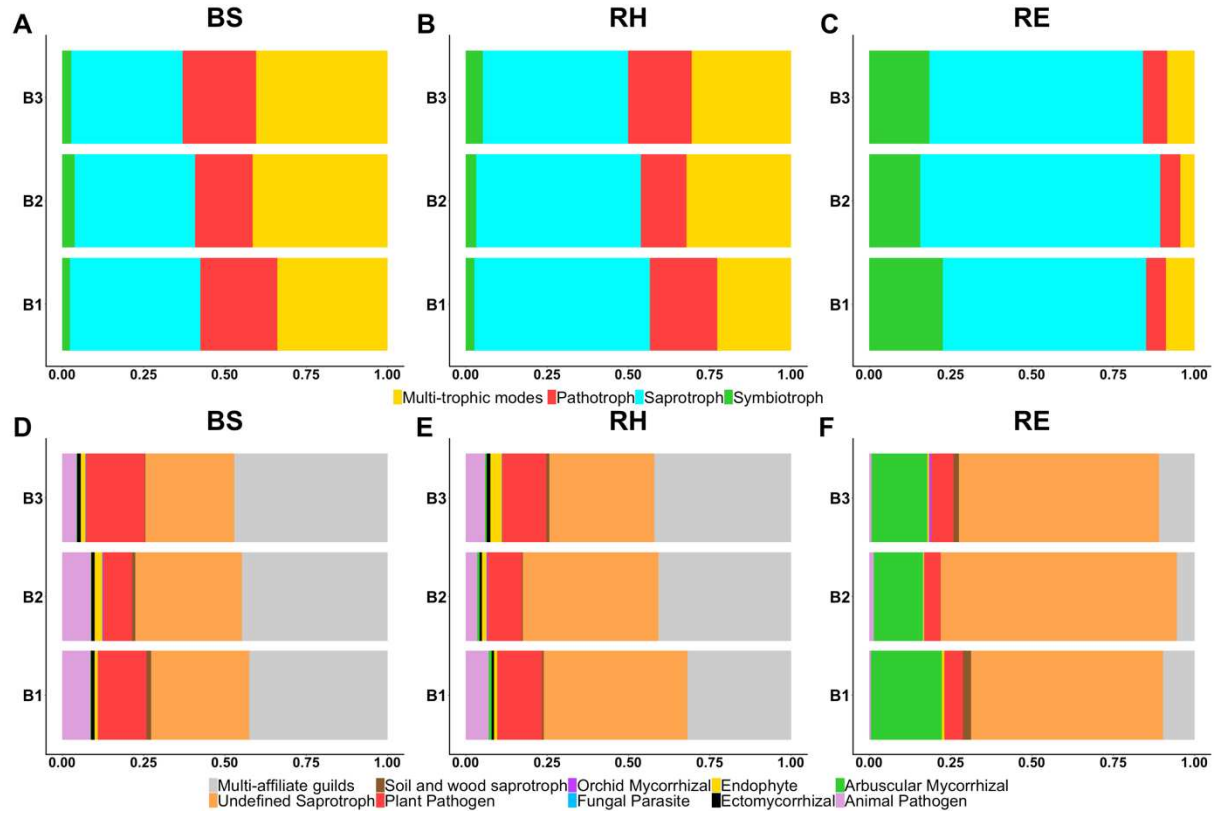


Figure S4: Comparison of the trophic modes and the guilds of fungi between blocks within the bulk soil (A and D), the rhizosphere (B and E) and the root endosphere (C and F) (n=54).

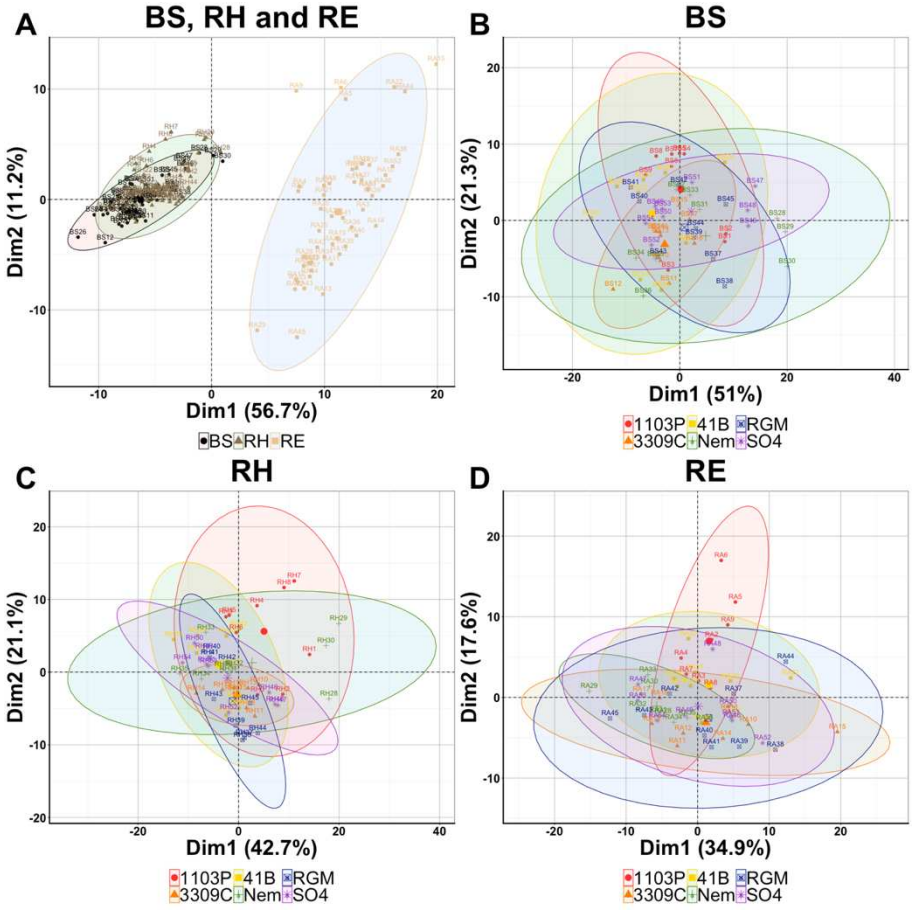


Figure S5: PCA analysis of the predicted functions of bacteria (121 variables) between root system compartments (n = 54), or rootstock genotypes in the bulk soil (B), therhizosphere (C) and the root endosphere (D) (n = 9).

Discussion de la thèse

I- Synthèse des résultats acquis dans la thèse

Dans leur environnement, tous les organismes multicellulaires sont colonisés par des microorganismes, mais ce n'est que récemment qu'il est devenu possible d'étudier la composition de ces communautés microbiennes, ainsi que leur influence sur l'écologie et l'évolution de leurs hôte. Depuis quelques années, une approche de réflexion sur le sujet consiste à considérer l'écosystème hôte-microbiome comme un « holobionte » (Morris, 2018). En effet, le développement récent des technologies de type OMICS a permis l'identification des microorganismes présents au sein d'un microbiote, ainsi que l'élucidation d'une partie des interactions étroites qu'ils mènent avec leur hôte (Xu et al., 2021). La diversité des microorganismes (e.g., bactéries, champignons, archaea, virus, protistes) associés au système racinaire des plantes est de l'ordre de dizaines de milliers d'espèces, présentes en abondance variable, constituant un second génome chez la plante (Berendsen et al., 2012). En interagissant avec leur hôte de manière neutre, bénéfique ou néfaste, il est aujourd'hui indéniable que le microbiome du système racinaire joue un rôle fondamental dans la croissance et le développement de la plante, ainsi que son adaptation aux contraintes environnementales (Philippot et al., 2013; Kumar and Dubey, 2020). Comme nous l'avons vu dans l'introduction, la viticulture est un secteur économique et culturel majeur, en France et dans le monde, soumis à différentes problématiques pour assurer sa pérennité, tels que l'adaptation au changement climatique, à l'agriculture durable et aux nouvelles attentes des consommateurs (Bucur and Dejeu, 2022; Cataldo et al., 2021; Noceto et al., 2021). De nombreux auteurs ont récemment proposé que l'adaptation de la viticulture à ces problématiques actuelles pourrait reposer sur l'utilisation des microorganismes du sol et du système racinaire, présentant des propriétés bénéfiques pour la plante, tels que les PGPR ou les CMA (Bettenfeld et al., 2022; Darriaut et al., 2022; Dries et al., 2021b; Torres et al., 2018; Trouvelot et al., 2015).

Dans ce contexte, il nous paraissait fondamental de comprendre l'influence des deux génotypes du plant greffé de vigne sur la composition du microbiote du système racinaire, notamment sur l'association avec des organismes bénéfiques, ainsi que de comprendre son rôle sur le développement de la vigne, afin de fournir des connaissances applicables pour de futur programmes d'amélioration variétale ou le développement de technologies promouvant les associations symbiotiques. Des études ont déjà démontré un rôle du porte-greffe sur la diversité des communautés bactériennes et/ou

fongiques du système racinaire (Berlanas et al., 2019; Darriaut et al., 2022a; D'Amico et al., 2018; Dries et al., 2021a; Marasco et al., 2022; Vink et al., 2021a; Swift et al., 2021), quand seulement trois autres ont étudié la contribution du greffon (Marasco et al., 2022; Vink et al., 2021b; Dries et al., 2023). A notre connaissance, une seule étude publiée a démontré l'effet du porte-greffe sur la diversité des CMA dans les racines (Moukarzel et al., 2021a). Même si l'effet du génotype de porte-greffe sur la diversité des communautés microbiennes du système racinaire de la vigne semble bien accepté par la communauté scientifique, la contribution du greffon reste encore discutable. De plus, à part l'étude de Marasco et al. (2018), aucune d'entre elles ne se s'est intéressée aux rôles de ces communautés microbiennes sur l'environnement et sur la plante. Enfin, aucune de ces équipes n'a encore étudié les mécanismes impliqués dans la sélection différentielle des microorganismes du sol par les porte-greffes.

Dans le chapitre 1, nous avons comparé par des approches de cultivable, de qPCR et de métabarcoding, la quantité et/ou la diversité des communautés bactériennes, fongiques et de CMA, associées à la rhizosphère et l'endosphère racinaire de dix combinaisons porte-greffe × greffon (i.e., six porte-greffes greffés avec CS et cinq cépages greffés sur RGM), prélevés en Mai 2021 sur deux blocs (2 et 3) de la parcelle GreffAdapt. Nous avons démontré que les deux génotypes du plant greffé exercent une influence sur la composition et la structure des microorganismes du système racinaire, ainsi que leurs fonctions associées, prédites *in silico*. Nos résultats démontrent aussi une contribution du génotype de cépage sur les communautés bactériennes et fongiques, principalement sur la diversité-β. De plus, ce travail était la première étude montrant une influence du génotype du porte-greffe sur la communauté de CMA du système racinaire de la vigne avec une approche de métabarcoding, principalement observée au sein de l'endosphère racinaire. Les observations occasionnelles d'un effet du bloc ou de son interaction avec le génotype, démontrent que les paramètres physicochimiques du sol influencent les communautés microbiennes du système racinaire, mais aussi que l'influence du génotype peut être dépendante du bloc. Enfin, nous avons établi plusieurs corrélations entre la composition des microbiotes du système racinaire et le phénotype ou le statut minéral de la plante, confirmant le rôle crucial de ces communautés microbiennes sur le développement de la plante.

Dans le chapitre 2, comme un seul article avant nous a étudié l'influence du génotype de porte-greffe sur la communauté de CMA du système racinaire, nous avons décidé de réanalyser la diversité des CMA au sein de l'endosphère racinaire chez les mêmes combinaisons porte-greffe × greffon, grâce à des échantillons prélevés en octobre 2021, uniquement sur le bloc 1 de la parcelle GreffAdapt. Nos analyses de microscopies ont montré que les génotypes de porte-greffe et de greffon ne semblent pas influencer la capacité de colonisation du système racinaire par les CMA. En revanche, nous avons

confirmé que le génotype de porte-greffe influence significativement la diversité et la structure des communautés de CMA dans les racines avec deux approches de métabarcoding. Cependant, l'effet du génotype de cépage est resté faible ou inexistant. Enfin, l'observation de corrélations significatives entre le phénotype du plant et les variables mesurées pour caractériser les CMA racinaires, confirme le rôle bénéfique de ces communautés sur le développement de la plante.

Après avoir confirmé l'influence du génotype de porte-greffe sur la composition des communautés microbiennes du système racinaire pour les trois groupes de microorganismes, nous avons souhaité étudier dans le troisième chapitre par quels mécanismes moléculaires les porte-greffes induisent cette sélection. Nous avons donc réalisé une dernière campagne de prélèvement du système racinaire, chez les six porte-greffes greffés avec CS, sur les trois blocs du dispositif GreffAdapt en octobre 2022. Ici, nous avons décidé de collecter également des échantillons de sol brut à proximité des plants étudiés, afin de voir si l'influence du porte-greffe sur les communautés microbiennes peut s'étendre au-delà de la rhizosphère. Pour caractériser les communautés microbiennes des trois compartiments, nous avons alors mené les mêmes analyses que celles effectuées dans les deux chapitres précédents (qPCR, métabarcoding, microscopie). Les nouveaux résultats acquis ici ont alors permis de confirmer ceux obtenus précédemment et sont comparés entre les expérimentations dans la discussion du Chapitre 3. De plus, certains d'entre eux suggèrent que l'influence du porte-greffe ne s'arrêterait pas à la rhizosphère, mais pourrait s'étendre au-delà. Nous avons aussi analysé la diversité des bactéries dans la rhizosphère grâce à une approche de profilage physiologique des communautés microbiennes (CLPP) qui confirme les résultats de métabarcoding. De plus, la réalisation de tests d'activités d'enzymes impliquées dans les cycles biogéochimiques des nutriments de la rhizosphère, confirme une influence du génotype sur les fonctions des communautés microbiennes du système racinaire. Enfin, nous avons extrait les métabolites de tous les échantillons prélevés pour les analyser en LC-MS/MS, afin de comparer entre les différents génotypes de porte-greffe, le métabolome des différents compartiments avec leur profil taxonomique. Les résultats d'analyses ne nous ont malheureusement pas encore été restitués par la plateforme MetaboHub. Cependant, l'intégration des données de métabarcoding et de métabolomique sera discutée dans la partie suivante.

II- Continuer et améliorer le décryptage des interactions de la vigne avec son microbiome racinaire

a) Le couplage des approches de métabarcoding et de métabolomique pour comprendre l'influence du porte-greffe sur le microbiome du sol

Les plantes influencent la composition des microbiotes rhizosphérique et racinaire grâce à l'exsudation de composés dans la rhizosphère, qui vont jouer le rôle d'élément nutritif pour les microorganismes, attirer des organismes bénéfiques ou non, ainsi que lutter contre les agents pathogènes (Philippot et al., 2013; Haichar et al., 2014). De plus, les microorganismes du système racinaire interagissent aussi entre eux par le biais de molécules signal tels que l'acyl-homosérine pour le quorom sensing (QS), ainsi que la production de composés antimicrobiens lors de la compétition pour l'accès au nutriments ou à une niche écologique (Compant et al., 2013; Jamil et al., 2022). Chez la vigne, des études réalisées *in vitro* ont déjà démontré que la composition et la quantité des composés présents dans les exsudats racinaires pouvaient varier entre différents génotypes de porte-greffe, tels que les acides organiques (Cançado et al., 2009), les acides aminés (Marastoni et al., 2020) ou les strigolactones (Lailheugue et al., 2023). Nous avons donc émis l'hypothèse que les différences de composition des microbiotes rhizosphérique et racinaire entre les six génotypes de porte-greffe, pourraient s'expliquer en partie par des variations dans la composition de leurs exsudats racinaires.

De récentes études menées chez d'autres modèles végétaux ont couplé des analyses de métabarcoding et de métabolomique pour comprendre, par exemple, le rôle du sol ou d'une communauté microbienne sur la promotion de la croissance de la plante (Duan et al., 2022a; Duan et al., 2022b), l'effet d'une plante parasite sur la composition taxonomique de sa rhizosphère (Clerissi et al., 2023) ou encore celui de cultures d'inter-rang sur la composition et les activités enzymatiques du microbiote du sol (Duan et al., 2023). Pour rechercher des corrélations entre la composition des microorganismes et le métabolome, ces études utilisent des outils tels que SmartPLS4 pour réaliser des approches de type PLS-PM (Partial Least Squares Path Model) ou OmicShare Tools pour conduire des analyses de corrélation canonique (CCA). Une autre étude a utilisé la combinaison des deux méthodes de type Omics pour examiner les performances d'espèces bactériennes du genre *Trichoderma* en tant que biostimulant chez *A. thaliana*, soumises à la sécheresse et/ou la chaleur, ainsi que leur impact sur le microbiote de la plante (Senizza et al., 2023). Les auteurs ont corrélé le métabolome des racines avec la composition bactérienne de la rhizosphère, à l'aide de l'outil DIABLO

(Data Integration Analysis for Biomarker discovery using Latent variable approaches for Omics studies), disponible dans le package de R « mixOmics » (Rohart et al., 2017). Cette approche supervisée a permis l'analyse intégrée des deux jeux de données de type Omics et l'identification des caractéristiques discriminantes qui déterminent les différences entre les groupes de traitement.

Dans notre dernière expérimentation, nous avons conduit le même type d'approche couplant le métabarcoding et la métabolomique, pour tenter de relier la composition taxonomique (bactéries, champignons et CMA) des échantillons de sol brut, de rizosphère et de racines, avec leurs métabolomes. Cela permettrait d'identifier quelles familles de métabolites sont impliquées dans la sélection différentielle des microorganismes du sol par les génotypes de porte-greffe. Nous avons donc caractérisé le métabolome des trois compartiments étudiés chez les six porte-greffes sélectionnés dans la thèse, grâce à une approche de LC-MS/MS non ciblée. Après réception des données, elles seront traitées grâce au logiciel MetaboAnalyst, disponible en ligne (https://www.metaboanalyst.ca). Nous devrions observer des métabolomes différents entre les différents compartiments étudiés. Même si nous nous attendons à retrouver une partie commune des métabolites entre tous les porte-greffes en termes de qualité et de quantité, nous espérons en identifier une autre différentiellement produite en fonction des génotypes, principalement dans la rhizosphère et l'endosphère racinaire. Enfin, nous espérons établir des corrélations entre certains métabolites et les différents taxons microbiens associés aux différents compartiments du système racinaire de la vigne, grâce à l'outil DIABLO.

b) Relier la composition du microbiome du système racinaire au développement de la plante

En parcelle viticole, la vigne constitut un véritable biotope qui héberge plusieurs centaines de taxons, dont seulement quelques dizaines ont des rôles et des modes d'action connus (Fournier et al., 2022). L'étude des microorganismes du sol et du système racinaire de la vigne, en particulier des champignons et des bactéries, est un domaine scientifique prometteur pour améliorer l'adaptation de la vigne au changement climatique et la prévention des maladies liées aux infections par des agents pathogènes (Darriaut et al., 2022b). À ma connaissance, il existe deux grandes voies pour étudier le rôle de ces microorganismes sur la croissance et le développement de la plante à partir de données de métabarcoding.

Bien que les données de métabarcoding soient principalement dédiées à la caractérisation taxonomique, elles peuvent être utilisées pour se faire une idée du potentiel fonctionnel d'un microbiome grâce à la prédiction des fonctions microbiennes *in silico*. Lors de nos différentes expérimentations, nous avons utilisé l'outil PICRUSt2 pour prédire les fonctions des bactéries (Douglas et al., 2020). Ce dernier intègre des outils open-source existants pour prédire les génomes à partir des séquences du gène de l'ARNr 16S. Les OTUs sont placées dans un arbre de référence, qui sera utilisé pour prédire les fonctions ou les voies métaboliques, à partir de base de données publiques de génomes annotés. Pour l'étude des champignons, nous avons utilisé l'outil FUNGuild (Nguyen et al., 2016). Ce dernier permet de prédire le régime trophique ou la guilde de différents taxons fongiques, indépendamment de la plateforme de séquençage ou du pipeline d'analyse. Il fonctionne simplement en entrant le genre ou l'espèce fongique sur sa base de données. Nous sommes satisfaits des résultats obtenus avec PICRUSt2 pour la prédiction des voies métaboliques des bactéries. En revanche, nous n'avons pu prédire les fonctions des champignons que pour seulement 30% des OTUs lors de nos expérimentations. Même si cet outil semble prometteur, il est nécessaire de l'améliorer en implémentant sa base de données, notamment pour les microorganismes du sol. Cependant, il existe d'autres outils qui mériteraient d'être testés pour améliorer la prédiction des fonctions des microorganismes identifiés dans nos études. Il existe par exemple EsMeCaTa, un package codé en python, permettant de prédire le protéome des microorganismes en s'appuyant sur la base de donnée UniProt (Belcour et al., 2022). Dans l'étude de Marasco et al. (2018), les auteurs ont prédit et comparé *in silico* les traits PGPR des bactéries identifiées dans le système racinaire de différents porte-greffes, à partir des données de l'ARNr 16S grâce au package R Tax4Fun (Aßhauer et al., 2015). Dans notre contexte, il serait intéressant de mener la même analyse, avec la nouvelle version Tax4Fun2 (Wemheuer et al., 2020) ou PICRUSt2 (Manter et al., 2023). Enfin, pour améliorer la résolution des fonctions des champignons, il serait intéressant de coupler les informations obtenues par FUNGuild avec celle d'une autre base de données telle que FUN^{Fun} (Zanne et al., 2020).

La seconde approche est de relier statistiquement la composition du microbiote à des traits écophysiologiques de la vigne représentatifs de sa tolérance à divers stress d'origine abiotique tels que la sécheresse (Gambetta et al., 2020) ou les fortes températures (Merrill et al., 2020), à la fréquence et à l'intensité des maladies au niveau de la plante (Rolshausen et al., 2010) ou de la parcelle (Darriaut et al., 2023), ou encore à des variables agronomiques tels que la qualité ou le rendement des baies (Popescu and Popescu, 2018). Dans chacune des expérimentations réalisées pendant la thèse, nous avons essayé de comprendre le rôle des microorganismes du système sur le développement de la plante en cherchant des corrélations entre les variables mesurées pour caractériser le microbiome, avec le

phénotype et la nutrition minérale de la plante. Cependant, comme cela a été rapporté par Fournier et al. (2022), d'autres outils statistiques plus puissants peuvent être utilisés sur les données de métabarcoding, afin d'évaluer la contribution de la composition du microbiome sur la variation d'un trait fonctionnel, et ainsi d'identifier les propriétés du microbiome qui ont un pouvoir explicatif. Ces propriétés explicatives peuvent être de différentes natures, telles que la présence ou l'abondance de taxons / groupes fonctionnels. Elles peuvent aussi correspondre à des propriétés agrégées au niveau de la communauté ou du réseau, telles que les indices de diversité-α, ou de diversité-β après conversion de la matrice de dissimilarité en vecteurs explicatifs, grâce à la méthode des vecteurs propres PCNM (principal coordinates of neighbor matrices). Il est alors possible de créer un modèle contenant le trait fonctionnel d'intérêt comme variable dépendante, ainsi que les propriétés du microbiome et les facteurs environnementaux comme variables explicatives (Fournier et al., 2022). Lorsque le microbiome contribue de manière significative au trait fonctionnel étudié (e.g., rendement, vigueur, $\delta^{13}C$), il est possible d'identifier quel sont les principaux taxons microbiens impliqués grâce à différentes méthodes telles que celle du package R TITAN2 (Baker et al., 2015), les analyses différentielles de l'abondance des taxons (Nearing et al., 2022), ou encore d'autres basées sur l'intelligence artificielle en utilisant par exemple l'algorithme Random Forest (Smucker et al., 2020).

Pour confirmer les fonctions putatives du microbiome obtenues avec ces deux types d'approches, il est possible de les vérifier avec des méthodes d'isolation et de culture des microorganismes du système racinaire (Basu et al., 2015). Après identification de l'espèce par une approche de séquençage ou d'analyse au MALDI-TOF MS (Darriaut et al., 2022a), il est alors possible de tester expérimentalement leurs activités PGP-R/F (Karagöz et al., 2012), ou d'étudier leurs impact sur la plante après inoculation en condition contrôlées (Sabir et al., 2012) ou en parcelle (Nogales et al., 2021).

c) Proposition d'une approche intégrative pour l'étude du microbiome de la vigne

En prenant du recul sur ma thèse, le principal reproche visible sur ces travaux est le fait de ne pas pouvoir étudier dans le même modèle l'intégralité des résultats acquis au cours des trois expérimentations. Cela s'explique par les différentes stratégies de métabarcoding utilisées pour étudier la composition taxonomique des microorganismes, telles que le choix du gène cible pour l'étude des CMA (ARNr 18S ou 28S), ou l'utilisation de PNA clamp pour limiter l'amplification de l'ARNr 16S des organites des cellules végétales de l'hôte. Les expérimentations diffèrent aussi par le choix des

compartiments (endosphère racinaire, rhizosphère, sol brut) et des blocs du dispositif étudiés, de la méthode de collection de la rhizosphère, ainsi que des dates des prélèvements. Dans un monde utopique ou le temps et les ressources ne compteraient pas, cette partie présente une proposition d'expérimentation pour une étude plus robuste et intégrative de l'effet de la combinaison porte-greffe × greffon de vigne sur le microbiome du système racinaire.

Avec ces 275 combinaisons, réparties simultanément sur trois blocs, au nombre de cinq réplicas biologiques par combinaison, le dispositif GreffAdapt, dont le suivi phénotypique annuel est réalisé chaque année, représente une parcelle de choix dans l'étude de l'influence exercée par les deux génotypes du plant greffé sur le microbiome du système racinaire de la vigne (Marguerit et al., 2019). En plus d'étudier séparément les effets des génotypes de porte-greffe et de greffon, certaines études prennent en compte l'effet de l'interaction des deux génotypes (Marasco et al., 2022; Vink et al., 2021). L'objectif serait de faire la même chose ici en prélevant le sol brut, la rhizosphère et l'endosphère racinaire, chez 25 combinaisons porte-greffe × greffon, c'est-à-dire cinq porte-greffes présentant des caractéristiques agronomiques différentes, chacun greffés avec les 5 cépages du dispositif. Comme nous avons observé des effets du blocs, ainsi qu'une forte variabilité biologique entre certains échantillons de la même modalité, il faudrait donc prélever les 5 réplicas biologiques sur chacun des blocs pour toutes les combinaisons, soit 375 plants.

En effectuant un suivi du nombre et de la longueur des racines chez le porte-greffe 99R greffé avec le cépage Colombar, une étude réalisée dans l'hémisphère Sud montre deux grandes phases de croissance du système racinaire (Van Zyl, 1984). La première débute quelques jours après le débourrement et se termine à la floraison, quand la seconde s'effectue pendant la phase de maturation du raisin jusqu'aux vendanges. Ces phases de croissance correspondent à des besoins minéraux importants pour la plante, permettant le développement de la partie végétative, puis la mise en place de réserves avant la période de repos hivernal. Il serait donc pertinent d'effectuer deux prélèvements au cours de la même année, lorsque la surface d'exploration du sol par le système racinaire est maximale. Pour améliorer la robustesse des résultats, il faudrait conduire ces campagnes de prélèvement au cours de deux années successives, comme cela a été réalisé dans plusieurs études (Berlanas et al., 2019; Darriaut et al., 2022b). Les échantillons seraient collectés de la même manière que celle utilisée dans le Chapitre 3.

Pour étudier la composition des bactéries, des champignons et des CMA, au sein des trois compartiments, nous réutiliserions les mêmes méthodes de métabarcoding que celles du Chapitre 3,

basées sur l'amplification du gène de l'ARNr 16S des bactéries (Marasco et al., 2022), des séquences ITS des champignons (Darriaut et al., 2022a) et du gène de l'ARNr 18S des CMA (Suzuki et al., 2020). Comme le métabarcoding devrait être progressivement remplacé par la métagénomique de type "Shotgun" dans les années à venir, il serait envisageable de compléter les résultats obtenus avec cette nouvelle approche. En séquençant l'intégralité de l'ADN présent dans les échantillons, cette technique fournit la composition en gènes fonctionnels des communautés microbiennes et constituent donc une analyse beaucoup plus large que les études phylogénétiques réalisées à l'aide des méthodes de métabarcoding (Azevedo-Silva et al., 2021). De plus, cette approche est également indépendante de la communauté, ce qui signifie qu'avec le même protocole, elle permet d'analyser différents groupes d'organismes tels que les bactéries, les archées, les virus, les phages, les plasmides, les levures, les champignons, les procaryotes, les algues, les plantes et les autres eucaryotes. Cela permettrait d'étudier l'influence de la combinaison porte-greffe × greffon de vigne sur l'ensemble des communautés du système racinaire, et fournirait des informations plus qualitatives pour l'étude de leurs fonctions que celles prédites *in silico* avec des outils tels que PICRUSt2 et FUNGuild.

Dans cette expérimentation, nous conserverions l'analyse non ciblée du métabolome des différents compartiments du système racinaire, afin de relier la composition des métabolites au profil taxonomique des communautés microbiennes (Senizza et al., 2023). Si des différences significatives sont observées entre les différentes combinaisons pour certains composés putatifs, notamment connus dans le recrutement de microorganismes du sol ou la lutte contre les agents pathogènes, il serait intéressant de confirmer les résultats par une approche de métabolomique ciblée. Par exemple, nous pourrions quantifier les phytoalexines ou certains stilbènes impliqués dans la défense de la plante (Haichar et al., 2014), ou les flavonoïdes impliqués dans la mise en place d'endosymbioses avec les bactéries des taxons *Rhizobium* ou des actinomycètes, ainsi que les CMA (Abdel-Lateif et al., 2012). Dans une étude précédente nous avons concentré et purifié deux formes de strigolactones (vitislactone et héliolactone) à partir d'exsudats racinaires de plants de RGM cultivés en condition de carence azotée (Lailheugue et al., 2023). Comme cette hormone est impliquée dans la mise en place de la symbiose mycorhizienne (Yoneyama et al., 2018), il pourrait donc être judicieux d'en utiliser une partie dans la préparation des standards pour une approche de LC-MS/MS en mode ciblé.

La métatranscriptomique a été appliquée à de nombreuses études récentes sur les interactions entre les plantes et les micro-organismes. En effet, elle permet de caractériser les membres d'un microbiome responsables de fonctions spécifiques et d'élucider les gènes qui déterminent la relation entre le microbiome et son hôte (Shakya et al., 2019). Ce type d'approche est basée sur l'extraction et

le séquençage de tous les ARN d'un échantillons (RNA seq), après une étape de rétrotranscription (Carvalhais et al., 2012). Comme la superposition de différentes méthodes de Omics est coûteuse, il est envisageable de mesurer l'expression de gènes d'intérêts par RT-qPCR. On pourrait par exemple mesurer l'expression de gènes de la plante impliqués dans les voies de biosynthèses hormonales (Cochetel et al., 2018; Li et al., 2022), le prélèvement et le transport des nutriments (Vannozzi et al., 2017), la mise en place de symbiose avec les microorganismes du sol (Duret et al., 2022), ou les réponses de défense de la plante contre les agents pathogènes (Dubreuil-Maurizi et al., 2010). Le recours à des techniques de qPCR à haut débit représente ici une bonne alternative au RNAseq. Dufour et al. (2016) ont par exemple développé une puce (NeoViGen96) permettant le profilage de l'expression de 85 gènes liés aux mécanismes de défense de la vigne. Il est aussi intéressant de mesurer l'expression de gènes microbiens impliqués dans les cycles des nutriments et des minéraux (Trevors, 2010), ainsi que dans la mise en place d'associations bénéfiques ou néfastes avec la plante hôte (Balestrini and Lanfranco, 2006; Belair et al., 2022).

Dans cette expérimentation fictive, nous pourrions finir par ajouter toutes les méthodologies utilisées pendant la thèse pour caractériser le microbiome du système racinaire, telles que la qPCR pour la quantification des grandes communautés microbiennes (Darriaut et al., 2021), la microscopie pour évaluer la capacité de colonisation des racines par les CMA (Trouvelot et al., 1986), le profilage physiologique des communautés microbiennes (Nerva et al., 2022) ou encore les tests d'activités d'enzymes microbiennes du sol (Acosta-Martinez and Tabatabai, 2000). Le recours à la protéomique permettrait aussi d'améliorer l'étude intégrative des interactions entre la plante et les microorganismes du sol (Kumar and Dubey, 2020). En vue du faible nombre de publications sur le sujet, il serait très novateur d'étudier le rôle du microbiome sur l'épigénome de la plante (Chen et al., 2022).

Les données collectées avec les différentes méthodes d'analyse du microbiome du système racinaire pourraient être corrélées entre elles, ainsi qu'avec le phénotype de la plante, grâce aux outils de bio-informatiques présentés précédemment (Fournier et al., 2022; Rohart et al., 2017). Conscient du travail et de l'expertise nécessaires pour mener à bien un tel projet, il est nécessaire de réaliser cette étude intégrative en équipe, avec des chercheurs de différents profils tels que des biologistes microbiens et végétaux, des écologistes, des informaticiens, et des statisticiens (Xu et al., 2021). Enfin, cette expérimentation serait aussi l'occasion d'isoler des microorganismes du sol et du système racinaire afin de construire une collection, pouvant être utilisée pour des projets d'étude futur, tels que la recherche de caractéristiques bénéfiques pour la plante (Zhao et al., 2016).

III- Conclusion et perspectives

Ces travaux démontrent grâce à différentes approches que les deux génotypes du plant greffé de vigne exercent une influence sur la composition des microorganismes du système racinaire en parcelle viticole. Comme nous l'avons vu au cours des trois études présentées, cette sélection exercée par les génotypes de porte-greffe et de cépage impacte les fonctions du microbiome racinaire, et par conséquent le développement et l'adaptation de la plante hôte aux contraintes environnementales. Ces résultats laissent entrevoir qu'un levier d'adaptation de la filière viticole aux problématiques actuelles pourrait se baser sur l'identification de génotypes de porte-greffe ou de cépages, promouvant la mise en place d'associations symbiotiques avec des organismes bénéfiques, ou à l'inverse, naturellement tolérants à certains agents pathogènes du sol. Cependant, d'autres recherches sont nécessaires avant d'établir quelles combinaisons de porte-greffe × greffon interagiront le mieux avec les communautés microbiennes du sol. Ce travail sera d'autant plus compliqué car beaucoup d'autres facteurs environnementaux influencent les communautés du sol et du système racinaire de la vigne. Il faudra donc établir plusieurs études similaires aux nôtres, dans une multitude d'environnements différents, afin d'identifier plusieurs combinaisons adaptables selon l'appellation ou elles sont plantées. Dans ce but, les données de plusieurs études peuvent être réutilisées pour des métanalyses, soulevant le besoin de protocoles communs entre les différentes équipes de recherche.

Il est maintenant nécessaire de comprendre par quels mécanismes les deux composants du plant recrutent différentiellement les communautés microbiennes du sol. Le récent développement des méthodes de type Omics, ainsi que leur démocratisation, présentent des perspectives prometteuses dans la compréhension de ces processus. D'ici la soutenance, j'espère réussir à traiter les données de LC-MS/MS, afin de mettre en évidence des différences dans la composition des métabolites présents au sein des différents compartiments du système racinaire entre les génotypes de porte-greffe. Cela permettrait de fournir des éléments pour discuter des mécanismes moléculaires impliqués dans la sélection des microorganismes du sol. Cependant, je ne pense pas réussir d'ici là à intégrer dans la même analyse les données de métabarcoding et de métabolomique. Enfin, il aurait été intéressant de mener d'autres analyses de transcriptomique ou de protéomique, afin d'améliorer la compréhension des mécanismes impliqués dans le recrutement des microorganismes du sol, ainsi que les fonctions de ces communautés microbiennes sur le développement du plant. La compréhension de ces processus pourrait permettre la création de nouveaux porte-greffes favorisant les interactions bénéfiques avec les microorganismes du sol, au détriment des interactions néfastes, ainsi que le développement de nouvelles biomolécules à utiliser en parcelle pour induire la mise en place d'un microbiome bénéfique.

Discussion de la thèse

Dans ce manuscrit de thèse, nous avons choisi de présenter uniquement les expérimentations réalisées en parcelle viticole. Cependant, nous avons réalisé deux autres expérimentations en conditions contrôlées, afin de caractériser la réponse de différents génotypes de porte-greffes à la nutrition azotée, au niveau de leurs exsudats racinaires. Dans la première expérience, nous avons caractérisé la structure de deux composés appartenant à la famille des strigolactones, présents dans les exsudats racinaires de RGM, cultivé en condition de carence azotée. Ces composés correspondent à une forme connue des strigolactones, appelée héliolactone. En revanche, la seconde forme n'avait encore été jamais décrite, nous l'avons donc baptisé « vitislactone ». Nous avons ensuite comparé par LC-MS/MS la quantité des strigolactones dans les exsudats racinaires de RGM et 1103P, soumis ou non, à la carence azotée. Les résultats montrent que l'application de ce stress nutritif induit l'exsudation de la vitislactone par les racines des deux génotypes. Cependant, le composé de type héliolactone ne fût détecté que dans les exsudats racinaires de RGM, suggérant que les deux génotypes répondent différemment à la carence azotée. Ces résultats ont déjà été publiés dans la revue Phytochemistry en 2023, et sont présentés à la fin du manuscrit. Dans une autre expérience, nous avons étudié la réponse à la carence azotée des six génotypes de porte-greffes étudiés pendant la thèse. Les plants ont été cultivés en condition hydroponique dans une solution contenant tous les nutriments nécessaires à la croissance des plantes, pendant une semaine. Ensuite, la moitié des plants a été transférée dans une solution sans azote, tandis que l'autre moitié est resté dans la même solution. Au bout de sept jours, nous avons fait exsuder les plants des différentes modalités dans de l'eau pendant 24h. Nous avons ensuite caractérisé la composition du métabolome des exsudats et des racines par LC-MS/MS, en mode non ciblée. Les résultats montrent que la nutrition azotée, ainsi que le génotype de porte-greffe influencent significativement la composition des métabolites des racines et leurs exsudats. Cependant, il reste encore beaucoup de travail pour rendre ces travaux publiables. Ensemble, ces deux expérimentations suggèrent que les génotypes de porte-greffe exsudent différents composés par les racines. Cela pourrait expliquer une partie des différences observées en parcelle dans la composition des microorganismes du système racinaire. Il est donc crucial de coupler des expérimentations en parcelle et en conditions contrôlées, afin d'améliorer la compréhension des processus par lesquels les porte-greffes influencent la composition des microorganismes du système racinaire.

Bibliographie

Abdel-Lateif, K., Bogusz, D., Hocher, V., 2012. The role of flavonoids in the establishment of plant roots endosymbioses with arbuscular mycorrhiza fungi, rhizobia and Frankia bacteria. Plant Signal. Behav. 7, 636–641. https://doi.org/10.4161/psb.20039

Acosta-Martinez, V., Tabatabai, M.A., 2000. Arylamidase Activity of Soils. SOIL SCI SOC AM J 64, 7.

Aguilera, P., Ortiz, N., Becerra, N., Turrini, A., Gaínza-Cortés, F., Silva-Flores, P., Aguilar-Paredes, A., Romero, J.K., Jorquera-Fontena, E., Mora, M.D.L.L., Borie, F., 2022. Application of Arbuscular Mycorrhizal Fungi in Vineyards: Water and Biotic Stress Under a Climate Change Scenario: New Challenge for Chilean Grapevine Crop. Front. Microbiol. 13, 826571. https://doi.org/10.3389/fmicb.2022.826571

Akiyama, K., Ogasawara, S., Ito, S., Hayashi, H., 2010. Structural Requirements of Strigolactones for Hyphal Branching in AM Fungi. Plant Cell Physiol. 51, 1104–1117. https://doi.org/10.1093/pcp/pcq058

Almeida, R.P.P., Daane, K.M., Bell, V.A., Blaisdell, G.K., Cooper, M.L., Herrbach, E., Pietersen, G., 2013. Ecology and management of grapevine leafroll disease. Front. Microbiol. 4. https://doi.org/10.3389/fmicb.2013.00094

Alonso González, P., Parga-Dans, E., 2020. Natural wine: do consumers know what it is, and how natural it really is? J. Clean. Prod. 251, 119635. https://doi.org/10.1016/j.jclepro.2019.119635

Álvarez-Pérez, J.M., González-García, S., Cobos, R., Olego, M.Á., Ibañez, A., Díez-Galán, A., Garzón-Jimeno, E., Coque, J.J.R., 2017. Use of Endophytic and Rhizosphere Actinobacteria from Grapevine Plants To Reduce Nursery Fungal Graft Infections That Lead to Young Grapevine Decline. Appl. Environ. Microbiol. 83, e01564-17. https://doi.org/10.1128/AEM.01564-17

Andrews, S., 2010. FastQC: a quality control tool for high throughput sequence data. Available Httpwwwbioinformaticsbabrahamacukprojectsfastqc.

Armijo, G., Schlechter, R., Agurto, M., Muñoz, D., Nuñez, C., Arce-Johnson, P., 2016. Grapevine Pathogenic Microorganisms: Understanding Infection Strategies and Host Response Scenarios. Front. Plant Sci. 7. https://doi.org/10.3389/fpls.2016.00382

Aßhauer, K.P., Wemheuer, B., Daniel, R., Meinicke, P., 2015. Tax4Fun: predicting functional profiles from metagenomic 16S rRNA data: Fig. 1. Bioinformatics 31, 2882–2884. https://doi.org/10.1093/bioinformatics/btv287

Azevedo-Silva, D., Rasmussen, J.A., Carneiro, M., Gilbert, M.T.P., Azevedo, H., 2021. Feasibility of applying shotgun metagenomic analyses to grapevine leaf, rhizosphere and soil microbiome characterisation. Aust. J. Grape Wine Res. 27, 519–526. https://doi.org/10.1111/ajgw.12508

Baldi, E., Miotto, A., Ceretta, C.A., Quartieri, M., Sorrenti, G., Brunetto, G., Toselli, M., 2018. Soil-applied phosphorous is an effective tool to mitigate the toxicity of copper excess on grapevine grown in rhizobox. Sci. Hortic. 227, 102–111. https://doi.org/10.1016/j.scienta.2017.09.010

Balestrini, R., Lanfranco, L., 2006. Fungal and plant gene expression in arbuscular mycorrhizal symbiosis. Mycorrhiza 16, 509–524. https://doi.org/10.1007/s00572-006-0069-2

Bazoche P., Deola C. and Soler L.G., 2008. An experimental study of wine consumers' willingness to pay for environmental characteristics.

Belair, M., Grau, A.L., Chong, J., Tian, X., Luo, J., Guan, X., Pensec, F., 2022. Pathogenicity Factors of Botryosphaeriaceae Associated with Grapevine Trunk Diseases: New Developments on Their Action on Grapevine Defense Responses. Pathogens 11, 951. https://doi.org/10.3390/pathogens11080951

Belcour, A., Ruiz, B., Frioux, C., Blanquart, S., Siegel, A., n.d. EsMeCaTa: Estimating metabolic capabilities from taxonomic affiliations.

Bibliographie

Belda, I., Zarraonaindia, I., Perisin, M., Palacios, A., Acedo, A., 2017. From Vineyard Soil to Wine Fermentation: Microbiome Approximations to Explain the "terroir" Concept. Front. Microbiol. 8, 821. https://doi.org/10.3389/fmicb.2017.00821

Berendsen, R.L., Pieterse, C.M.J., Bakker, P.A.H.M., 2012. The rhizosphere microbiome and plant health. Trends Plant Sci. 17, 478–486. https://doi.org/10.1016/j.tplants.2012.04.001

Berg, G., Rybakova, D., Fischer, D., Cernava, T., Vergès, M.-C.C., Charles, T., Chen, X., Cocolin, L., Eversole, K., Corral, G.H., Kazou, M., Kinkel, L., Lange, L., Lima, N., Loy, A., Macklin, J.A., Maguin, E., Mauchline, T., McClure, R., Mitter, B., Ryan, M., Sarand, I., Smidt, H., Schelkle, B., Roume, H., Kiran, G.S., Selvin, J., Souza, R.S.C.D., Van Overbeek, L., Singh, B.K., Wagner, M., Walsh, A., Sessitsch, A., Schloter, M., 2020. Microbiome definition re-visited: old concepts and new challenges. Microbiome 8, 103. https://doi.org/10.1186/s40168-020-00875-0

Berger, M.M.J., Lailheugue, V., Zhelyazova, G., Stammitti, L., Lauvergeat, V., Barrieu, F., Gallusci, P., 2022. One prep to catch them all: "2 in 1", an efficient method for the simultaneous extraction of DNA and RNA from Grapevine tissues. OENO One 56, 1–13. https://doi.org/10.20870/oeno-one.2022.56.2.5000

Berlanas, C., Berbegal, M., Elena, G., Laidani, M., Cibriain, J.F., Sagües, A., Gramaje, D., 2019. The Fungal and Bacterial Rhizosphere Microbiome Associated With Grapevine Rootstock Genotypes in Mature and Young Vineyards. Front. Microbiol. 10, 1142. https://doi.org/10.3389/fmicb.2019.01142

Bernard, M., Rué, O., Mariadassou, M., Pascal, G., 2021. FROGS: a powerful tool to analyse the diversity of fungi with special management of internal transcribed spacers. Brief. Bioinform. 22, bbab318. https://doi.org/10.1093/bib/bbab318

Besserer, A., Puech-Pagès, V., Kiefer, P., Gomez-Roldan, V., Jauneau, A., Roy, S., Portais, J.-C., Roux, C., Bécard, G., Séjalon-Delmas, N., 2006. Strigolactones Stimulate Arbuscular Mycorrhizal Fungi by Activating Mitochondria. PLoS Biol. 4, e226. https://doi.org/10.1371/journal.pbio.0040226

Bettenfeld, P., Cadena I Canals, J., Jacquens, L., Fernandez, O., Fontaine, F., Van Schaik, E., Courty, P.-E., Trouvelot, S., 2022. The microbiota of the grapevine holobiont: A key component of plant health. J. Adv. Res. 40, 1–15. https://doi.org/10.1016/j.jare.2021.12.008

Biasi, R., Brunori, E., Ferrara, C., Salvati, L., 2019. Assessing Impacts of Climate Change on Phenology and Quality Traits of Vitis vinifera L.: The Contribution of Local Knowledge. Plants 8, 121. https://doi.org/10.3390/plants8050121

Binet, M.-N., van Tuinen, D., Souard, F., Sage, L., Périgon, S., Gallet, C., Legay, N., Lavorel, S., Mouhamadou, B., 2017. Responses of above- and below-ground fungal symbionts to cessation of mowing in subalpine grassland. Fungal Ecol. 25, 14–21. https://doi.org/10.1016/j.funeco.2016.10.001

Blanco-Pérez, R., Sáenz-Romo, M.G., Vicente-Díez, I., Ibáñez-Pascual, S., Martínez-Villar, E., Marco-Mancebón, V.S., Pérez-Moreno, I., Campos-Herrera, R., 2020. Impact of vineyard ground cover management on the occurrence and activity of entomopathogenic nematodes and associated soil organisms. Agric. Ecosyst. Environ. 301, 107028. https://doi.org/10.1016/j.agee.2020.107028

Bodenhausen, N., 2021. Relative qPCR to quantify colonization of plant roots by arbuscular mycorrhizal fungi 12.

Boso, S., Alonso-Villaverde, V., Santiago, J.L., Gago, P., Dürrenberger, M., Düggelin, M., Kassemeyer, H.H., Martinez, M.C., 2010. Macro- and microscopic leaf characteristics of six grapevine genotypes (Vitis spp.) with different susceptibilities to grapevine downy mildew.

Bouffaud, M.-L., Bernaud, E., Colombet, A., Van Tuinen, D., Wipf, D., Redecker, D., 2016. Regional-scale analysis of arbuscular mycorrhizal fungi: the case of Burgundy vineyards. OENO One 50, 1. https://doi.org/10.20870/oeno-one.2016.50.1.49

Bruez, E., Haidar, R., Alou, M.T., Vallance, J., Bertsch, C., Mazet, F., Fermaud, M., Deschamps, A., Guerin-Dubrana, L., Compant, S., Rey, P., 2015. Bacteria in a wood fungal disease: characterization of bacterial communities in wood tissues of esca-foliar symptomatic and asymptomatic grapevines. Front. Microbiol. 6. https://doi.org/10.3389/fmicb.2015.01137

Brunetto, G., Marques, A.C.R., Trentin, E., Sete, P.B., Soares, C.R.F.S., Ferreira, P.A.A., De Melo, G.W.B., Zalamena, J., Da Silva, L.O.S., Marchezan, C., Da Silva, I.C.B., Dos Santos, J.P.J., Morsch, L., 2023. Arbuscular mycorrhizal fungi

inoculation as strategy to mitigate copper toxicity in young field-grown vines. Ciênc. E Téc. Vitivinícola 38, 60–66. https://doi.org/10.1051/ctv/ctv20233801060

Bucur, G.M., Dejeu, L., 2022. Research on Adaptation Measures of Viticulture to Climate Change: Overview. Sci. Pap. Ser. B Hortic. 66, 177–190. https://horticulturejournal.usamv.ro/pdf/2022/issue_2/Art22.pdf

Bukin, Yu.S., Galachyants, Yu.P., Morozov, I.V., Bukin, S.V., Zakharenko, A.S., Zemskaya, T.I., 2019. The effect of 16S rRNA region choice on bacterial community metabarcoding results. Sci. Data 6, 190007. https://doi.org/10.1038/sdata.2019.7

Caldwell, B.A., 2005. Enzyme activities as a component of soil biodiversity: A review. Pedobiologia 49, 637–644. https://doi.org/10.1016/j.pedobi.2005.06.003

Cameron, D.D., Neal, A.L., Van Wees, S.C.M., Ton, J., 2013. Mycorrhiza-induced resistance: more than the sum of its parts? Trends Plant Sci. 18, 539–545. https://doi.org/10.1016/j.tplants.2013.06.004

Cançado, G.M.A., Ribeiro, A.P., Piñeros, M.A., Miyata, L.Y., Alvarenga, Â.A., Villa, F., Pasqual, M., n.d. Evaluation of aluminium tolerance in grapevine rootstocks.

Cao, Y., Dong, Q., Wang, D., Zhang, P., Liu, Y., Niu, C., 2022. microbiomeMarker: an R/Bioconductor package for microbiome marker identification and visualization. Bioinformatics 38, 4027–4029. https://doi.org/10.1093/bioinformatics/btac438

Carvalhais, L.C., Dennis, P.G., Tyson, G.W., Schenk, P.M., 2012. Application of metatranscriptomics to soil environments. J. Microbiol. Methods 91, 246–251. https://doi.org/10.1016/j.mimet.2012.08.011

Carvalho, L.C., Coito, J.L., Gonçalves, E.F., Chaves, M.M., Amâncio, S., 2016. Differential physiological response of the grapevine varieties Touriga Nacional and Trincadeira to combined heat, drought and light stresses. Plant Biol. 18, 101–111. https://doi.org/10.1111/plb.12410

Cataldo, E., Eichmeier, A., Mattii, G.B., 2023. Effects of Global Warming on Grapevine Berries Phenolic Compounds—A Review.

Cataldo, E., Fucile, M., Mattii, G.B., 2021. A Review: Soil Management, Sustainable Strategies and Approaches to Improve the Quality of Modern Viticulture. Agronomy 11, 2359. https://doi.org/10.3390/agronomy11112359

Challacombe, J.F., Hesse, C.N., Bramer, L.M., McCue, L.A., Lipton, M., Purvine, S., Nicora, C., Gallegos-Graves, L.V., Porras-Alfaro, A., Kuske, C.R., 2019. Genomes and secretomes of Ascomycota fungi reveal diverse functions in plant biomass decomposition and pathogenesis. BMC Genomics 20, 976. https://doi.org/10.1186/s12864-019-6358-x

Chen, C., Wang, M., Zhu, J., Tang, Y., Zhang, H., Zhao, Q., Jing, M., Chen, Y., Xu, X., Jiang, J., Shen, Z., 2022. Long-term effect of epigenetic modification in plant–microbe interactions: modification of DNA methylation induced by plant growth-promoting bacteria mediates promotion process. Microbiome 10, 36. https://doi.org/10.1186/s40168-022-01236-9

Clerissi, C., Chaïb, S., Raviglione, D., Espiau, B., Bertrand, C., Meyer, J.-Y., 2023. Metabarcoding and Metabolomics Reveal the Effect of the Invasive Alien Tree Miconia calvescens DC. on Soil Diversity on the Tropical Island of Mo'orea (French Polynesia). Microorganisms 11, 832. https://doi.org/10.3390/microorganisms11040832

Cobos, R., Ibañez, A., Diez-Galán, A., Calvo-Peña, C., Ghoreshizadeh, S., Coque, J.J.R., 2022. The Grapevine Microbiome to the Rescue: Implications for the Biocontrol of Trunk Diseases. Plants 11, 840. https://doi.org/10.3390/plants11070840

Cochetel, N., Météier, E., Merlin, I., Hévin, C., Pouvreau, J.-B., Coutos-Thévenot, P., Hernould, M., Vivin, P., Cookson, S.J., Ollat, N., Lauvergeat, V., 2018. Potential contribution of strigolactones in regulating scion growth and branching in grafted grapevine in response to nitrogen availability. J. Exp. Bot. 69, 4099–4112. https://doi.org/10.1093/jxb/ery206

Compant, S., Brader, G., Muzammil, S., Sessitsch, A., Lebrihi, A., Mathieu, F., 2013. Use of beneficial bacteria and their secondary metabolites to control grapevine pathogen diseases. BioControl 58, 435–455. https://doi.org/10.1007/s10526-012-9479-6

Bibliographie

Contreras, F., Díaz, J., Rombolà, A.D., De La Luz Mora, M., 2019. Prospecting intercropping between subterranean clover and grapevine as potential strategy for improving grapevine performance. Curr. Plant Biol. 19, 100110. https://doi.org/10.1016/j.cpb.2019.100110

Corso, M., Bonghi, C., 2014. Grapevine rootstock effects on abiotic stress tolerance. Plant Sci. Today 1, 108–113. https://doi.org/10.14719/pst.2014.1.3.64

Cruz-Silva, A., Figueiredo, A., Sebastiana, M., 2021. First Insights into the Effect of Mycorrhizae on the Expression of Pathogen Effectors during the Infection of Grapevine with Plasmopara viticola. Sustainability 13, 1226. https://doi.org/10.3390/su13031226

D'Amico, F., Candela, M., Turroni, S., Biagi, E., Brigidi, P., Bega, A., Vancini, D., Rampelli, S., 2018. The Rootstock Regulates Microbiome Diversity in Root and Rhizosphere Compartments of Vitis vinifera Cultivar Lambrusco. Front. Microbiol. 9, 2240. https://doi.org/10.3389/fmicb.2018.02240

Darriaut, R., Antonielli, L., Martins, G., Ballestra, P., Vivin, P., Marguerit, E., Mitter, B., Masneuf-Pomarède, I., Compant, S., Ollat, N., Lauvergeat, V., 2022a. Soil composition and rootstock genotype drive the root associated microbial communities in young grapevines. Front. Microbiol. 13, 1031064. https://doi.org/10.3389/fmicb.2022.1031064

Darriaut, R., Lailheugue, V., Masneuf-Pomarède, I., Marguerit, E., Martins, G., Compant, S., Ballestra, P., Upton, S., Ollat, N., Lauvergeat, V., 2022b. Grapevine rootstock and soil microbiome interactions: Keys for a resilient viticulture. Hortic. Res. 9, uhac019. https://doi.org/10.1093/hr/uhac019

Darriaut, R., Martins, G., Dewasme, C., Mary, S., Darrieutort, G., Ballestra, P., Marguerit, E., Vivin, P., Ollat, N., Masneuf-Pomarède, I., Lauvergeat, V., 2021. Grapevine decline is associated with difference in soil microbial composition and activity. OENO One 55. https://doi.org/10.20870/oeno-one.2021.55.3.4626

Darriaut, R., Tran, J., Martins, G., Ollat, N., Masneuf-Pomarède, I., Lauvergeat, V., 2023. In grapevine decline, microbiomes are affected differently in symptomatic and asymptomatic soils. Appl. Soil Ecol. 183, 104767. https://doi.org/10.1016/j.apsoil.2022.104767

De Bem, B.P., Bogo, A., Everhart, S.E., Casa, R.T., Gonçalves, M.J., Filho, J.L.M., Rufato, L., Da Silva, F.N., Allebrandt, R., Da Cunha, I.C., 2016. Effect of four training systems on the temporal dynamics of downy mildew in two grapevine cultivars in southern Brazil. Trop. Plant Pathol. 41, 370–379. https://doi.org/10.1007/s40858-016-0110-8

Dewasme, C., Inchboard, L., Tandonnet, J.-P., Roby, J.-P., 2023. Dynamics of grapevine fanleaf virus (GFLV) infection in the vineyard and study of the response of different rootstocks.

Deyett, E., Rolshausen, P.E., 2020. Endophytic microbial assemblage in grapevine. FEMS Microbiol. Ecol. 96, fiaa053. https://doi.org/10.1093/femsec/fiaa053

Diaz-Lara, A., Klaassen, V., Stevens, K., Sudarshana, M.R., Rowhani, A., Maree, H.J., Chooi, K.M., Blouin, A.G., Habili, N., Song, Y., Aram, K., Arnold, K., Cooper, M.L., Wunderlich, L., Battany, M.C., Bettiga, L.J., Smith, R.J., Bester, R., Xiao, H., Meng, B., Preece, J.E., Golino, D., Al Rwahnih, M., 2018. Characterization of grapevine leafroll-associated virus 3 genetic variants and application towards RT-qPCR assay design. PLOS ONE 13, e0208862. https://doi.org/10.1371/journal.pone.0208862

Dong, Y., Duan, S., Xia, Q., Liang, Z., Dong, X., Margaryan, K., Musayev, M., Goryslavets, S., Zdunić, G., Bert, P.-F., Lacombe, T., Maul, E., Nick, P., Bitskinashvili, K., Bisztray, G.D., Drori, E., De Lorenzis, G., Cunha, J., Popescu, C.F., Arroyo-Garcia, R., Arnold, C., Ergül, A., Zhu, Yifan, Ma, C., Wang, Shufen, Liu, S., Tang, L., Wang, C., Li, D., Pan, Y., Li, J., Yang, L., Li, X., Xiang, G., Yang, Z., Chen, B., Dai, Z., Wang, Yi, Arakelyan, A., Kuliyev, V., Spotar, G., Girollet, N., Delrot, S., Ollat, N., This, P., Marchal, C., Sarah, G., Laucou, V., Bacilieri, R., Röckel, F., Guan, P., Jung, A., Riemann, M., Ujmajuridze, L., Zakalashvili, T., Maghradze, D., Höhn, M., Jahnke, G., Kiss, E., Deák, T., Rahimi, O., Hübner, S., Grassi, F., Mercati, F., Sunseri, F., Eiras-Dias, J., Dumitru, A.M., Carrasco, D., Rodriguez-Izquierdo, A., Muñoz, G., Uysal, T., Özer, C., Kazan, K., Xu, M., Wang, Yunyue, Zhu, S., Lu, J., Zhao, M., Wang, L., Jiu, S., Zhang, Y., Sun, L., Yang, H., Weiss, E., Wang, Shiping, Zhu, Youyong, Li, S., Sheng, J., Chen, W., 2023. Dual domestications and origin of traits in grapevine evolution. Science 379, 892–901. https://doi.org/10.1126/science.add8655

Bibliographie

Douglas, G.M., Maffei, V.J., Zaneveld, J.R., Yurgel, S.N., Brown, J.R., Taylor, C.M., Huttenhower, C., Langille, M.G.I., 2020. PICRUSt2 for prediction of metagenome functions. Nat. Biotechnol. 38, 685–688. https://doi.org/10.1038/s41587-020-0548-6

Dries, L., Bussotti, S., Pozzi, C., Kunz, R., Schnell, S., Löhnertz, O., Vortkamp, A., 2021a. Rootstocks Shape Their Microbiome—Bacterial Communities in the Rhizosphere of Different Grapevine Rootstocks. Microorganisms 9, 822. https://doi.org/10.3390/microorganisms9040822

Dries, L., Hendgen, M., Schnell, S., Löhnertz, O., Vortkamp, A., 2021b. Rhizosphere engineering: leading towards a sustainable viticulture? OENO One 55, 353–363. https://doi.org/10.20870/oeno-one.2021.55.2.4534

Dries, L., Ratering, S., Bussotti, S., Löhnertz, O., Vortkamp, A., Schnell, S., 2023. The transcriptionally active bacterial communities of grapevine rhizosphere in dependence on rootstock and scion variety. OENO One 57, 86–97. https://doi.org/10.20870/oeno-one.2023.57.3.5547

Duan, B., Li, L., Chen, G., Su-Zhou, C., Li, Y., Merkeryan, H., Liu, W., Liu, X., 2021. 1-Aminocyclopropane-1-Carboxylate Deaminase-Producing Plant Growth-Promoting Rhizobacteria Improve Drought Stress Tolerance in Grapevine (Vitis vinifera L.). Front. Plant Sci. 12, 706990. https://doi.org/10.3389/fpls.2021.706990

Duan, M., Li, Y., Zhu, G., Wu, X., Huang, H., Qin, J., Long, S., Li, X., Feng, B., Qin, S., Liu, Q.-H., Li, C., Wang, L., Li, Q., He, T., Wang, Z., 2023. Soil chemistry, metabarcoding, and metabolome analyses reveal that a sugarcane—Dictyophora indusiata intercropping system can enhance soil health by reducing soil nitrogen loss. Front. Microbiol. 14, 1193990. https://doi.org/10.3389/fmicb.2023.1193990

Duan, M., Lu, J., Yang, W., Lu, M., Wang, J., Li, S., Chen, Y., Hu, L., Wang, L., 2022a. Metabarcoding and Metabolome Analyses Reveal Mechanisms of Leymus chinensis Growth Promotion by Fairy Ring of Leucocalocybe mongolica. J. Fungi 8, 944. https://doi.org/10.3390/jof8090944

Duan, M., Lu, M., Lu, J., Yang, W., Li, B., Ma, L., Wang, L., 2022b. Soil Chemical Properties, Metabolome, and Metabarcoding Give the New Insights into the Soil Transforming Process of Fairy Ring Fungi Leucocalocybe mongolica. J. Fungi 8, 680. https://doi.org/10.3390/jof8070680

Dubreuil-Maurizi, C., Trouvelot, S., Frettinger, P., Pugin, A., Wendehenne, D., Poinssot, B., 2010. β-Aminobutyric Acid Primes an NADPH Oxidase–Dependent Reactive Oxygen Species Production During Grapevine-Triggered Immunity. Mol. Plant-Microbe Interactions® 23, 1012–1021. https://doi.org/10.1094/MPMI-23-8-1012

Dufour, M.-C., Magnin, N., Dumas, B., Vergnes, S., Corio-Costet, M.-F., 2016. High-throughput gene-expression quantification of grapevine defense responses in the field using microfluidic dynamic arrays. BMC Genomics 17, 957. https://doi.org/10.1186/s12864-016-3304-z

Duret, M., Zhan, X., Belval, L., Le Jeune, C., Hussenet, R., Laloue, H., Bertsch, C., Chong, J., Deglène-Benbrahim, L., Valat, L., 2022. Use of a RT-qPCR Method to Estimate Mycorrhization Intensity and Symbiosis Vitality in Grapevine Plants Inoculated with Rhizophagus irregularis. Plants 11, 3237. https://doi.org/10.3390/plants11233237

Edgar, R.C., Haas, B.J., Clemente, J.C., Quince, C., Knight, R., 2011a. UCHIME improves sensitivity and speed of chimera detection. Bioinformatics 27, 2194–2200. https://doi.org/10.1093/bioinformatics/btr381

Eivazi, F., Tabatabai, M.A., 1988. Glucosidases and galactosidases in soils. Soil Biol. Biochem. 20, 601–606. https://doi.org/10.1016/0038-0717(88)90141-1

Enespa, Chandra, P., 2022. Tool and techniques study to plant microbiome current understanding and future needs: an overview. Commun. Integr. Biol. 15, 209–225. https://doi.org/10.1080/19420889.2022.2082736

Erdogan, U., Turan, M., Ates, F., Kotan, R., Çakmakçi, R., Erdogan, Y., Kitir, N., Tüfenkçi, S., 2018. Effects of Root Plant Growth Promoting Rhizobacteria Inoculations on the Growth and Nutrient Content of Grapevine. Commun. Soil Sci. Plant Anal. 49, 1731–1738. https://doi.org/10.1080/00103624.2018.1474910

Escudié, F., Auer, L., Bernard, M., Mariadassou, M., Cauquil, L., Vidal, K., Maman, S., Hernandez-Raquet, G., Combes, S., Pascal, G., 2018. FROGS: Find, Rapidly, OTUs with Galaxy Solution. Bioinformatics 34, 1287–1294. https://doi.org/10.1093/bioinformatics/btx791

Bibliographie

Fahad, S., Hussain, S., Bano, A., Saud, S., Hassan, S., Shan, D., Khan, F.A., Khan, F., Chen, Y., Wu, C., Tabassum, M.A., Chun, M.X., Afzal, M., Jan, A., Jan, M.T., Huang, J., 2015. Potential role of phytohormones and plant growth-promoting rhizobacteria in abiotic stresses: consequences for changing environment. Environ. Sci. Pollut. Res. 22, 4907–4921. https://doi.org/10.1007/s11356-014-3754-2

Fitzpatrick, C.R., Lu-Irving, P., Copeland, J., Guttman, D.S., Wang, P.W., Baltrus, D.A., Dlugosch, K.M., Johnson, M.T.J., 2018. Chloroplast sequence variation and the efficacy of peptide nucleic acids for blocking host amplification in plant microbiome studies. Microbiome 6, 144. https://doi.org/10.1186/s40168-018-0534-0

Fournier, P., Pellan, L., Barroso-Bergadà, D., Bohan, D.A., Candresse, T., Delmotte, F., Dufour, M.-C., Lauvergeat, V., Le Marrec, C., Marais, A., Martins, G., Masneuf-Pomarède, I., Rey, P., Sherman, D., This, P., Frioux, C., Labarthe, S., Vacher, C., 2022. The functional microbiome of grapevine throughout plant evolutionary history and lifetime, in: Advances in Ecological Research. Elsevier, pp. 27–99. https://doi.org/10.1016/bs.aecr.2022.09.001

Fraga, H., Malheiro, A.C., Moutinho-Pereira, J., Santos, J.A., 2012. An overview of climate change impacts on European viticulture. Food Energy Secur. 1, 94–110. https://doi.org/10.1002/fes3.14

Gambetta, G.A., Herrera, J.C., Dayer, S., Feng, Q., Hochberg, U., Castellarin, S.D., 2020. The physiology of drought stress in grapevine: towards an integrative definition of drought tolerance. J. Exp. Bot. 71, 4658–4676. https://doi.org/10.1093/jxb/eraa245

Gaši, E., Radić, T., Čarija, M., Gambino, G., Balestrini, R., Hančević, K., 2023. Arbuscular Mycorrhizal Fungi Induce Changes of Photosynthesis-Related Parameters in Virus Infected Grapevine. Plants 12, 1783. https://doi.org/10.3390/plants12091783

Gautier, A., Cookson, S.J., Lagalle, L., Ollat, N., Marguerit, E., 2020. Influence of the three main genetic backgrounds of grapevine rootstocks on petiolar nutrient concentrations of the scion, with a focus on phosphorus. OENO One 54, 1–13. https://doi.org/10.20870/oeno-one.2020.54.1.2458

Gazioglu Sensoy, R.I., Gazioglu Sensoy, R.I., 2022. Effects of Arbuscular Mycorrhizal Fungus (AMF) and whey applications on the grapevine (Vitis vinifera L.) cuttings exposed to salt stress. J. Elem. https://doi.org/10.5601/jelem.2022.27.2.2295

Gerdemann, J.W., Nicolson, T.H., 1963. Spores of mycorrhizal Endogone species extracted from soil by wet sieving and decanting. Trans. Br. Mycol. Soc. 46, 235–244. https://doi.org/10.1016/S0007-1536(63)80079-0

Giblot-Ducray, D., Correll, R., Collins, C., Nankivell, A., Downs, A., Pearce, I., Mckay, A.C., Ophel-Keller, K.M., 2016. Detection of grape phylloxera (Daktulosphaira vitifoliae Fitch) by real-time quantitative PCR: development of a soil sampling protocol: Sampling protocol for phylloxera detection by qPCR. Aust. J. Grape Wine Res. 22, 469–477. https://doi.org/10.1111/ajgw.12237

Gobbi, A., Acedo, A., Imam, N., Santini, R.G., Ortiz-Álvarez, R., Ellegaard-Jensen, L., Belda, I., Hansen, L.H., 2022. A global microbiome survey of vineyard soils highlights the microbial dimension of viticultural terroirs. Commun. Biol. 5, 241. https://doi.org/10.1038/s42003-022-03202-5

Goicoechea, N., Torres, N., Garmendia, I., Hilbert, G., Antolín, M.C., 2023. Mycorrhizal symbiosis improve fruit quality in Tempranillo grapevine sensitive to low-moderate warming. Sci. Hortic. 315, 111993. https://doi.org/10.1016/j.scienta.2023.111993

Goswami, D., Pithwa, S., Dhandhukia, P., Thakker, J.N., 2014. Delineating Kocuria turfanensis 2M4 as a credible PGPR: a novel IAA-producing bacteria isolated from saline desert. J. Plant Interact. 9, 566–576. https://doi.org/10.1080/17429145.2013.871650

Goulson, D., 2013. REVIEW: An overview of the environmental risks posed by neonicotinoid insecticides. J. Appl. Ecol. 50, 977–987. https://doi.org/10.1111/1365-2664.12111

Grassi, F., De Lorenzis, G., 2021. Back to the Origins: Background and Perspectives of Grapevine Domestication. Int. J. Mol. Sci. 22, 4518. https://doi.org/10.3390/ijms22094518

Bibliographie

Gryta, A., Fr, M., 2014. The Application of the Biolog EcoPlate Approach in Ecotoxicological Evaluation of Dairy Sewage Sludge. Appl Biochem Biotechnol.

Haichar, F. el Z., Santaella, C., Heulin, T., Achouak, W., 2014. Root exudates mediated interactions belowground. Soil Biol. Biochem. 77, 69–80. https://doi.org/10.1016/j.soilbio.2014.06.017

Halleen, F., Fourie, P.H., Lombard, P.J., 2016. Protection of Grapevine Pruning Wounds against Eutypa lata by Biological and Chemical Methods. South Afr. J. Enol. Vitic. 31. https://doi.org/10.21548/31-2-1409

Hassani, M.A., Durán, P., Hacquard, S., 2018. Microbial interactions within the plant holobiont. Microbiome 6, 58. https://doi.org/10.1186/s40168-018-0445-0

Hazarika, S.N., Thakur, D., 2020. Actinobacteria, in: Beneficial Microbes in Agro-Ecology. Elsevier, pp. 443–476. https://doi.org/10.1016/B978-0-12-823414-3.00021-6

Hernandez, M.M., Menéndez, C.M., 2019. Influence of seasonality and management practices on diversity and composition of fungal communities in vineyard soils. Appl. Soil Ecol. 135, 113–119. https://doi.org/10.1016/j.apsoil.2018.11.008

Basu, S., Bose, C., Ojha, N., Das, N., Das, J., Pal, M., Khurana, S., 2015. Evolution of bacterial and fungal growth media. Bioinformation 11, 182–184. https://doi.org/10.6026/97320630011182

Islam, W., Noman, A., Naveed, H., Huang, Z., Chen, H.Y.H., 2020. Role of environmental factors in shaping the soil microbiome. Environ. Sci. Pollut. Res. 27, 41225–41247. https://doi.org/10.1007/s11356-020-10471-2

Jamil, F., Mukhtar, H., Fouillaud, M., Dufossé, L., 2022. Rhizosphere Signaling: Insights into Plant–Rhizomicrobiome Interactions for Sustainable Agronomy. Microorganisms 10, 899. https://doi.org/10.3390/microorganisms10050899

Kalam, S., Basu, A., Ahmad, I., Sayyed, R.Z., El-Enshasy, H.A., Dailin, D.J., Suriani, N.L., 2020. Recent Understanding of Soil Acidobacteria and Their Ecological Significance: A Critical Review. Front. Microbiol. 11, 580024. https://doi.org/10.3389/fmicb.2020.580024

Kang, S.-M., Khan, A.L., You, Y.-H., Kim, J.-G., Kamran, M., Lee, I.-J., 2014. Gibberellin Production by Newly Isolated Strain Leifsonia soli SE134 and Its Potential to Promote Plant Growth. J. Microbiol. Biotechnol. 24, 106–112. https://doi.org/10.4014/jmb.1304.04015

Kaniganti, S., Bhattacharya, J., Petla, B.P., Reddy, P.S., 2022. Strigolactone, a neglected plant hormone, with a great potential for crop improvement: Crosstalk with other plant hormones. Environ. Exp. Bot. 204, 105072. https://doi.org/10.1016/j.envexpbot.2022.105072

Karagöz, K., Ateş, F., Karagöz, H., Kotan, R., Çakmakçı, R., 2012. Characterization of plant growth-promoting traits of bacteria isolated from the rhizosphere of grapevine grown in alkaline and acidic soils. Eur. J. Soil Biol. 50, 144–150. https://doi.org/10.1016/j.ejsobi.2012.01.007

Khan, M.M., Akram, M.T., Qadri, R.W.K., Al-Yahyai, R., 2020. Role of grapevine rootstocks in mitigating environmental stresses: A review. J. Agric. Mar. Sci. JAMS 25, 1. https://doi.org/10.24200/jams.vol25iss2pp1-12

Kjøller, R., Rosendahl, S., 2014. Cultivated and fallow fields harbor distinct communities of Basidiomycota. Fungal Ecol. 9, 43–51. https://doi.org/10.1016/j.funeco.2014.02.005

Koch, B., Oehl, F., 2018. Climate Change Favors Grapevine Production in Temperate Zones. Agric. Sci. 09, 247–263. https://doi.org/10.4236/as.2018.93019

Koh, C.-L., Sam, C.-K., Yin, W.-F., Tan, L., Krishnan, T., Chong, Y., Chan, K.-G., 2013. Plant-Derived Natural Products as Sources of Anti-Quorum Sensing Compounds. Sensors 13, 6217–6228. https://doi.org/10.3390/s130506217

Krebelj, A.J., Čepin, U., Ravnikar, M., Novak, M.P., 2015. Spatio-temporal distribution of Grapevine fanleaf virus (GFLV) in grapevine. Eur. J. Plant Pathol. 142, 159–171. https://doi.org/10.1007/s10658-015-0600-4

Bibliographie

Kumar, A., Dubey, A., 2020. Rhizosphere microbiome: Engineering bacterial competitiveness for enhancing crop production. J. Adv. Res. 24, 337–352. https://doi.org/10.1016/j.jare.2020.04.014

Lacroix, R., Kurrasch, D.M., 2023. Glyphosate toxicity: in vivo, in vitro , and epidemiological evidence. Toxicol. Sci. 192, 131–140. https://doi.org/10.1093/toxsci/kfad018

Lailheugue, V., Merlin, I., Boutet, S., Perreau, F., Pouvreau, J.-B., Delgrange, S., Ducrot, P.-H., Cottyn-Boitte, B., Mouille, G., Lauvergeat, V., 2023. Vitislactone, a non-canonical strigolactone exudated by grapevine rootstocks in response to nitrogen starvation. Phytochemistry 215, 113837. https://doi.org/10.1016/j.phytochem.2023.113837

Landi, L., Foglia, R., Murolo, S., Romanazzi, G., 2021. The Mycorrizal Status in Vineyards Affected by Esca. J. Fungi 7, 869. https://doi.org/10.3390/jof7100869

Lavrinienko, A., Jernfors, T., Koskimäki, J.J., Pirttilä, A.M., Watts, P.C., 2021. Does Intraspecific Variation in rDNA Copy Number Affect Analysis of Microbial Communities? Trends Microbiol. 29, 19–27. https://doi.org/10.1016/j.tim.2020.05.019

Li, J., Li, D., Liu, B., Wang, R., Yan, Y., Li, G., Wang, L., Ma, C., Xu, W., Zhao, L., Li, X., Wang, S., 2022. Effects of root restriction on phytohormone levels in different growth stages and grapevine organs. Sci. Rep. 12, 1323. https://doi.org/10.1038/s41598-021-04617-6

Likar, M., Regvar, M., 2017. Arbuscular Mycorrhizal Fungi and Dark Septate Endophytes in Grapevine: The Potential for Sustainable Viticulture?, in: Varma, A., Prasad, R., Tuteja, N. (Eds.), Mycorrhiza - Function, Diversity, State of the Art. Springer International Publishing, Cham, pp. 275–289. https://doi.org/10.1007/978-3-319-53064-2_13

Likar, M., Stres, B., Rusjan, D., Potisek, M., Regvar, M., 2017. Ecological and conventional viticulture gives rise to distinct fungal and bacterial microbial communities in vineyard soils. Appl. Soil Ecol. 113, 86–95. https://doi.org/10.1016/j.apsoil.2017.02.007

Liu, Q., Zhang, L., Wang, L., Wu, Q., Li, K., Guo, X., 2022. Autotoxin affects the rhizosphere microbial community structure by influencing the secretory characteristics of grapevine roots. Front. Microbiol. 13, 953424. https://doi.org/10.3389/fmicb.2022.953424

López-Rayo, S., Di Foggia, M., Rodrigues Moreira, E., Donnini, S., Bombai, G., Filippini, G., Pisi, A., Rombolà, A.D., 2015. Physiological responses in roots of the grapevine rootstock 140 Ruggeri subjected to Fe deficiency and Fe-heme nutrition. Plant Physiol. Biochem. 96, 171–179. https://doi.org/10.1016/j.plaphy.2015.07.034

Lou, J., Fu, L., Peng, Y., Zhou, L., 2013. Metabolites from Alternaria Fungi and Their Bioactivities. Molecules 18, 5891–5935. https://doi.org/10.3390/molecules18055891

Loupit, G., Fonayet, J.V., Lorensen, M.D.B.B., Franc, C., De Revel, G., Janfelt, C., Cookson, S.J., 2023. Tissue-specific stilbene accumulation is an early response to wounding/grafting as revealed by using spatial and temporal metabolomics. Plant Cell Environ. pce.14693. https://doi.org/10.1111/pce.14693

Luna, E., Flandin, A., Cassan, C., Prigent, S., Chevanne, C., Kadiri, C.F., Gibon, Y., Pétriacq, P., 2020. Metabolomics to Exploit the Primed Immune System of Tomato Fruit. Metabolites 10, 96. https://doi.org/10.3390/metabo10030096

Ma, W., Tang, S., Dengzeng, Z., Zhang, D., Zhang, T., Ma, X., 2022. Root exudates contribute to belowground ecosystem hotspots: A review. Front. Microbiol. 13, 937940. https://doi.org/10.3389/fmicb.2022.937940

Mahé, F., Rognes, T., Quince, C., De Vargas, C., Dunthorn, M., 2014. Swarm: robust and fast clustering method for amplicon-based studies. PeerJ 2, e593. https://doi.org/10.7717/peerj.593

Manter, D.K., Hamm, A.K., Deel, H.L., 2023. Community structure and abundance of ACC deaminase containing bacteria in soils with 16S-PICRUSt2 inference or direct acdS gene sequencing. J. Microbiol. Methods 211, 106740. https://doi.org/10.1016/j.mimet.2023.106740

Marasco, R., Alturkey, H., Fusi, M., Brandi, M., Ghiglieno, I., Valenti, L., Daffonchio, D., 2022. Rootstock–scion combination contributes to shape diversity and composition of microbial communities associated with grapevine root system. Environ. Microbiol. 1462-2920.16042. https://doi.org/10.1111/1462-2920.16042

Bibliographie

Marasco, R., Rolli, E., Fusi, M., Michoud, G., Daffonchio, D., 2018. Grapevine rootstocks shape underground bacterial microbiome and networking but not potential functionality. Microbiome 6, 3. https://doi.org/10.1186/s40168-017-0391-2

Marastoni, L., Lucini, L., Miras-Moreno, B., Trevisan, M., Sega, D., Zamboni, A., Varanini, Z., 2020. Changes in physiological activities and root exudation profile of two grapevine rootstocks reveal common and specific strategies for Fe acquisition. Sci. Rep. 10, 18839. https://doi.org/10.1038/s41598-020-75317-w

Marastoni, L., Sandri, M., Pii, Y., Valentinuzzi, F., Cesco, S., Mimmo, T., 2019. Morphological Root Responses and Molecular Regulation of Cation Transporters Are Differently Affected by Copper Toxicity and Cropping System Depending on the Grapevine Rootstock Genotype. Front. Plant Sci. 10, 946. https://doi.org/10.3389/fpls.2019.00946

Martin, M., 2011b. Cutadapt removes adapter sequences from high-throughput sequencing reads. EMBnet.journal 17, 10. https://doi.org/10.14806/ej.17.1.200

Massa, N., Bona, E., Novello, G., Todeschini, V., Boatti, L., Mignone, F., Gamalero, E., Lingua, G., Berta, G., Cesaro, P., 2020. AMF communities associated to Vitis vinifera in an Italian vineyard subjected to integrated pest management at two different phenological stages. Sci. Rep. 10, 9197. https://doi.org/10.1038/s41598-020-66067-w

McMurdie, P.J., Holmes, S., 2013. phyloseq: An R Package for Reproducible Interactive Analysis and Graphics of Microbiome Census Data. PLoS ONE 8, e61217. https://doi.org/10.1371/journal.pone.0061217

Mekureyaw, M.F., Pandey, C., Hennessy, R.C., Nicolaisen, M.H., Liu, F., Nybroe, O., Roitsch, T., 2022. The cytokinin-producing plant beneficial bacterium Pseudomonas fluorescens G20-18 primes tomato (Solanum lycopersicum) for enhanced drought stress responses. J. Plant Physiol. 270, 153629. https://doi.org/10.1016/j.jplph.2022.153629

Merrill, N.K., García De Cortázar-Atauri, I., Parker, A.K., Walker, M.A., Wolkovich, E.M., 2020. Exploring Grapevine Phenology and High Temperatures Response Under Controlled Conditions. Front. Environ. Sci. 8, 516527. https://doi.org/10.3389/fenvs.2020.516527

Mezzasalma, V., Sandionigi, A., Bruni, I., Bruno, A., Lovicu, G., Casiraghi, M., Labra, M., 2017. Grape microbiome as a reliable and persistent signature of field origin and environmental conditions in Cannonau wine production. PLOS ONE 12, e0184615. https://doi.org/10.1371/journal.pone.0184615

Monteiro, E., Gonçalves, B., Cortez, I., Castro, I., 2022. The Role of Biostimulants as Alleviators of Biotic and Abiotic Stresses in Grapevine: A Review. Plants 11, 396. https://doi.org/10.3390/plants11030396

Morris, J.J., 2018. What is the hologenome concept of evolution? F1000Research 7, 1664. https://doi.org/10.12688/f1000research.14385.1

Moukarzel, R., Ridgway, H.J., Guerin-Laguette, A., Jones, E.E., 2021a. Grapevine rootstocks drive the community structure of arbuscular mycorrhizal fungi in New Zealand vineyards. J. Appl. Microbiol. 131, 2941–2956. https://doi.org/10.1111/jam.15160

Moukarzel, R., Ridgway, H.J., Guerin-Laguette, A., Jones, E.E., 2021b. Grapevine rootstocks drive the community structure of arbuscular mycorrhizal fungi in New Zealand vineyards. J. Appl. Microbiol. 131, 2941–2956. https://doi.org/10.1111/jam.15160

Moukarzel, R., Ridgway, H.J., Liu, J., Guerin-Laguette, A., Jones, E.E., 2022. AMF Community Diversity Promotes Grapevine Growth Parameters under High Black Foot Disease Pressure. J. Fungi 8, 250. https://doi.org/10.3390/jof8030250

Moukarzel, R., Ridgway, H.J., Waller, L., Guerin-Laguette, A., Cripps-Guazzone, N., Jones, E.E., 2023. Soil Arbuscular Mycorrhizal Fungal Communities Differentially Affect Growth and Nutrient Uptake by Grapevine Rootstocks. Microb. Ecol. 86, 1035–1049. https://doi.org/10.1007/s00248-022-02160-z

Naitam, M.G., Kaushik, R., 2021. Archaea: An Agro-Ecological Perspective. Curr. Microbiol. 78, 2510–2521. https://doi.org/10.1007/s00284-021-02537-2

Bibliographie

Nearing, J.T., Douglas, G.M., Hayes, M.G., MacDonald, J., Desai, D.K., Allward, N., Jones, C.M.A., Wright, R.J., Dhanani, A.S., Comeau, A.M., Langille, M.G.I., 2022. Microbiome differential abundance methods produce different results across 38 datasets. Nat. Commun. 13, 342. https://doi.org/10.1038/s41467-022-28034-z

Németh, I., Molnár, S., Vaszita, E., Molnár, M., 2021. The Biolog EcoPlate™ Technique for Assessing the Effect of Metal Oxide Nanoparticles on Freshwater Microbial Communities. Nanomaterials 11, 1777. https://doi.org/10.3390/nano11071777

Nerva, L., Giudice, G., Quiroga, G., Belfiore, N., Lovat, L., Perria, R., Volpe, M.G., Moffa, L., Sandrini, M., Gaiotti, F., Balestrini, R., Chitarra, W., 2022. Mycorrhizal symbiosis balances rootstock-mediated growth-defence tradeoffs. Biol. Fertil. Soils 58, 17–34. https://doi.org/10.1007/s00374-021-01607-8

Nerva, L., Pagliarani, C., Pugliese, M., Monchiero, M., Gonthier, S., Gullino, M.L., Gambino, G., Chitarra, W., 2019. Grapevine Phyllosphere Community Analysis in Response to Elicitor Application against Powdery Mildew. Microorganisms 7, 662. https://doi.org/10.3390/microorganisms7120662

Nguyen, N.H., Song, Z., Bates, S.T., Branco, S., Tedersoo, L., Menke, J., Schilling, J.S., Kennedy, P.G., 2016. FUNGuild: An open annotation tool for parsing fungal community datasets by ecological guild. Fungal Ecol. 20, 241–248. https://doi.org/10.1016/j.funeco.2015.06.006

Nicolás, E., Maestre-Valero, J.F., Alarcón, J.J., Pedrero, F., Vicente-Sánchez, J., Bernabé, A., Gómez-Montiel, J., Hernández, J.A., Fernández, F., 2015. Effectiveness and persistence of arbuscular mycorrhizal fungi on the physiology, nutrient uptake and yield of Crimson seedless grapevine. J. Agric. Sci. 153, 1084–1096. https://doi.org/10.1017/S002185961400080X

Nilsson, R.H., Larsson, K.-H., Taylor, A.F.S., Bengtsson-Palme, J., Jeppesen, T.S., Schigel, D., Kennedy, P., Picard, K., Glöckner, F.O., Tedersoo, L., Saar, I., Kõljalg, U., Abarenkov, K., 2019. The UNITE database for molecular identification of fungi: handling dark taxa and parallel taxonomic classifications. Nucleic Acids Res. 47, D259–D264. https://doi.org/10.1093/nar/gky1022

Noceto, P.-A., Bettenfeld, P., Boussageon, R., Hériché, M., Sportes, A., Van Tuinen, D., Courty, P.-E., Wipf, D., 2021. Arbuscular mycorrhizal fungi, a key symbiosis in the development of quality traits in crop production, alone or combined with plant growth-promoting bacteria. Mycorrhiza 31, 655–669. https://doi.org/10.1007/s00572-021-01054-1

Noceto, PA., Durney, C., van Tuinen, D., De Sousa, J., Wipf, D., Courty, P.E., 2023. Arbuscular mycorrhizal fungal communities differ in neighboring vineyards of different ages. Mycorrhiza 33, 241–248. https://doi.org/10.1007/s00572-023-01117-5

Nogales, A., Rottier, E., Campos, C., Victorino, G., Costa, J.M., Coito, J.L., Pereira, H.S., Viegas, W., Lopes, C., 2021. The effects of field inoculation of arbuscular mycorrhizal fungi through rye donor plants on grapevine performance and soil properties. Agric. Ecosyst. Environ. 313, 107369. https://doi.org/10.1016/j.agee.2021.107369

Noller, H.F., Lancaster, L., Mohan, S., Zhou, J., 2017. Ribosome structural dynamics in translocation: yet another functional role for ribosomal RNA. Q. Rev. Biophys. 50, e12. https://doi.org/10.1017/S0033583517000117

Ollat, N., Cookson, S.J., Lauvergeat, V., Marguerit, E., Barrieu, F., Gambetta, G., Goutouly, J.-P., Tandonnet, J.-P., Vivin, P., Delrot, S., 2017. Grapevine roots: the dark side. Acta Hortic. 213–226. https://doi.org/10.17660/ActaHortic.2017.1188.28

Öpik, M., Vanatoa, A., Vanatoa, E., Moora, M., Davison, J., Kalwij, J.M., Reier, Ü., Zobel, M., 2010. The online database MaarjAM reveals global and ecosystemic distribution patterns in arbuscular mycorrhizal fungi (Glomeromycota). New Phytol. 188, 223–241. https://doi.org/10.1111/j.1469-8137.2010.03334.x

Orozco-Mosqueda, Ma.D.C., Fadiji, A.E., Babalola, O.O., Glick, B.R., Santoyo, G., 2022. Rhizobiome engineering: Unveiling complex rhizosphere interactions to enhance plant growth and health. Microbiol. Res. 263, 127137. https://doi.org/10.1016/j.micres.2022.127137

Orozco-Mosqueda, Ma.D.C., Glick, B.R., Santoyo, G., 2020. ACC deaminase in plant growth-promoting bacteria (PGPB): An efficient mechanism to counter salt stress in crops. Microbiol. Res. 235, 126439. https://doi.org/10.1016/j.micres.2020.126439

Bibliographie

Oyuela Aguilar, M., Gobbi, A., Browne, P.D., Ellegaard-Jensen, L., Hansen, L.H., Semorile, L., Pistorio, M., 2020. Influence of vintage, geographic location and cultivar on the structure of microbial communities associated with the grapevine rhizosphere in vineyards of San Juan Province, Argentina. PLOS ONE 15, e0243848. https://doi.org/10.1371/journal.pone.0243848

Ozimek, E., Hanaka, A., 2020. Mortierella Species as the Plant Growth-Promoting Fungi Present in the Agricultural Soils. Agriculture 11, 7. https://doi.org/10.3390/agriculture11010007

Parker, A.K., García De Cortázar-Atauri, I., Trought, M.C.T., Destrac, A., Agnew, R., Sturman, A., Van Leeuwen, C., 2020. Adaptation to climate change by determining grapevine cultivar differences using temperature-based phenology models: This article is published in cooperation with the XIIIth International Terroir Congress November 17-18 2020, Adelaide, Australia. Guests editors: Cassandra Collins and Roberta De Bei. OENO One 54, 955–974. https://doi.org/10.20870/oeno-one.2020.54.4.3861

Philippot, L., Raaijmakers, J.M., Lemanceau, P., van der Putten, W.H., 2013. Going back to the roots: the microbial ecology of the rhizosphere. Nat. Rev. Microbiol. 11, 789–799. https://doi.org/10.1038/nrmicro3109

Poni, S., Gatti, M., Palliotti, A., Dai, Z., Duchêne, E., Truong, T.-T., Ferrara, G., Matarrese, A.M.S., Gallotta, A., Bellincontro, A., Mencarelli, F., Tombesi, S., 2018. Grapevine quality: A multiple choice issue. Sci. Hortic. 234, 445–462. https://doi.org/10.1016/j.scienta.2017.12.035

Popescu, G.C., Popescu, M., 2018. Yield, berry quality and physiological response of grapevine to foliar humic acid application. Bragantia 77, 273–282. https://doi.org/10.1590/1678-4499.2017030

Pouzoulet, J., Mailhac, N., Couderc, C., Besson, X., Daydé, J., Lummerzheim, M., Jacques, A., 2013. A method to detect and quantify Phaeomoniella chlamydospora and Phaeoacremonium aleophilum DNA in grapevine-wood samples. Appl. Microbiol. Biotechnol. 97, 10163–10175. https://doi.org/10.1007/s00253-013-5299-6

Quast, C., Pruesse, E., Yilmaz, P., Gerken, J., Schweer, T., Yarza, P., Peplies, J., Glöckner, F.O., 2012. The SILVA ribosomal RNA gene database project: improved data processing and web-based tools. Nucleic Acids Res. 41, D590–D596. https://doi.org/10.1093/nar/gks1219

Quince, C., Walker, A.W., Simpson, J.T., Loman, N.J., Segata, N., 2017. Shotgun metagenomics, from sampling to analysis. Nat. Biotechnol. 35, 833–844. https://doi.org/10.1038/nbt.3935

Redecker, D., Kodner, R., Graham, L.E., 2000. Glomalean Fungi from the Ordovician. Science 289, 1920–1921. https://doi.org/10.1126/science.289.5486.1920

Redecker, D., Schüßler, A., Stockinger, H., Stürmer, S.L., Morton, J.B., Walker, C., 2013. An evidence-based consensus for the classification of arbuscular mycorrhizal fungi (Glomeromycota). Mycorrhiza 23, 515–531. https://doi.org/10.1007/s00572-013-0486-y

Rillig, M.C., Aguilar-Trigueros, C.A., Bergmann, J., Verbruggen, E., Veresoglou, S.D., Lehmann, A., 2015. Plant root and mycorrhizal fungal traits for understanding soil aggregation. New Phytol. 205, 1385–1388. https://doi.org/10.1111/nph.13045

Rodriguez, R., Durán, P., 2020. Natural Holobiome Engineering by Using Native Extreme Microbiome to Counteract the Climate Change Effects. Front. Bioeng. Biotechnol. 8, 568. https://doi.org/10.3389/fbioe.2020.00568
Rognes, T., Flouri, T., Nichols, B., Quince, C., Mahé, F., 2016a. VSEARCH: a versatile open source tool for metagenomics. PeerJ 4, e2584. https://doi.org/10.7717/peerj.2584

Rognes, T., Flouri, T., Nichols, B., Quince, C., Mahé, F., 2016. VSEARCH: a versatile open source tool for metagenomics. PeerJ 4, e2584. https://doi.org/10.7717/peerj.2584

Rohart, F., Gautier, B., Singh, A., Lê Cao, K.-A., 2017. mixOmics: An R package for 'omics feature selection and multiple data integration. PLOS Comput. Biol. 13, e1005752. https://doi.org/10.1371/journal.pcbi.1005752

Rolshausen, P.E., Úrbez-Torres, J.R., Rooney-Latham, S., Eskalen, A., Smith, R.J., Gubler, W.D., 2010. Evaluation of Pruning Wound Susceptibility and Protection Against Fungi Associated with Grapevine Trunk Diseases. Am. J. Enol. Vitic. 61, 113–119. https://doi.org/10.5344/ajev.2010.61.1.113

Bibliographie

Rossdeutsch, L., Schreiner, R.P., Skinkis, P.A., Deluc, L., 2021. Nitrate Uptake and Transport Properties of Two Grapevine Rootstocks With Varying Vigor. Front. Plant Sci. 11, 608813. https://doi.org/10.3389/fpls.2020.608813

Sabir, A., Yazici, M.A., Kara, Z., Sahin, F., 2012. Growth and mineral acquisition response of grapevine rootstocks (Vitis spp.) to inoculation with different strains of plant growth-promoting rhizobacteria (PGPR). J. Sci. Food Agric. 92, 2148–2153. https://doi.org/10.1002/jsfa.5600

Salmeron-Santiago, I.A., Martínez-Trujillo, M., Valdez-Alarcón, J.J., Pedraza-Santos, M.E., Santoyo, G., Pozo, M.J., Chávez-Bárcenas, A.T., 2021. An Updated Review on the Modulation of Carbon Partitioning and Allocation in Arbuscular Mycorrhizal Plants. Microorganisms 10, 75. https://doi.org/10.3390/microorganisms10010075

Salomon, M.V., Bottini, R., De Souza Filho, G.A., Cohen, A.C., Moreno, D., Gil, M., Piccoli, P., 2014. Bacteria isolated from roots and rhizosphere of Vitis vinifera retard water losses, induce abscisic acid accumulation and synthesis of defense-related terpenes in in vitro cultured grapevine. Physiol. Plant. 151, 359–374. https://doi.org/10.1111/ppl.12117

Savo, V., Kumbaric, A., Caneva, G., 2016. Grapevine (Vitis vinifera L.) Symbolism in the Ancient Euro-Mediterranean Cultures. Econ. Bot. 70, 190–197. https://doi.org/10.1007/s12231-016-9347-x

Schreiner, R.P., 2020. Depth structures the community of arbuscular mycorrhizal fungi amplified from grapevine (Vitis vinifera L.) roots. Mycorrhiza 30, 149–160. https://doi.org/10.1007/s00572-020-00930-6

Schreiner, R.P., 2005. Mycorrhizas and Mineral Acquisition in Grapevines. Soil Environment and Vine Mineral Symposium. https://api.semanticscholar.org/CorpusID:30760777

Schreiner, R.P., Mihara, K.L., 2009. The diversity of arbuscular mycorrhizal fungi amplified from grapevine roots (Vitis vinifera L.) in Oregon vineyards is seasonally stable and influenced by soil and vine age. Mycologia 101, 599–611. https://doi.org/10.3852/08-169

Seaton, F.M., George, P.B.L., Lebron, I., Jones, D.L., Creer, S., Robinson, D.A., 2020. Soil textural heterogeneity impacts bacterial but not fungal diversity. Soil Biol. Biochem. 144, 107766. https://doi.org/10.1016/j.soilbio.2020.107766

Senizza, B., Araniti, F., Lewin, S., Wende, S., Kolb, S., Lucini, L., 2023. Trichoderma spp.-mediated mitigation of heat, drought, and their combination on the Arabidopsis thaliana holobiont: a metabolomics and metabarcoding approach. Front. Plant Sci. 14, 1190304. https://doi.org/10.3389/fpls.2023.1190304

Shah, A., Nazari, M., Antar, M., Msimbira, L.A., Naamala, J., Lyu, D., Rabileh, M., Zajonc, J., Smith, D.L., 2021. PGPR in Agriculture: A Sustainable Approach to Increasing Climate Change Resilience. Front. Sustain. Food Syst. 5, 667546. https://doi.org/10.3389/fsufs.2021.667546

Shakya, M., Lo, C.-C., Chain, P.S.G., 2019. Advances and Challenges in Metatranscriptomic Analysis. Front. Genet. 10, 904. https://doi.org/10.3389/fgene.2019.00904

Sharma, M.P., Buyer, J.S., 2015. Comparison of biochemical and microscopic methods for quantification of arbuscular mycorrhizal fungi in soil and roots. Appl. Soil Ecol. 95, 86–89. https://doi.org/10.1016/j.apsoil.2015.06.001

Shirani Bidabadi, S., Sabbatini, P., 2020. Bioaccumulation, Ionome and Physiological Responses to Copper Toxicity of Iranian Grapevine Rootstocks Grafted with 'Asgari' Seedless Grape. Int. J. Fruit Sci. 20, 451–470. https://doi.org/10.1080/15538362.2019.1652133

Si Ammour, M., Bove, F., Toffolatti, S.L., Rossi, V., 2020. A Real-Time PCR Assay for the Quantification of Plasmopara viticola Oospores in Grapevine Leaves. Front. Plant Sci. 11, 1202. https://doi.org/10.3389/fpls.2020.01202

Smith, P., Cotrufo, M.F., Rumpel, C., Paustian, K., Kuikman, P.J., Elliott, J.A., McDowell, R., Griffiths, R.I., Asakawa, S., Bustamante, M., House, J.I., Sobocká, J., Harper, R., Pan, G., West, P.C., Gerber, J.S., Clark, J.M., Adhya, T., Scholes, R.J., Scholes, M.C., 2015. Biogeochemical cycles and biodiversity as key drivers of ecosystem services provided by soils. SOIL 1, 665–685. https://doi.org/10.5194/soil-1-665-2015

Smucker, N.J., Pilgrim, E.M., Nietch, C.T., Darling, J.A., Johnson, B.R., 2020. DNA metabarcoding effectively quantifies diatom responses to nutrients in streams. Ecol. Appl. 30, e02205. https://doi.org/10.1002/eap.2205

Bibliographie

Song, F., Bai, F., Wang, J., Wu, L., Jiang, Y., Pan, Z., 2020. Influence of Citrus Scion/Rootstock Genotypes on Arbuscular Mycorrhizal Community Composition under Controlled Environment Condition. Plants 9, 901. https://doi.org/10.3390/plants9070901

Souza Gonzaga, L., Capone, D.L., Bastian, S.E.P., Jeffery, D.W., 2021. Defining wine typicity: sensory characterisation and consumer perspectives. Aust. J. Grape Wine Res. 27, 246–256. https://doi.org/10.1111/ajgw.12474

Stosiek, N., Terebieniec, A., Ząbek, A., Młynarz, P., Cieśliński, H., Klimek-Ochab, M., 2019. N-phosphonomethylglycine utilization by the psychrotolerant yeast Solicoccozyma terricola M 3.1.4. Bioorganic Chem. 93, 102866. https://doi.org/10.1016/j.bioorg.2019.03.040

Subbarao, G.V., Rondon, M., Ito, O., Ishikawa, T., Rao, I.M., Nakahara, K., Lascano, C., Berry, W.L., 2007. Biological nitrification inhibition (BNI)—is it a widespread phenomenon? Plant Soil 294, 5–18. https://doi.org/10.1007/s11104-006-9159-3

Suzuki, K., Takahashi, K., Harada, N., 2020. Evaluation of primer pairs for studying arbuscular mycorrhizal fungal community compositions using a MiSeq platform. Biol. Fertil. Soils 56, 853–858. https://doi.org/10.1007/s00374-020-01431-6

Swift, J.F., Hall, M.E., Harris, Z.N., Kwasniewski, M.T., Miller, A.J., 2021. Grapevine Microbiota Reflect Diversity among Compartments and Complex Interactions within and among Root and Shoot Systems. Microorganisms 9, 92. https://doi.org/10.3390/microorganisms9010092

Tabatabai, M.A., Bremner, J.M., 1969. Use of p-nitrophenyl phosphate for assay of soil phosphatase activity. Soil Biol. Biochem. 1, 301–307. https://doi.org/10.1016/0038-0717(69)90012-1

Tandonnet, J.-P., Cookson, S.J., Vivin, P., Ollat, N., 2009. Scion genotype controls biomass allocation and root development in grafted grapevine: Scion/rootstock interactions in grapevine. Aust. J. Grape Wine Res. 16, 290–300. https://doi.org/10.1111/j.1755-0238.2009.00090.x

Tedersoo, L., Bahram, M., Zinger, L., Nilsson, R.H., Kennedy, P.G., Yang, T., Anslan, S., Mikryukov, V., 2022. Best practices in metabarcoding of fungi: From experimental design to results. Mol. Ecol. 31, 2769–2795. https://doi.org/10.1111/mec.16460

Terral, J.-F., Tabard, E., Bouby, L., Ivorra, S., Pastor, T., Figueiral, I., Picq, S., Chevance, J.-B., Jung, C., Fabre, L., Tardy, C., Compan, M., Bacilieri, R., Lacombe, T., This, P., 2010. Evolution and history of grapevine (Vitis vinifera) under domestication: new morphometric perspectives to understand seed domestication syndrome and reveal origins of ancient European cultivars. Ann. Bot. 105, 443–455. https://doi.org/10.1093/aob/mcp298

Torres, N., Antolín, M.C., Goicoechea, N., 2018. Arbuscular Mycorrhizal Symbiosis as a Promising Resource for Improving Berry Quality in Grapevines Under Changing Environments. Front. Plant Sci. 9, 897. https://doi.org/10.3389/fpls.2018.00897

Torres, N., Yu, R., Kurtural, S.K., 2021. Arbuscular Mycrorrhizal Fungi Inoculation and Applied Water Amounts Modulate the Response of Young Grapevines to Mild Water Stress in a Hyper-Arid Season. Front. Plant Sci. 11, 622209. https://doi.org/10.3389/fpls.2020.622209

Tourna, M., Stieglmeier, M., Spang, A., Könneke, M., Schintlmeister, A., Urich, T., Engel, M., Schloter, M., Wagner, M., Richter, A., Schleper, C., 2011. Nitrososphaera viennensis , an ammonia oxidizing archaeon from soil. Proc. Natl. Acad. Sci. 108, 8420–8425. https://doi.org/10.1073/pnas.1013488108

Trevors, J.T., 2010. One gram of soil: a microbial biochemical gene library. Antonie Van Leeuwenhoek 97, 99–106. https://doi.org/10.1007/s10482-009-9397-5

Trouvelot, A., Kough, J.L., Gianinazzi-Pearson, V., Estimation of VA mycorhizal infection levels. Research for method having a functional significance. European symposium on mycorrhizae (1 ; Dijon 1985-07-01) http://pascal-francis.inist.fr/vibad/index.php?action=getRecordDetail&idt=8758731

Bibliographie

Trouvelot, S., Bonneau, L., Redecker, D., van Tuinen, D., Adrian, M., Wipf, D., 2015. Arbuscular mycorrhiza symbiosis in viticulture: a review. Agron. Sustain. Dev. 35, 1449–1467. https://doi.org/10.1007/s13593-015-0329-7

Uroz, S., Oger, P., Tisserand, E., Cébron, A., Turpault, M.-P., Buée, M., De Boer, W., Leveau, J.H.J., Frey-Klett, P., 2016. Specific impacts of beech and Norway spruce on the structure and diversity of the rhizosphere and soil microbial communities. Sci. Rep. 6, 27756. https://doi.org/10.1038/srep27756

Van Dam, N.M., Bouwmeester, H.J., 2016. Metabolomics in the Rhizosphere: Tapping into Belowground Chemical Communication. Trends Plant Sci. 21, 256–265. https://doi.org/10.1016/j.tplants.2016.01.008

Van Horn, C., Somera, T.S., Mazzola, M., 2021. Comparative Analysis of the Rhizosphere and Endophytic Microbiomes across Apple Rootstock Genotypes in Replant Orchard Soils. Phytobiomes J. 5, 231–243. https://doi.org/10.1094/PBIOMES-08-20-0058-R

Van Leeuwen, Destrac-Irvine, Dubernet, Duchêne, Gowdy, Marguerit, Pieri, Parker, De Rességuier, Ollat, 2019. An Update on the Impact of Climate Change in Viticulture and Potential Adaptations. Agronomy 9, 514. https://doi.org/10.3390/agronomy9090514

Van Zyl, J.L., 2017. Response of Colombar Grapevines to Irrigation as Regards Quality Aspects and Growth. South Afr. J. Enol. Vitic. 5. https://doi.org/10.21548/5-1-2365

Vannozzi, A., Donnini, S., Vigani, G., Corso, M., Valle, G., Vitulo, N., Bonghi, C., Zocchi, G., Lucchin, M., 2017. Transcriptional Characterization of a Widely-Used Grapevine Rootstock Genotype under Different Iron-Limited Conditions. Front. Plant Sci. 7. https://doi.org/10.3389/fpls.2016.01994

Venios, X., Korkas, E., Nisiotou, A., Banilas, G., 2020. Grapevine Responses to Heat Stress and Global Warming.
Vierheilig, H., Coughlan, A.P., Wyss, U., Piché, Y., 1998. Ink and Vinegar, a Simple Staining Technique for Arbuscular-Mycorrhizal Fungi. Appl. Environ. Microbiol. 64, 5004–5007. https://doi.org/10.1128/AEM.64.12.5004-5007.1998

Vink, Stefanie N., Chrysargyris, A., Tzortzakis, N., Salles, J.F., 2021. Bacterial community dynamics varies with soil management and irrigation practices in grapevines (Vitis vinifera L.). Appl. Soil Ecol. 158, 103807. https://doi.org/10.1016/j.apsoil.2020.103807

Vink, Stefanie Nicoline, Dini-Andreote, F., Höfle, R., Kicherer, A., Salles, J.F., 2021. Interactive Effects of Scion and Rootstock Genotypes on the Root Microbiome of Grapevines (Vitis spp. L.). Appl. Sci. 11, 1615. https://doi.org/10.3390/app11041615

Wang, W., Min, Z., Wu, J., Liu, B., Xu, X., Fang, Y., Ju, Y., 2021. Physiological and transcriptomic analysis of Cabernet Sauvginon (Vitis vinifera L.) reveals the alleviating effect of exogenous strigolactones on the response of grapevine to drought stress. Plant Physiol. Biochem. 167, 400–409. https://doi.org/10.1016/j.plaphy.2021.08.010

Wang, W., Shi, J., Xie, Q., Jiang, Y., Yu, N., Wang, E., 2017. Nutrient Exchange and Regulation in Arbuscular Mycorrhizal Symbiosis. Mol. Plant 10, 1147–1158. https://doi.org/10.1016/j.molp.2017.07.012

Wang, Z., Song, Y., 2022. Toward understanding the genetic bases underlying plant-mediated “cry for help” to the microbiota. iMeta 1, e8. https://doi.org/10.1002/imt2.8

Wemheuer, F., Taylor, J.A., Daniel, R., Johnston, E., Meinicke, P., Thomas, T., Wemheuer, B., 2020. Tax4Fun2: prediction of habitat-specific functional profiles and functional redundancy based on 16S rRNA gene sequences. Environ. Microbiome 15, 11. https://doi.org/10.1186/s40793-020-00358-7

Wilson, G.W.T., Rice, C.W., Rillig, M.C., Springer, A., Hartnett, D.C., 2009. Soil aggregation and carbon sequestration are tightly correlated with the abundance of arbuscular mycorrhizal fungi: results from long-term field experiments. Ecol. Lett. 12, 452–461. https://doi.org/10.1111/j.1461-0248.2009.01303.x

Wipf, D., Krajinski, F., Van Tuinen, D., Recorbet, G., Courty, P., 2019. Trading on the arbuscular mycorrhiza market: from arbuscules to common mycorrhizal networks. New Phytol. 223, 1127–1142. https://doi.org/10.1111/nph.15775

Bibliographie

Wright, A.H., Ali, S., Migicovsky, Z., Douglas, G.M., Yurgel, S., Bunbury-Blanchette, A., Franklin, J., Adams, S.J., Walker, A.K., 2022. A Characterization of a Cool-Climate Organic Vineyard's Microbiome. Phytobiomes J. 6, 69–82. https://doi.org/10.1094/PBIOMES-03-21-0019-R

Xiao, J.F., Zhou, B., Ressom, H.W., 2012. Metabolite identification and quantitation in LC-MS/MS-based metabolomics. TrAC Trends Anal. Chem. 32, 1–14. https://doi.org/10.1016/j.trac.2011.08.009

Xu, L., Pierroz, G., Wipf, H.M.-L., Gao, C., Taylor, J.W., Lemaux, P.G., Coleman-Derr, D., 2021. Holo-omics for deciphering plant-microbiome interactions. Microbiome 9, 69. https://doi.org/10.1186/s40168-021-01014-z

Ye, Q., Wang, H., Li, H., 2022. Arbuscular Mycorrhizal Fungi Improve Growth, Photosynthetic Activity, and Chlorophyll Fluorescence of Vitis vinifera L. cv. Ecolly under Drought Stress. Agronomy 12, 1563. https://doi.org/10.3390/agronomy12071563

Yoneyama, K., Brewer, P.B., 2021. Strigolactones, how are they synthesized to regulate plant growth and development? Curr. Opin. Plant Biol. 63, 102072. https://doi.org/10.1016/j.pbi.2021.102072

Yoneyama, Kaori, Mori, N., Sato, T., Yoda, A., Xie, X., Okamoto, M., Iwanaga, M., Ohnishi, T., Nishiwaki, H., Asami, T., Yokota, T., Akiyama, K., Yoneyama, Koichi, Nomura, T., 2018. Conversion of carlactone to carlactonoic acid is a conserved function of MAX 1 homologs in strigolactone biosynthesis. New Phytol. 218, 1522–1533. https://doi.org/10.1111/nph.15055

Yoneyama, Koichi, Xie, X., Yoneyama, Kaori, Kisugi, T., Nomura, T., Nakatani, Y., Akiyama, K., McErlean, C.S.P., 2018. Which are the major players, canonical or non-canonical strigolactones? J. Exp. Bot. 69, 2231–2239. https://doi.org/10.1093/jxb/ery090

Yu, G., Fadrosh, D., Goedert, J.J., Ravel, J., Goldstein, A.M., 2015. Nested PCR Biases in Interpreting Microbial Community Structure in 16S rRNA Gene Sequence Datasets. PLOS ONE 10, e0132253. https://doi.org/10.1371/journal.pone.0132253

Zaller, J.G., Cantelmo, C., Santos, G.D., Muther, S., Gruber, E., Pallua, P., Mandl, K., Friedrich, B., Hofstetter, I., Schmuckenschlager, B., Faber, F., 2018. Herbicides in vineyards reduce grapevine root mycorrhization and alter soil microorganisms and the nutrient composition in grapevine roots, leaves, xylem sap and grape juice. Environ. Sci. Pollut. Res. 25, 23215–23226. https://doi.org/10.1007/s11356-018-2422-3

Zanne, A.E., Abarenkov, K., Afkhami, M.E., Aguilar-Trigueros, C.A., Bates, S., Bhatnagar, J.M., Busby, P.E., Christian, N., Cornwell, W.K., Crowther, T.W., Flores-Moreno, H., Floudas, D., Gazis, R., Hibbett, D., Kennedy, P., Lindner, D.L., Maynard, D.S., Milo, A.M., Nilsson, R.H., Powell, J., Schildhauer, M., Schilling, J., Treseder, K.K., 2020. Fungal functional ecology: bringing a trait-based approach to plant-associated fungi. Biol. Rev. 95, 409–433. https://doi.org/10.1111/brv.12570

Zarraonaindia, I., Owens, S.M., Weisenhorn, P., West, K., Hampton-Marcell, J., Lax, S., Bokulich, N.A., Mills, D.A., Martin, G., Taghavi, S., Van Der Lelie, D., Gilbert, J.A., 2015. The Soil Microbiome Influences Grapevine-Associated Microbiota. mBio 6, e02527-14. https://doi.org/10.1128/mBio.02527-14

Zhang, H., Ullah, F., Ahmad, R., Ali Shah, S.U., Khan, A., Adnan, M., 2022. Response of Soil Proteobacteria to Biochar Amendment in Sustainable Agriculture- A mini review. J. Soil Plant Environ. 1, 16–30. https://doi.org/10.56946/jspae.v1i2.56

Zhang, L., Liu, Q., Li, K., Guo, X., Guo, Y., Liu, Z., Lin, H., An, D., Yang, F., 2022. Transcriptomic and metabolomic analyses reveal defense mechanism in 'Beta' grapevine root border cells under ρ-hydroxybenzoic acid stress. Sci. Hortic. 302, 111169. https://doi.org/10.1016/j.scienta.2022.111169

Zhang, L., Marguerit, E., Rossdeutsch, L., Ollat, N., Gambetta, G.A., 2016. The influence of grapevine rootstocks on scion growth and drought resistance. Theor. Exp. Plant Physiol. 28, 143–157. https://doi.org/10.1007/s40626-016-0070-x

Zhao, P., Xia, W., Lei, C., Omer, S.H.S., Zhang, X., Zhuang, Y., Chen, S., 2016. Isolation, Identification and Physiological Activity of Endophytes from the Roots of <I>Vitis vinifera</I>. Nanosci. Nanotechnol. Lett. 8, 532–538. https://doi.org/10.1166/nnl.2016.2164

Publications

Berger, M.M.J., Lailheugue, V., Zhelyazova, G., Stammitti, L., Lauvergeat, V., Barrieu, F., Gallusci, P., 2022. One prep to catch them all: "2 in 1", an efficient method for the simultaneous extraction of DNA and RNA from Grapevine tissues. OENO One 56, 1–13. https://doi.org/10.20870/oeno-one.2022.56.2.5000

Abstract:

Recent advances in our understanding of plant physiology and adaptation to the environment are tightly related to the development of 'omics'technologies such as metabolomics, transcriptomics, genomics and epigenomics that allow a more comprehensive view of the plant functioning. In this context, the ability to extract DNA and RNA from small amounts of plant material can be a limiting factor, worse in the case of non-model plants for which efficient nucleic extraction procedures are lacking. In the case of grapevine, extraction of high-quality DNA is typically limited by the high polyphenolic and polysaccharide contents of the different tissues. Here, we propose an adaptation of the method of Reid et al. (2006) that allows the simultaneous and efficient extraction of DNA and RNA from grapevine vegetative and berry tissues from in vitro grown grapevine plants and cells and from other plants. The protocol allows the extraction of high-quality RNA and DNA for standard molecular biology methods as well as for Next Generation Sequencing (NGS). It also works with a limited amount of plant material, such as young developing buds, and provides the means to analyse "omics" data from a single plant sample.

Darriaut, R., Lailheugue, V., Masneuf-Pomarède, I., Marguerit, E., Martins, G., Compant, S., Ballestra, P., Upton, S., Ollat, N., Lauvergeat, V., 2022. Grapevine rootstock and soil microbiome interactions: Keys for a resilient viticulture. Horticulture Research 9, uhac019. https://doi.org/10.1093/hr/uhac019

Abstract:

Soil microbiota has increasingly been shown to play an integral role in viticulture resilience. The emergence of new metagenomic and culturomic technologies has led to significant advances in the study of microbial biodiversity. In the agricultural sector, soil and plant microbiomes have been found to significantly improve resistance to environmental stressors and diseases, as well as inf luencing crop yields and fruit quality thus improving sustainability under shifting environments. Grapevines are

usually cultivated as a scion grafted on rootstocks, which are selected according to pedoclimatic conditions and cultural practices, known as terroir. The rootstock connects the surrounding soil to the vine's aerial part and impacts scion growth and berry quality. Understanding rootstock and soil microbiome dynamics is a relevant and important field of study, which may be critical to improve viticulture sustainability and resilience. This review aims to highlight the relationship between grapevine roots and telluric microbiota diversity and activity. In addition, this review explores the concept of core microbiome regarding potential applications of soil microbiome engineering with the goal of enhancing grapevine adaptation to biotic and abiotic stress.

Lailheugue, V., Merlin, I., Boutet, S., Perreau, F., Pouvreau, J.-B., Delgrange, S., Ducrot, P.-H., Cottyn-Boitte, B., Mouille, G., Lauvergeat, V., 2023. Vitislactone, a non-canonical strigolactone exudated by grapevine rootstocks in response to nitrogen starvation. Phytochemistry 215, 113837. https://doi.org/10.1016/j.phytochem.2023.113837

Abstract :

Strigolactones are compounds produced by plant roots in response to nutrient deficiency, acting both as local and systemic signals to control development and nutrition. Strigolactones are exuded in the rhizosphere to positively influence interactions with beneficial microbes. LC-MS/MS analysis shows that two genetically distinct grapevine rootstocks exudate one or two non-canonical strigolactones when subjected to low nitrogen conditions. Gene expression profiles and orobanche seed germination assays confirm that the biosynthesis and exudation of noncanonical compounds is the preferred pathway. The first compound, corresponding to heliolactone or 6- epiheliolactone, is only exuded by the rootstock showing lower shoot branching and a higher level of mycorrh ization with arbuscular mycorrhizal fungi. The structure of the second compound exuded by both rootstocks was identified by NMR and LC-MS/MS analysis. It is a non-canonicalstrigolactone, which has never been identified in another species. This first identification of a natural compound with the potential to stimulate beneficial rootmicrobe interactions in grapevines opens new perspectives in viticulture.

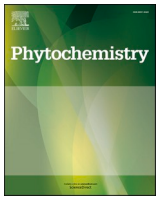
Phytochemistry 215 (2023) 113837



Contents lists available at ScienceDirect

Phytochemistry

journal homepage: www.elsevier.com/locate/phytochem





Vitislactone, a non-canonical strigolactone exudated by grapevine rootstocks in response to nitrogen starvation

Vincent Lailheugue [a,1], Isabelle Merlin [a,1], Stéphanie Boutet [b], François Perreau [b], Jean-Bernard Pouvreau [c], Sabine Delgrange [c], Paul-Henri Ducrot [b], Betty Cottyn-Boitte [b], Gregory Mouille [b], Virginie Lauvergeat [a,*]

[a] EGFV, Univ. Bordeaux, Bordeaux Sciences Agro, INRAE, ISVV, F-33882, Villenave d'Ornon, France
[b] Université Paris-Saclay, INRAE, AgroParisTech, Institut Jean-Pierre Bourgin (IJPB), 78000, Versailles, France
[c] Nantes Université, CNRS, US2B, UMR 6286, F-44000, Nantes, France

ARTICLE INFO

Keywords:
Vitis riparia
Grapevine
Exudates
Nitrogen
LC-MS/MS
NMR
Strigolactones
Vitislactone

ABSTRACT

Strigolactones are compounds produced by plant roots in response to nutrient deficiency, acting both as local and systemic signals to control development and nutrition. Strigolactones are exuded in the rhizosphere to positively influence interactions with beneficial microbes. LC-MS/MS analysis shows that two genetically distinct grapevine rootstocks exudate one or two non-canonical strigolactones when subjected to low nitrogen conditions. Gene expression profiles and orobanche seed germination assays confirm that the biosynthesis and exudation of non-canonical compounds is the preferred pathway. The first compound, corresponding to heliolactone or 6-*epi*-heliolactone, is only exuded by the rootstock showing lower shoot branching and a higher level of mycorrhization with arbuscular mycorrhizal fungi. The structure of the second compound exuded by both rootstocks was identified by NMR and LC-MS/MS analysis. It is a non-canonical strigolactone, which has never been identified in another species. This first identification of a natural compound with the potential to stimulate beneficial root-microbe interactions in grapevines opens new perspectives in viticulture.

1. Introduction

Throughout their life cycle, plants face different types of abiotic stresses. They must detect environmental modifications in order to adapt their development, but also interact with their environment to better respond to constraints such as drought, lack of nutrients, heat or cold, and limestone in the soil. In low phosphorus or nitrogen availability conditions, the root system adapts its growth and architecture in response to endogenous signals (phosphorus or nitrogen plant status), and exogenous signals (sensing of phosphate or nitrate soil content) (Lyzenga et al., 2023). Furthermore, during such adaptation processes, the roots exude a number of molecules into the soil whose biochemical composition and/or biological function are not always identified (Chai and Schachtman et al., 2022). Due to the difficulty of sampling root exudates in the field (Oburger and Jones, 2018), the interactions between roots and soil, according to nutrient availability, is still poorly understood, particularly for perennial woody plants (Wen et al., 2022). Different systems have been developed to overcome this problem of access to the root system on the one hand and to control the level of available nutrients in the medium on the other hand (Williams et al., 2021; Lopez-Guerrero et al., 2022). Hydroponic cultivation is the system most frequently used to harvest the culture medium in which roots have exuded for a few hours, and to analyze the composition of exudates depending on the nutrient availability in the nutritive solution (Strehmel et al., 2014; van Dam and Bouwmeester, 2016; Xie et al., 2021).

Strigolactones (SLs) are carotenoid-derived compounds that have been found to increase in root exudates when plants are subjected to phosphorus and nitrogen deficient conditions (for all species or depending on the species, respectively) (Yoneyama et al., 2012). Strigolactones were initially discovered as germination stimulants of

* Corresponding author.
E-mail addresses: vincent.lailheugue@u-bordeaux.fr (V. Lailheugue), merlin.isabelle@gmail.com (I. Merlin), stephanie.boutet@inrae.fr (S. Boutet), francois.perreau@inrae.fr (F. Perreau), Jean-Bernard.Pouvreau@univ-nantes.fr (J.-B. Pouvreau), Sabine.Delgrange@univ-nantes.fr (S. Delgrange), paul-henri.ducrot@inrae.fr (P.-H. Ducrot), betty.cottyn@inrae.fr (B. Cottyn-Boitte), gregory.mouille@inrae.fr (G. Mouille), virginie.lauvergeat@inrae.fr (V. Lauvergeat).
[1] Both authors contributed equally to this work.

https://doi.org/10.1016/j.phytochem.2023.113837
Received 12 June 2023; Received in revised form 21 August 2023; Accepted 22 August 2023
Available online 26 August 2023
0031-9422/© 2023 Elsevier Ltd. All rights reserved.

parasitic plants such as Striga spp (Cook et al., 1966). Due to the high sensitivity of seeds of Orobanche and Striga species to very low concentration of SL, bioassays using these seeds are still frequently performed to test the presence of SL-like compounds in an extract (Xie et al., 2019; Wakabayashi et al., 2022; Ge et al., 2023). SLs were then identified as root-derived signals involved in the establishment of arbuscular mycorrhizal symbiosis in the rhizosphere (Akiyama et al., 2005) before being classified as hormone-like compounds produced mainly by the roots in nutrient deficiency conditions, which act in a variety of ways, such as reducing shoot branching (root-shoot long distance signaling) and increasing root development (local response) (Guercio et al., 2023), in association with other phytohormones (Wu et al., 2022).

SLs are divided into two classes: canonical and non-canonical SLs (Guercio et al., 2023). Canonical SLs are composed of a tricyclic lactone (ABC-rings) connected to a (R)-configurated butenolide ring (D-ring) through an enol-ether bridge (Fig. 1). According to the stereochemistry of the C-ring, canonical SLs are divided into orobanchol- (β-oriented C-ring) and strigol-type (α-oriented C-ring). In contrast, non-canonical SLs are characterized by the lack of the A, B or C ring but retain the enol-ether bridge and the D-ring moieties (Mashiguchi et al., 2021).

The biosynthetic pathway to canonical and non-canonical strigolactones has not been fully identified. Carlactonoic acid (CLA) appears to be the common precursor of all SLs (Mashiguchi et al., 2021) (Fig. 1). SL canonical biosynthetic pathway downstream CLA has been partly identified in several plant species (Fig. 1). The non-canonical SL biosynthetic pathway is currently poorly characterized. The shared chemical substructure of methyl carlactonoate (MeCLA) with known non-canonical SLs suggests its involvement as an intermediate (Yoneyama et al., 2018). In *Arabidopsis thaliana*, the MeCLA is converted in a SL-like compound by the LATERAL BRANCHING OXIDOREDUCTASE (LBO), a 2-oxoglutarate-dependent dioxygenase (2OGD) (Brewer et al., 2016). The product of this reaction has been shown to be hydroxymethyl carlactonoate (1′–OH–MeCLA) but also CLA, in Arabidopsis, sorghum, maize and tomato (Yoneyama et al., 2020). 1′-OH'MeCLA is unstable and its role *in planta* is still not identified (Yoneyama and Brewer, 2021; Mashiguchi et al., 2021).

By screening for SL-defect mutants, Mori et al. (2020) discovered a novel 2OGD called LOTUSLACTONE-DEFECTIVE (LLD) in the non-canonical SL biosynthetic pathway. *LLD*-defective mutant could not produce lotuslactone in root exudates while its production was restored in transgenic roots expressing the WT *LLD* cDNA. However, the substrate and product of LLD remain to be determined.

Although it is logical to think that different forms of SLs must have different biological functions, no specific functions for canonical or non-canonical SLs have been clearly identified to date. Yoneyama et al. (2018) suggest that the two families of molecules can act as signal molecules in the rhizosphere for plant-plant or plant-microorganism communication, but that the molecules involved in regulating the internal root-shoot signal are likely non-canonical.

Vitis vinifera, the vine species cultivated for its fruit, is a woody perennial plant grown grafted onto rootstocks tolerant to a phylloxera, a soil-born parasite. These rootstocks are mainly American species of Vitis, which have different capacities to adapt to pedoclimatic constraints and control of the growth of the shoots (also called conferred vigor), yield and quality of the berry. We previously demonstrated that in response to heterogeneous nitrate availability, the transcription of genes of the SL biosynthetic pathway was activated in roots subjected to low nitrate concentrations in grafted grapevine plants (Cochetel et al., 2017). Further analysis showed that rootstock exudates exhibited SL-like activity (i.e., stimulation of parasitic plant seed germination) when grown hydroponically in a nitrate-free solution compared to a high nitrate solution (Cochetel et al., 2018). Comparative analysis of two rootstock genotypes showed differences between them. The rootstock Vitis riparia Gloire de Montpellier (RGM), well known for inducing low scion vigor and being poorly resistant to drought, seems to produce more strigolactone-like compounds and significantly reduces scion branching in low nitrate conditions, whereas the rootstock 1103Paulsen (1103P, a hybrid of Vitis berlandieri x Vitis rupestris) seems to be less sensitive to the difference in nitrogen nutrition. Understanding the molecular processes involved in these responses would make it possible to identify avenues for genetic improvement of grapevine rootstocks. The first aim of the present work was to confirm and quantify the presence of molecules of the SL family in exudates of both rootstocks grown hydroponically with a solution without nitrate. The related molecules were then purified, and their structure was elucidated using LC-MS/MS followed by NMR analysis. The activity of the crude exudates and purified compounds was evaluated using P. ramosa germination bioassays. The transcriptional regulation of genes involved in canonical and non-canonical SL biosynthesis and transport was studied in both rootstocks.

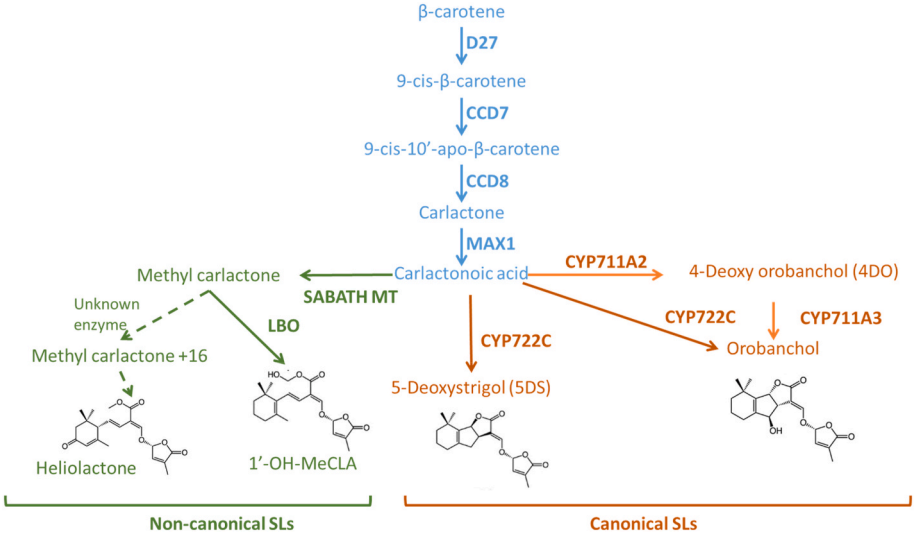


Fig. 1. SL putative biosynthetic pathway. Plastid-localized D27 (DWARF27), CCD7 (CAROTENOID CLEAVAGE DIOXYGENASE 7) and CCD8 (CAROTENOID CLEAVAGE DIOXYGENASE 8) lead to the formation of carlactone from all-*trans*-β-carotene. Carlactone would be oxidized by MAX1 (MORE AXILLARY GROWTH 1), a member of the CYP711A family to produce carlactonoic acid (CLA). CLA appears to be the precursor of both canonical and non-canonical SL. Members of the CYP711A and CYP722C families have been shown to produce canonical SLs (either Strigol-type or Orobanchol-type) from CLA in some species such as *Lotus japonicus*, *Gossypium arboreum*, *Solanum lycopersicum*, *Sorghum bicolor* and *Oryza sativa* (Mashiguchi et al., 2021). The first step of the synthesis of non-canonical SLs from CLA is the formation of MeCLA. A SABATH methyltransferase able to convert CLA to MeCLA has been recently identified (Wakabayashi et al., 2021). LBO (LATERAL BRANCHING OXIDOREDUCTASE) then allows the conversion of MeCLA to 1′–OH–MeCLA and CLA, as demonstrated in *Arabidopsis*, maize and sorghum. The enzymes involved in the last steps of non-canonical SLs such as heliolactone (produced by *Helianthus annuus*) are not yet identified. Solid arrows indicate the confirmed pathways, and the pathways with dashed arrows have not been fully established. 5-Deoxystrigol (5DS) is a Strigol-type SL.

2. Results and discussion

2.1. Two non-canonical strigolactones were identified in exudates of the Vitis riparia RGM rootstock by LC-MS/MS

We first selected the exudates of the RGM rootstock genotype in order to evaluate the presence, type and quantity of SL under N- and N+ conditions. This genotype had previously been shown to exhibit the most SL-like activity in its exudates compared to 1103P (Cochetel et al., 2018). The most sensitive mode of LC-MS/MS, multiple reaction monitoring (MRM), was used to monitor signals for specific existing strigolactones based on literature, to propose an identification based on the responding MRM transitions and to quantify them when they are present (Ravazzolo et al., 2019). Two molecules **1** and **2** eluting at the respective retention times of 10.76 and 10.26 min were proposed as SLs and quantified (Table 1 and Fig. S1).

1 (RT = 10.76 min) was quantified and confirmed to be a SL, on the one hand by the typical MRM signal of strigolactones from literature producing the butenolide fragment ion *m/z* 97 (*m/z* 363 > 97), and on the other hand by numerous other MRM transitions for strigolactones deduced from MS/MS data of Brewer et al. (2016) (*m/z* 363 > 231, 363 > 203, 363 > 249, 363 > 267 and 363 > 327). This suggested that **1** was a strigolactone with a MW of 362. Moreover, the sample exhibited a signal at the same RT for two supplementary new MRM transitions from known strigolactones with precursor ion *m/z* 345, 345 > 248 and 345 > 97. This precursor ion could have been a fragment produced by a water loss from MH + *m/z* 363 in the ionization source of the mass spectrometer. The two transitions from *m/z* 345 precursor are characteristic of SLs by fragment and neutral loss of the butenolide ring, supporting the hypothesis of a strigolactone for **1**. In order to obtain a MS/MS spectrum of *m/z* 363 and greater structural insights, we had to purify a larger sample (5 times 40 mL of exudate sample pooled together). The MS/MS spectrum of *m/z* 363 did indeed show numerous fragments (*m/z* 345, 327, 267, 249, 231, 203, 187 and 171) that corresponded to the those of the non-canonical SL hydroxymethylcarlactonoate MW 362 (Brewer et al., 2016; Yoneyama et al., 2020). This led us to believe that **1** could be a form of non-canonical SLs and might be a putative hydroxymethylcarlactonoate. In order to clarify the identity of **1** and determine the raw formula of this compound, more exudates were concentrated and purified by SPE and preparative HPLC to be submitted to LC-HRMS and MS/MS. **1** exhibited a protonated molecular ion $[M+H]^+$ that was measured at *m/z* 363.1802, corresponding to a raw formula of $C_{20}H_{27}O_6^+$ (0.2 ppm error, 2.7 msigma indicating an excellent isotope profile adequacy), as determined with the software SmartFormula from Bruker. High resolution MS/MS spectra of this $[M+H]^+$ gave a list of fragments similar to the previous low-resolution MS/MS fragment list, which determined the raw formula of the fragments (Fig. 2). All of these indications supported the hypothesis of a non-canonical SL, with similar characteristics to hydroxymethylcarlactonoate as measured by mass spectrometry. We decided to purify higher amounts of **1** from 25.5 L of grapevine exudates in order to be able to analyze its structure by NMR.

NMR spectra of **1** were recorded on less than 0.1 mg of **1** in different solvents at 400 MHz, in order to observe as many molecule signals as possible without being impacted by unavoidable signal overlap due to residual nondeuterated solvent and water. D_6-acetone, d_6-benzene and d-chloroform were used successively. In these three solvents, **1** exhibited similar spectra with only slight changes in chemical shifts (see Table 2 and Fig. S1-S3; some chemical shifts are lacking for quaternary carbons due to the very low quantity of **1**). Five systems of protons were observed from the COSY and HSQC spectra (Fig. S4-S14). The first one, composed of one methyl group and two methine protons (H-7′, 4′ and 5′), was easily assigned to the butenolide moiety as observed in all strigolactones. The second one, composed of three methine and two methylene protons (H-6′, 3a, 4 and 8b), is very similar to what has been described for the avenaol's γ-lactone (Kim et al., 2014) (Fig. 3), except for the chemical shifts of H-3a and H-4: the chemical shift of H-4 in **1** around 5 ppm (δ_C > 120 ppm) led us to propose the presence of a $\Delta^{4\text{-}5}$ double bond, but the very peculiar chemical shift of H-3a (δ_H > 5.2 ppm, δ_C around 38 ppm) has yet to be explained. The three last proton systems were a *gem*-dimethyl group, three coupled aliphatic methylenes and a very peculiar system composed of a methyl group coupled to the proton of an hydroxy group that was observed in all solvents (see Table 2 and Fig. S5-S7), even in the presence of a large excess of residual water. These results led us to propose structure **1** (Fig. 3), considering that a NOE (Fig. S16-S17) between H-4 and one of the methyl groups of the *gem*-dimethyl group allowed us to fix the stereochemistry of the $\Delta^{4\text{-}5}$ double bond as depicted on Fig. 3. Nevertheless, for the time being, none of the further NMR data has allowed us to choose between the four stereoisomers **1a**-**1d** (Fig. 4).

In an attempt to differentiate between these four isomers, we then sought to explain the peculiar chemical shift of H-3a and the lack of exchange between water and the labile proton at C-10 as well as its coupling with the methyl protons H-11. These two features led us to advocate a very peculiar constrained 3D structure for the molecule with a strong stabilization of the OH proton through a hydrogen bond with one of the oxygen atoms of the molecule. In all isomers, a hydrogen bond may be formed between the OH proton and the enol oxygen at C-6'. In the case of **1a**, a hydrogen bond is also possible with the oxygen 1' but leads to a lower stabilization of the molecule. However, the main feature arising when looking to the 3D model of **1a** (Fig. 5) is the almost coplanarity of the enol oxygen, C-10 and the oxygen and hydrogen atoms of the hydroxy group at C-10. This very peculiar geometry, which is not observed in isomers **1b**-**d**, may account for a rigidification of the structure, allowing for the long-range coupling between the labile proton and the methyl group H-11. In this conformation of **1a**, H-3a is observed in the orthogonal plane at the oxygen atom at C-10 to the plane described above at a distance of about 2.28 Å from the oxygen atom at C-10. This disposition, not observed in the other isomers (Fig. S18), may allow the anisotropic effect of the oxygen to induce the very high chemical shift observed for H-3a. We therefore propose that structure **1a** is the most suitable to explain the NMR data of 1. The closest molecule, whose structure is not published to date, seems to be cannalactone, purified from hemp root exudate (Hamzaoui et al., 2019; Fornier et al., 2022). The trivial name of vitislactone was therefore proposed for this compound.

2 (RT = 10.26 min) was quantified and confirmed by typical MRM channels of strigolactones *m/z* 361 > 97 and *m/z* 361 > 233. *m/z* 361 > 97 and is characteristic of the butenolide ring of strigolactones. These

Table 1
MRM signals responding in LC-MS of grapevine exudates, corresponding to putative strigolactones (RT: retention time, Q: main transition used for quantification, C: secondary transition used for confirmation purpose).

MRM transitions	RT (min)	Q/C	Strigolactone ions known to respond for this transition
361 > 97	10.26	Q	[M+H]+ of 7-oxoorobanchol, methoxy-5-deoxystrigol or heliolactone
361 > 233	10.26	C	[M+H]+ of 7-oxoorobanchol, methoxy-5-deoxystrigol or heliolactone
363 > 97	10.76	Q	[M+H]+ of 7-hydroxyorobanchol or peogol or MeCLA+16
363 > 231	10.76	C	[M+H]+ of 7-hydroxyorobanchol or peogol or MeCLA+16
363 > 203	10.76	C	[M+H]+ of 7-hydroxyorobanchol or peogol or MeCLA+16
363 > 249	10.76	C	[M+H]+ of 7-hydroxyorobanchol or peogol or MeCLA+16
363 > 267	10.76	C	[M+H]+ of 7-hydroxyorobanchol or peogol or MeCLA+16
363 > 327	10.76	C	[M+H]+ of 7-hydroxyorobanchol or peogol or MeCLA+16
345 > 248	10.76	C	[M + H–H_2O]+ of 7-hydroxyorobanchol or peogol or MeCLA+16
345 > 97	10.76	C	[M + H–H_2O]+ of 7-hydroxyorobanchol or peogol or MeCLA+16

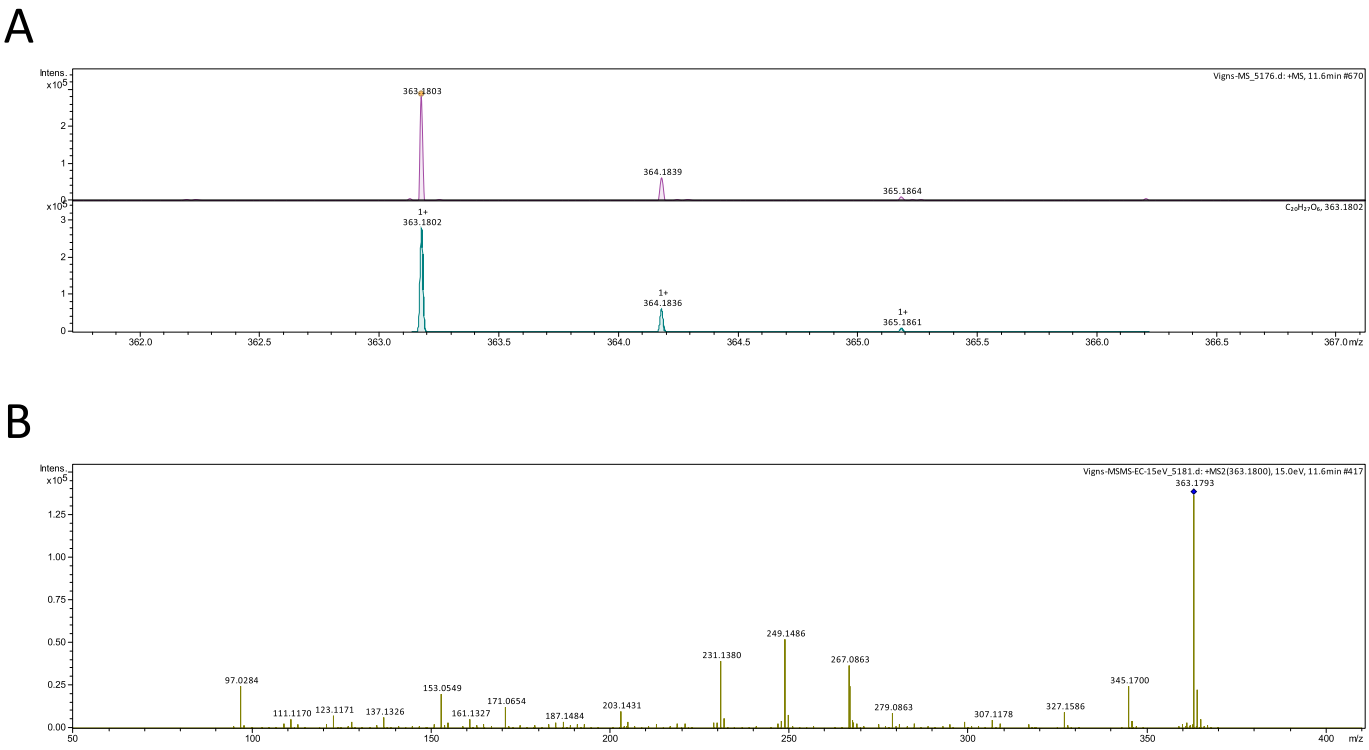


Fig. 2. LC-HRMS spectra of 1 from grapevine root exudate in positive mode. A) MS spectrum of 1, experimental and theoretical isotope profiles for the proposed chemical formula: $C_{20}H_{27}O_6^+$ and B) MS/MS spectrum of the parent ion *m/z* 363.1803 from **1.**

Table 2
NMR chemical shifts of the main observed signals for 1.

No.	CD_3COCD_3		C_6D_6		$CDCl_3$	
	δ^H (ppm) mult. *J* (Hz)	δ^C (ppm)	δ^H (ppm) mult. *J* (Hz)	δ^C (ppm)	δ^H (ppm) mult. *J* (Hz)	δ^C (ppm)
2′	–	170.6	–	n.o.	–	170.5
3′	–	134.7	–	n.o.	–	136.5
4′	7.33 m	142.3	5.64 m	140.0	6.98 m	140.2
5′	6.55 m	101.4	4.85 m	101.2	6.13 m	100.7
6′	7.57 d *2.8*	150.7	7.18 bs	150.7	7.51 d *2.3*	150.7
7′	1.98 bs	9.7	1.39 bs	1.39	2.03 t *1.5*	10.5
2	–	n.o.	–	n.o.	–	n.o.
3	–	n.o.	–	n.o.	–	n.o.
3a	5.26 m	36.7	5.15 m	36.7	5.27 m	36.4
8b	4.54 t *8.8* 3.92 dd *8.8* *6.3*	71.7	3.94 bt *9.0* 3.42 bt *9.0*	71.1	4.52 t *8.3* 3.95 dd *8.3* *5.9*	72.1
4	5.36 d *9.5*	123.3	4.99 d *9.3*	122.8	5.27 m	122.4
5	–	152.6	–	n.o.	–	153.9
6	–	36.5	–	n.o.	–	39.5
7	1.7 m 1.25 m	30.3	n.o.	n.o.	1.30	29.3
8	1.59 m 1.55 m	19.2	1.37 m 1.33 m	19.3	1.58 m	19.2
9	1.46 m 1.43 m	42.9	1.75 m 1.4 m	45.3	1.88 m 1.36 m	43.7
10	–	73.5	–	n.o.	–	74.6
11	1.39 bs	30.3	1.28 bs	29.9	1.41 bs	30.0
12	1.09 s	30.7	0.96 s	31.7	1.10 s	31.8
13	1.07 s	31.4	0.83 s	31.3	1.08 s	31.8
OH	2.95 bs	–	2.25 bs	–	2.38 bs	–

MRM signals suggested that the molecular weight (MW) of this molecule is 360 g/mol. Only three strigolactones with this mass were previously known in the literature, 7-oxoorobanchol and methoxy-5-deoxystrigol (two main transitions *m/z* 361 > 247 and *m/z* 361 > 97, Cardoso et al., 2014) and heliolactone (two main transitions *m/z* 361 > 233 and *m/z* 361 > 97, Charnikhova et al., 2017). As corresponding standard was not available, a sunflower exudate was produced as described in Chabaud et al. (2022) except that the medium was slightly modified (TT/2) and concentrated with SPE following the same method as for grapevine exudates. Then, grapevine exudate was compared under the same analysis conditions to this sunflower exudate, which is known to contain heliolactone (Ueno et al., 2014) and inducing germination of *Orobanche cumana* seeds (90%, data not shown). The retention times as well as the peak area ratios between the main MRM transitions 361 > 97 361 > 233 and 361 > 247 were found to be identical between both exudates. However, as 6-*epi*-heliolactone found in root exudates of *Avena strigosa* has been shown to be highly difficult to separate using UPLC or reverse-phase HPLC (Moriyama et al., 2022), we concluded that **2** is heliolactone or 6-*epi*-heliolactone.

2.2. The two rootstocks exudate different profiles of biologically active non-canonical strigolactone compounds in nitrogen deficient conditions

Since the two rootstock genotypes have different genetic origins, it was then important to verify the presence of similar molecules in the root exudates of both rootstocks under N- conditions.

Exudates from both rootstocks cultivated in N- or N+ conditions were harvested, and the presence of biologically active compounds was first assessed using P. ramosa bioassays. We used two ecotypes with different sensitivity to canonical and non-canonical strigolactones: *P. ramosa* 2a hosted by hemp *C. sativa* and *P. ramosa* 1 from oilseed rape *B. napus* (Stojanova et al., 2019). It has been previously demonstrated that the germination of the seeds of *P. ramosa* can be selectively induced by different SLs. *P. ramosa* 1 is more sensitive to canonical SL (de Saint Germain et al., 2019; Dvorakova et al., 2019; Huet et al., 2020) and *P. ramosa* 2a is more sensitive to non-canonical strigolactones than *P. ramosa 1* (Hamzaoui et al., 2019; Fornier et al., 2022). The exudates of both rootstocks showed a higher germination activity, regardless of the *P. ramosa* genotype, when plants were subjected to N- treatment than N+ treatment (Fig. 6 A-D and Fig. S19). This result confirms that the two grapevine rootstocks exudate SL-like compounds when they are grown

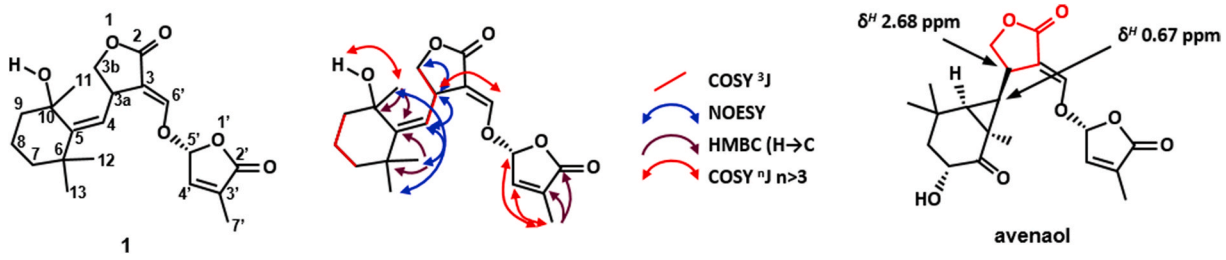


Fig. 3. Structure of vitislactone **1**, diagram of the most important correlations extracted from 2D homo and heteronuclear spectra, and structure of avenaol as a comparison.

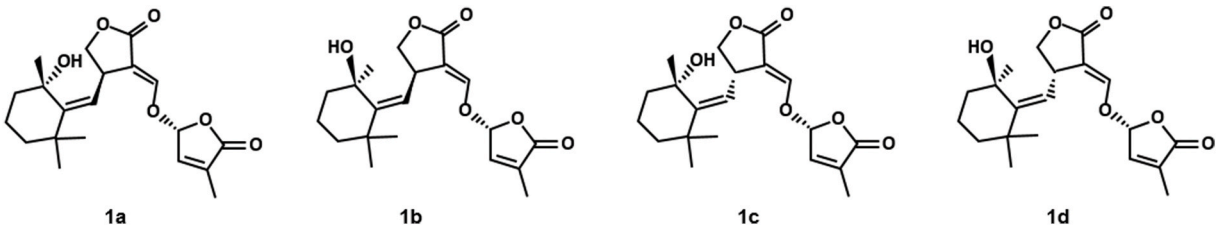


Fig. 4. Structures of the four isomer hypotheses for 1, vitislactone being proposed as the structure 1a.

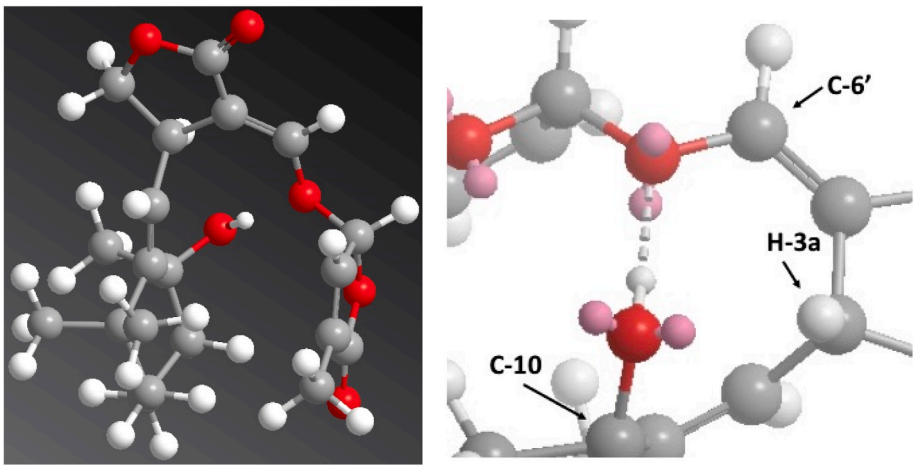


Fig. 5. Molecular model of isomer 1a: general view and close-up showing the possible influence of the oxygen atom at C-10 on the chemical shift of H-3a, taking into account the hydrogen bond between (O)H at C-10 and the oxygen atom at C-6.

in nitrogen depleted nutritive solution, as previously published (Cochetel et al., 2018). The germination stimulant activity is higher for *P. ramosa* 2a than for *P. ramosa* 1 for all samples, which is in accordance with the presence of non-canonical SLs in those exudates. Root exudates from N+ condition also showed a stimulant germination activity on *P. ramosa* 2a (25–60% of germination relative to GR24 when diluted at 1:10).

LC-MS/MS analysis confirmed that the N- condition induced the presence of strigolactones in the exudates of both genotypes (Fig. 6E and F). Vitislactone (MW 362) was detected in both genotypes and was significantly increased in N- condition (10–20 times higher) compared to N+ condition. The heliolactone-like compound (MW 360) compound was detected in exudates of 11 out of 12 RGM plants grown in N- condition (Fig. 6F)), but was not detected in 1103P exudates (over 10 individual plants). Heliolactone-like compound was detected in only one sample of exudates from RGM grown in N+ condition over a total of 13 plants. All these data suggest either that the heliolactone-like compound is specifically produced by RGM genotype in N- conditions or that this compound is present in 1103P exudates but at levels too low to be detected by LC-MS/MS.

The ability of purified vitislactone and heliolactone-like compound to induce the germination of seeds of broomrape species have been assayed (Fig. 7 and Fig. S20). Whereas (±)-GR24, analog of canonical SL, exhibited a lower activity for *P. ramosa* 2a than *P. ramosa* 1 (EC50 ± SE, $7.2 \pm 3.2\ 10^{-10}$ mol L^{-1} and $4.5 \pm 1.5\ 10^{-11}$ mol L^{-1}, respectively), vitislactone was more efficient on *P. ramosa* 2a than on *P. ramosa 1* which is consistent with its non-canonical type structure (EC50 ± SE, $3.4 \pm 0.2\ 10^{-11}$ mol L^{-1} and $1.0 \pm 0.1\ 10^{-9}$ mol L^{-1} respectively). The same result was found for cannalactone (Hamzaoui et al., 2019), a non-canonical strigolactone produced by hemp, and with a structure that seems highly similar to vitislactone (data not shown). Heliolactone-like compound purified from RGM root exudates was as effective in inducing the germination of *P. ramosa* 2a as of *P. ramosa* 1 (EC50 ± SE, $5.0 \pm 1.8\ 10^{-10}$ mol L^{-1} and $5.6 \pm 0.4\ 10^{-10}$ mol L^{-1}, respectively). These results confirm that the stimulation activity of the parasitic plant seed germination of grapevine rootstock root exudates cultivated in N+ and N- solution is mainly due to the presence of vitislactone. RGM exudates induce more efficiently the *P. ramosa* 1 germination than 1103P exudates. This difference in activity between the two genotypes may be due to the presence and increase in heliolactone-like

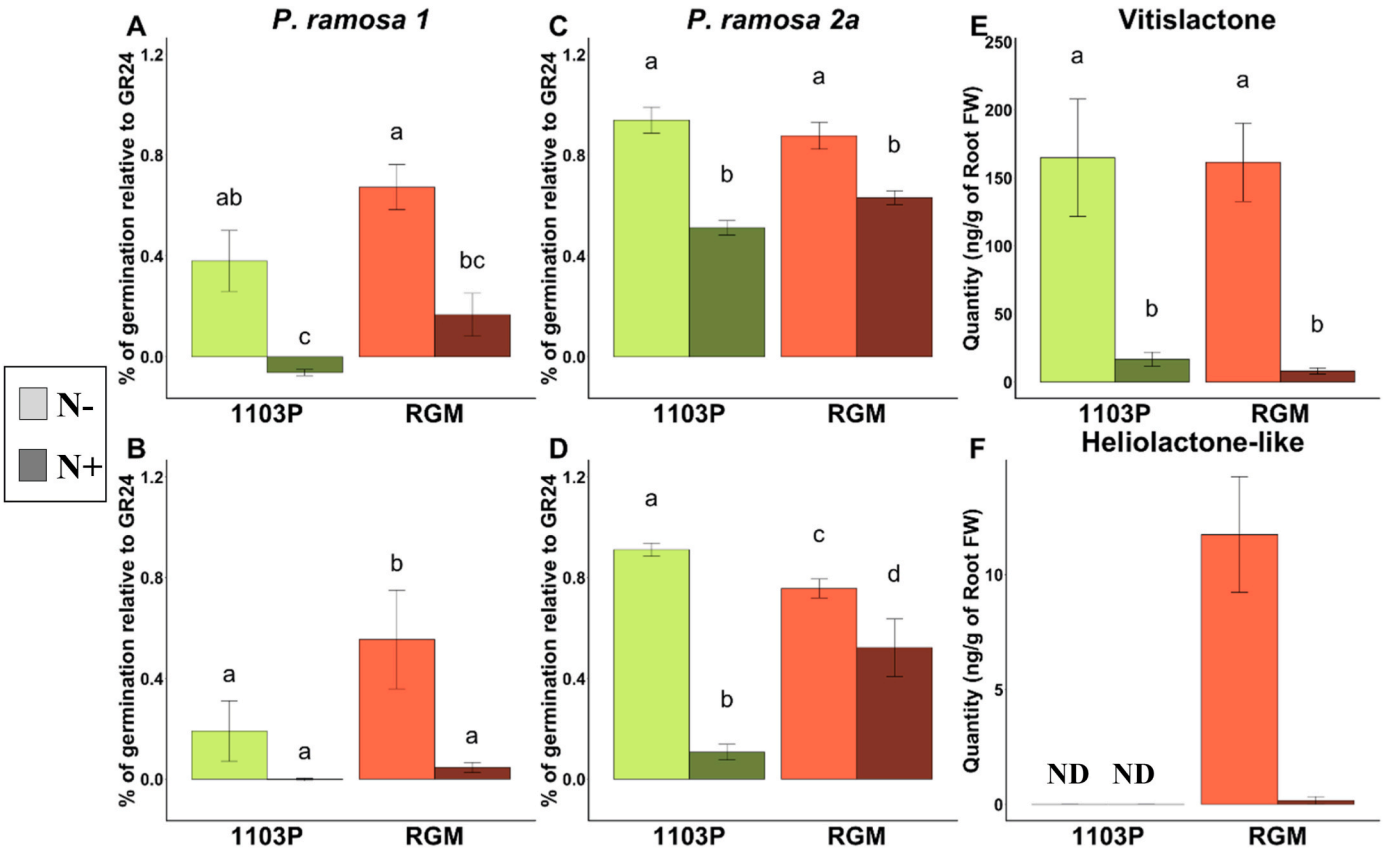


Fig. 6. Quantification of SLs in root exudates of both rootstocks and *P. ramosa* seed germination stimulant activities of grapevine root exudates. Activity of exudates on *P. ramosa* 1 (A–B) and *P. ramosa* 2a (C–D) seed germination. Germination stimulant activities are presented as a percentage relative to the positive control GR24 (1 μM). The root exudates samples were diluted 1:2 (A, C) and 1:10 (B, D). Data are presented as means ± SE, n = 5 (five biological replicates repeated two times). Letters indicate significant differences between treatments (i.e., condition × genotype) using a paired *t*-test ($P < 0.05$). Quantitative analysis of the relative amounts of vitislactone (E), b) heliolactone-like compound (F) in root exudates for both genotypes 1103P (green) and RGM (red), in N+ (dark colors) and N- (light colors) conditions as determined by LC-MS/MS MRM. Data are presented in ng equivalent GR24 per gram of root fresh weight, as means ± SE ($10 \leq n \leq 13$). ND = not detected. Only one biological sample over 13 showed a detectable heliolactone-like compound level from RGM grown in N+.

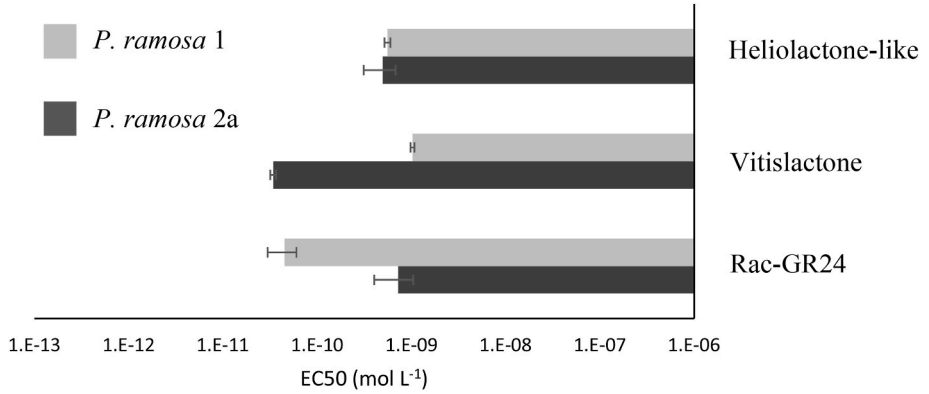


Fig. 7. Bioactivity on *P. ramosa* 1 and *P. ramosa* 2a seed germination of purified heliolactone-like compound and vitislactone from RGM root exudates. EC50 (half maximal effective concentration) ($mol.L^{-1}$) of heliolactone-like compound and vitislactone purified from RGM exudates, and racemic-GR24 EC50 values are presented ± SE, ($6 \leq n \leq 12$).

compound in RGM genotype.

Even though the germination stimulant activity was higher in N- than N+ root exudates for both *P. ramosa* ecotypes would suggest the presence of biologically active non-canonical strigolactones, the absence of clear correlation between the level of detected compounds and the biological activity indicates that other compounds are able to selectively stimulate the germination of Phelipanche seeds. Molecules other than SLs have indeed been shown to play a role in the recognition of a plant host by broomrape seeds (Auger et al., 2012; Joel et al., 2011; Nelson, 2021; Miura et al., 2022).

2.3. *Gene expression profiles confirm that the biosynthetic pathway leading to non-canonical strigolactone production is induced by nitrogen deficiency in grapevines*

Transcript level patterns of genes involved in SL biosynthetic and

transport pathways (Fig. 8) showed that genes encoding enzymes involved in the synthesis of carlactonoic acid (*CCD7*, *CCD8* and *MAX1*) are all significantly induced in N- conditions compared to N+ conditions in both genotypes. The same result was obtained for *D27* (data not shown). The general precursor of canonical and non-canonical SLs is therefore significantly induced by nitrogen deficiency in both genotypes of grapevine rootstocks.

CYP722C was a good candidate for studying whether the canonical biosynthesis pathway is activated by low nutrient level in the medium because it was described as being involved in orobanchol or 5DS synthesis, depending on the species (Mori et al., 2020; Wakabayashi et al., 2019, 2020). The transcripts of a grapevine homolog of *CYP722C* were weakly detected in all samples and the expression of this gene was not affected by N treatment.

On the other hand, the expression level of a homolog of *LBO* gene fits perfectly with those of the carlactonoic acid general pathway. Transcript level was significantly higher in N- condition compared to N+ condition for both genotypes. LBO was shown to be involved in the synthesis of 1′–OH–MeCLA in *Arabidopsis*, maize, tomato and sorghum (Brewer et al., 2016; Yoneyama, 2020; Yoneyama and Brewer, 2021). Even if the role of this strigolactone-like compound is still not elucidated, the induction of expression of the grapevine *LBO* gene during N-treatment suggests that the pathway leading to non-canonical SLs is efficient in grapevine, which is in accordance with the detection of non-canonical SLs in the exudates.

The level of expression of a gene encoding a SL transporter, PDR1 (PLEIOTROPIC DRUG RESISTANCE 1, Shiratake et al., 2019), was also studied and this gene was significantly induced by N- treatment compared to N+ treatment in both genotypes. In Petunia, PDR1 has been demonstrated to be involved in SLs exudation from the hypodermis to the soil rather than root-shoot long distance transport (Shiratake et al., 2019). The high expression of the homologous gene in grapevine

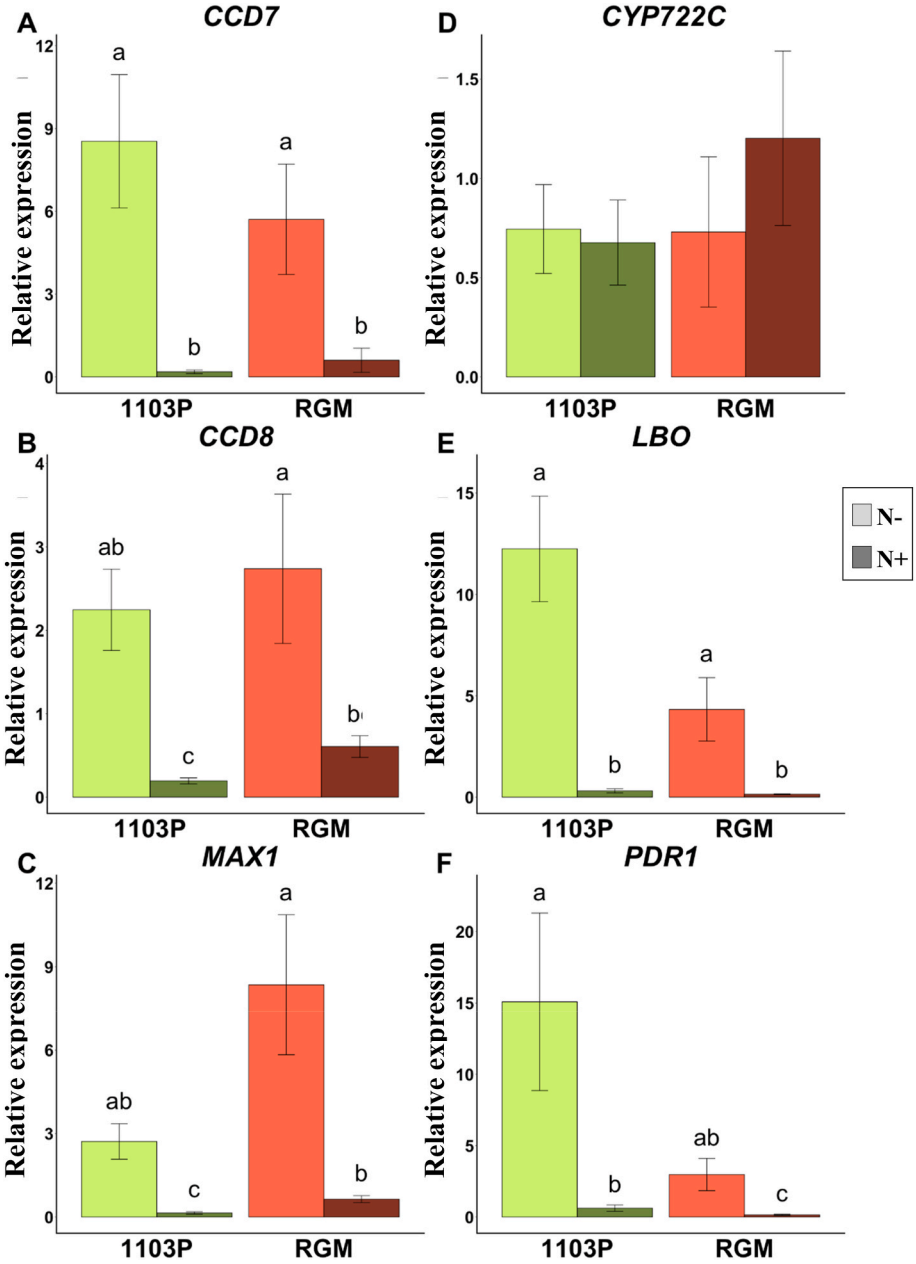


Fig. 8. Transcript levels of SL-related biosynthesis and transport in roots of 1103P (green) and RGM (red) grapevine roots grown hydroponically and subjected to N- (light colors) and N+ (dark colors) conditions. Data are presented as means ± SE (n = 5). Letters indicate significant differences between treatments (i.e., condition x genotype) using a pairwise.t.test ($P < 0.05$).

rootstocks when nitrogen is depleted from the medium is therefore consistent with the higher presence of both SLs in exudates compared to the medium with high nitrate level. No clear significant difference in the level of expression between the two genotypes could be identified for any of these genes.

3. Conclusions

This study represents the first identification of grapevine SLs in root exudates. Two non-canonical SLs were identified and purified from root exudates of *Vitis* plants cultivated hydroponically in medium without nitrogen. The most abundant, which we have named Vitislactone, is a SL with a new structure. The second one is an heliolactone-like compound and has been detected only in RGM exudates. No signals related to canonical SLs were detected in either of the *Vitis* exudates. Canonical SLs have been found in roots of *Vitis vinifera* cv. 'Muscat Hamburg' using a targeted approach by Xu et al. (2021), and Jiu et al. (2022). Strigol and ent-2′-epi-5DS have been identified and the content of these SLs in roots was associated with the restriction of root development in greenhouse experiments (Xu et al., 2021). In our work, both non-canonical SLs were able to stimulate parasitic plant seeds of broomrape species. The two rootstocks induced symbiosis with *Rhizophagus irregularis* when grown in nitrate deficiency conditions (Fig. S21) in a controlled experiment in a growth chamber, indicating that the roots produce a signal able to stimulate this interaction. Interestingly, RGM rootstock showed a significantly higher intensity of colonization and a higher relative abundance of Glomeromycota sequences than 1103P when grown in symptomatic vineyard soils (Darriaut et al., 2022). Further studies are needed to clarify the pathway of SL biosynthesis in grapevine rootstocks and their roles in the control of biotic interactions, especially with soil microbiome under stress conditions such as drought.

4. Experimental

4.1. Plant material and growth conditions

Vitis berlandieri x *V. rupestris* cv. 1103 Paulsen (1103P) and *V. riparia* cv. Riparia Gloire de Montpellier (RGM) cuttings were propagated *in vitro* and transferred in hydroponic conditions as described in Cochetel et al. (2018). *In vitro* cuttings were grown on McCown Woody Plant Medium (Duchefa) supplemented with 30 g L^{-1} sucrose, 0.27 μM 1-naphtalene acetic acid and 7 g L^{-1} agar. The growth conditions were 22 °C with a 16 h light/8 h dark photoperiod and a light intensity of 55 μmol m^{-2} s^{-1}. One-month-old plantlets were acclimated on perlite substrate, irrigated with tap water for one month in a growth chamber at 26 °C and subjected to the same photoperiod with a light intensity of 145 μmol photons m^{-2} s^{-1}. Plants were transferred into aerated hydroponic jars containing 8 L of a McCown-derived nutrient solution deprived of vitamins and with 5 mM of NH_4NO_3 and 2.35 mM of Ca $(NO_3)_2$ $4H_2O$ (HN nutritive solution) for 1 week, followed by 1 week of culture in a solution without any source of N (0N nutritive solution). Calcium concentration was adjusted by adding 0.65 or 3 mM of $CaCl_2$ to HN and 0N solutions respectively. Plants were then separated into two groups and moved to the HN condition or kept in the 0N condition for 48 h.

4.2. Root exudate collection and root sampling

At the end of the 48 h, each plant was transferred to a 50 mL tube containing a new nutrient solution (ON or HN depending on the treatment), covered with aluminum foil, and incubated for 24 h in the growth chamber. The exudates were weighted and filtered through 0.2 μm filters and stored at 4 °C in the dark. A 2 mL aliquot was used to do the *Phelipanche ramosa* seed germination assays, and the rest for LC-MS/MS MRM analysis. The fresh weight of the root system was measured for each plant at the end of the experiment. The roots were frozen immediately in liquid nitrogen and kept at −80 °C pending further analysis.

For strigolactone identification, the exudates were collected from 250 individual RGM plants in 0N condition each day for five consecutive days, resulting in 25.5 L of exudates, which were filtered and stored at 4 °C in the dark before the extraction step.

4.3. LC-MS/MS quantification and identification of strigolactones compounds in grapevine root exudates

SL quantification was obtained using the same conditions of extraction of 50 mL of root exudate from the two rootstock genotypes and LC-MS/MS analysis as described in Ravazzolo et al. (2019). Two independent experiments were carried out on five to seven individual plants to confirm the results.

SL identification was performed on 25.5 L of root exudates from the RGM rootstock that underwent several concentration and purification steps. The 25.5 L were first concentrated by Solid Phase Extraction (SPE). Root exudates were loaded 1 L by 1 L onto Strata-X 33 μm Polymeric Solid Phase Extraction (SPE, Phenomenex) columns and then washed with 4 mL of distilled water. Flow and wash volumes were pooled (FT). Elution was carried out with 4 mL of acetonitrile (ACN). Twenty eight SPEs were performed and the eluates were pooled to obtain 112 mL of eluate. The acetonitrile of this eluate was then evaporated using a Rotavapor R II (Buchi) and the aqueous phase concentrated again by SPE plus evaporation to reduce the volume to 0.4 mL. In a second step, the fraction was resuspended and subsequently purified by SPE silica cartridge Upti Clean Si–S 10g/60 mL (Interchim, Montluçon, France) previously activated with 30 mL heptane and pre-equilibrated with 30 mL of heptane/ethyl acetate (90/10, v:v). The SPE column was washed with 30 mL heptane/ethyl acetate 40/60 v:v, the fraction containing SLs 362 was obtained by elution of 30 mL heptane/ethyl acetate 17/83 v:v. This fraction was evaporated to dryness and then redissolved in 140 μL acetonitrile. At each step the germination stimulant activity of each fraction (crude exudates, FT, eluates), was controlled as described below (section 4.5), to confirm the presence or absence of strigolactone activity.

A third step of purification was required for NMR analyses and was performed by HPLC, using a BEH C18 column (2.1 * 100 mm, particle size 1.7 μm, Waters, Milford, MA, USA) at 40 °C, an ACQUITY UPLC I-class system (Waters, Milford, MA, USA), equipped with an ACQUITY Binary Solvent Manager and ACQUITY Sample Manager with a flow rate of 0.4 mL/min, for 10 μL injected. Eluents A and B were water and acetonitrile, respectively. Elution was as follows: 5% B for 2 min, 5–50% B in 8 min, 50–100% B in 3 min, 100% B for 3 min, 5% B for 3 min. Only the fraction corresponding to the retention time range between 10.3 min and 11.3 min were collected (Fig. S1). This HPLC purification step was repeated 16 times, representing 160 μL of the previous SPE fraction. All the HPLC fractions obtained were then pooled to give a concentrated and highly purified extract and evaporated for NMR analyses.

To confirm the raw formula, an UHPLC system (Ultimate 3000 Thermo) coupled to quadrupole time of flight mass spectrometer (Q TOF Impact II Bruker Daltonics, Bremen, Germany) was used. The LC conditions were similar to the purification conditions previously described. A data dependent acquisition (DDA) method was used for mass spectrometer acquisition in positive ESI mode using the following parameters: capillary voltage, 4.5 kV; nebulizer gas flow, 2.1 bar; dry gas flow, 6 L/min; drying gas in the heated electrospray source temperature, 140 °C; acquisition frequency, 8Hz; mass range, 100–1500 m/z. Stepping acquisition parameters were created to improve the fragmentation profile with a collision RF from 200 to 700 Vpp, a transfer time from 20 to 70 μs and a collision energy from 20 to 40 eV. Each cycle included a MS full scan and 5 MS/MS CID on the 5 main ions of the previous MS spectrum.

4.4. NMR analysis

1D ^{1}H and ^{13}C as well as homo and hetero 2D spectra were recorded successively in d_6-acetone, d_6-benzene and d-chloroform (the same tube was used for all experiments and solvents were carefully evaporated under argon between the different sets of experiments) on a BRUKER Ascend 400 spectrometer (400 MHz) equipped with a BBO probe. Topspin 3.2 was used for the setting of standard pulse sequences and data analysis. Signal of residual solvent was used in each case for chemical shift calibration.

4.5. P. ramosa seed germination assays

The germination-stimulant activity of grapevine exudates on seeds of *Phelipanche ramosa* L. *Pomel*, was measured using 3-(4,5-dimethylthiazol-2-yl)-2,5-diphenyltetrazolium bromide assays as described by Pouvreau et al. (2021). Assays were done with two *Phelipanche ramosa* associated to different genetic groups (Stojanova et al., 2019). The first one, *P. ramosa* 1 corresponds to *Phelipanche ramosa* (L.) Pomel harvested in St Jean d'Angely, France, on broomrape parasitizing winter oilseed rape *(Brassica napus* L.) in 2015 (US2B code: Pram120). The second, identified as *P. ramosa* 2a, corresponds to *Phelipanche ramosa* harvested in Saint Martin de Bossenay, France, on broomrape developed on *Cannabis sativa*, in 2012 (US2B code: Pram76). Data were reported as a percentage relative to the positive control (±)-GR24 (kindly provided by François-Didier Boyer CNRS, ICSN, Gif/Yvette, France). To confirm the results, two independent experiments (dilution and germination assays) were done with at least five biological replicates. For both purified compounds tested, response curves (Germination stimulation = f(c), Germination Stimulant activity relative to (±)-GR24 1 µmol.L^{-1}; c: concentration (mol.L^{-1}), half maximal effective concentration (EC50), and maximum of germination stimulant activity were determined using a Four Parameter Logistic Curve computed with SigmaPlot® 10.0.

4.6. Transcript level quantification

Total RNA was isolated from root samples as described in Cookson et al. (2013). Total RNA (1.5 µg) was reverse transcribed into cDNA using the iScript™ Advanced cDNA Synthesis Kit (Bio-Rad). Quantitative PCRs were performed using GoTaq® qPCR Master Mix (Promega) on a iCycler iQH (Bio-Rad) according to the procedure provided by the supplier. Primer sequences used for *CCD7*, *CCD8*, *MAX1* and *PDR1* were the same as described in Cochetel et al. (2018). LBO and CYP722C protein sequences from *Arabidopsis thaliana* (AT3G21420) and *Gossypium arboretum* (LC528626.1), respectively, were used to identify Vitis genes encoding homologous proteins using tblastn (*XM_034829441.1* and XM_034827578.1, respectively). The following primers were then used for qPCR: F-VrLBO: 5′-GAGATTGAGCTTGGCCCCAT; R-VrLBO: 5′-CCCTCCAGCTTGCTAGTCAC; F-VrCYP722C: 5′- GCTTGAAACTCATGAAGGGCT and R-VrCYP722C: 5′-CTCATCGCAACTCCCTGCTT. Normalized Relative Quantities were determined according to Hellemans et al. (2007), using GAPDH and EF1γ references genes.

4.7. Statistical analyses

All statistical analyses were performed using the software R (version 4.2.1). The figures illustrating the results of parasitic seed germination assays, transcript level quantification and SLs concentration were generated using *ggtheme* (version 4.2.4) and *ggplot2* (version 3.4.1) packages and arranged with *ggpubr* (version 0.4.0). A variable with four levels was created to compare the treatments (1103P N-, 1103P N+, RGM N-, RGM N+). The comparison between groups was done using pairwise *t*-test ($\alpha = 0.05$) after one-way Anova. Residuals were checked for their normality and variance homogeneity with the Shapiro–Wilk and Levene tests, respectively. When assumptions for parametric tests were not respected, a multiple comparison using a Wilcoxon test was performed after a Kruskal-Wallis test.

Declaration of competing interest

The authors declare that they have no known competing financial interests or personal relationships that could have appeared to influence the work reported in this paper.

Data availability

Data will be made available on request.

Acknowledgments

The authors would like to thank Cyril Hévin (EGFV) for his assistance with *in vitro* and hydroponic cultures. This work was supported by IJPB's Plant Observatory technological platforms. The IJPB receives support from Saclay Plant Sciences-SPS (ANR-17-EUR-0007).

Appendix A. Supplementary data

Supplementary data to this article can be found online at https://doi.org/10.1016/j.phytochem.2023.113837.

References

Akiyama, K., Matsuzaki, K., Hayashi, H., 2005. Plant sesquiterpenes induce hyphal branching in arbuscular mycorrhizal fungi. Nature 435, 824–827. https://doi.org/10.1038/nature03608.

Auger, B., Pouvreau, J.-B., Pouponneau, K., Yoneyama, Kaori, Montiel, G., Le Bizec, B., Yoneyama, Koichi, Delavault, P., Delourme, R., Simier, P., 2012. Germination stimulants of *Phelipanche ramosa* in the rhizosphere of *Brassica napus* are derived from the glucosinolate pathway. Mol. Plant Microbe Interact. 25, 993–1004. https://doi.org/10.1094/MPMI-01-12-0006-R.

Brewer, P.B., Yoneyama, Kaori, Filardo, F., Meyers, E., Scaffidi, A., Frickey, T., Akiyama, K., Seto, Y., Dun, E.A., Cremer, J.E., Kerr, S.C., Waters, M.T., Flematti, G. R., Mason, M.G., Weiller, G., Yamaguchi, S., Nomura, T., Smith, S.M., Yoneyama, Koichi, Beveridge, C.A., 2016. *LATERAL BRANCHING OXIDOREDUCTASE* acts in the final stages of strigolactone biosynthesis in *Arabidopsis*. Proc. Natl. Acad. Sci. U.S.A. 113, 6301–6306. https://doi.org/10.1073/pnas.1601729113.

Cardoso, C., Charnikhova, T., Jamil, M., Delaux, P.-M., Verstappen, F., Amini, M., Lauressergues, D., Ruyter-Spira, C., Bouwmeester, H., 2014. Differential activity of *Striga hermonthica* seed germination stimulants and *Gigaspora rosea* hyphal branching factors in rice and their contribution to underground communication. PLoS One 9, e104201. https://doi.org/10.1371/journal.pone.0104201.

Chabaud, M., Auriac, M.-C., Boniface, M.-C., Delgrange, S., Folletti, T., Jardinaud, M.-F., Legendre, A., Pérez-Vich, B., Pouvreau, J.-B., Velasco, L., Delavault, P., Muños, S., 2022. Wild *Helianthus* species: a reservoir of resistance genes for sustainable pyramidal resistance to broomrape in sunflower. Front. Plant Sci. 13, 1038684 https://doi.org/10.3389/fpls.2022.1038684.

Chai, Y.N., Schachtman, D.P., 2022. Root exudates impact plant performance under abiotic stress. Trends Plant Sci. 27, 80–91. https://doi.org/10.1016/j.tplants.2021.08.003.

Charnikhova, T.V., Gaus, K., Lumbroso, A., Sanders, M., Vincken, J.-P., De Mesmaeker, A., Ruyter-Spira, C.P., Screpanti, C., Bouwmeester, H.J., 2017. Zealactones. Novel natural strigolactones from maize. Phytochemistry 137, 123–131. https://doi.org/10.1016/j.phytochem.2017.02.010.

Cochetel, N., Escudié, F., Cookson, S.J., Dai, Z., Vivin, P., Bert, P.-F., Muñoz, M.S., Delrot, S., Klopp, C., Ollat, N., Lauvergeat, V., 2017. Root transcriptomic responses of grafted grapevines to heterogeneous nitrogen availability depend on rootstock genotype. J. Exp. Bot. 68, 4339–4355. https://doi.org/10.1093/jxb/erx224.

Cochetel, N., Météier, E., Merlin, I., Hévin, C., Pouvreau, J.-B., Coutos, P., Hernould, M., Vivin, P., Cookson, S.J., Ollat, N., Lauvergeat, V., 2018. Potential contribution of strigolactones in regulating scion growth and branching in grafted grapevine in response to nitrogen availability. J. Exp. Bot. 69, 4099–4112. https://doi.org/10.1093/jxb/ery206.

Cook, C.E., Whichard, L.P., Turner, B., Wall, M.E., Egley, G.H., 1966. Germination of Witchweed (*Striga lutea* Lour.): isolation and properties of a potent stimulant. Science 154, 1189–1190. https://doi.org/10.1126/science.154.3753.1189.

Cookson, S.J., Clemente Moreno, M.J., Hevin, C., Nyamba Mendome, L.Z., Delrot, S., Trossat-Magnin, C., Ollat, N., 2013. Graft union formation in grapevine induces transcriptional changes related to cell wall modification, wounding, hormone signalling, and secondary metabolism. J. Exp. Bot. 64, 2997–3008. https://doi.org/10.1093/jxb/ert144.

Darriaut, R., Antonielli, L., Martins, G., Ballestra, P., Vivin, P., Marguerit, E., Mitter, B., Masneuf-Pomarède, I., Compant, S., Ollat, N., Lauvergeat, V., 2022. Soil composition and rootstock genotype drive the root associated microbial communities in young

grapevines. Front. Microbiol. 13, 1031064 https://doi.org/10.3389/fmicb.2022.1031064.
De Saint Germain, A., Retailleau, P., Norsikian, S., Servajean, V., Pelissier, F., Steinmetz, V., Pillot, J.-P., Rochange, S., Pouvreau, J.-B., Boyer, F.-D., 2019. Contalactone, a contaminant formed during chemical synthesis of the strigolactone reference GR24 is also a strigolactone mimic. Phytochemistry 168, 112112. https://doi.org/10.1016/j.phytochem.2019.112112.
Dvorakova, M., Hylova, A., Soudek, P., Petrova, S., Spichal, L., Vanek, T., 2019. Triazolide strigolactone mimics as potent selective germinators of parasitic plant *Phelipanche ramosa*. Pest Manag. Sci. 75, 2049–2056. https://doi.org/10.1002/ps.5330.
Fornier, S.D., de Saint Germain, A., Retailleau, P., Pillot, J.-P., Taulera, Q., Andna, L., Miesch, L., Rochange, S., Pouvreau, J.-B., Boyer, F.-D., 2022. Noncanonical strigolactone analogues highlight selectivity for stimulating germination in two *Phelipanche ramosa* populations. J. Nat. Prod. 85, 1976–1992. https://doi.org/10.1021/acs.jnatprod.2c00282.
Ge, Y., Chen, X., Khan, S.N., Jia, S., Chen, G., 2023. Synthesis and germination activity study of novel strigolactam/strigolactone analogues. Tetrahedron Lett. 115, 154315 https://doi.org/10.1016/j.tetlet.2022.154315.
Guercio, A.M., Palayam, M., Shabek, N., 2023. Strigolactones: diversity, perception, and hydrolysis. Phytochemistry Rev. https://doi.org/10.1007/s11101-023-09853-4.
Hamzaoui, O., Maciuk, A., Delgrange, S., Kerdja, K., Thouminot, C., De Saint Germain, A., Rochange, S., Boyer, F.-D., Simier, P., Pouvreau, J.-B., 2019. Cannalactone: a new non-canonical strigolactone exudated by *Cannabis sativa* roots with a pivotal role in host specialization within French broomrape (*Phelipanche ramosa*) populations. In: 15th World Congress on Parasitic Plants, vol. 32. Amsterdam, Netherlands. https://hal.archives-ouvertes.fr/hal-02326484.
Hellemans, J., Mortier, G., De Paepe, A., Speleman, F., Vandesompele, J., 2007. qBase relative quantification framework and software for management and automated analysis of real-time quantitative PCR data. Genome Biol. 8, R19. https://doi.org/10.1186/gb-2007-8-2-r19.
Huet, S., Pouvreau, J.-B., Delage, E., Delgrange, S., Marais, C., Bahut, M., Delavault, P., Simier, P., Poulin, L., 2020. Populations of the parasitic plant *Phelipanche ramosa* influence their seed microbiota. Front. Plant Sci. 11, 1075. https://doi.org/10.3389/fpls.2020.01075.
Jiu, S., Xu, Y., Wang, J., Haider, M.S., Xu, J., Wang, L., Wang, S., Li, J., Liu, X., Sun, W., Xu, W., Zhang, C., 2022. Molecular mechanisms underlying the action of strigolactones involved in grapevine root development by interacting with other phytohormone signaling. Scientia Hort 293, 110709. https://doi.org/10.1016/j.scienta.2021.110709.
Joel, D.M., Chaudhuri, S.K., Plakhine, D., Ziadna, H., Steffens, J.C., 2011. Dehydrocostus lactone is exuded from sunflower roots and stimulates germination of the root parasite *Orobanche cumana*. Phytochemistry 72, 624–634. https://doi.org/10.1016/j.phytochem.2011.01.037.
Kim, H.I., Kisugi, T., Khetkam, P., Xie, X., Yoneyama, Kaori, Uchida, K., Yokota, T., Nomura, T., McErlean, C.S.P., Yoneyama, Koichi, 2014. Avenaol, a germination stimulant for root parasitic plants from *Avena strigosa*. Phytochemistry 103, 85–88. https://doi.org/10.1016/j.phytochem.2014.03.030.
Lopez-Guerrero, M.G., Wang, P., Phares, F., Schachtman, D.P., Alvarez, S., van Dijk, K., 2022. A glass bead semi-hydroponic system for intact maize root exudate analysis and phenotyping. Plant Methods 18, 25. https://doi.org/10.1186/s13007-022-00856-4.
Lyzenga, W.J., Liu, Z., Olukayode, T., Zhao, Y., Kochian, L.V., Ham, B.-K., 2023. Getting to the roots of N, P, and K uptake. J. Exp. Bot. erad035. https://doi.org/10.1093/jxb/erad035.
Mashiguchi, K., Seto, Y., Yamaguchi, S., 2021. Strigolactone biosynthesis, transport and perception. Plant J. 105, 335–350. https://doi.org/10.1111/tpj.15059.
Miura, H., Ochi, R., Nishiwaki, H., Yamauchi, S., Xie, X., Nakamura, H., Yoneyama, Koichi, Yoneyama, Kaori, 2022. Germination stimulant activity of isothiocyanates on Phelipanche spp. Plants 11, 606. https://doi.org/10.3390/plants11050606.
Mori, N., Nomura, T., Akiyama, K., 2020. Identification of two oxygenase genes involved in the respective biosynthetic pathways of canonical and non-canonical strigolactones in Lotus japonicus. Planta 251, 40. https://doi.org/10.1007/s00425-019-03332-x.
Moriyama, D., Wakabayashi, T., Shiotani, N., Yamamoto, S., Furusato, Y., Yabe, K., Mizutani, M., Takikawa, H., Sugimoto, Y., 2022. Identification of 6-epi-heliolactone as a biosynthetic precursor of avenaol in Avena strigosa. Biosci. Biotehnol. Biochem. 86, 998–1003. https://doi.org/10.1093/bbb/zbac069.
Nelson, D.C., 2021. The mechanism of host-induced germination in root parasitic plants. Plant Physiol. 185, 1353–1373. https://doi.org/10.1093/plphys/kiab043.
Oburger, E., Jones, D.L., 2018. Sampling root exudates – mission impossible? Rhizosphere 6, 116–133. https://doi.org/10.1016/j.rhisph.2018.06.004.
Pouvreau, J.-B., Poulin, L., Huet, S., Delavault, P., 2021. Strigolactone-like bioactivity via parasitic plant germination bioassay. In: Prandi, C., Cardinale, F. (Eds.), Strigolactones, Methods in Molecular Biology. Springer US, New York, NY, pp. 59–73. https://doi.org/10.1007/978-1-0716-1429-7_6.
Ravazzolo, L., Trevisan, S., Manoli, A., Boutet-Mercey, S., Perreau, F., Quaggiotti, S., 2019. The control of zealactone biosynthesis and exudation is involved in the response to nitrogen in maize root. Plant Cell Physiol. 60, 2100–2112. https://doi.org/10.1093/pcp/pcz108.
Shiratake, K., Notaguchi, M., Makino, H., Sawai, Y., Borghi, L., 2019. Petunia PLEIOTROPIC DRUG RESISTANCE 1 is a strigolactone short-distance transporter with long-distance outcomes. Plant Cell Physiol. 60, 1722–1733. https://doi.org/10.1093/pcp/pcz081.
Stojanova, B., Delourme, R., Duffé, P., Delavault, P., Simier, P., 2019. Genetic differentiation and host preference reveal non-exclusive host races in the generalist parasitic weed Phelipanche ramosa. Weed Res 59, 107–118. https://doi.org/10.1111/wre.12353.
Strehmel, N., Böttcher, C., Schmidt, S., Scheel, D., 2014. Profiling of secondary metabolites in root exudates of Arabidopsis thaliana. Phytochemistry 108, 35–46. https://doi.org/10.1016/j.phytochem.2014.10.003.
Ueno, K., Furumoto, T., Umeda, S., Mizutani, M., Takikawa, H., Batchvarova, R., Sugimoto, Y., 2014. Heliolactone, a non-sesquiterpene lactone germination stimulant for root parasitic weeds from sunflower. Phytochemistry 108, 122–128. https://doi.org/10.1016/j.phytochem.2014.09.018.
van Dam, N.M., Bouwmeester, H.J., 2016. Metabolomics in the rhizosphere: tapping into belowground chemical communication. Trends Plant Sci. 21, 256–265. https://doi.org/10.1016/j.tplants.2016.01.008.
Wakabayashi, T., Hamana, M., Mori, A., Akiyama, R., Ueno, K., Osakabe, K., Osakabe, Y., Suzuki, H., Takikawa, H., Mizutani, M., Sugimoto, Y., 2019. Direct conversion of carlactonoic acid to orobanchol by cytochrome P450 CYP722C in strigolactone biosynthesis. Sci. Adv. 5, eaax9067 https://doi.org/10.1126/sciadv.aax9067.
Wakabayashi, T., Shida, K., Kitano, Y., Takikawa, H., Mizutani, M., Sugimoto, Y., 2020. CYP722C from *Gossypium arboreum* catalyzes the conversion of carlactonoic acid to 5-deoxystrigol. Planta 251, 97. https://doi.org/10.1007/s00425-020-03390-6.
Wakabayashi, T., Yasuhara, R., Miura, K., Takikawa, H., Mizutani, M., Sugimoto, Y., 2021. Specific methylation of (11R)-carlactonoic acid by an Arabidopsis SABATH methyltransferase. Planta 254, 88. https://doi.org/10.1007/s00425-021-03738-6.
Wakabayashi, T., Moriyama, D., Miyamoto, A., Okamura, H., Shiotani, N., Shimizu, N., Mizutani, M., Takikawa, H., Sugimoto, Y., 2022. Identification of novel canonical strigolactones produced by tomato. Front. Plant Sci. 13, 1064378 https://doi.org/10.3389/fpls.2022.1064378.
Wen, Z., White, P.J., Shen, J., Lambers, H., 2022. Linking root exudation to belowground economic traits for resource acquisition. New Phytol. 233, 1620–1635. https://doi.org/10.1111/nph.17854.
Williams, A., Langridge, H., Straathof, A.L., Fox, G., Muhammadali, H., Hollywood, K.A., Xu, Y., Goodacre, R., de Vries, F.T., 2021. Comparing root exudate collection techniques: an improved hybrid method. Soil Biol. Biochem. 161, 108391 https://doi.org/10.1016/j.soilbio.2021.108391.
Wu, F., Gao, Y., Yang, W., Sui, N., Zhu, J., 2022. Biological functions of strigolactones and their crosstalk with other phytohormones. Front. Plant Sci. 13, 821563 https://doi.org/10.3389/fpls.2022.821563.
Xie, X., Mori, N., Yoneyama, K., Nomura, T., Uchida, K., Yoneyama, K., Akiyama, K., 2019. Lotuslactone, a non-canonical strigolactone from *Lotus japonicus*. Phytochemistry 157, 200–205. https://doi.org/10.1016/j.phytochem.2018.10.034.
Xie, X., Yoneyama, K., Nomura, T., Yoneyama, K., 2021. Evaluation and quantification of natural strigolactones from root exudates. In: Strigolactones: Methods and Protocols. Springer US, New York, NY, pp. 3–12.
Xu, Y., Wang, J., Wang, R., Wang, L., Zhang, C., Xu, W., Wang, S., Jiu, S., 2021. The role of strigolactones in the regulation of root system architecture in grapevine (*Vitis vinifera* L.) in response to root-restriction cultivation. Int. J. Mol. Sci. 22, 8799. https://doi.org/10.3390/ijms22168799.
Yoneyama, Kaori, Xie, X., Kim, H.I., Kisugi, T., Nomura, T., Sekimoto, H., Yokota, T., Yoneyama, Koichi, 2012. How do nitrogen and phosphorus deficiencies affect strigolactone production and exudation? Planta 235, 1197–1207. https://doi.org/10.1007/s00425-011-1568-8.
Yoneyama, Koichi, Xie, X., Yoneyama, Kaori, Kisugi, T., Nomura, T., Nakatani, Y., Akiyama, K., McErlean, C.S.P., 2018. Which are the major players, canonical or non-canonical strigolactones? J. Exp. Bot. 69, 2231–2239. https://doi.org/10.1093/jxb/ery090.
Yoneyama, Kaori, Akiyama, K., Brewer, P.B., Mori, N., Kawano-Kawada, M., Haruta, S., Nishiwaki, H., Yamauchi, S., Xie, X., Umehara, M., Beveridge, C.A., Yoneyama, Koichi, Nomura, T., 2020. Hydroxyl carlactone derivatives are predominant strigolactones in *Arabidopsis*. Plant Direct 4. https://doi.org/10.1002/pld3.219.
Yoneyama, K., 2020. Recent progress in the chemistry and biochemistry of strigolactones. J. Pestic. Sci. 45, 45–53. https://doi.org/10.1584/jpestics.D19-084.
Yoneyama, K., Brewer, P.B., 2021. Strigolactones, how are they synthesized to regulate plant growth and development? Curr. Opin. Plant Biol. 63, 102072 https://doi.org/10.1016/j.pbi.2021.102072.